T. R.
ONDOKUZ MAYIS UNIVERSITY
INSTITUTE OF GRADUATE STUDIES
DEPARTMENT OF HISTOLOGY AND EMBRYOLOGY

EFFECT OF GUM ARABIC IN HEALING OF GIT MUCOSAL INJURY INDUCED BY DICLOFENAC: A STEREOLOGICAL STUDY IN A RAT MODEL

PhD Thesis

Mohammed Kheir Eltigani Awad Elkarim AHMED

Supervisor

Prof. Dr. Süleyman KAPLAN

SAMSUN
2022

T. R.
ONDOKUZ MAYIS UNIVERSITY
INSTITUTE OF GRADUATE STUDIES
DEPARTMENT OF HISTOLOGY AND EMBRYOLOGY

EFFECT OF GUM ARABIC IN HEALING OF GIT MUCOSAL INJURY INDUCED BY DICLOFENAC: A STEREOLOGICAL STUDY IN A RAT MODEL

PhD Thesis

Mohammed Kheir Eltigani Awad Elkarim AHMED

Supervisor

Prof. Dr. Süleyman KAPLAN

SAMSUN
2022

ACCEPTANCE AND APPROVAL OF THE THESIS

The study entitled "Effect of Gum Arabic in healing of GIT mucosal injury induced by diclofenac: A Stereological Study in a Rat Model" prepared by Mohammed Kheir Eltigani Awad Elkarim AHMED and supervised by Prof. Dr. Süleyman KAPLAN was found successful and unanimously accepted by committee members as PhD thesis of the Department of Histology and Embryology, following the examination on the date 11/03/2022

	Title Name Surname **University** **Department**	**Signature**	**Final decision**
Chairman:	Prof. Dr. Cafer MARANGOZ Istanbul Medipol University Faculty of Medicine Department of Physiology		☐ Accept ☐ Reject
Member: **(Supervisor)**	Prof. Dr. Süleyman KAPLAN Ondokuz Mayıs University Faculty of Medicine Department of Histology and Embryology		☐ Accept ☐ Reject
Member:	Prof. Dr. Mustafa AYYILDIZ Ondokuz Mayıs University Faculty of Medicine Department of Physiology		☐ Accept ☐ Reject
Member:	Prof. Dr. Abdurrahman AKSOY Ondokuz Mayıs University Faculty of Veterinary Medicine Department of Pharmacology and Toxicology		☐ Accept ☐ Reject
Member:	Prof. Dr. Levent TÜMKAYA Recep Tayyip Erdoğan University Faculty of Medicine Department of Histology and Embryology		☐ Accept ☐ Reject

This thesis has been approved by the committee members that already stated above and determined by the Institute Executive Board.

CONFIRMATION
… / … / …
Prof. Dr. Ali BOLAT
Head of Institute of Graduate Studies

DECLARATION OF COMPLIANCE WITH SCIENTIFIC ETHIC

I hereby declare and undertake that I complied with scientific ethics and academic rules in all stages of my PhD thesis, that I have referred to each quotation that I use directly or indirectly in the study and that the works I have used consist of those shown in the sources, that it was written in accordance with the institute writing guide and that the situations stated in the article 3, section 9 of the Regulation for TÜBİTAK Research and Publication Ethics Board were not violated.

11 /03 / 2022

Mohammed Kheir Eltigani Awad Elkarim AHMED

DECLERATION OF THESIS ORIGINALITY REPORT

Thesis title: Effect of Gum Arabic in healing of GIT mucosal injury induced by diclofenac: A Stereological and Histological Study in a Rat Model

As a result of the originality report, which was received by me from the plagiarism detection program on 27/01/2022 for the thesis work with the above title;

Similarity rate: 10%
Single source rate:1%

27 /01 / 2022

Prof. Dr. Süleyman KAPLAN

ÖZET

DİKLOFENAKIN NEDEN OLDUĞU GİT MUKOZAL YARALANMALARININ İYİLEŞTİRİLMESİNDE ARAP SAKIZININ ETKİSİ: SIÇAN MODELİNDE STEREOLOJİK VE HİSTOLOJİK BİR ÇALIŞMA

Mohamed Kheir Eltigani Awad Elkarim AHMED
Ondokuz Mayıs Üniversitesi
Lisansüstü Eğitim Enstitüsü
Histoloji ve Embriyoloji Ana Bilim Dalı
Doktora, Mart /2022
Danışman: Prof. Dr. Süleyman KAPLAN

Amaç: Bu çalışma, bir sıçan modelinde diklofenak sodyumun neden olduğu gastrointestinal sistem (GIT) mukozal hasarının iyileştirilmesinde Arap sakızının etkisini stereolojik ve histolojik teknikler kullanarak araştırmayı amaçlamaktadır.

Gereç ve Yöntem: On iki haftalık kırk erkek Wistar albino sıçanı, her biri on sıçandan oluşan dört gruba ayrıldı. Bunlar kontrol grubu (Cont), diklofenak sodyum, 3,6 mg/kg grubu (DS), Arap zamkı 7,5 g/kg grubu (GA) ve diklofenak sodyum + Arap zamkı grubudur (DS+GA). Tüm gruplara 15 gün süreyle oral gavaj ile maddeler verildi. Sakrifikasyondan sonra GİT dokuları (mide, ince ve kalın bağırsaklar) histolojik ve stereolojik analizler için çıkarıldı.

Bulgular: Stereolojik analizlere göre grupların hacim fraksiyonları arasında anlamlı bir fark bulunamadı. Histopatolojik değerlendirmeler açısından, Cont ve GA gruplarının aksine, GIT mukozası 15 günlük DS maruziyetinden sonra ciddi şekilde etkilenmiştir. DS'ye maruz kaldıktan sonra Arap zamkı ile yapılan tedavide hafif bir koruyucu etki görülmüştür. GA tedavisinden sonra mide mukozası normal, yüzey epiteli ince, lamina propriada kollajen lifler ve normale yakın mide bezleri arasında gözlendi. Histolojik analizler, diklofenak sodyuma maruz kalan sıçanlarda, bağırsak mukozasında önemli modifikasyonların olduğunu, hem diklofenak sodyum hem de Arap zamkı verilen sıçanlarda, mukozada yüzeysel lezyon ve orta derecede tahriş gibi küçük patolojik anormalliklerin olduğunu göstermiştir.

Sonuç: GIT'in mukozal tabakasının morfolojisi nicel ve nitel yöntemler kullanılarak değerlendirildi. Gruplar arasında epitel, lamina propria ve muskularis mukoza volümü oranlarında anlamlı bir farklılık yoktu. DS, kalitatif verilere dayanarak GIT mukozasına zarar verir; yine de, GA DS ile birlikte alındığında GIT mukozasını kısmen korumaktadır. GA, NSAID'lerin yeni bir anti-COX-1 ve anti-COX-2'si gibi görünüyor.

Anahtar Kelimeler: GIT, diklofenak sodyum, Arap sakızı, stereoloji

ABSTRACT

EFFECT OF GUM ARABIC IN HEALING OF GIT MUCOSAL INJURY INDUCED BY DICLOFENAC: A STEREOLOGICAL AND HISTOLOGICAL STUDY IN A RAT MODEL

Mohamed Kheir Eltigani Awad Elkarim AHMED
Ondokuz Mayıs University
Institute of Graduate Studies
Department of Histology and Embryology
Ph.D., March /2022
Supervisor: Prof. Dr. Süleyman KAPLAN

Aim: This study aims to investigate the effect of gum Arabic in the healing of gastrointestinal tract (GIT) mucosal injury induced by diclofenac sodium in a rat model, using stereological and histological techniques.

Material and Method: Forty male 12-week-old Wistar albino rats were divided into four groups (each consisting of ten rats); in addition to the control group (Cont), the other groups received diclofenac sodium 3.6 mg/kg (DS group), gum Arabic group, 7.5 g/kg (GA), and diclofenac sodium + gum Arabic group (DS+GA). All groups were received substance by oral gavage for 15 days, after sacrification, the GIT tissues (stomach, small and large intestines) were removed for histological and stereological analyses.

Results: Based on the stereological analyses, there was no significant difference found between volume fractions of groups. In terms of histopathological evaluations, the GIT mucosa was seriously affected after 15 days of DS exposure in contrast to the Cont and GA groups. Treatment with gum Arabic after DS exposure, a slight protective effect was seen. The stomach mucosa was found to be normal, with thin surface epithelial lining, collagen fibers in the lamina propria, and between the near-normal gastric glands after GA treatment. In diclofenac sodium-treated rats, histological analyses revealed considerable modifications in the mucosal layer of the intestines, as well as minor pathological abnormalities such as superficial lesion and moderate irritation in rats that given both diclofenac sodium and gum Arabic.

Conclusion: The morphology of the mucosal layer of the GIT was assessed using quantitative and qualitative methods. There were no significant differences in the ratios of epithelium, lamina propria, and muscularis mucosae volume between groups. DS harms the GIT mucosa, based on qualitative data; yet, the mucosa of GIT is slightly protected when GA taken with DS. GA looks a novel anti-COX-1 and anti-COX-2 of NSAIDs.

Keywords: GIT, diclofenac sodium, gum Arabic, stereology

ACKNOWLEDGMENT

First and foremost, I want to express my gratitude to Allah Almighty for providing me with the strength and encouragement to embark on this study effort and endure until it is completed.

I would like to convey my heartfelt gratefulness and appreciation to my exceptional supervisor, Professor Dr. Süleyman Kaplan, who has been a constant source of encouragement and counsel during my Ph.D. path. I learned the scientific mindset and behaviour from him and the scientific mind of searching and discovering answers to our life's questions. I would like to express my sincere thanks to Prof. Dr. Mohamed Abdelsalam Nurein who helps me on this research subject. I want to thank the professors of the PhD Thesis Following Committee, Prof. Dr. Mustafa Ayyıldız, and Prof. Dr. Abdurrahman Aksoy, for following up on this research from its beginning to the end.

Dr. Gamze Altun deserves a special thank you for her unwavering support, invaluable guidance, kind collaboration and unwavering assistance, which she provided from the beginning to the finish of my thesis. Thank you to everyone in the Histology and Embryology Department for their assistance and support.

I would like to express my sincere gratitude to Res. Assist. Ayşenur Kaya for her invaluable assistance in the laboratory during the histology procedures as well as aesthetic works on the images of light micrographs in this thesis. From her, I learned a lot about tissue processing.

I would like to thank the Department of Histology and Embryology faculty members for their assistance and contributions to my Ph.D. studies. My gratitude also goes out to the department's staffs, which includes secretary Ayşegül Sakallı and technician Hüseyin Sarıcaoğlu.

I would like to thank with profound gratitude to the soul of my father Eltigani who passed away, my mother Shama, my wife, Dr. Rania, my brothers, my sisters, my sons, and my daughters for their unquestionable and unlimited encouragement and support.

CONTENTS

ACCEPTANCE AND APPROVAL OF THE THESIS ..... **i**
DECLARATION OF COMPLIANCE WITH SCIENTIFIC ETHIC ..... **ii**
DECLERATION OF THESIS ORIGINALITY REPORT ..... **ii**
ÖZET ..... **iii**
ABSTRACT ..... **iv**
ACKNOWLEDGMENT ..... **v**
LIST OF ABBREVIATIONS ..... **x**
LIST OF FIGURES ..... **xii**
LIST OF TABLES ..... **xix**
1. INTRODUCTION **1**
1.2. Justification 4
1.2. Objectives of the Study 4
1.2.1. Generally, to 4
1.2.2. Specifically 4
2. GENERAL INFORMATION AND SUMMARY OF LITERATURE REVIEW **6**
2.1. Gum Arabic 6
2.1.2. Introduction and Historical Background 6
3.1.3. GA Belt 7
2.1.4. Physical Characteristics of Gum Arabic 7
2.1.5. Digestion and Absorption of Gum Arabic 8
2.1.6. Applications of Gum Arabic 8
2.1.6.1. In the Food Manufacturing 8
2.1.6.2. Printing and Paint Industry 9
2.1.6.3. Pharmaceuticals 9
2.1.7. Biological Properties of Gum Arabic 9
2.2. Diclofenac Sodium 14
2.2.1. Introduction 14
2.2.2. Diclofenac Sodium 14
2.2.2.1. Description 14
2.2.2.2. Forms 15
2.2.2.3. Indications 15
2.2.2.4. Dose 15
2.2.2.5. Mechanism of Action 15
2.2.2.6. Side Effects 16

2.2.2.6.1. Side Effects on Cardiovasculr System 16
2.2.2.6.2. Side Effects on the Renal System 17
2.2.2.6.3. Side Effects on Respiratory System 18
2.2.2.6.4. Side Effects on Gastrointestinal Tract 18
2.2.2.6.5. Side Effects on Nervous System 20
2.3. The Gastrointestinal Tract of Albino Rat 20
2.3.1. Stomach 20
2.3.2. Small Intestine 21
2.3.3. Large Intestine 21
2.3.4. Histology of the Stomach 22
2.3.5. Histology of the Intestine 23
2.3.5.1. Histology of the Small Intestine 23
2.3.5.2. Histology of the Large Intestine 24
2.4. Development of the Gastrointestinal Tract 24
2.4.1. Development of the Stomach 24
2.4.2. Development of the Midgut 25
2.4.3. Development of Hind Gut 26
2.5. Histogenesis 26
2.5.1. Histogenesis of Stomach 26
2.5.2. Histogenesis of the Intestine 27
3. MATERIAL AND METHODS 29
3.1. Materials 29
3.1.1. The Study Drug 29
3.1.2. The Study Plant 29
3.1.3. The Study Animals 29
3.2. Methods 29
3.2.1. Study Design 29
3.2.2. Formation of Experimental Animal Groups 30
3.3. Preparation of Tissue Samples 31
3.3.1. Perfusion 31
3.3.2. Routine Histological Tissue Procedures 32
3.4. Tissue Sampling Protocol 32
3.4.1. Stomach: 32
3.4.2. Intestine 32
3.5. Sectioning Methods 34
3.6. Staining Process 36
3.7. Tissue Preparation for Electron Microscopy 36

3.8. Stereology ... 37
3.8.1. Stereological Analysis: ... 38
3.9. Statistical Analysis ... 40
4. RESULTS AND DISCUSSION ... 41
4.1. Result ... 41
4.1.1. Stereological Findings ... 41
4.1.1.1. Estimation of the Volume Fraction of the Surface and Glandular Epithelium ... 41
4.1.1.1.1. Stomach ... 41
4.1.1.1.2. Small Intestine ... 42
4.1.1.1.3. Large Intestine ... 43
4.1.1.2. Estimation of the Volume Fraction of the Lamina Propria ... 44
4.1.1.2.1. Stomach ... 44
4.1.1.2.2. Small Intestine ... 45
4.1.1.2.3. Large Intestine ... 46
4.1.1.3. Estimation of the Volume Fraction of the Muscularis Mucosae ... 47
4.1.1.3.1. Stomach ... 47
4.1.1.3.2. Small Intestine ... 48
4.1.1.3.3. Large Intestine ... 49
4.1.1.4. Estimation of the Volume Fraction of the Mucosal Layers ... 50
4.1.1.4.1. Stomach ... 50
4.1.1.4.2. Small Intestine ... 50
4.1.1.4.3. Large Intestine ... 51
4.1.2. Light Microscopic Findings ... 52
4.1.2.1. Stomach ... 52
4.1.2.1.1. Control Group ... 52
4.1.2.1.2. Diclofenac Sodium Group ... 63
4.1.2.1.3. Diclofenac Sodium +Gum Arabic Group ... 75
4.1.2.1.4. Gum Arabic Group ... 86
4.1.2.2. Small Intestine ... 96
4.1.2.2.1. Control Group ... 96
4.1.2.2.2. Diclofenac Sodium Group ... 108
4.1.2.2.3. Diclofenac Sodium + Gum Arabic Group ... 123
4.1.2.2.4. Gum Arabic Group ... 135
4.1.2.3. Large Intestine ... 146
4.1.2.3.1. Control Group ... 146

4.1.2.3.2. Diclofenac Sodium Group 156
4.1.2.3.3. Diclofenac Sodium + Gum Arabic Group 166
4.1.2.3.4. Gum Arabic Group 177
4.2. Discussion 185
5. CONCLUSION AND RECOMMENDATION 194
5.1. Conclusion 194
5.2. Recommendation 194
6. REFERENCES 195
APPENDICES 211
Ethical Committee Approval Certificate 211
CURRICULUM VITAE 212

LIST OF ABBREVIATIONS

AG	**:** Arabinogalactan
AGP	**:** Arabinogalactan protein
AIA	**:** Aspirin induced asthma
BC	**:** Before Christ
BE	**:** Balloon enteroscopy
Ca	**:** Calcium
CE	**:** Capsule endoscopy
CE	**:** Coefficient of error
COX-1	**:** Cyclooxygenase 1 enzyme
COX-2	**:** Cyclooxygenase 2 enzyme
CV	**:** Coefficient of variance
DS	**:** Diclofenac sodium
GA	**:** Gum Arabic
GALT	**:** Gut associated lymphoid tissue
GI	**:** Gastrointestinal
GIT	**:** Gastrointestinal tract
GP	**:** Glycoprotein
H2RAs	**:** Histamine 2-Receptor Antagonists
H&E	**:** Hematoxylin and eosin
IBS	**:** Irritable bowel syndrome
K	**:** Potassium
LTA4	**:** Leukotriene A4
MCV	**:** Mean corpuscular volume
MCH	**:** Mean corpuscular hemoglobin
Mg	**:** Magnesium
MI	**:** Myocardial infarction
MTL	**:** Melatonin
Na	**:** Sodium
NSAIDs	**:** Non-steroidal anti-inflammatory drugs
NO	**:** Nitric oxide
NOS	**:** Nitric oxide synthase
PG	**:** Prostaglandin
PH	**:** Potential of hydrogen
PPIs	**:** Proton pump inhibitors

ROS	**:** Reactive oxygen species
SGLT1	**:** Sodium-glucose transporter 1
SRS	**:** Systemic random sampling
VCE	**:** Video capsule endoscopy

LIST OF FIGURES

Figure 3.1. Housing conditions of the animals……...30
Figure 3.2. Wistar albino rats in a cage……..31
Figure 3.3. Automated dehydration……33
Figure 3. 4. A rotary microtome (Leica Rm2125rt, Nussloch, Germany)…….....35
Figure 3.5. Laboratory drying oven……35
Figure 3.6. Stereological analysis system…….....38
Figure 3.7. The stomach section is seen in the imagej program…….....39
Figure 3.8. The stomach section is seen in the imagej program…….....40
Figure 4.1. A volume ratio of the epithelium to the mucosal layer of the stomach, control (Cont.), gum Arabic (GA), diclofenac sodium (DS), diclofenac sodium + gum Arabic (DS+GA)……...……...……..……42
Figure 4.2. A volume ratio of the epithelium to the mucosal layer of the small intestine, control (Cont.), gum Arabic (GA), diclofenac sodium (DS), diclofenac sodium + gum Arabic (DS+GA)……..……..…..…..43
Figure 4.3. A volume ratio of the epithelium to the mucosal layer of the large intestine, control (Cont.), gum Arabic (GA), diclofenac sodium (DS), diclofenac sodium + gum Arabic (DS+GA)……...……..…..44
Figure 4.4. A volume ratio of lamina propria to the mucosal layer of the stomach, control (Cont.), gum Arabic (GA), diclofenac sodium (DS), diclofenac sodium + gum Arabic (DS+GA)…….……..……..45
Figure 4.5. A volume ratio of lamina propria to the mucosal layer of the small intestine, control (Cont.), gum Arabic (GA), diclofenac sodium (DS), diclofenac sodium + gum Arabic (DS+GA)……..…….……....46
Figure 4.6. A volume ratio of lamina propria to the mucosal layer of the large intestine, control (Cont.), gum Arabic (GA), diclofenac sodium (DS), diclofenac sodium + gum Arabic (DS+GA)……..……..……....47
Figure 4.7. A volume ratio of muscularis mucosae to the mucosal layer of the stomach, control (Cont.), gum Arabic (GA), diclofenac sodium (DS), diclofenac sodium + gum Arabic (DS+GA)…….…...……...48
Figure 4.8. A volume ratio of muscularis mucosae to the mucosal layer of the small intestine, Control (Cont.), gum Arabic (GA), diclofenac sodium (DS), diclofenac sodium + gum Arabic (DS+GA)……..……...……....49
Figure 4.9. A volume ratio of muscularis mucosae to the mucosal layer of the large Intestine, Control (Cont.), gum Arabic (GA), diclofenac sodium (DS), diclofenac sodium + gum Arabic (DS+GA)……..…….……....50
Figure 4.10. General structure of the stomach is seen. the whole layers of the stomach have a well-protected structure.…….…….....53
Figure 4.11. General structure of the stomach is seen. the whole layers of the stomach have a well-protected structure. 54
Figure 4.12. (A, B) High magnification of the stomach layers is seen. the whole layers of the stomach have a well-protected structure.. 55
Figure 4.13. (A, B) High magnification of the stomach layers, the epithelium (ep) and lamina propria (lp), are seen.. 56
Figure 4.14. (A, B) High magnification of the glands (gld) in the stomach, the epithelium (ep), and lamina propria (lp) are seen.. 57
Figure 4.15. (A, B) High magnification of the glands (gld), muscularis mucosa (mm), and submucosa layers in the stomach are seen..... 58

Figure 4.16. (A, B) High magnification images of the lower part of glands, lamina propria (lp), and muscularis mucosae layers (mm) of the stomach are observed.. 60
Figure 4.17. (A, B) The image of the lower part of glands (gld) lamina propria, muscularis mucosae layers (between arrowheads), and submucosa (sm) of the stomach are observed.. 60
Figure 4.18. (A, B) The image of the lower part of glands (gld) and connective tissue of the lamina propria are observed.. 61
Figure 4.19. (A, B) The images of muscularis externa that consists of two layers, interna (in) and externa (ex) of the stomach are observed. 62
Figure 4.20. General structure of stomach layers belonging to the diclofenac sodium (DS) group is seen. 64
Figure 4.21. A high magnification of the general structure of stomach layers belonging to the diclofenac sodium group is seen.. 65
Figure 4.22. (A, B) A high magnification of the surface epithelium in the stomach belonging to the diclofenac sodium (DS) group is seen..... 66
Figure 4.23. (A, B) A high magnification of transverse sections of the gastric pits (Gld) in the stomach belonging to the diclofenac sodium (DS) group is seen 67
Figure 4.24. A high magnification of the longitudinal section of the gastric mucosa from the stomach belonging to the diclofenac sodium (DS) group is seen.... 68
Figure 4.25. (A, B) High magnification images of a longitudinal section of the gastric glands (Gld) from the stomach belonging to the diclofenac sodium (DS) group are seen..... 70
Figure 4.26. (A, B) Images of the gastric glands from the stomach belonging to the diclofenac sodium (DS) group are observed.. 70
Figure 4.27. (A, B) Transverse sections from the base of gastric glands (Gld) group are observed..... 71
Figure 4.28. (A) A transverse section from the base of gastric glands (Gld) and lamina propria (Lp) in the stomach belonging to the diclofenac sodium (DS) group is seen..... 72
Figure 4.29. (A) A transverse section from the muscularis externa of the stomach belonging to the diclofenac sodium (DS) group is seen..... 73
Figure 4.30. (A) A transverse section from the muscularis externa of the stomach belonging to the diclofenac sodium (DS) group is seen..... 74
Figure 4.31. General structure of stomach layers belonging to the diclofenac sodium + gum Arabic (DS + GA) group is seen..... 76
Figure 4.32. A high magnification of the general structure of stomach layers belonging to the diclofenac sodium + gum Arabic (DS + GA) group is seen. 77
Figure 4.33. (A, B) High magnification images of the general structure of stomach mucosal layers belonging to the diclofenac sodium + gum Arabic (DS + GA) group are seen,..... 78
Figure 4.34. High magnification image of the general structure of stomach mucosal layers belonging to the diclofenac sodium + gum Arabic (DS + GA) group is seen.. 80
Figure 4.35. A high magnification image of the general structure of the stomach mucosal layer belonging to the diclofenac sodium + gum Arabic (DS + GA) group is seen..... 80

Figure 4.36. (A, B) High magnified images of the glands (Gld) in the stomach belonging to the diclofenac sodium + gum Arabic (DS + GA) group are seen. 81
Figure 4.37. (A, B) Images of the stomach layers belonging to the diclofenac sodium + gum Arabic (DS + GA) group are seen..... 82
Figure 4.38. An image of the stomach wall layers belonging to the diclofenac sodium + gum Arabic (DS + GA) group is seen.. 83
Figure 4.39. (A, B) Images of the stomach wall layers that are submucosa (SM) and muscularis externa (ME) belonging to the diclofenac sodium + gum Arabic (DS + GA) group are seen.. 84
Figure 4.40. An image of the stomach layers that are submucosa (SM) and muscularis externa (ME) belonging to the diclofenac sodium + gum Arabic (DS + GA) group is seen.. 85
Fgure 4.41. General structures of the stomach belonging to the gum Arabic (GA) group are seen. 87
Figure 4.42. Whole layers in the wall of the stomach belonging to the gum Arabic (GA) group are seen. 88
Figure 4.43. A part of mucosal layer in the wall of the stomach belonging to the gum Arabic (GA) group is seen.. 90
Figure 4.44. (A, B) Magnified images of a glandular part in the tunica mucosa of the stomach wall belonging to the gum Arabic (GA) group are seen.. 90
Figure 4.45. (A, B) Magnified images of a glandular part in the wall of stomach belonging to the gum Arabic (GA) group are seen. 91
Figure 4.46. (A, B, C) Magnified images of the stomach layers belonging to the gum Arabic (GA) group are seen.. 92
Figure 4.47. (A, B) Magnified images of the vessels in the submucosa layer in the wall of the stomach belonging to the gum Arabic (GA) group are seen..... 93
Figure 4.48. (A, B) Magnified images of the muscularis externa in the wall of the stomach belonging to the gum Arabic (GA) group are seen. 94
Figure 4.49. (A, B) Magnified images of the muscularis externa (ME) in the wall of the stomach belonging to the gum Arabic (GA) group are seen. 95
Figure 4.50. (A, B) General structures of the small intestine belonging to the control group are seen……..….97
Figure 4.51. General structures of the tubular gland in the small intestine belonging to the control group are seen 98
Figure 4.52. (A, B) High magnification of the small intestine images belonging to the control group is seen 100
Figure 4.53. (A) A high magnification of the surface epithelium belonging to the small intestine image from the control group is seen.. 100
Figure 4.54. (A, B) High magnification of the surface epithelium (Ep) and its lamina propria (Lp) belonging to the small intestine image from the control group is seen.. 101
Figure 4.55. A high magnification of the surface epithelium, its lamina propria (Lp), and intestinal gland with a lumen (L) belonging to the small intestine from the control group is seen. 102
Figure 4.56. (A) A longitudinal section of the intestinal gland with a lumen (L), at the base of it, an accumulation of the Paneth cells from the control group is observed.. 103
Figure 4.57. (A, B) Longitudinal and transverse sections of the intestinal glands (Gld) from the control group are seen. 104

Figure 4.58. (A, B) Longitudinal sections of the intestinal glands (Gld) from the control group are seen.. 105
Figure 4.59. (A) Longitudinal sections of the intestinal glands (Gld) from the control group are seen. A rich and well-developed connective tissue and submucosal ganglionic cells (dashed circled area) are visible.. 106
Figure 4.60. (A) A section of the intestinal glands (Gld), lamina propria, muscularis mucosae, submucosa, and muscularis externa (ME) belonging to the control group are seen..... 107
Figure 4.61. A general view of the small intestine belongs to the diclofenac sodium (DS) group. All layers of the organ are seen.. 109
Figure 4.62. A high magnification of the general view of the small intestine belongs to the diclofenac sodium (DS) group. 110
Figure 4.63. A high magnification of simple columnar epithelium of the small intestine belongs to the diclofenac sodium (DS) group.. 111
Figure 4.64. (A) A high magnification of simple columnar epithelium (Ep) of the small intestine belongs to the diclofenac sodium (DS) group. 112
Figure 4.65. (A) A high magnification of simple columnar epithelium (Ep) of the small intestine belongs to the diclofenac sodium (DS) group.. 113
Figure 4.66. (A) A high magnification of intestinal gland, it is lined by simple columnar epithelium (Ep) that has many Goblet cells (arrows) that belongs to the diclofenac sodium (DS) group. 114
Figure 4.67. (A) A high magnification of lamina propria (Lp) and glandular epithelium of the small intestine belongs to the diclofenac sodium (DS) group..... 115
Figure 4.68. (A, B) Longitudinally sectioned intestinal glands (Gld) with a lumen (L) belonging to the diclofenac sodium (DS) group is seen. 116
Figure 4.69. (A) A longitudinal section of the intestinal gland with a thick basal membrane (arrowhead) belonging to the diclofenac sodium (DS) group is seen..... 117
Figure 4.70. (A) A longitudinal section of the intestinal gland with a thick basal membrane (arrowhead) belonging to the diclofenac sodium (DS) group is observed 118
Figure 4.71. (A, B) Longitudinal sections of intestinal glands (Gld) with a thick basal membrane (arrowhead) belonging to the diclofenac sodium (DS) group are observed. 119
Figure 4.72. A unified image of sections belonging to the small intestinal glands (Gld) with a thick basal membrane to the diclofenac sodium (DS) group is observed.. 120
Figure 4.73. A submucosal ganglion that is surrendered by a connective tissue capsule (dashed circled area) belonging to the diclofenac sodium (DS) group is observed 121
Figure 4.74. A longitudinal section of muscularis externa that has internal and external layers of muscle belonging to the diclofenac sodium (DS) group is observed. 122
Figure 4.75. A general view of the small intestine belonging to the DS + GA group 124
Figure 4.76. A high magnification of the small intestine belonging to the DS + GA group is seen..... 125
Figure 4.77. A high magnification of epithelium (Ep) and lamina propria (Lp) of the small intestine belonging to the DS + GA group is seen. 126

Figure 4.78. A high magnification of epithelium (Ep) and lamina propria (Lp) of the small intestine belonging to the DS + GA group is observed.. 127
Figure 4.79. (A, B) High magnification of lamina propria (Lp) of the small intestine belonging to the DS + GA group are observed. 128
Figure 4.80. A high magnification of an intestinal gland (Gld) and surrounding connective (Ct) in the small intestine belonging to the DS + GA group is seen 129
Figure 4.81. A high magnification of two intestinal glands (Gld) that were cut longitudinally belonging to the DS + GA group is seen.. 130
Figure 4.82. (A, B) High magnification of two intestinal glands (Gld) that were cut longitudinally belonging to the DS + GA group are seen.. 131
Figure 4.83. (A) A high magnification of two intestinal glands (Gld) belonging to the DS + GA group is seen.. 132
Figure 4.84. (A) A high magnification of muscularis externa that consists of an inner (In) and external (Ex) layer belonging to the DS + GA group is seen.. 133
Figure 4.85. (A) A high magnification of muscularis externa that consists of an inner (In) and external (Ex) and submucosa layer (SM) belonging to the DS + GA group is seen 134
Figure 4.86. (A, B) General structure of the small intestine belonging to the GA group is seen ……..……...136
Figure 4.87. (A, B) High magnification of the small intestine images belonging to the GA group is seen. 137
Figure 4.88. (A, B) General structures of the tubular gland in the small intestine image belonging to the GA group are seen. 138
Figure 4.89. Magnified and unified images of the small intestine belonging to the GA group are observed.. 139
Figure 4.90. Transverse sections of the intestinal glands (Gld) belonging to the GA group are seen..... 140
Figure 4.91. (A, B) A partly longitudinal sections of the intestinal glands (Gld) belonging to the GA group are seen.. 141
Figure 4.92. The sections of the intestinal glands (Gld) in the small intestine belonging to the GA group are seen.. 142
Figure 4.93. (A, B) The sections of the intestinal glands (Gld) in the small intestine belonging to the GA group are observed.. 143
Figure 4.94. (A, B) The sections of the intestinal glands (Gld) in the small intestine belonging to the GA group are seen.. 144
Figure 4.95. (A) The sections of the intestinal glands (Gld) in the small intestine belonging to the GA group are seen.. 145
Figure 4.96. A general view of the large intestine belongs to the control (Cont) group ……..……..... 147
Figure 4.97. A high magnification of the general view of the large intestine belongs to the control (Cont) group all layers of the organ are found healthy. 148
Figure 4.98. A high magnification of the general view of the large intestine belonging to the control (Cont) group is seen. 149
Figure 4.99. A high magnification of the epithelium (Ep) and lamina propria (Lp) of the large intestine belonging to the control (Cont) group are seen. 150
Figure 4.100. (A, B) A high magnification of the epithelium (Ep) and lamina propria (Lp) of the large intestine belonging to the control (Cont) group are seen .. 151

Figure 4.101. (A, B, C) A high magnification of intestinal glands (Gld) and its lamina propria (Lp) of the large intestine belongs to the control (Cont) group is seen.. 152
Figure 4.102. A high magnification of intestinal glands (Gld), its lamina propria, muscularis mucosae (MM), submucosa (SM), and muscularis externa (ME) of the large intestine belong to the control (Cont) group is seen..... 153
Figure 4.103. (A, B) A high magnification of connective tissue (Ct) in the submucosa of the large intestine belonging to the control (Cont) group is seen. 154
Figure 4.104. A high magnification of muscularis externa of the large intestine belonging to the control (Cont) group is seen.. 155
Figure 4.105. A general view of the large intestine belongs to the diclofenac sodium (DS) group. 157
Figure 4.106. Whole layers of the large intestine wall belonging to the diclofenac sodium (DS) group are seen 158
Figure 4.107. (A, B) Images of the simple columnar epithelium (Ep) and lamina propria (Lp) belonging to the diclofenac sodium (DS) group are seen..... 159
Figure 4.108. (A, B) The simple columnar epithelium (Ep) and lamina propria belonging to the diclofenac sodium (DS) group is seen..... 160
Figure 4.109. (A, B) Longitudinal sections of intestinal glands belonging to the diclofenac sodium (DS) group are seen. 161
Figure 4.110. (A, B) Intestinal glands belonging to the diclofenac sodium (DS) group are seen 162
Figure 4.111. (A, B) The images of the epithelium (Ep) and lamina propria (Lp) of intestinal glands belonging to the diclofenac sodium (DS) group are seen. 163
Figure 4.112. A high magnification of submucosa (SM) and muscularis externa that consists of two layers named interna (In) and externa (Ex) are seen. 164
Figure 4.113. (A, B) A high magnification of submucosa (SM) and muscularis externa that consists of two layers named interna (In) and externa (Ex) are seen.. 165
Figure 4.114. A general view of the large intestine belongs to the diclofenac sodium + gum Arabic (DS + GA) group..... 167
Figure 4.115. A high magnification of the large intestine belongs to the diclofenac sodium + gum Arabic (DS + GA) group. 168
Figure 4.116. A high magnification of the large intestine belongs to the diclofenac sodium + gum Arabic (DS + GA) group. 169
Figure 4.117. (A, B) High magnification images of the large intestine belonging to the diclofenac sodium + gum Arabic (DS + GA) group are seen.. 170
Figure 4.118. (A, B) High magnification images of two large intestines belonging to the diclofenac sodium + gum Arabic (DS + GA) group are observed.. 171
Figure 4.119. A high magnification image of the large intestine belonging to the diclofenac sodium + gum Arabic (DS + GA) group is seen.. 172
Figure 4.120. (A, B) Images of the large intestine belonging to the diclofenac sodium + gum Arabic (DS + GA) group are seen..... 173

Figure 4.121. (A, B) Images of large intestine belonging to the diclofenac sodium + gum Arabic (DS + GA) group is seen…. .. 174
Figure 4.122. An image of a large intestine belonging to the diclofenac sodium + gum Arabic (DS+ GA) group is seen. 175
Figure 4.123. (A, B) Images of the large intestine belonging to the diclofenac sodium + gum Arabic (DS+ GA) group are observed.. 176
Figure 4.124. A general view of the large intestine belongs to the gum Arabic (GA) group. 178
Figure 4.125. (A, B, C) General views of the large intestine belong to the gum Arabic (GA) group. All layers of the organ are seen intact at this magnification. Partly an enlarged mucosa and large size crypt of Lieberkühn (i.e. intestinal crypt) are observed 179
Figure 4.126. (A, B) General views of the large intestine belong to the gum Arabic (GA) group. (A) Epithelium (Ep) and lamina propria (Lp) of mucosal layers in the organ is seen intact at this magnification.. 180
Figure 4.127. (A, B) General views of the large intestine glands belong to the gum Arabic (GA) group. (A) An intestinal gland with many Goblet cells (arrows) and a large lumen (L) are seen.. 181
Figure 4.128. (A, B) General views of the large intestine glands belong to the gum Arabic (GA) group. Three intestinal glands (Gld) with many Goblet cells (arrows) are partly seen.. 182
Figure 4.129. (A, B) General views of the large intestine belong to the gum Arabic (GA) group. (A) Epithelium and lamina propria (Lp) of mucosal layers in the organ is seen intact at this magnification. 183
Figure 4.130. (A, B) General views of the large intestine layers belong to the gum Arabic (GA) group. The submucosa that has many healthy vessels (V) and connective tissue (Ct) is seen. 184

LIST OF TABLES

Table 3.1. Chemical solutions and duration of follow-up of git tissues…….....33

Table 3.2. Chemicals and duration used for h&e staining of the sections……....36

Table 4.1. A volume ratio of the epithelium to the mucosal layer of the stomach, control (Cont.), gum Arabic (GA), diclofenac sodium (DS), diclofenac sodium + gum Arabic (D+GA) ……..…….....41

Table 4.2. A volume ratio of the epithelium to the mucosal layer of the small intestine, control (Cont.), gum Arabic (GA), diclofenac sodium (DS), diclofenac sodium + gum Arabic (DS+GA) …….....42

Table 4.3. A volume ratio of the epithelium to the mucosal layer of the large intestine, control (Cont.), gum Arabic (GA), diclofenac sodium (DS), diclofenac sodium + gum Arabic (DS+GA)……43

Table 4.4. A volume ratio of lamina propria to the mucosal layer of the stomach, control (Cont.), gum Arabic (GA), diclofenac sodium (DS), diclofenac sodium + gum Arabic (DS+GA)……...…….…..44

Table 4.5. A volume ratio of lamina propria to the mucosal layer of the small intestine, control (Cont.), gum Arabic (GA), diclofenac sodium (DS), diclofenac sodium + gum Arabic (DS+GA)……....45

Table 4.6. A volume ratio of lamina propria to the mucosal layer of the large intestine, control (Cont.), gum Arabic (GA), diclofenac sodium (DS), diclofenac sodium + gum Arabic (DS+GA)……....46

Table 4.7. A volume ratio of muscularis mucosae to the mucosal layer of the stomach, control (Cont.), gum Arabic (GA), diclofenac sodium (DS), diclofenac sodium + gum Arabic (DS+GA)……....47

Table 4.8. A volume ratio of muscularis mucosae to the mucosal layer of the small intestine, control (Cont.), gum Arabic (GA), diclofenac sodium (DS), diclofenac sodium + gum Arabic (DS+GA)……..…….....48

Table 4.9. A volume ratio of muscularis mucosae to the mucosal layer of the large intestine, control (Cont.), gum Arabic (GA), diclofenac sodium (DS), diclofenac sodium + gum Arabic (DS+GA)……..…..49

Table 4.10. A volume ratio of the mucosal layers of the stomach, control (Cont.), gum Arabic (GA), diclofenac sodium (DS), diclofenac sodium + gum Arabic (DS+GA)……...……...……..……..50

Table 4.11. A volume ratio of the mucosal layers of the small intestine, control (Cont.), gum Arabic (GA), diclofenac sodium (DS), diclofenac sodium + gum Arabic (DS+GA)……..…….…...51

Table 4.12. A volume ratio of the mucosal layers of the large intestine, control (Cont.), gum Arabic (GA), diclofenac sodium (DS), diclofenac sodium + gum Arabic (DS+GA)…….……...…..51

Table 4.13. The coefficient of error CE and the coefficient of variance CV for the volume fraction of, the epithelium, lamina propria, muscularis mucosae of the stomach of the control (Cont.), gum Arabic (GA), diclofenac sodium (DS), diclofenac sodium + gum Arabic (DS+GA)……....….51

Table 4.14. The coefficient of error CE and the coefficient of variance CV for the volume fraction of, the epithelium, lamina propria, muscularis mucosae of the small intestine of the control (Cont.), gum Arabic (GA), diclofenac sodium (DS), diclofenac sodium + gum Arabic (DS+GA)……..51

Table 4.15. The coefficient of error CE and the coefficient of variance CV for the volume fraction of, the epithelium, lamina propria, muscularis mucosae of the large intestine of the control (Cont), gum Arabic (GA), diclofenac sodium (DS), diclofenac sodium + gum Arabic (DS+GA) groups……..52

1. INTRODUCTION

Gum Arabic (GA), similarly recognized as gum Acacia, stands as an exudate from a tree that has been used as a marketable constituent since ancient times. According to the Joint Expert Committee on Food Additives, is defined as an exudate produced by all the parts of Acacia plants (JECFA) (Phillips and Williams, 2001).

The genus Acacia Gums contains more than 1000 species, but only two are commercially important: *Acacia senegal* and *Acacia seyal* (Abuarra et al., 2014). *Acacia senegal* is the best grade and accounts for the majority of global trade due to the low number of tannins (Egadu et al., 2007). The trees develop extensively through the Sahelian belt of Africa, a region estimated at four million kilometres crescentic-like landmass directly south of the Sahara desert that extends from Somalia in the east to Senegal in the west. GA is the balm that discharges by the entire parts of plants. The making of GA is started by `tapping,' which implicates eliminating units of the cortex. The sticky, gummy material dehydrates on the trees, forming hard nodules that must be picked by hand and categorized by color and size. GA has additional names: Acacia gum, Kordofan gum, gum Hashab, gum Arabic (*Acacia seyal*), gum Talha, Arabic gum, gum Arabic (*Acacia senegal*) (Phillips and Williams, 2000).

The earliest Egyptians had used gum Arabic from the second millennium BC as a glue for preserving bodies and in mineral dyes for producing hieroglyphs (Verbeken et al., 2003). In current years, however, there has been a renewed attention in gum Arabic, resulting in more papers regarding its constitution, properties, and novel uses in food and medicines, among other fields (Rodge et al., 2012).

GA has a complicated chemical make-up. It is primarily composed of high-molecular-weight polysaccharides and their magnesium, potassium, and calcium salts, which when hydrolyzed harvest three chief polysaccharides with protein elements: arabinogalactan (AG), AG protein (AGP), and glycoprotein (GP), each of them has differs molecular weight and chemical structure (Desplanques et al., 2012).

It is used widely as an additive and stabilizer to many food and drug products as well as to enhance the elimination of liquids and electrolytes from the GIT

(Wapnir et al., 1997; Rehman et al., 2003; Codipilly et al., 2006), so it is used in oral rehydration solution (Alam et al., 2000). Its oligosaccharides and fermentable fibers aid in releasing nitrogenous products in the cecum lumen, resulting in the breakdown of these ions in the stool and therefore lowering blood urea levels (Younes et al., 1995). Moreover, in a study on albino rats, gum Arabic was proved to have a protective effect on the mucosa of the intestine and enhance a product of the enzymes of the pancreas (El-Mawla and Osman, 2011).

Non-steroidal anti-inflammatory drugs (NSAIDs) are one of the best usually recommended drugs. There are prescription and non-prescription versions available. The similar pharmacological qualities that make them beneficial in treating several painful and/or arthritic illnesses also cause various gastrointestinal adverse effects, extending from slight dyspepsia to the possibility of stomach cancer (Bidaut-Russell and Gabriel, 2001).

NSAIDs, such as diclofenac sodium (DS), have long been used in clinical settings to treat and prevent inflammatory diseases such as joint pain, connective tissue diseases, ache, fever, and cerebrovascular ischemic disorders (Matsui et al., 2011). This is due to antipyretic, analgesic, anti-inflammatory, and antiplatelet effects (Higuchi et al., 2009). Traditional (selective) and non-selective cyclooxygenase-2 inhibitors (COX-2 inhibitors) are the two main forms of NSAIDs (Venerito et al., 2010). Traditional (NSAIDs) are recognized to have substantial gastrointestinal (GI) adverse effects (Allison et al., 1992). The COX-2 inhibitors were created to decrease the GI adverse effects but preserve the value of the traditional NSAIDs. The COX-2 inhibitors have been linked to an augmented hazard of cardiovascular complications (Jüni et al., 2005). Diclofenac's particular way of action, similar to that of other NSAIDs, is uncertain. Anti-inflammatory, antipyretic, and painkilling effects have been discovered. NSAIDs are hypothesized to have these effects through inhibiting cyclooxygenase (COX) enzymes, which causes prostaglandin (PG) production to be inhibited. On the other hand, PG has imperative roles in maintaining the homeostasis of the gastrointestinal mucosa (Higuchi et al., 2009). As a result, NSAIDs can have substantial side effects in both experimental animals and humans, such as gastrointestinal damage (Bjarnason et al., 1987;Allison et al., 1992; Tanaka et al., 2002). Because of the recent increase in NSAIDs prescriptions, it is necessary to be mindful of the gastrointestinal adverse effects.

Previous studies reported the hazards of NSAID mainly on the upper GIT. The current reports utilized new emerging diagnostic modalities like video capsule endoscopy (VCE), capsule endoscopy (CE), device-assisted enteroscopy, and balloon enteroscopy (BE) to display involvement of the whole GIT (Higuchi et al., 2009). This raised the awareness of researchers to the seriousness of the hazards of uncontrolled NSAID use (Kameda et al., 2008; Sunada and Yamamoto, 2009). Some studies showed involvement of the lower GIT in 55% while other studies showed lower GIT involvement in 75% of the population (Goldstein et al., 2005; Graham et al., 2005; Maiden et al., 2005;Maiden et al., 2007; Maiden, 2009; Fujimori et al., 2010). Further studies reported the ratio of upper GIT/lower GIT problems was reversed from 4.1 in 1996 to 1.4 in 2005 (Lanas et al., 2009; Lanas and Sopeña, 2009). This indicated that NSAIDs enhance the hazard of lower GI haemorrhage and damage in the same way they do in the upper GI tract, the frequency of NSAID enteropathy was reported to vary between 55% (Goldstein et al., 2005), (68% and 75%) (Maiden et al., 2005). In the UK, admission for bleeding from gastric and duodenal ulcers was 8528 per annum: 20-25% of them were found to be resulted by are reasonably related to the consumption of NSAIDs, and the death rate was found to be about 700-900 (Langman, 2001).

The pathophysiology of NSAID injuries varies between different parts of the GIT. In the upper GIT, the tissue insults were found to be multifactorial. Some researchers attributed it to tissue dehydration due to the acidic nature of the drug (Scheiman, 1994; Scarpignato, 1995). Other studies described it as a result of inhibition of mucus production, leading to the breaking of mucus barrier and disrupting the tied junction between the cells (Rainsford, 1978; Scheiman, 2001). A third group attributed the cause of insult to the reduction of submucosal blood flow hence mucosal ischemia and impairment of mucosal repair in addition to impairment of mucosal cell proliferation (Sun et al., 2000; Funatsu et al., 2007). On the other hand, the mechanism by which NSAID cause injury in the lower GIT was reported to have resulted from the metabolism of the drug through the enterohepatic circulation assisted the uncontrolled growth of the lower GIT bacterial flora (Reuter et al., 1997; Goldstein et al., 2005; Maiden et al., 2005; Fujimori et al., 2010).

1.2. Justification

For centuries, traditional herbal medicine has been utilized by indigenous societies all over the world to cure a variety of ailments. The World Health Organization (WHO) estimates that up to 80% of the residents in developing nations practice traditional herbal medicine for primary health care (Verma and Singh, 2008). In 2008, WHO issued a declaration calling for collaboration between modern and traditional herbal medicine to help close the equity hole in public health and highlighting the importance of the investigation to support traditional herbal medicine's development in providing suitable, safe, and effective treatments. On the other side, the annual expense of treating NSAID-related gastrointestinal side effects is exorbitant. For example, in the United States, only it exceeds US$ 4 billion (Bidaut-Russell and Gabriel, 2001). The GIT was chosen for this study because, firstly, GIT symptoms usually bring patients urgently seeking medical advice. Secondly, symptomatology of GIT could be a red flag alarming for serious NSAIDs pathology affecting other systems. Thirdly, treatment to GIT may result without irreversible damage to it.

Knowledge about stereological studies investigating the effect of GA on the GIT histology is scanty. This study was aimed to apply stereology in quantifying the role of gum Arabic in the healing of GIT injury induced by diclofenac sodium in a rat model.

1.1. Objectives of the Study

The study's goals are as follows:

1.1.1.Generally, to

1. Examine the ability of gum Arabic on the healing of GIT mucosal injury caused by diclofenac sodium in rats using stereological technique.
2. Evaluate the efficiency of light microscopy in detecting GIT injuries induced by diclofenac sodium.

1.1.2. Specifically

- To compare:

1. The volume fraction of each of the three portions of the mucosal layer in each part of the GIT.

2. Features of the mucosal cells among rats treated with diclofenac sodium, diclofenac sodium + gum Arabic, gum Arabic, and the control.
3. To compare the results obtained by stereological analysis with those obtained by routine microscopy.

2. GENERAL INFORMATION AND SUMMARY OF LITERATURE REVIEW

2.1. Gum Arabic

2.1.2. Introduction and Historical Background

For eras, gum has been used in baking elements, medicines, tools, and trades. It has a lengthy history in culture, dating back to the Egyptians and Australian native communities. Acacia was engaged in a number of methods by these countries and peoples, from candies to hemorrhoids management. In 1700, the first species of acacia was discovered and named by Swedish scientist Carl Linnaeus as *Acacia nilotica*, and after that, the acacia genus was developed by now around 1000 species were identified (Meena and Datta, 2015).

Since 4000 B.C., GA has been employed in the manufacture of ink, watercolors, and dyes in Egypt, where it was widely used under the Pharaoh's civilization. GA gets its name because it was first imported to Europe from Arabian ports. Trees between the ages of three and thirty years produce the gum, especially if they are in poor health (Blunt, 1926).

Gum Arabic is a minor forest product derived from *Acacia senegal* (Hashab) and *Acacia seyal* (Talh). The *Acacia senegal* tree can be found across Africa, as well as on the Indian subcontinent. The GA belt includes many African countries like Mauritania, Senegal, Mali, in the west, Chad, Cameroon, Sudan, in the middle, Eritrea, Ethiopia, Somalia, in the east, where the main residents of gum-producing Acadia species may be originating. The greatest of the world's GA, however, derives from Sudan. The Hashab tree produces over 90% of Sudan's total GA production, with the remaining 10% coming from other sources. With its two states (Southern and Northern Kordofan), the Great Kordofan Region is the primary producer of high-quality natural GA known as Kordofan gum (Abd- Allah et al., 2002). GA is naturally created as enormous swellings through a procedure called gummosis to bind sores in the tree's cortex and is made from exudates from the stalks and boughs of two types of acacia trees. It has a lower consistency than other hydrocolloids (Verbeken et al., 2003).

3.1.3. GA Belt

The African gum belt, which runs east-west from between latitudes 4 and 18, is a desert zone situated north of the Equator and south of the Sahara desert. Tanzania, Zimbabwe, Malawi, and South Africa are examples of countries south of the Equator where they can be found. The Arabian Peninsula and India in Asia are both home to *Acacia senegal* (Adam et al., 2016).

2.1.3. Chemical Behaviors of GA

Gum Arabic is a highly heterogeneous material (glycoprotein), composed mainly of sugars and shallow protein content. It's a branched-chain, complex polysaccharide with neutral sugars (arabinose, rhamnose, and galactose) and slightly acidic sugar derivatives (4-methoxyglucuronic acid and glucuronic acid), and it comes in potassium, magnesium, and calcium salts (Tonon et al., 2011).

The backbone consists of 1,3-linked b-D-galactopyranosyl units, whereas the side chains consist of two to five 1,3-linked b-D-galactopyranosyl units joined to the chief chain by 1,6-linkages (Verbeken et al., 2003). The primary amino acids found in the protein component of GA are hydroxyproline, serine, and proline (Verbeken et al., 2003). GA is made up of polysaccharides with a lower molecular weight (0.25 x 106 Daltons primary component) and hydroxyproline-rich glycoproteins with greater molecular weight (2.5 x 106 Daltons minor component) (Renard et al., 2006). GA's chemical composition changes according to its source, the oldness of the trees collected, weather circumstances, and the soil atmosphere (Renard et al., 2006)

2.1.4. Physical Characteristics of Gum Arabic

GA has different physical qualities according to the tree's origin and age, exudation time, and climate. Physical properties of gums were altered by post-harvest treatment, such as washing, drying, and sun bleaching, as well as storage conditions (Hu et al., 2018). It is tear-shaped, spherical, orange-brown, and of great quality. The particles become paler in color and appear vitreous after being crushed or shattered. It can be dissolved in water, resulting in an acidic liquid solution. The resultant solution is colorless, odorless, and has little interaction with other chemicals (Daoub et al., 2018).

2.1.5. Digestion and Absorption of Gum Arabic

Both humans and animals have difficulty-digesting GA. It is fermented particularly into propionic acids by normal flora in the colon, pretty than destroying it in the small intestine. The human colon absorbs these breakdown products, which are then used energetically in metabolism (Kishimoto et al., 2006).

2.1.6. Applications of Gum Arabic

GA is widely utilized as a preservative, thickener, emulsifier, and encapsulated in sustenance manufacturing, as well as in fabrics, porcelains, lithography, makeups, and drugs industries to a lesser extent (Verbeken et al., 2003). GA is principally utilized as a microencapsulating substance in the aliment sector and confectionery, bakery, dairy, and beverage. Its powder is most commonly used in the creation of soft beverages, as well as in cooking and baking, to maintain product texture, enhance liquid viscosity, and aid in the rising of backed items. Other uses include imparting shine or a glossy appearance to some dishes, coating foods, and preventing sugar crystallization. Acacia gum is moreover applied in producing syrups and the linking of sweeteners with other flavors.

2.1.6.1. In the Food Manufacturing

Flavor

Gum Arabic is commonly utilized to spray-dry a gum-flavor-produced mixture into a fixed or encapsulated flavor in dry powder form that can be packed in dry mixes of desserts, puddings, beverages, cakes, and soups (Al Assaf et al., 2005).

Soft drinks

Gum Arabic's versatility as an emulsifier has led to broad use in meals; as a citrus oil emulsion stabilizer, it maintains a unique position in the soft drink industry (Al Assaf et al., 2005).

Confectionery

GA can be found in gum, lozenges, chocolates, and sweets, to name a few. GA has two important functions in these products: Sugar crystallization is slowed or prevented, and fat is emulsified to maintain it equally distributed throughout the product (Sanchez et al., 2002).

Food Additive

It would be valuable if a somewhat costly hydrocolloid extract, texturizer, and film-former, which are routinely utilized in beverage production to steady aromas and crucial fats (Sanchez et al., 2002).

Cosmetics

Lotions, protective creams, and emulsions are all stabilized by gum Arabic. By increasing viscosity, it serves to impart a spreading action, offers a smooth sensation to the skin, and provides a protective layer.

2.1.6.2. Printing and Paint Industry

Both watercolor and gouache paints use GA as a binder. To make a paint that is more opaque and gives the surface a dusty appearance, pigments are ground up and a liquid GA solution is added (Sanchez et al., 2002). Its powder is a basic paper adhesive that can be used immediately after dissolving two or three times its weight in water. In the suspension of carbon black inks and printing pastes, GA additionally acts as a colloid protection agent. It has found special applications in lithography due to its easy wet and spread ability, viscosity control, lithography chemical stabilization, and ready removal ability (Al Assaf et al., 2005).

2.1.6.3. Pharmaceuticals

Gum Arabic is only used in limited amounts in pharmaceuticals. These applications are based on their emulsifying, suspending, demulcent, or coating properties. Insoluble compounds are kept suspended when GA is employed in reasonably high doses. It's used both internally and topically to manage irritation of the GIT mucosa, as well as skin, tender nipples, and nodular leprosy. Treatment of urinary tract infection, GIT upsets, bleeding, some eye problems, gonorrhea, sore throat, and typhoid are some of the other uses (Verbeken et al., 2003). It is act as a carrier in capsules and as a tableting excipient; cough syrups are one of its oldest and most well-known applications. It can be found in face masks, hair treatments, fixatives, protective creams, and lotions, among other things (Ahmed, 2018).

2.1.7. Biological Properties of Gum Arabic

While GA has long been studied as a hydrocolloid with a diversity of dietary applications, it has only lately been investigated for its potential to improve human

health. Human subjects' physiological states can be positively influenced by GA (Khalid et al., 2014).

Gum Arabic as Prebiotic

Prebiotics are defined as non-digestible substances that support the growth of some bacterial species in the intestine (Slavin, 2013). Because it can cross the small intestine deprived of being digested and enter the large intestine, GA could be regarded as nutritional fiber or a non-digestible carbohydrate. It is also classified as a prebiotic and it benefits the host's health and fitness by promoting the progress and/or motion of one or a small amount of gut normal flora while inhibiting the accretion of undesired bacteria (Calame et al., 2008).

The Outcome of Gum Arabic on Kidney Function

GA has long been utilized in Arab traditional medicine, to lessen the rate and need of hemodialysis in patients suffering from long-lasting kidney disease (Younes et al., 2006). Supplementing with GA rises fecal nitrogen elimination while lowering blood urea levels, and it has also been demonstrated to increase urea elimination in the cecum and so minimize urine nitrogen excretion (Ali et al., 2008). It almost acts by creating bulk in the intestines, causing urea, uric acids, and cholesterol to be transported to the intestinal loop and feces. GA fermentation provides energy for growth and nitrogen incorporation for colonic bacteria, as well as a variety of breakdown yields such as serum butyrate. Butyrate inhibits the signaling cascade involving extracellular mitogen-activated protein kinase, absorbs nitrogen and can decompose urea to ammonia, decreasing serum urea levels in rats and humans, and has favorable impacts on kidney pro-fibrotic cytokine production in vitro (Bliss et al., 2001). GA can fix cations, particularly divalent cations such as calcium and magnesium. As a result of this influence, the quantity of calcium and magnesium in the caecum increases dramatically, resulting in an increased supply of these cations in the large intestine as well as increased Mg^{2+} and Ca^{2+} excretion via the intestinal and renal systems. This was associated with lower urinary inorganic phosphate excretion and lower blood emphasis of 1, 25-dihydroxy vitamin D. Furthermore, it improves dietary sodium and potassium absorption, increases fecal weight and potassium excretion, and reduces daily urine Na (+) excretion. GA also lowers daily

urine production while improving 24-hour creatinine clearance and urinary antidiuretic hormone excretion (Matsumoto et al., 2006; Ali et al., 2008).

Impact of Gum Arabic on Blood Glucose Concentration

Several studies have found that gum Arabic lowers blood glucose levels and triggers insulin release from pancreatic B cells, as well as lowers postprandial blood glucose levels (Turvill et al., 2000). GA's blood-glucose-lowering ability may be due to its interaction with sodium-glucose transporter 1 (SGLT1) membrane abundance, which restricts glucose absorption in the intestine (Nasir et al., 2016), or by prolonging intestinal transit time, delaying stomach emptying, and delaying glucose absorption (Macrae et al., 1993).

Effects of Gum Arabic on Lipid Metabolism

Gum Arabic can influence stool bile acid evacuation and reduce blood cholesterol levels while also boosting critical cholesterol metabolism enzymes (Pasquier et al., 1996). The limy of fermentable nutritional fibers, according to some studies, contributes significantly to the fat-reducing impacts in equally animals and humans; raised stool bile acid and neutral sterol emission, as well as changes in lipid digestion and absorption, are the mechanisms most likely to be involved. Dietary fibers are thought to drag or isolate bile acids, reducing active reuptake in the small intestine and resulting in feces elimination, which promotes cholesterol diversion to bile acid synthesis while also increasing the number of hepatic lipoprotein receptors and lowering cholesterol levels (Codipilly et al., 2006).

Gum Arabic may bind a lot of cations, especially calcium (Ca^{2+}). Sequestered bile acids are rendered insoluble by the acidic nature released during the fermentation procedure; calcium that has been bound is too liberated and makes unsolvable compounds with bile acids, which aids in their evacuation (Stephen and Phillips, 2016).

Effect of Gum Arabic on the Gastrointestinal Tract

In the small intestine, GA enhances salt and water absorption. It was also connected to an increase in water and sodium absorption by expanding the gaps between the absorptive epithelial cells and the underline layer. It also improves the absorption of solutes given via transcellular or trans junctional channels (Ibrahim et al., 2004). When animals were given GA dissolved in isotonic fluids, it improved

zinc and Ca^{2+} absorption (Ibrahim et al., 2004). Mechanisms of GA action influences nitric oxide (NO) production by acting as both a forager of NO and a competing inhibitor of NO synthase (NOS) (Rehman et al., 2004; Codipilly et al., 2006). This is confirmed GA's possible efficacy in cases of diarrhea or malabsorption produced by communicable or serviceable causes (Codipilly et al., 2006). In research done in South Korea, compound yogurt enhanced with gum and *Bifidobacterium lactis* was found to have more substantial therapeutic effects than ordinary yogurt in patients with IBS, and it relieved constipation in the test set (Min et al., 2012).

Gum Arabic as an Antioxidant

Gum Arabic contains numerous antioxidants, and it has been discovered that it protects against experimental toxicity in the liver, kidney, and heart by regulating toxic elements in the upper intestine such as nitric oxide (NO), either by eliminating NO formed in enterocytes and dispersing to the gut cavity, or suppressing inducible NO synthase (Rehman et al., 2004). Both *in vivo* and *in vitro*, its antioxidant effects were demonstrated (Abd- Allah et al., 2002).

Dental Effect of Gum Arabic

Dental caries develop when the demineralization and remineralization phases are out of balance, and prevention can be accomplished by augmenting the remineralization phase; various chemicals, including fluoride, have been used for this tenacity (Cheng et al., 2007). Affording to a current study employing histological methods, GA can help with remineralization (Onishi et al., 2008), most likely through assisting other remineralization efforts. Its large number of Ca^{2+}, Mg^{2+}, and K^{+} polysaccharide salts, as well as the gum's effect on Ca^{2+} and possibly phosphate metabolism, were credited with this supportive function. It is also known to include cyanogenetic glycosides and antibacterial enzymes (such as oxidases, peroxidases, and pectinases) that fight bacteria including *Prophyromonas gingivalis* and *Prevotella intermedia* (Aoba, 2004).

The Effect of Gum Arabic on Liver

In vitro, GA has been found to inhibit macrophage activation, which creates superoxide anions. This demonstrates that GA can almost totally inhibit macrophages free radical production, and this merits consideration of GA in the treatment of chronic liver disease, especially because in this situation, an unbalanced gathering of

Kupffer cells happens, which is linked to complications like endotoxemia (Pasquier et al., 1996).

Hematological Effect of Gum Arabic

GA's capacity to boost fetal hemoglobin levels in Sudanese sickle cell patients is one of its recently found unique effects. GA has been proven to enhance MCV volume while decreasing MCH levels (Kaddam et al., 2015). It also has a minor anticoagulant impact, according to studies. It significantly enhanced prothrombin time within the functional rate in a two-arm controlled experiment (Abdalla et al., 2014).

The Effect of Gum Arabic on Cancer

One of GA's most impressive and promising properties is its capability to lower angiogenin transcript level expression and increase colon cancer endurance. The ability of GA to elevate serum butyrate appears to be the key mediator of its activity (Nasir et al., 2010). On the other hand, gold nanoparticles are microscopic gold particles could be the future of cancer detection and therapy. Due to their high surface reactivity, gold nanoparticles are suited for *in vivo* molecular imaging and therapeutic applications, such as cancer diagnosis and therapy (Liu et al., 2007).

The challenge of producing gold nanoparticles in a stable, harmless state that can be injected into a patient has limited their potential. According to new research from the University of Missouri-Columbia, GA can be used to alleviate this problem, resulting in a stable and harmless gold nanoparticle that can be ingested orally or injected (Katti et al., 2009).

Dietary fiber is thought to minimize the risk of lower GIT cancer. The adsorption of carcinogens to insoluble dietary fiber in the digestive tract is one of the methods through which dietary fiber is thought to protect against colorectal cancer. 1, 8-dinitropyrene, a hydrophobic carcinogen, binds to insoluble plant cell wall components and causes cancer (Calame et al., 2008). The number of aberrant crypts was lower in mice with colorectal carcinogenesis treated with GA than in the control group. Similarly, genotoxicity and oxidative stress in the colon, hepatic, and systemic organs decreased. These findings support GA's antioxidant effect and could lead to the development of medicines to prevent colorectal cancer (Avelino et al., 2021).

Side Effects

Only the first week was used to assess GA-related adverse effects. A few people noticed an unpleasant viscous taste in their oral cavity, allergy, morning sickness, minor diarrhea, and stomach distending (Babiker et al., 2012).

2.2. Diclofenac Sodium

2.2.1. Introduction

Non-steroidal anti-inflammatory medications were first documented in ancient Roman and Greek literature as extracts of salicylate-containing plants (Rao et al., 2010). Willow tree extracts' antipyretic, analgesic; and anti-inflammatory effects were particularly well-known (Steinmeyer, 2000).

Salicylic acid was widely utilized for a variety of diseases in the late nineteenth century (Rao and Knaus, 2008). In 1897, Felix Hoffiman and Arthur Eichengrun prepared the salicylic acid molecule, to be more pleasant in taste, which was patented in 1899 as aspirin (Sneader, 2000). Phenylbutazone, a pyrazolidine derivative, was discovered in the early 1950s and became the first non-salicylate NSAID (Domenjoz, 1960; Brune and Hinz, 2004).

Following John Vane's detection of the NSAID mechanism of action in 1971, a flood of novel NSAIDs was developed, including fenamic acid derivatives (e.g., mefenamic acid) and propionic acid derivatives (e.g., ibuprofen) (Schlansky and Hwang, 2009; Sinha et al., 2013).

2.2.2. Diclofenac Sodium

Voltaren, Pennsaid, Solaraze, Zipsor, Cataflam, and Zorvolex are all brand names for DS, which is a prescription pain reliever. After Alfred Sallmann and Rudolf Pfister developed diclofenac sodium (DS), Novartis began marketing it in 1973 (Altman et al., 2015). In aqueous and hydrophobic circumstances, DS is a weak phenylacetic acid with partial solubility (Sallmann, 1986). The suppression of COX enzymes is liable for their anti-inflammatory properties; COX-2 is inhibited more potently than COX-1 (Warner et al., 1999; Altman et al., 2015).

2.2.2.1. Description

Diclofenac sodium is present in form of a crystal-like powder that is only slightly solvable in water at room temperature. Monosodium salt, 2-[(2, 6-

dichlorophenyl) amino] benzene acetic acid, is the chemical name. The structural formula is C14H10Cl2NNaO2 with some inactive constituents in Voltaren.

2.2.2.2. Forms

Diclofenac is available in the pharmaceutical market in the compound formulae of acid, potassium salt, or sodium salt in a wide range of dosage formulations and delivery modes (Joshi and Rapoport, 2017). Among these are modified-release oral dosage forms (tablets, capsules), suppositories dosage forms, injections, topical or sprayed medicines, and eye drops (Amin et al., 2013). The sodium version of diclofenac is most typically seen in medicinal forms.

2.2.2.3. Indications

It is administered as a first-line pain killer in all the disorders that affect the bones like osteoarthritis, joints like rheumatoid arthritis, abdominal and ureteric colic, and all conditions in which diclofenac sodium is utilized to dismiss pain, discharge swelling, and release inflammation (Maksymowych, 2007; Poddubnyy et al., 2009). They are also used after dental and minor surgery to relieve pain and inflammation (Ebell, 2004). NSAIDs have been shown to lessen the risk of cancers in the stomach, lungs, brain, breast, and biliary tract (Kashfi and Rigas, 2005). NSAIDs are also used to prevent Alzheimer's disease, according to epidemiological research that has not yet been confirmed in clinical trials (Szekely and Zandi, 2010).

2.2.2.4. Dose

Following the initial response of the patient to DS therapy, the amount and rate should be a disciple to fit the patient's unique wants. For osteoarthritis reprieve, a daily dose of 100-150 mg divided into two doses is indicated (50 mg twice or triple a day, or 75 mg two times a day). For rheumatoid arthritis treatment, up to 200 mg/day in divided dosages is advised (50 mg triple times a day or 75 mg twice per day, or four times per day.). The recommended dosage for ankylosing spondylitis alleviation is up to 125 mg per day, divided into four doses of 25 mg each, with a 25-mg dose at night if needed.

2.2.2.5. Mechanism of Action

The NSAIDs' main activity is to inhibit the COX enzyme. (Vane and Botting, 1998). Two enzymes known to act in the pain pathway are COX-1, which constantly

exists in the body, and COX-2, which is only expressed during the context of inflammation. COX enzymes alter arachidonic acid to prostaglandin H2, which is then converted to bioactive lipids like thromboxane A2, prostaglandins D2, E2, F2, and prostacyclin through a variety of routes. NSAIDs can be categorized by their affinity for inhibiting the COX-1 and, or COX-2 into selective and non-selective (Antman et al., 2007).

Diclofenac sodium belongs to the non-selective NSAIDs. Most NSAIDs are active upon administering the drug, meaning that they do not need to be metabolized by the body to serve their function. The clearance of NSAIDs is performed by the liver through the action of the enzyme CYP2C9, a cytochrome P450 enzyme. This enzyme puts the NSAID through several cycles of glucuronidation. The inactive form of the NSAID is eliminated by the kidney when this procedure is completed (Ulrich et al., 2006).

2.2.2.6. Side Effects

NSAIDs have a unique method of achievement that renders them extremely beneficial medicinally while also causing adverse things, especially common following oral administration. NSAIDs are thought to be responsible for about 21–25 percent of all known adverse drug reactions (ADR). Functional abnormalities of the GIT, kidneys, cardiovascular, and central nervous systems are NSAID medication's most common side effects, especially when taken long-term. In terms of side effects, contraindications, and use limitations, NSAIDs have been demonstrated to differ greatly (Kowalski et al., 2011).

2.2.2.6.1. Side Effects on Cardiovascular System

Some COX-2 selective and nonselective NSAIDs have been linked to an elevated hazard of dangerous cardiovascular (CV) thrombotic conditions, like angina pectoris and cerebrovascular attack, in up to three-year clinical investigations (Bresalier et al., 2005; Solomon et al., 2005). Based on the existing evidence, it's uncertain whether all NSAIDs carry the same threat of CV thrombotic problems. The comparative surge in major CV thrombotic conditions provided by NSAID consumption seems to be equal in those with and deprived of recognized CV illness or CV threat reasons. Due to their higher baseline rate, excess significant CV thrombotic events were more common in those with existing CV disease or risk

factors (Schmidt et al., 2018). The augmented hazard of significant CV thrombotic conditions commenced within the initial several weeks of management, according to several observational studies. The surge in CV thrombotic hazard has been repeatedly found at large amounts (Bombardier et al., 2000).

The imbalance induced by decreasing COX-2-mediated prostacyclin synthesis without lowering COX-1-mediated thromboxane generation may rise the jeopardy of thrombotic problems with COX-2 selective medicines (Rostom et al., 2009 b; Trelle et al., 2011). There is no clue if taking aspirin and an NSAID simultaneously reduces the hazard of serious CV thrombotic events, but if it does, combining aspirin and an NSAID like diclofenac upsurges the hazard of a serious GI problem.

According to studies done in the Danish National Registry, patients administered with NSAIDs in the post-MI time had an augmented hazard to develop reattack, death due to CV problem, and mortality starting in the first few days of therapy. In the first year following MI, NSAID-treated patients died at a rate of 20 per 100 person-years, compared to 12 per 100 patient-years in non-NSAID-treated individuals in the same cohort. Despite the fact that the total degree of death dropped next to the first year post-MI, the higher comparative hazard of mortality among NSAID takers persevered for at minimum the following four years of pursuing (Schmidt et al., 2018). Furthermore, NSAIDs have been shown to raise blood pressure and cause congestive heart failure in vulnerable people, mainly when COX-2 inhibitors are used (Antman et al., 2007).

2.2.2.6.2. Side Effects on the Renal System

Nephrotoxicity is another side effect of NSAIDs that is well recognized. Although rare, such events occur in a small proportion of people, ranging from less than 1 to 5% of NSAIDs users (Whelton, 1999). The pathophysiological process inhibits prostaglandin production through the COX enzymes blockade conferred by NSAIDs (Musu et al., 2011). Prostaglandins regulate blood flow within the kidney by modulating vascular tone, sodium balance, and renin release (Musu et al., 2011). COX-1 is conveyed immanently in the kidney, as it is in many other tissues, and COX-2 has been discovered to be expressed to a lesser amount in some regions of the kidney (Crofford, 1997). A variety of prostaglandin receptors exist in the kidney and impact the hemodynamics and overall function of the kidney. The inhibition of prostaglandin production resulting from NSAIDs use causes a reduction in blood

flow and subsequent injury. Although NSAIDs-induced nephropathy is rare, an elevation in blood pressure of roughly 5 mmHg is expected in chronic NSAIDs users (Johnson, 1997). Patients with predisposing factors such as old age, diabetes, diuretic use, congestive heart failure, cirrhosis, and nephrosis are more likely to suffer renal injury (Musu et al., 2011). However, patients without predisposing factors are also at risk for renal complications (Huerta et al., 2005). The nephrotoxic effect of NSAIDs is dose-dependent, with lower doses having a lower like the hood of causing renal injury (Stillman and Schlesinger, 1990; Griffin, 2000).

Although the nephrotoxic effects are usually reversible and the chance of getting them disappears when therapy is stopped, there is still a danger with both short and long-term NSAIDs use.

2.2.2.6.3. Side Effects on Respiratory System

NSAID-induced asthma, more commonly known as Aspirin-Induced Asthma (AIA) (Palaian et al., 2010), is a phenomenon that was well documented by Samter and Beers in the 1960s (Samter and Beers, 1968). AIA is observed in a constellation of clinical findings recognized as Samter's triad and consists of aspirin hypersensitivity, nasal polyps, and asthma. The mechanism for AIA is related to COX-1 inhibition results from the local accumulation of arachidonic acid. As mentioned above, arachidonic acid is altered to prostaglandins by COX-1. In the setting of NSAID-induced inhibition of this enzyme, arachidonic acid enters an alternate pathway leading to the production of a leukotriene LTA4. LTA4 is metabolized into the byproduct cysteine leukotriene, which causes bronchoconstriction (Neighbour, 2014). Finally, a patient with AIA or a clinical presentation suggestive with Samter's triad is treated primarily by avoiding the use of NSAIDs (Gazarian and Graudins, 2006).

2.2.2.6.4. Side Effects on Gastrointestinal Tract

NSAIDs have several documented side effects, including gastropathy (NSAID-induced gastropathy) and enteropathy (NSAID-induced enteropathy), ranging from gastroesophageal reflux to gastrointestinal bleeding. These adverse effects are caused by the suppression of the COX-1 enzyme and the exhaustion of prostaglandin in the stomach mucosa (Abraham et al., 2010). Prostaglandin (PGE2) and prostacyclin (PGI2) enhance the creation and discharge of mucus and bicarbonate, encouraging

epithelial propagation and aggregate mucosal blood run, and are thought to be gastroprotective. Gastric protective mechanisms are classified as primary (mucous, bicarbonate, and immunoglobulin released into the lumen), secondary (epithelium), and tertiary (microcirculation) (Wallace and Chin, 1997). Microcirculation, in particular, acts to neutralize acid, preventing it from building up to hazardous levels. In the absence of these protective features, NSAIDs use can lead to petechiae, erosion, and, less commonly, ulcerations, bleeding, perforation, and obstruction of the stomach outlet. The purpose of preventative therapy is to keep ulcers and bleeding from developing as a result of mucosal injury (Moore et al., 2009), and dyspepsia, as it is often a limiting factor in its therapeutic use (Cullen et al., 1998). Continuous aspirin use for cardio protection, ulcer history, age >60, corticosteroid use, antiplatelet or anticoagulant drug use, and significant cardiovascular impairment are all risk factors for gastrointestinal issues. Before putting patients on long-term NSAID medication, modifiable risk factors such as aspirin, corticosteroid, and anticoagulant use should be addressed. In addition, the treatment of H. Pylori can also help to prevent ulcers from forming. Patients on non-selective NSAIDs with gastrointestinal risk factors should be monitored closely. When compared to placebo, gastroprotective pharmacological interventions have been found to reduce unfavorable gastrointestinal outcomes (Hooper et al., 2004). There are three main medications that can be used for gastroprotection: synthetic prostaglandin, H2-receptor blockers, and proton pump inhibitors (PPI). Misoprostol has long been the most often used synthetic prostaglandin in clinical practice, and it is beneficial in gastroprotection for continuing NSAIDs consumption (Silverstein et al., 1995; De Groot et al., 2013). However, because of its side effects, which include nausea, vomiting, diarrhea, and pyrexia (Watanabe et al., 2008), anaphylaxis, and the inability to take it during pregnancy due to the risk of abortion (Weeks, 2015), its use for ulcer prevention has been limited. H2-receptor blockers work by inhibiting the histamine receptor in the gastric parietal cells, preventing acid from being released into the stomach. They are not beneficial in reducing the incidence of stomach ulcers, although they successfully reduce the total incidence of gastrointestinal ulcers (Rostom et al., 2002). PPIs, or proton pump inhibitors, reduce acid-related mucosal injury and disease by inhibiting the H/K ATPase, blocking gastric acid output. PPIs have been found in multiple meta-analyses to minimize symptomatology, and endoscopic evidence of peptic ulcer disease (Rostom et al., 2002; Hooper et al.,

2004) and are now commonly used for gastroprotection in the setting of NSAID use (Patrignani et al., 2011).

2.2.2.6.5. Side Effects on Nervous System

The inducible isoform of COX has been discovered to be expressed in the cerebral hemisphere, hippocampus formation, and amygdaloidal body (Andreasson et al., 2001). In the dentate gyrus neurons, side effects of DS acquaintance have been observed, including significant cell loss. The hippocampus's granular and pyramidal cells have both shown adverse effects from DS exposure (Gokcimen et al., 2007). Additional investigation on the impact of prenatal DS contact on peripheral nerves found that DS-treated rats had considerably less axons and a slighter mean axonal cross-sectional area (Keskin et al., 2015). DS moreover has certain outcomes that are distinct from those of other NSAIDs. It inhibits proliferation and decreases the development of neural stem cells into neurons by inducing apoptosis. Because of its widespread and long-term usage, it is critical to investigate the potential impacts of DS. In addition to decreasing harmful effects, the main focus of research is on toxic effects (Simon, 1997).

2.3. The Gastrointestinal Tract of Albino Rat

The rat was the first vertebrate kind tamed for methodical examination, with investigations reaching back to roughly 1850. From that time, the rat has played an essential part in physiology, pharmacology, genetics, and medical science investigation. Albino rats have played an innovative part in animal research since their foundation among rat strains (Kuramoto et al., 2012). The operator needs to understand normal tissue's basic anatomy and histology while analyzing alterations in the gastrointestinal system (or other organs), which is covered in standard textbooks (Oliveira et al., 2016).

2.3.1. Stomach

The stomach of the rat is the supreme enlarged part of the gastrointestinal tract, and it's in charge of storing and digesting food into a meal before passing it on to the duodenum in measured proportions (Treuting et al., 2012). It is found in the abdomen's left hypochondriac area (Adjene and Kendabie, 2007). The glandular and non-glandular components of the rat stomach are separated. The stomach's non-glandular section took up a greater part of the entire surface capacity. It was easily

parted from the glandular stomach by the limiting edge. Also, the glandular stomach was split into fundic and antral portions (Treuting et al., 2012; Nolte et al., 2016).

2.3.2. Small Intestine

This portion is the longest part of the gastrointestinal tract and is in charge of nutrition absorption. The pyloric sphincter is the start of the small intestine, which continues distally to the ileocecal valve (Treuting et al., 2012). The duodenum, jejunum, and ileum are three physiologically but not anatomically separate divisions in the rat. The first segment of the small intestine is the duodenum and it begins immediately after the pylorus and forms a C-shaped ring around the pancreas at the close of the umbilicus. It is also related to the pancreas (Liebelt, 1998). The bile duct transports the liver secretions to the duodenum, whereas the pancreatic duct transports digestive fluids from the pancreas (Treuting et al., 2012). After that, the duodenum gives way to the jejunum, which makes up the bulk of the small bowel. The ileum, which forms the small bowel's terminal end and connects to the cecum, follows the jejunum. The mesentery connects the intestine to the posterior abdominal wall for supporting, and the superior mesenteric artery provides the majority of the intestine's blood supply (Treuting et al., 2012).

2.3.3. Large Intestine

Principal job of the large intestine is to dehydrate and store fecal matter. The proximal colon undergoes extensive reabsorption of water and salt, which continues throughout the body. The colonic mucosa is lubricated and protected from harm by numerous mucus-secreting goblet cells that help move the increasingly solid colonic contents from proximal to distal. Bacterial flora is abundant within the colon that performs a rumen-like function (Treuting et al., 2011).

From the ileocecal junction, the large intestine spreads distally. The cecum, colon, and rectum are the three regions of the large bowel. The cecum is a blind-ended pouch that marks the starting of the big bowel and is packed with bacteria that ferment the digest. It took up a significant percentage of the rat's abdominal cavity, fluctuating in size and location depending on nutrition. The appendix is lacking in the rat. The colon is divided into two sections: the proximal colon, which is broader and has prominent mucosal folds, and the distal colon. The colon comes to an end in

the rectum and the anus in the cecum's ampulla. Taenia coli and haustra are not found in the mouse colon (Snipes, 1981).

2.3.4. Histology of the Stomach

The rat stomach is a buildup of four layers arranged from the inside out in the following manner: mucosa, submucosa, muscularis externa, as well as a serosa. Keratinized squamous epithelium lines the mucosa of the non-glandular section of the stomach. The degree of keratinization reduces along with the alteration among the glandular as well as non-glandular of the stomach portions (Ghoshal and Bal, 1989). The submucosa, on the other hand, has both a network of collagen, elastic, and reticular fibers as well as thick meshes of fenestrated capillaries underlying the epithelium's basement membrane (Dellmann and Eurell, 1998). Three layers make up the thickness of the muscularis externa, which appears to increase from non-glandular to glandular portions: inner layer composed of oblique smooth muscle, middle circular in orientation, and outer longitudinal (Ghoshal and Bal, 1989). The serosa is a loose connective tissue that is protected by the mesothelium. In the loose connective tissue, there are variable quantities of adipose tissue, arteries, lymph vessels, and nerves (Dellmann and Eurell, 1998).

According to Ojo et al. (2010), gastric folds or rugae were developed in the glandular region of the mucosa and faded after the stomach was completely dilated. The glands were found in the underline connective tissue, the membrane that separates the stomach pits. They also identified three histological sections established on the nature of the glands: cardiac, fundic, and pyloric. There were three layers to the muscularis mucosae: an inner rounded layer, an outside longitudinal layer, and a third, generally circular layer in some locations. Smooth muscle strands protruded into the lamina propria from the inner layer (Ojo et al., 2010).

The region of the cardiac gland that is present in the rat's stomach is a small crew that houses the glands near the esophageal aperture. These glands are simple tubular branched glands that are virtually entirely made up of mucous secreting cells (Ojo et al., 2010; Treuting et al., 2012).

The rat's stomach was mainly made up of the fundic or gastric region. The gastric glands in this location run upright to the surface epithelium and reach the muscularis mucosae. Each gastric pit had three to seven glands at its base. The base,

neck, and isthmus make up each gland. The glands are made up of parietal or oxyntic cells, mucous neck cells, zymogenic or chief cells, neuroendocrine or enteroendocrine cells, undifferentiated or stem cells (Ojo et al., 2010; Treuting et al., 2012).

The pyloric gland is similar to the cardiac gland in appearance. This portion of the stomach has deeper pits than the rest of the stomach. Pyloric glands are tubes that are short, simple, or branching. Mucous-secreting cells are the most common type of cell (Chandana et al., 2013). The submucosa is a dense connective tissue that maintains the mucosa and contains major blood arteries, lymph vessels, and the Meissner nerve plexus, besides smooth muscle (Ojo et al., 2010).

A robust inner spirally structured muscle layer and a modest outer circular layer make up the rat glandular region of the stomach's muscularis externa. Little ganglion cells are placed between these layers. The serosa in this region is extremely thin (Ghoshal and Bal, 1989).

2.3.5. Histology of the Intestine

The intestine is a muscular canal with a similar fundamental structure from top to bottom. The tube's lumen contains substances, while the wall's histology is made up of four layers from inside to out: mucosal surface, minimum connective tissue such as submucosa, muscularis externa, and serosa. GALT is a lymphoid tissue type that can be found throughout the intestine. Several smooth, elevated white-yellow structures are frequently detected macroscopically inside the small bowel wall, indicating planned lymphoid nodules known as payer's patches (Williams et al., 2016).

2.3.5.1. Histology of the Small Intestine

The rat lacks plicae circularis; therefore, villi and microvilli dictate the real surface area accessible for digestion and food absorption. The villi, which are highest in the duodenum and gradually get shorter towards the ileum, are the distinguishing feature of the small bowel. The Lieberkuhn crypts found at the base of villi contain the intestinal stem cell. The bulk of epithelial cells in the small bowel are absorptive enterocytes, which account for 80% of all epithelial cells (Watson and Pritchard, 2000). The remaining cells consist of Goblet cells, in addition to enteroendocrine cells and Paneth cells. Goblet cells, which can be seen in both the crypt and villus

areas are mainly responsible for mucus secretion, have a large Goblet-like clear area. Paneth cells, located close to the bottom of the crypts and characterized by an abundance of bright acidic, antibacterial properties, are thought to exist in granules at the topmost of the cytoplasm. The dome epithelium beneath the Payer's patches contains enteroendocrine (neuroendocrine) cells, microfold (M cells), and tuft cells, among other cell types. Only the first two millimeters of the rat's duodenum contain submucosal Brunner's glands (Williams et al., 2016).

2.3.5.2. Histology of the Large Intestine

The large intestine mucosa contains Lieberkuhn crypt, which is characterized by a high great number of goblet glands and a flat surface epithelium. The undifferentiated cell section in the large intestine (crypt base columnar cell) is identical to that present in the small bowel (Barker et al., 2007). The cecum is the initial portion of the large bowel, a closed-ended pouch with a lot of lymphoid tissue at the tip. Undulating mucosal folds can be found in together the cecum and the proximal large bowel. Also, these parts have more goblet cells, and their number decreases as the intestine moves further down. The mucosa of the mid colon is flat and unfurled, while the mucosa of the distal colon is moderately crumpled. Absorptive as well as enteroendocrine cells are two other cell types found in the colon. The large intestine of the rat does not include Paneth cells. The rat's rectum is exceedingly short, with a sudden change from the simple columnar epithelium to the squamous epithelium (Williams et al., 2016).

2.4. Development of the Gastrointestinal Tract

The digestive organs include the GIT, which is made up of an endoderm-derived epithelial lining and splanchnic mesoderm-derived surrounding mesenchyme. The digestive tract begins to develop as a simple undifferentiated tube and then, after the gastrulation, becomes divided into foregut, mid-gut, and hindgut (De Santa et al., 2003).

2.4.1. Development of the Stomach

The stomach develops from the embryonic foregut, which also differentiates to many other tissues. The embryonic stomach is produced from the posterior foregut and develops with a number of surrounding tissues, including the esophagus, intestine, liver, gallbladder, and pancreas. The promotion of stomach fate, as with all

endoderm organs, is based on a complex network of epithelial-mesenchymal interactions. Once identified, gastric progenitors are segregated further along the rostro-caudal axis. The proximal region is formed by the forestomach epithelium, whereas the distal section develops into the antral stomach (McCracken and Wells, 2017).

2.4.2. Development of the Midgut

The midgut developmental stage of a 13-day-old rat is easily seen as a loop. The loop can be broken down into three sections: A proximal dorsal or center section, a ventral section that enlarges distally in the umbilical coil, and a straight section between them. These three portions show no signs of synchronization as they progress. The midgut swells fast inside the luminal cavity of the umbilicus during the 15th and 17th days of the pregnancy, resulting in the creation of a plethora of coils of loops. The central component demonstrates more significant growth activity throughout (13 to 16 days), resulting in the establishment of the duodeno-jejunal coil. However, the ventral part's growth activities are unbalanced and not evenly distributed. The ileum's fast development is to blame for this imbalance. Although the duodenal and infra-umbilical sections of the midgut are very active during development, substantial alterations in the straight part do not occur until the 17th day (Kluth et al., 1995). The umbilical midgut's "return" begins on day 17. The ultimate coil that reaches the cavity of the abdomen, rather than the cecum, is the end of the ileum. Only the cecum is present inside the umbilical coelom, with the rest of the colorectal remaining inside the abdominal cavity. In day 18 of the pregnancy, the cecum enters the abdominal cavity and takes up a ventral position near the liver and abdominal wall. The normal location of the gut in newborns appears to be determined by two separate embryological processes. The most crucial appears to be the proper formation of the duodenal coil. The duodenum expands and lengthens locally in the early stages of development, forming a loop. Further growth pulls the duodenojejunal loop's tip behind the root of the mesenteric; it then reverts to its original left-to-right orientation. Another critical developmental stage is the intestines' return from the umbilicus to the abdominal cavity (Kluth et al., 2003).

2.4.3. Development of Hind Gut

The division of the hind intestine into a urogenital and anorectal component is explained by two major theories: Cloacal separation and rectum migration are two conditions that can occur. The primitive hind intestine requires a healthy division of the cloaca by a septum, known as the urorectal septum. During normal development, the rectum moves from a higher location to the anatomical position of the anal hole (Gans, 1961).

The hindgut epithelium is in close touch with the embryonic ectoderm in the zone of the cloacal membrane. The hindgut enters the cloaca from the dorsocranial side, whereas the urachus is a cranioventral diverticulum. The urorectal fold is found between the urachus and the hindgut. The cloacal sheath has arrived at its last resting place. Only a small portion of the cloaca is left for the anorectal component, as the urethral cloaca now occupies the majority of it. The urorectal fold begins to approach the cloaca membrane between 14.5 and 17.5 days. The urethra is significantly larger than the cloaca's anorectal portion. The urorectal fold comes close to touching the cloacal membrane. The urethral cloaca's top part now resembles a terminal urethra. The cloacal membrane is unaffected. The cloacal membrane disintegrates where the urorectal fold joins. The urorectal fold's tip epithelium has merged with the perineum's epithelium. The anal opening can be seen plainly (Dietrich et al., 2011).

2.5. Histogenesis

The process by which developing organs acquire their morphological and functional properties is known as morphogenesis. These morphogenic processes occur in organ systems that have already received the molecular instructions that will determine their final identity (Walton et al., 2018).

The three stages of GIT mucosa development (histogenesis) include cell propagation, morphogenesis, in addition, cell distinction, and functional maturation (Colony, 1983).

2.5.1. Histogenesis of Stomach

The stomach epithelium in adult rats is divided into two types: esophageal and gastric. The esophageal section of the adult stomach is made up of esophageal epithelium, whereas the right half is made up of ordinary glandular or gastric epithelium (Kammeraad, 1942).

In the esophageal portion, the establishment of an undifferentiated stratified epithelium and subsequent differentiation of this layer into four zones typical of the adult esophageal epithelium results in the development of the final, esophageal epithelium. The endoderm of this part is primarily made up of simple columnar cells with a well-defined basement membrane that separates it from the underlying mesoderm throughout the cell proliferation stage, which begins on the 14th day of intrauterine life. The creation of a typical stratified type of embryonic epithelium is the outcome of cell proliferation (Kammeraad, 1942).

The appearance of flattened superficial cells indicates the start of the histo-differentiation period: 19-day embryo histo-differentiation period. In the 20-day embryo, there is more histo-differentiation. The epithelium is divided into four zones: the first is the stratum germinativum, which is a basal or proliferative zone. The stratum granulosum is the second zone, where the most superficial cells are squamous. The third zone, also known as the stratum lucidum, is made up of one to two layers of cells. The fourth zone, also known as the stratum corneum, comprises severely flattened, degenerating cornified cells (Kammeraad, 1942).

The definitive glandular epithelium develops in three stages: cell proliferation, histo-differentiation, and chemo-differentiation. The epithelium's vacuolization is the first stage in differentiating. The primitive gastric pits are formed when the vacuoles break into the lumen. Gastric pits are formed by up growths of mesoderm toward the lumen between villi-form structures. The gastric glands emerge from the bottoms of gastric pits as invagination and expand into the adjacent mesoderm. Chief and parietal cells in the stomach glands can be distinguished one day after birth. Although the main and parietal cells have differentiated, the granules do not develop in any substantial quantity until around 15 days of life (Kammeraad, 1942).

2.5.2. Histogenesis of the Intestine

The simple epithelium thickens into pseudostratified epithelium with nuclei that arise at various stages once the gut tube is fully developed. As the mesenchyme, epithelium, and lumen expand from embryonic day 9.5 to 13.5, the gut cylinder expands and the diameter becomes wider. The epithelium of the intestinal tube is hypothesized to change into a stratified epithelium as it grows longer and wider (Dunn, 1967). The endoderm of the small intestine is stratified in the 14.5-day

embryo. Cell proliferation, vacuolization, and mesodermal up growth toward the lumen are all a component in villi development in the majority of the small intestine. In the duodenum, the creation of villus starts then proceeds to the terminal ileum as the morphogenic wave washes down the gut; Each villus unit is generated by a succession of cellular and molecular actions that occur in close proximity and are repeated over and again (Burgess, 1975; Walton et al., 2012). Intestinal glands form as a result of epithelial invagination between the villi's bases. In mice, intestine development continues after birth and is completed by the time they are weaned. The inter villus epithelium produces Lieberkuhn crypts, which comprise all primordial and proliferative cells in the adult intestinal epithelium. The place of nascent crypts attracts originator stem cells, which subsequently develop by the crypt-villus junction migrating upward (propelled by the movement of mesenchymal cells) rather than the inter villus epithelium moving downward, according to the current paradigm (Calvert and Pothier, 1990).

3. MATERIAL AND METHODS

3.1. Materials

3.1.1. The Study Drug

Tablets (Voltaren from Novartis Health, Food and Agricultural Products Industry and Trade Inc. Kurtköy, Pendik, Istanbul), dose: 3.6 mg/kg/day managed by oral gavage daily for 15 days. 90 mg/kg has been found as the lethal dosage (LD) for DS (Hirose et al., 1984). We used 0.04 of the LD 50 doses (3.6 mg/kg).

3.1.2. The Study Plant

Gum Arabic powder was acquired as clean and pure collected exudate from the Gum Arabic Company Limited in Khartoum, Sudan.

3.1.3. The Study Animals

Forty male albino rats with 280±30g weight and 12-14 weeks age were acquired from the Experimental Animal Research Centre and Surgical applications of Ondokuz Mayis University, Samsun, Turkey.

3.2. Methods

3.2.1. Study Design

The research was begun after the consent of the Ethical Committee and Animal Care of the Ondokuz Mayis University, Samsun, Turkey (approval number 2015/45). All experimental methods were carried out according to the institutional rules. The study's experimental components were carried out at Ondokuz Mayis University, Experimental Animal Research Centre and surgical applications. The animals were weighed and kept in stainless steel cages for a 12-hour light-dark cycle in a temperature-controlled environment (22±2 °C) and humidity (50-60 per cent). Food and water were freely available to the animal. For two weeks, the experiment was carried out (Figures 3.1 and 3.2).

Figure 3. 1. Housing conditions of the animals

3.2.2. Formation of Experimental Animal Groups

Four groups were formed at randomly and each group has 10 animals.

1. **Control group (Cont.):** The administration of any drugs to animals in this group was not done.
2. **Diclofenac sodium group (DS):** Animals in this group was given 3.6 mg/kg/day of DS by oral gavage (Voltaren from Novartis Health, Food and Agricultural Products Industry and Trade Inc. Kurtköy, Pendik, Istanbul, Turkey)
3. **Gum Arabic group (GA):** Animals in this group was subjected to 7.5 g/kg/day of GA by oral gavage (Gum Arabic Company, Khartoum, Sudan).
4. **Diclofenac + Gum Arabic group (DS+GA):** Animals in this group was subjected to both 3.6 mg/kg/day of DS by oral gavage (Voltaren, Novartis) and 7.5 g/kg/day of GA by oral gavage (Gum Arabic Company, Khartoum, Sudan).

Figure 3. 2. Wistar albino rats in a cage

3.3. Preparation of Tissue Samples

The histological and stereological studies were conducted out in the Department of Histology and Embryology at the Faculty of Medicine, Ondokuz Mayis University, Samsun, Turkey.

3.3.1. Perfusion

Animals were weighed before perfusion. The average weight of the rats is about 280±30 g. After the experiment, all rats were mercifully executed with an intraperitoneal dose of ketamine hydrochloride 80 mg/kg (Ketalar®, Eczacibasi, Istanbul, Turkey) and 10 mg/kg xylene (Rompun®, Bayer, Istanbul, Turkey). All perfusion solutions and supplies were made one day in advance and reserved at room temperature.

After the anesthesia, rats were put on the operating bench with their backs facing the operating table, and the heart was revealed by opening the chest with a pair of scissors and a scalpel from the lower part of the sternum up to the end of the chest. Then, a plastic cannula was inserted inside the apex of the left ventricle while the heart was still pumping to accomplish tissue perfusion. A tiny cut was made in the right atrium with the scalpel at the same time as the surgery to ensure that the solution was flowing freely. Tetanic contractions in the rat extremities were recorded throughout the perfusion procedure, which is a sign of formalin fixation. During the perfusion process, all of the rats in our study showed irregular contractions (formalin dance).

Dressing forceps were used to pull up mid-abdominal skin, which was then withdrawn towards the head and tail after a transverse tiny incision was made using scissors. A mid-laparotomy through (Linea Alba) was used to acquire entrance to the abdominal hole. The abdominal wall was explored from the lower end of the sternum to the symphysis pubis. From superiorly along the final rib to inferiorly at the inguinal region, the abdominal wall was severed on both sides. To expose the distal colon, rectum, and anal canal, the pubis, and ischium were removed with bone scissors. The gastroesophageal junction was severed, and the whole GIT was detached from its mesenteric connection and externalized.

3.3.2. Routine Histological Tissue Procedures

After the GIT was completely extracted, it was engaged in a plastic bottle having 10% formalin and stored in the fixation solution for two weeks. During the fixing period, the fixative fluid was altered three times a week. The purpose of this perfusion approach was to reduce artefacts during the fixation process. All GIT parts of each rat were processed using standard histology techniques: they were soaked in running water for one night after being removed from the 10% formalin fixative solution. After the tissue had been washed, the following techniques were used to prepare it:

3.4. Tissue Sampling Protocol

3.4.1. Stomach

The length of the resected stomach was measured then cut into two segments, upper and lower rings. One of the portions was randomly selected.

3.4.2. Intestine

Each intestine was freed of the attached mesentery and removed. Then the length was measured. Subsequently, every intestine was sliced transversely with a razor blade into three segments for the small intestine, and two segments for the large intestine of roughly equal length. Each segment was split in turn into smaller parts, from which one was selected randomly. Luminal contents were washed away with the fresh fixative solution before each segment was trimmed to a length of around two cm.

The Thermo Scientific TM Citadel 2000 Tissue Processor (Fisher Scientific UK Ltd Bishop Meadow Road Loughborough LE11 5RG) was used to process the

tissues (Figures 3.3). Tissue processing was carried out according to the protocol described in the tissue processing protocol (Table 3.1). A code number was given to each tissue sample so that stereological analyses would be done blindly (i.e., the investigator had no knowledge of the animals' allocation to groups and the transcription of the codes was kept until the experiments and stereological procedures were completed.

Table 3. 1. Chemical solutions and duration of follow-up of GIT tissues

Chemical Solution	Duration
70% of Alcohol (Ethyl Alcohol)	six hour
80% Alcohol	one night
96% Alcohol	one hour
96% Alcohol	one hour
100% Alcohol	one hours
100% Alcohol	two hours
Xylene (Sigma-Aldrich)	one hour
Xylene	one hour
Paraplast	one hour
Paraplast	one hour

Figure 3. 3. Automated dehydration

3.5. Sectioning Methods

A single tissue block was used in pilot research to determine the GIT tissue sectioning approach before obtaining transvers sections of GIT tissues for this experiment. After randomly selecting the beginning part, to select sampled parts for stereological analysis, systematic random sampling (SRS) method was applied. A stereological analysis technique that is named as the Cavalieri technique was used to find volume ratio of mucosal layers, epithelium, lamina propria, and muscularis mucosae to the mucosa. Sectioning continued until the entire specimen had been cut; approximately 15 systematic randomly selected sections were taken for each specimen. Serial sections from the tissue blocks of the 5 μm-thickness were cut in a coronal plane with section intervals of 1/100.

Disposable metal microtome blades (Type N35, Feather Company, Osaka, Japan) and rotary microtomes (Leica RM2125RT, Nussloch, Germany) were utilized to cut paraffin sections from the tissue blocks (Figure 3.4). Sampled portions of the stomach were collected on slides covered with one percent powdered gelatin (made by dissolving one gram of gelatin in 100 ml of distilled water), while sampled parts of the intestine were collected without the use of gelatin. This was achieved by adding distilled water to a flotation bath that had been heated to 42°C (MH8517 Paraffin Section Flotation Baths). As a result, the sections remain firmly attached to the glass slide during the staining process. Before beginning the staining procedure, the slides with selecting samples were placed in a 59° C oven for one night to remove the paraffin (deparaffinization) from the tissues (Figures 3.5). Hematoxylin and eosin (HE) staining were used to stain these sampled sections.

Figure 3. 4. A rotary microtome (Leica RM2125RT, Nussloch, Germany)

Figure 3. 5. Laboratory drying oven

3.6. Staining Process

HE staining was used to stain the tissue sections. Below is a list of the dyes and solutions used to stain the sections (Table 3.2). The duration of dye penetration into the sections was measured in a pilot study in a single section. After that, the same technique was used in all areas based on the pilot study. The quality of the HE-stained slices was examined using a light microscope (Olympus BX51, Japan).

Table 3. 2. Chemicals and duration used for HE staining of the sections

Chemicals	Duration
Xylene (x4) (Sigma-Aldrich)	45 minutes
100% Alcohol (x2)	5 minutes
96% Alcohol	5 minutes
80% of Alcohol (Ethyl Alcohol)	5 minutes
70% Alcohol	5 minutes
Distilled water	5 minutes
Hematoxylin	8 minutes
Distilled water	One minute
Eosin	6 minutes
70% Alcohol	Rinse once
80% Alcohol	Rinse once
96% Alcohol	Rinse once
100% Alcohol	1 minute
Xylene	15 minutes
Entellan	For mounting

3.7. Tissue Preparation for Electron Microscopy

For EM analysis, one animal from each group was perfused by means of "intra-cardiac perfusion" with 4% glutaraldehyde + 4% paraformaldehyde solutions through the left ventricle. The samples were then submerged into the same fixative for several weeks. After that, Milloning buffer was used to wash the segment samples. After washing with buffer, they were immersed in 1% osmium tetroxide in the dark for 1.5-2 hours. The samples were rewashed for 4x15 minutes with Milloning buffer, and the procedure was completed by dehydration.

For dehydration:

- 50% acetone for 15 minutes,
- 75% acetone for 15 minutes,
- 95% acetone for 15 minutes,
- 100% acetone for 20 minutes,

Subsequently:

- Propylene oxide for 20 minutes,
- Propylene oxide for 20 minutes,
- 50% of propylene oxide + 50% Araldite mixture for 1 hour,
- Araldite 100% for 1 hour was subjected to the infiltration process.

The GI tissues were then blocked at 45°C in a silicone embedding mould. Every 30 minutes, the temperature was raised by 5°C until it reached 62°C. To ensure polymerization, they were incubated at 62°C for 48 hours. At the end of the process, using an ultra-microtome (Leica Ultra cut UCT of the Leica Microsystems GmbH of Germany), semi-thin 0.5-micron thickness sections were taken from the resin blocks for LM examination.

3.8. Stereology

The earliest concepts of stereology were described in the 1930s by William Thompson (Kaplan et al., 2012). The term “stereology” itself was presented in 1961 by Hans Elias at a scientific meeting held in Germany (Miki et al., 2005). Stereological procedures are based on providing quantitative and unbiased estimates from two-dimensional sections to get three-dimensional data. Data that does not deviate systematically from the real value is obtained using the principles of these procedures. Furthermore, achieving the real value with a little mistake a few times would be conceivable (Altunkaynak et al., 2012).

Many investigations have employed unbiased and reliable stereological procedures (Schmitz et al., 2014). The application of stereological methods' rules is based on systematic random sampling (SRS). Analysis of tissue samples taken from the tissue to be held at equal intervals to offer each site sampling an equal opportunity (Brown, 2017).

3.8.1. Stereological Analysis:

The Cavalieri's principle, which is an impartial stereological method, was performed to evaluate the volume fraction of surface + glandular epithelium, lamina propria, and muscularis mucosae. To identify the appropriate sectioning interval and number of sampled sections, a pilot study was conducted. For this study, the sectioning interval ratio was 1/100. Each tissue block had serial 5 micron-thickness sections taken from it.

Using a light microscope (Olympus BX43F, Tokyo, Japan) and a microscope camera (Olympus SC50, Olympus Soft Imaging Solutions GmbH, Münster, Germany) linked to a desktop computer, many photographs of the sections at a magnification of x20 were taken (Figure 3.6). Olympus CellSens Entry 1.14 was used as the imaging software. To identify the appropriate imaging interval within the section, a pilot study was conducted (obtaining suitable coefficient of error CE) (Deniz et al., 2017). For this study, the imaging interval of 1/3 was determined. Selected pictures were shown in the ImageJ program.

Figure 3. 6. Stereological analysis system

The image was projected onto a point counting grid with square-shaped points. The pointed area measurement ruler (the area represented by the point is 5000 μm^2) was discarded on the photographs. The first image was picked at random from the specimens in each section, and then the interval of 1/3 was applied to the rest of the section. The magnification was adjusted so that each field of view could contain the

whole mucosal layers. In all selected fields of view, the number of points striking the surface and glandular epithelium, P (epithelium), the lamina propria, P (lamina propria), and the muscularis mucosae, P (muscularis), was tallied. The overall number of points for each field, P, is calculated by adding the three distinct counts. Each total number of points obtained for the structure is the total number of points that superimposed onto the point counting test grid (Figures 3.7 and 3.8). The percentage has been calculated. The Coefficient of error (CE) of each animal in the study and the coefficient of variation (CV) for each group was calculated.

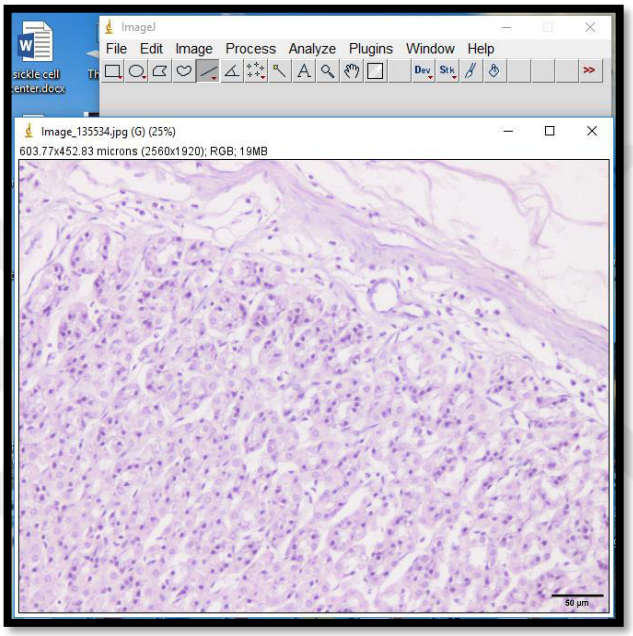

Figure 3. 7. The stomach section is seen in the ImageJ program

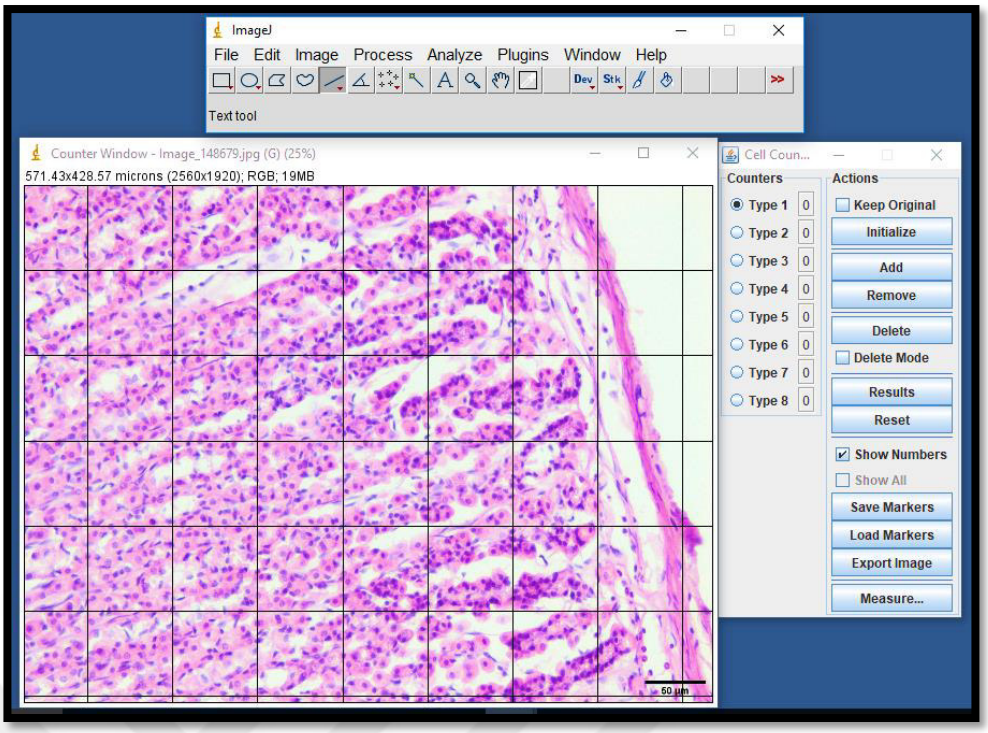

Figure 3. 8. The stomach section is seen in the ImageJ program

3.9. Statistical Analysis

The statistical comparison of the groups was done via the Statistical Program (SPSS version 25.0; SPSS Inc., Chicago, IL, USA). For regularly distributed data, the One-way ANOVA test (post-hoc Tukey test) was used, while for data that did not demonstrate normal distribution, the Kruskal Wallis test was utilized. In the analysis of all data, a $p \leq 0.05$ value was considered significant.

4. RESULTS AND DISCUSSION

4.1. Result

The goal of this study was to see if GA could help reduce the side histopathological effects of DS on the mucosa of the rat GIT. Histological and stereological analyses were carried out.

4.1.1. Stereological Findings

The volume fraction of all mucosal layers (surface + glandular epithelium, lamina propria, and muscularis mucosae) of the stomach, small intestine, and large intestine were estimated using Cavalieri's principle. Those estimations were done for the four groups: Cont group, GA group (rats receive GA by oral gavage), DS group (rats receive DS by oral gavage), and DS+GA group (rats received both DS and GA by oral gavage).

4.1.1.1. Estimation of the Volume Fraction of the Surface and Glandular Epithelium

4.1.1.1.1. Stomach

We estimated the volume ratio of the surface + glandular epithelium that were found no statistically significant difference among all groups. In brief, no significant difference was found when compared the Cont group to the DS, GA, and DS + GA groups ($p > 0.05$) (Table 4.1 and Figure 4.1)

Table 4. 1. The volume ratio of the epithelium to the mucosal layer of the stomach, control (Cont), gum Arabic (GA), diclofenac sodium (DS), diclofenac sodium + gum Arabic (DS+GA)

Groups	Mean (%)	Standard error of the mean
Cont	0.6010	0.01947
DS	0.5745	0.01487
DS + GA	0.5840	0.03343
GA	0.5986	0.02430
Mean	0.5897	0.01139

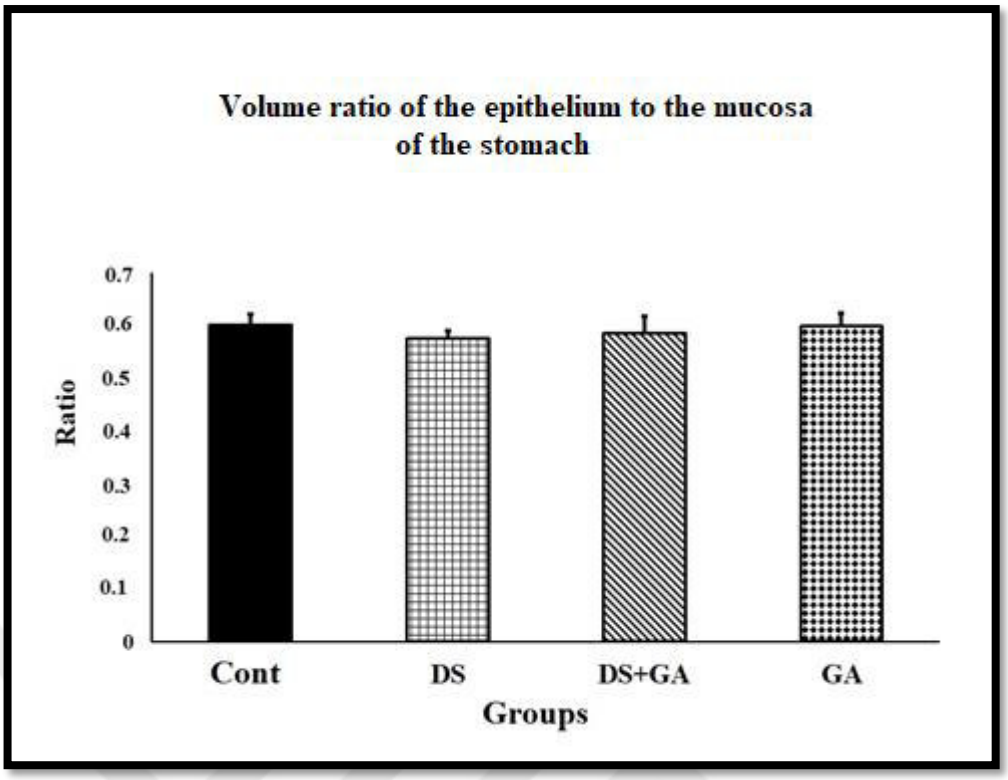

Figure 4. 1. A volume ratio of the epithelium to the mucosal layer of the stomach, control (Cont), gum Arabic (GA), diclofenac sodium (DS), diclofenac sodium + gum Arabic (DS+GA)

4.1.1.1.2. Small Intestine

The volume ratio of the surface + glandular epithelium was estimated, and no statistically significant differences were found between the groups. In summary, no significant differences were observed when the Cont group was compared to the DS, GA, and DS + GA groups ($p > 0.05$) (Table 4.2, and Figure 4.2).

Table 4. 2. The volume ratio of the epithelium to the mucosal layer of the small intestine, control (Cont), gum Arabic (GA), diclofenac sodium (DS), diclofenac sodium + gum Arabic (DS+GA)

Groups	Mean (%)	Standard error of the mean
Cont	0.5240	0.02087
DS	0.5241	0.02463
DS + GA	0.5078	0.01510
GA	0.4823	0.02619
Mean	0.5088	0.01105

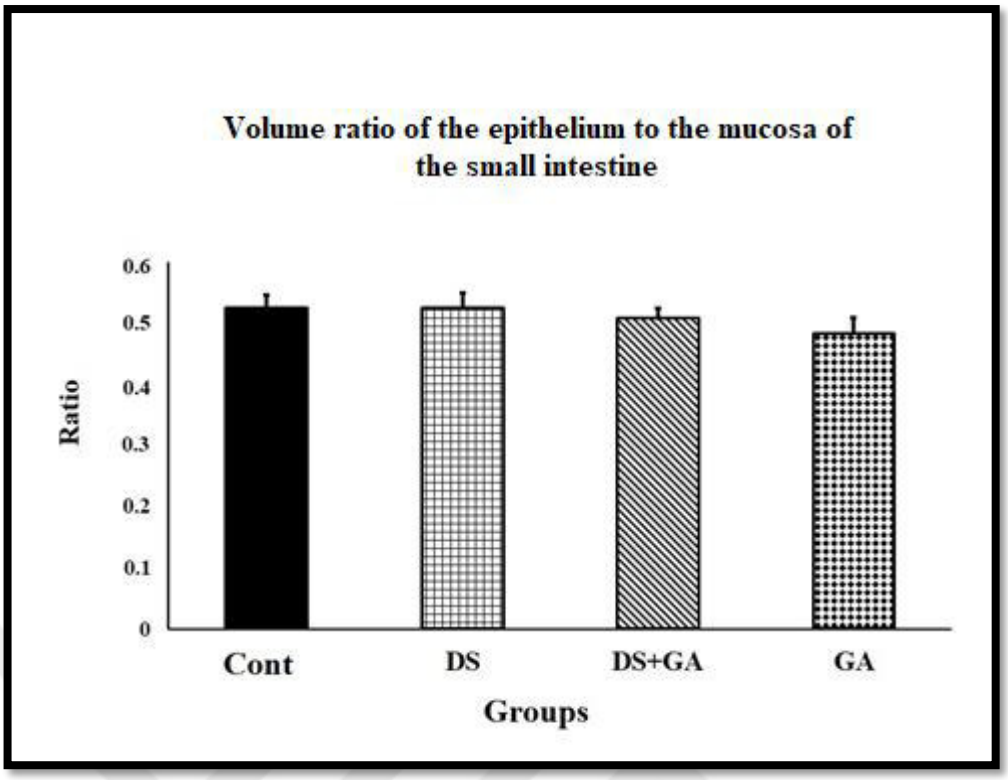

Figure 4. 2. A volume ratio of the epithelium to the mucosal layer of the small intestine, control (Cont), gum Arabic (GA), diclofenac sodium (DS), diclofenac sodium + gum Arabic (DS+GA)

4.1.1.1.3. Large Intestine

To all of the groups, the volume proportion of the surface + glandular epithelium was estimated. When comparing the Cont group to the DS, GA, and DS + GA groups, no significant differences were observed ($p > 0.05$) (Table 4.3 and Figure 4.3).

Table 4. 3. The volume ratio of the epithelium to the mucosal layer of the large intestine, control (Cont), gum Arabic (GA), diclofenac sodium (DS), diclofenac sodium + gum Arabic (DS+GA)

Groups	Mean (%)	Standard error of the mean
Cont	0.5684	0.00812
DS	0.5151	0.02528
DS + GA	0.5655	0.01758
GA	0.5752	0.02155
Mean	0.5556	0.01016

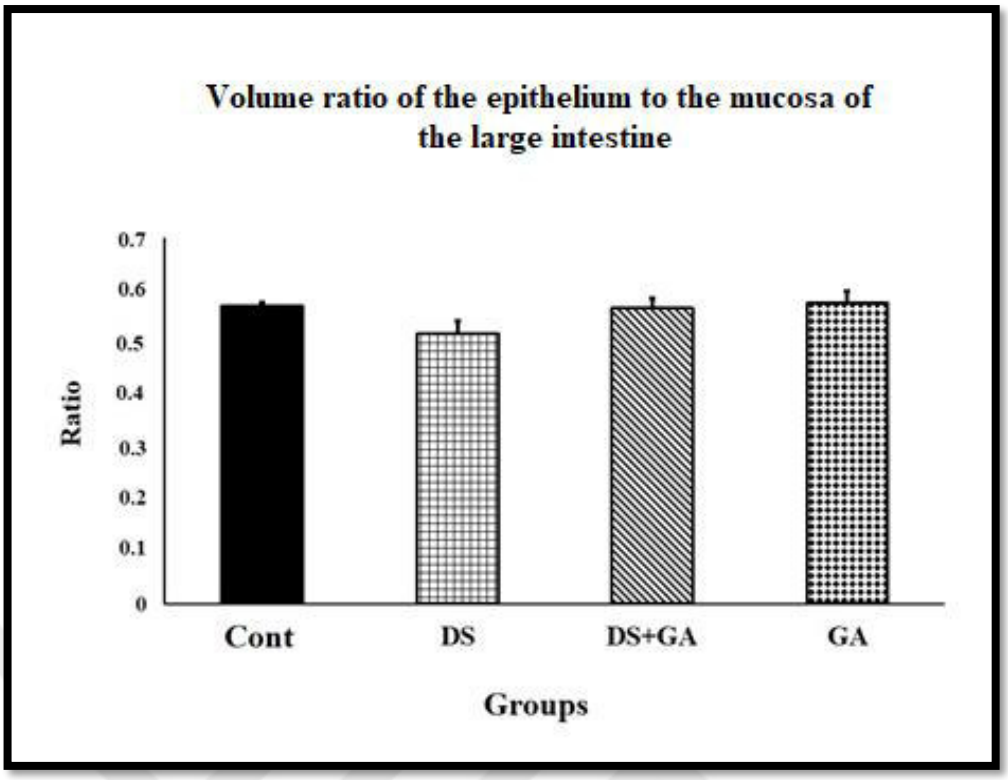

Figure 4. 3. A volume ratio of the epithelium to the mucosal layer of the large intestine, control (Cont), gum Arabic (GA), diclofenac sodium (DS), diclofenac sodium + gum Arabic (DS+GA)

4.1.1.2. Estimation of the Volume Fraction of the Lamina Propria

4.1.1.2.1. Stomach

In terms of volume fraction of the lamina propria, no significant differences were observed among the groups Cont, DS, DS + GA, and GA ($p > 0.05$) (Table 4.4 and Figure 4.4).

Table 4. 4. A volume ratio of lamina propria to the mucosal layer of the stomach, control (Cont), gum Arabic (GA), diclofenac sodium (DS), diclofenac sodium + gum Arabic (DS+GA)

Groups	Mean (%)	Standard error of the mean
Cont	0.3324	0.01497
DS	0.3437	0.01416
DS + GA	0.3439	0.03187
GA	0.3215	0.02076
Mean	0.3352	0.01018

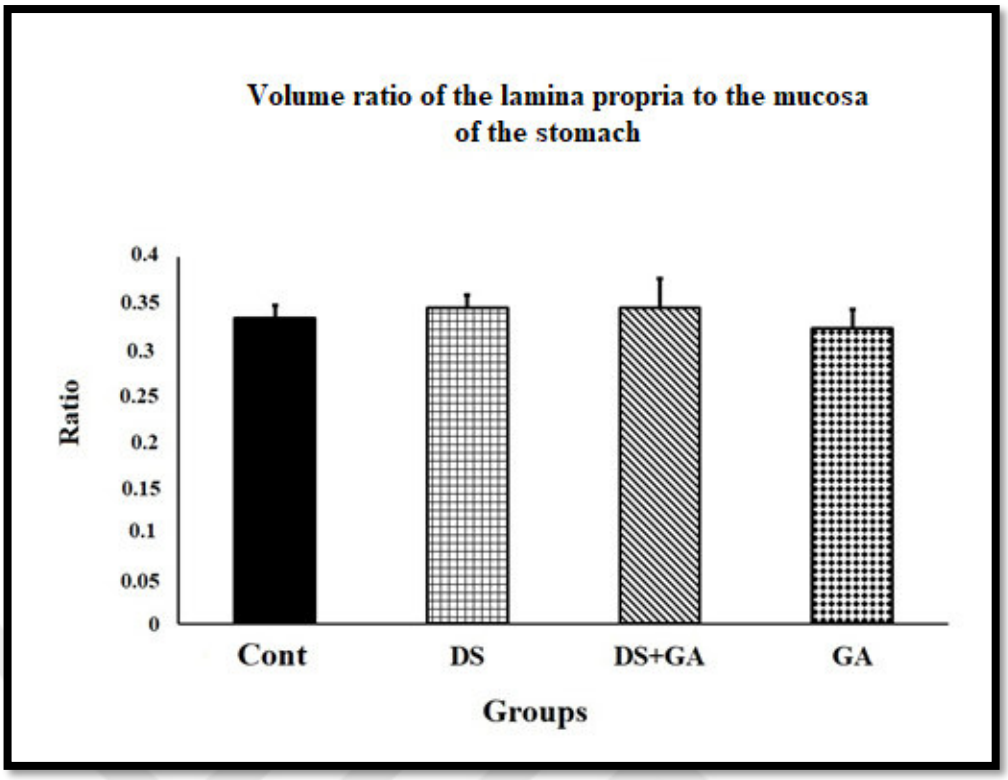

Figure 4. 4. A volume ratio of lamina propria to the mucosal layer of the stomach, control (Cont), gum Arabic (GA), diclofenac sodium (DS), diclofenac sodium + gum Arabic (DS+GA)

4.1.1.2.2. Small Intestine

There were no significant difference in the volume fraction of the lamina propria between the groups Cont, DS, DS + GA, and GA ($p > 0.05$) (Table 4.5, and Figure 4.5).

Table 4. 5. A volume ratio of lamina propria to the mucosal layer of the small intestine, control (Cont), gum Arabic (GA), diclofenac sodium (DS), diclofenac sodium + gum Arabic (DS+GA)

Groups	Mean (%)	Standard error of the mean
Cont	0.3944	0.01806
DS	0.3993	0.01930
DS + GA	0.4064	0.01620
GA	0.4181	0.02814
Mean	0.4048	0.01038

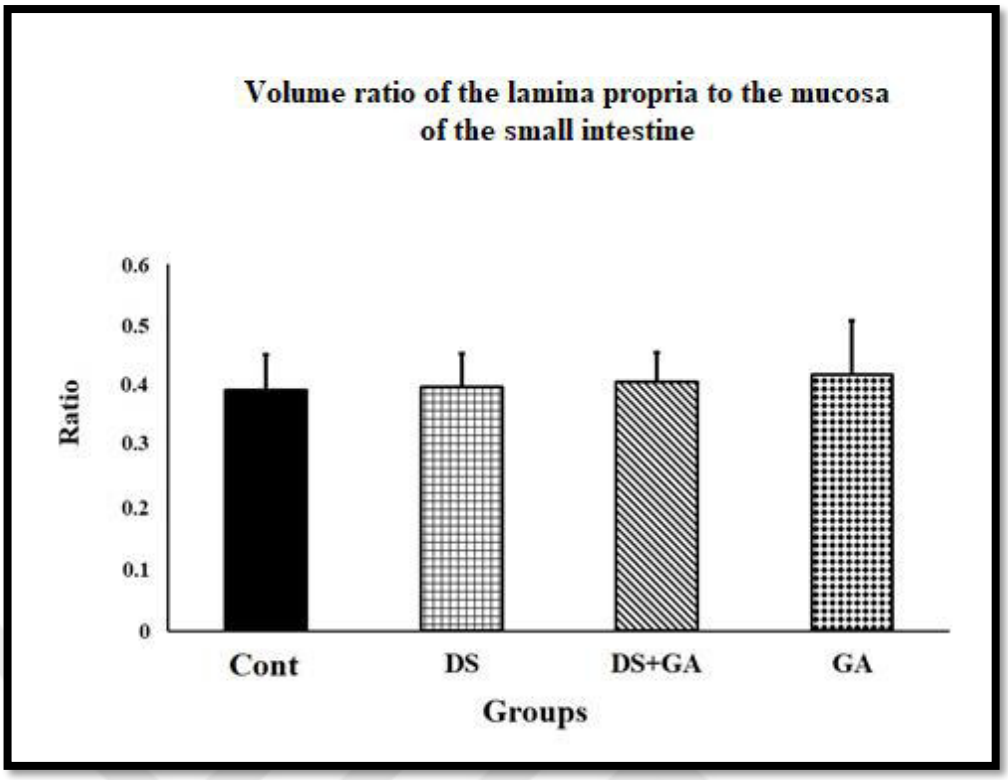

Figure 4. 5. A volume ratio of lamina propria to the mucosal layer of the small intestine, control (Cont), gum Arabic (GA), diclofenac sodium (DS), diclofenac sodium + gum Arabic (DS+GA)

4.1.1.2.3. Large Intestine

There were no significant difference in volume fraction of the lamina propria between the groups Cont, DS, DS + GA, and GA ($p>0.05$) (Table 4.6, and Figure 4.6).

Table 4. 6. A volume ratio of lamina propria to the mucosal layer of the large intestine, control (Cont), gum Arabic (GA), diclofenac sodium (DS), diclofenac sodium + gum Arabic (DS+GA)

Groups	Mean (%)	Standard error of the mean
Cont	0.3410	0.00988
DS	0.3842	0.02070
DS + GA	0.3520	0.01672
GA	0.3422	0.02015
Mean	0.3550	0.00891

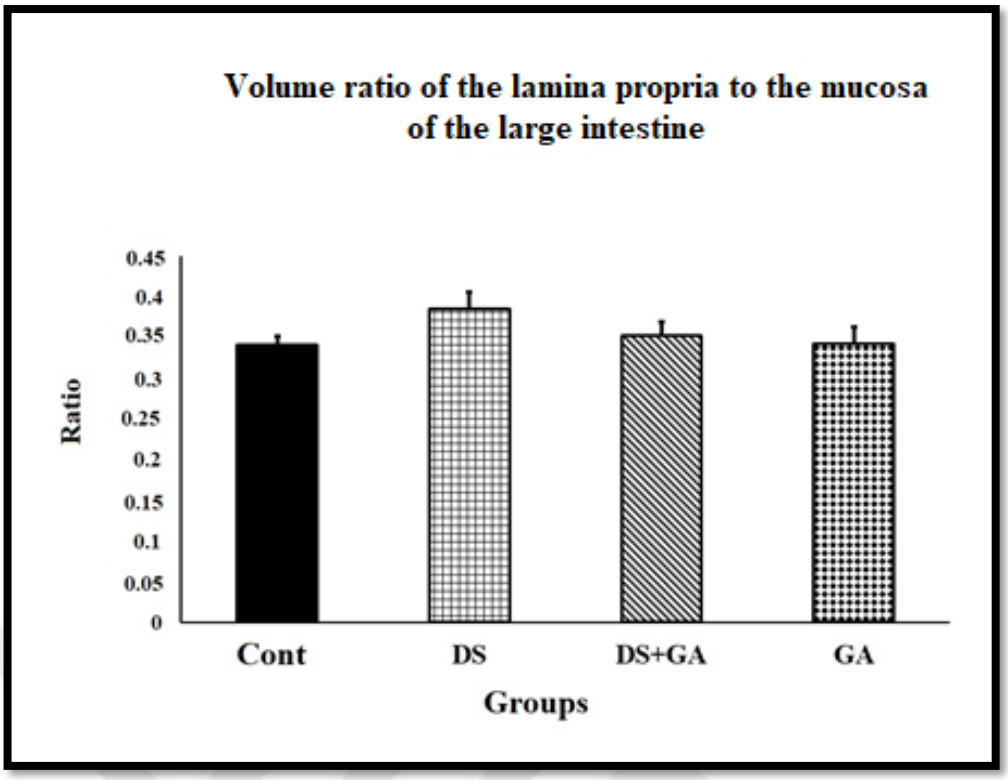

Figure 4. 6. A volume ratio of lamina propria to the mucosal layer of the large intestine, control (Cont), gum Arabic (GA), diclofenac sodium (DS), diclofenac sodium + gum Arabic (DS+GA)

4.1.1.3. Estimation of the Volume Fraction of the Muscularis Mucosae

4.1.1.3.1. Stomach

According to the statistical analysis of the stereological data obtained from the estimation of volume ratio of muscularis mucosae showed that no significant differences were found between the Cont, DS, DS + GA, and GA groups (Table 4.7, and Figure 4.7)

Table 4. 7. A volume ratio of muscularis mucosae to the mucosal layer of the stomach, control (Cont), gum Arabic (GA), diclofenac sodium (DS), diclofenac sodium + gum Arabic (DS+GA)

Groups	Mean (%)	Standard error of the mean
Cont	0.0666	0.00766
DS	0.0818	0.00379
DS + GA	0.0720	0.00875
GA	0.0801	0.00830
Mean	0.0752	0.00366

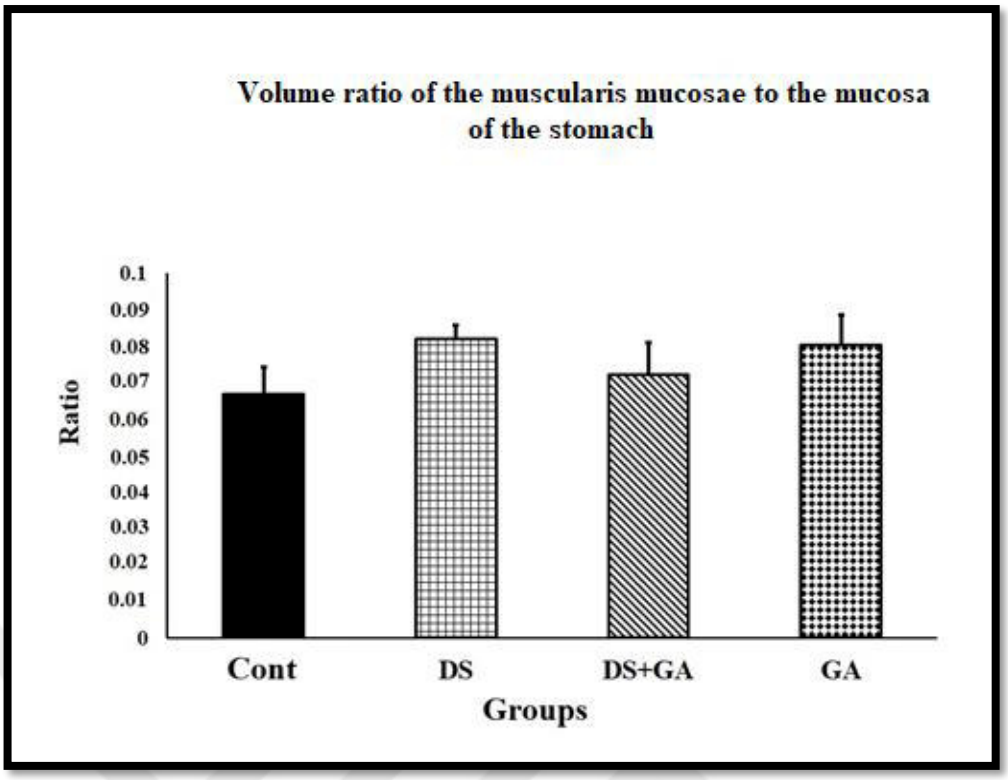

Figure 4. 7. A volume ratio of muscularis mucosae to the mucosal layer of the stomach, control (Cont), gum Arabic (GA), diclofenac sodium (DS), diclofenac sodium + gum Arabic (DS+GA)

4.1.1.3.2. Small Intestine

According to statistical analysis of stereological data collected from the estimation of volume ratio of muscularis mucosae, no significant differences between the Cont, DS, DS + GA, and GA groups were found ($p > 0.05$) (Table 4.8, and Figure 4.8).

Table 4. 8. A volume ratio of muscularis mucosae to the mucosal layer of the small intestine, control (Cont), gum Arabic (GA), diclofenac sodium (DS), diclofenac sodium + gum Arabic (DS+GA)

Groups	Mean (%)	Standard error of the mean
Cont	0.0814	0.00813
DS	0.0766	0.01118
DS + GA	0.0857	0.00540
GA	0.0994	0.00469
Mean	0.0863	0.00385

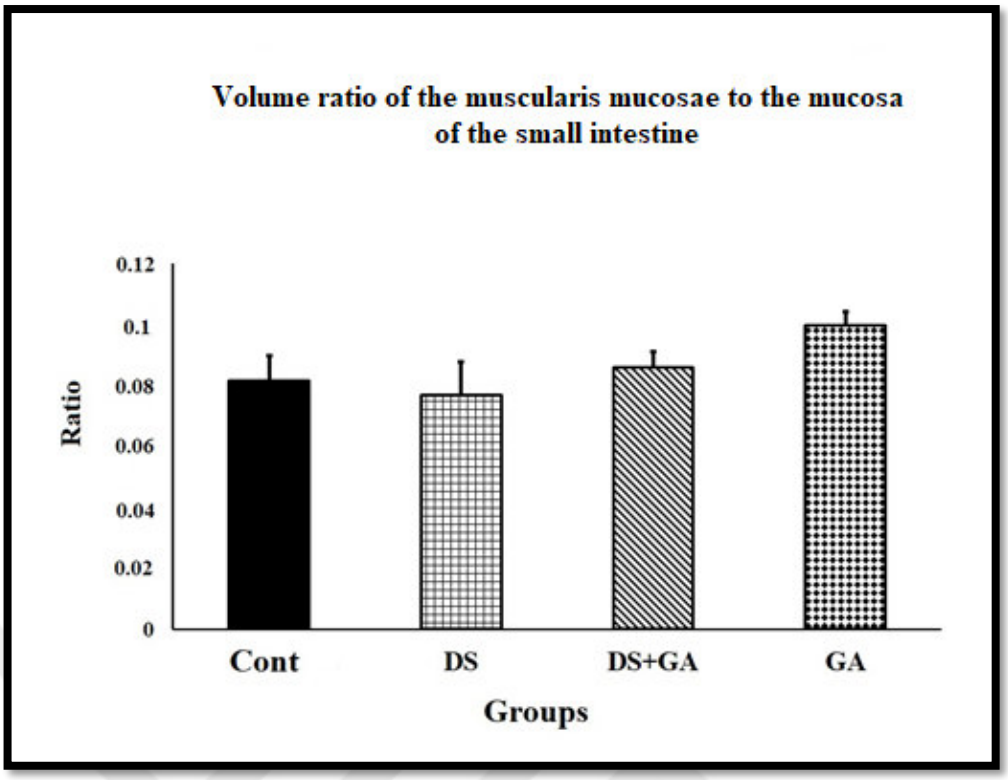

Figure 4. 8. A volume ratio of muscularis mucosae to the mucosal layer of the small intestine, control (Cont), gum Arabic (GA), diclofenac sodium (DS), diclofenac sodium + gum Arabic (DS+GA)

4.1.1.3.3. Large Intestine

According to stereological data collected from the estimation of volume ratio of muscularis mucosae, no significant differences between the Cont, DS, DS + GA, and GA groups were observed in the large intestine ($p>0.05$) (Table 4.9, and Figure 4.9).

Table 4. 9. A volume ratio of muscularis mucosae to the mucosal layer of the large intestine, control (Cont), gum Arabic (GA), diclofenac sodium (DS), diclofenac sodium + gum Arabic (DS+GA)

Groups	Mean (%)	Standard error of the mean
Cont	0.0905	0.00786
DS	0.1008	0.01058
DS + GA	0.0823	0.00682
GA	0.0826	0.00743
Mean	0.0894	0.00425

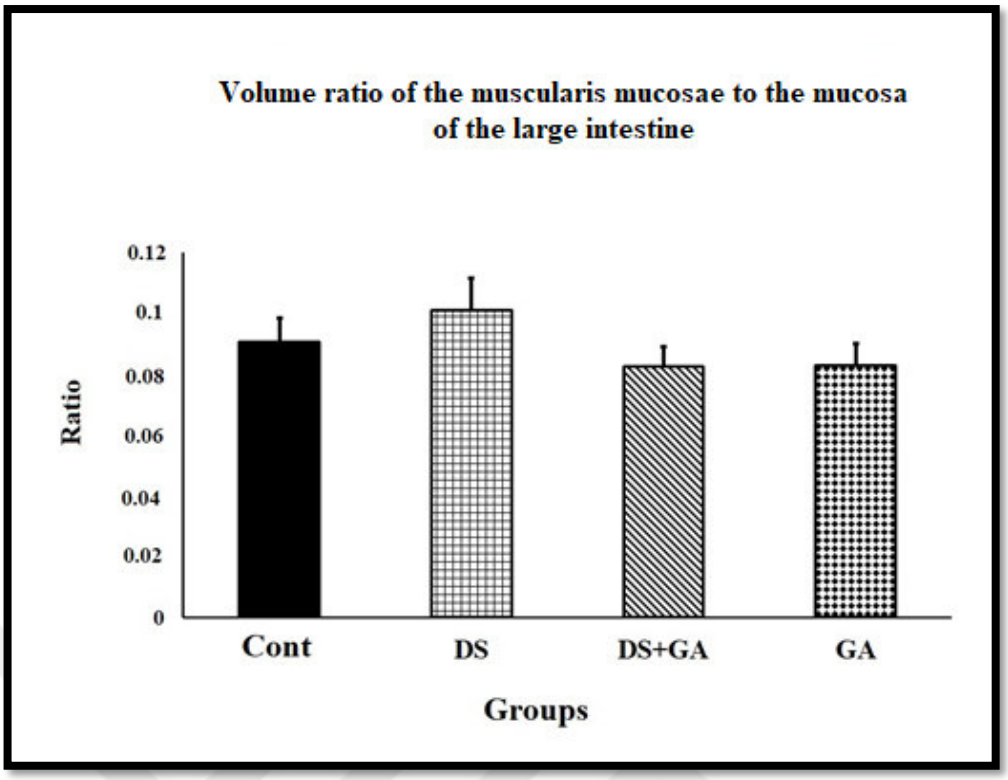

Figure 4. 9. A volume ratio of muscularis mucosae to the mucosal layer of the large intestine, control (Cont), gum Arabic (GA), diclofenac sodium (DS), diclofenac sodium + gum Arabic (DS+GA)

4.1.1.4. Estimation of the Volume Fraction of the Mucosal Layers

4.1.1.4.1. Stomach

Estimation of the volume ratio of different layers of the mucosal layer of the stomach to the different groups Cont, DS, DS + GA, and GA were given in below (Table 4.10)

Table 4. 10. A volume ratio of the mucosal layers of the stomach, control (Cont), gum Arabic (GA), diclofenac sodium (DS), diclofenac sodium + gum Arabic (DS+GA)

	Epithelium (%)	LP (%)	MM (%)
Cont	60.1	33.2	6.7
DS	57.5	34.4	8.2
DS+GA	58.4	34.4	7.2
GA	59.8	32.1	8.1

4.1.1.4.2. Small Intestine

The volume ratio of the mucosal layer of the small intestine to the various groups was estimated. Below are the terms Cont, DS, DS + GA, and GA (Table 4.11).

Table 4. 11. A volume ratio of the mucosal layers of the small intestine, control (Cont), gum Arabic (GA), diclofenac sodium (DS), diclofenac sodium + gum Arabic (DS+GA)

	Epithelium (%)	LP (%)	MM (%)
Cont	52.4	39.4	8.2
DS	52.4	39.9	7.7
DS+GA	50.8	40.6	8.6
GA	48.2	41.8	9.9

4.1.1.4.3. Large Intestine

The volume ratio of the mucosal layer of the large intestine to the various groups was estimated. Below are the definitions of Cont, DS, DS + GA, and GA (Table 4.12).

Table 4. 12. A volume ratio of the mucosal layers of the large intestine, control (Cont), gum Arabic (GA), diclofenac sodium (DS), diclofenac sodium + gum Arabic (DS+GA)

	Epithelium (%)	LP (%)	MM (%)
Cont	56.8	34.1	9.1
DS	51.5	38.4	10.1
DS+GA	56.6	35.2	8.2
GA	57.5	34.2	8.3

The coefficient of error CE, and the coefficient of variance CV for the volume fraction of, the epithelium, lamina propria, muscularis mucosae of the stomach, small intestine and large intestine are shown in (Table 4.13 - 4.15).

Table 4. 13. The coefficient of error (CE) and the coefficient of variance (CV) for the volume fraction estimation of, the epithelium, lamina propria, muscularis mucosae of the stomach of the control (Cont), diclofenac sodium (DS), diclofenac sodium + gum Arabic, gum Arabic (GA)

Groups	**CE**			**CV**		
	Epithelium	**Lamina propria**	**Muscularis mucosae**	**Epithelium**	**Lamina propria**	**Muscularis mucosae**
Cont	0.018	0.025	0.056	0.097	0.135	0.346
DS	0.016	0.021	0.043	0.077	0.124	0.138
DS+GA	0.022	0.029	0.063	0.162	0.499	0.529
GA	0.019	0.026	0.055	0.122	0.194	0.311

Table 4. 14. The coefficient of error (CE) and the coefficient of variance (CV) for the volume fraction estimation of, the epithelium, lamina propria, muscularis mucosae of the small intestine of the control (Cont), diclofenac sodium (DS), diclofenac sodium + gum Arabic (DS+GA), gum Arabic (GA) groups

Groups	**CE**			**CV**		
	Epithelium	**Lamina propria**	**Muscularis mucosae**	**Epithelium**	**Lamina propria**	**Muscularis mucosae**
Cont	0.030	0.035	0.080	0.120	0.137	0.301
DS	0.033	0.037	0.091	0.124	0.128	0.385
DS+GA	0.032	0.036	0.079	0.372	0.317	0.364
GA	0.037	0.039	0.081	0.163	0.202	0.142

Table 4. 15. The coefficient of error (CE) and the coefficient of variance (CV) for the volume fraction estimation of, the epithelium, lamina propria, muscularis mucosae of the large intestine of the control (Cont), diclofenac sodium (DS), diclofenac sodium + gum Arabic (DS+GA), gum Arabic (GA) groups

Groups	**CE**			**CV**		
	Epithelium	**Lamina propria**	**Muscularis mucosae**	**Epithelium**	**Lamina propria**	**Muscularis mucosae**
Cont	0.018	0.029	0.055	0.043	0.087	0.259
DS	0.033	0.039	0.076	0.147	0.162	0.314
DS+GA	0.026	0.033	0.069	0.082	0.126	0.220
GA	0.027	0.035	0.072	0.112	0.117	0.268

The statistical analysis of the data revealed that there is no discernible disparity among the groups regarding the volume fraction of the mucosal layer components.

4.1.2. Light Microscopic Findings

Semi-thin sections (0.5 µm thickness) from the resin blocks were taken and stained with toluidine blue. Following the examination of all layers in the wall, the findings are given below:

4.1.2.1. Stomach

4.1.2.1.1. Control Group

The entire structure of the stomach layers is well protected in this group. The organ's glandular layer (part of the mucosa), submucosa, and muscularis externa are all intact. The stomach's simple columnar epithelial layer appears to be a healthy structure. The stomach gland's parietal cells are big size cells. The glands' lumens are somewhat enlarged. The connective tissue that surrounds glands is extremely loose. The glands and connective tissue cells have normal morphology. The parietal cells are the largest cells in the glands. The vascular and fibrillar arrangements are well organized. The stomach's muscularis externa, which is mostly made up of two layers, internal and external, is visible. Tunica serosa protects this layer. A myenteric plexus can be visible between these smooth muscles layers. All of the buildings in these strata appear to be in good structure. The basal membrane surrounds each muscle cell (Figures 4.10-4.19).

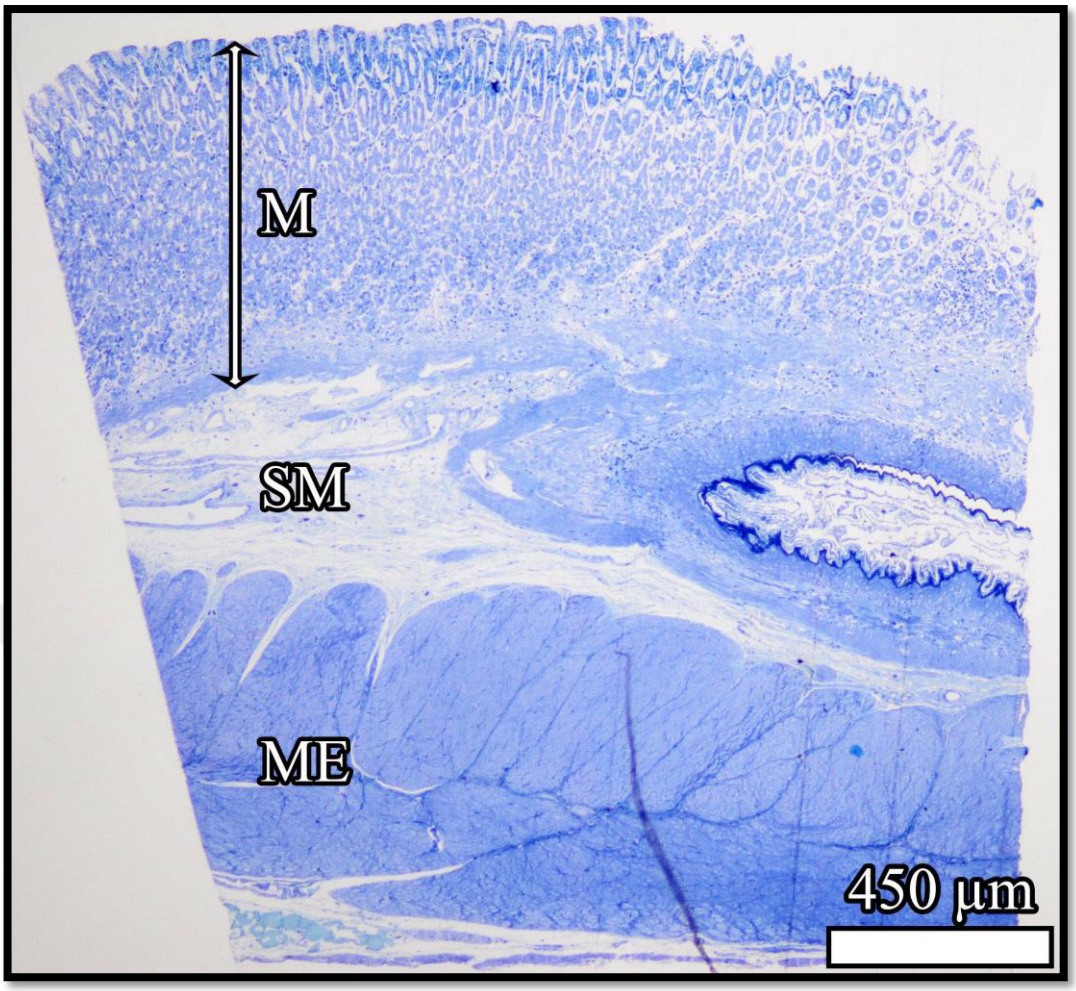

Figure 4. 10. General structure of the stomach is seen. The whole layers of the stomach have a well-protected structure. Glandular layer of organ (arrow) i.e. a part of mucosa (M), submucosa (SM) and muscularis externa (ME) are intact. At the right center side of image, non-glandular part of stomach that is lined by cornified stratified squamous epithelium is observed. Semithin section of resin embedded tissue (0.5 µm thickness) and stained with toluidine blue

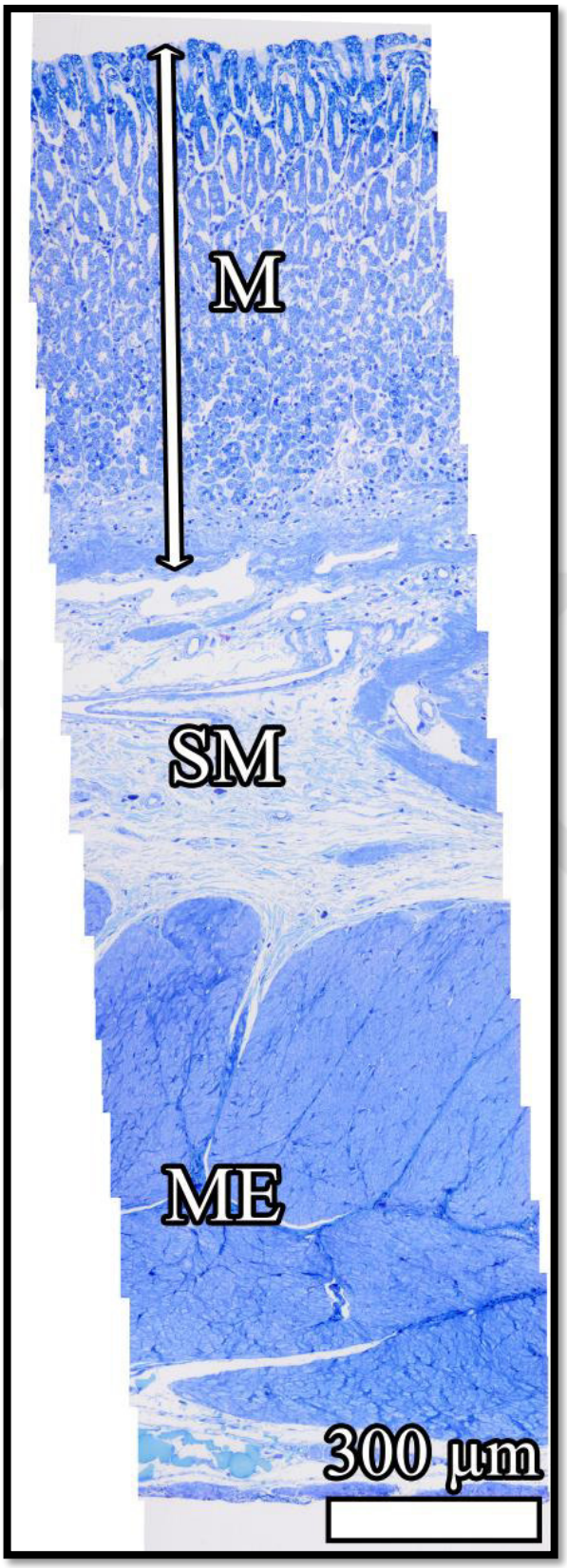

Figure 4. 11. General structure of the stomach is seen. The whole layers of the stomach have a well-protected structure. Epithelium and a glandular layer of organ, a part of mucosa (M), submucosa (SM), and muscularis externa (ME) are seen intact. Semithin section of resin embedded tissue (0.5 µm thickness) and stained with toluidine blue

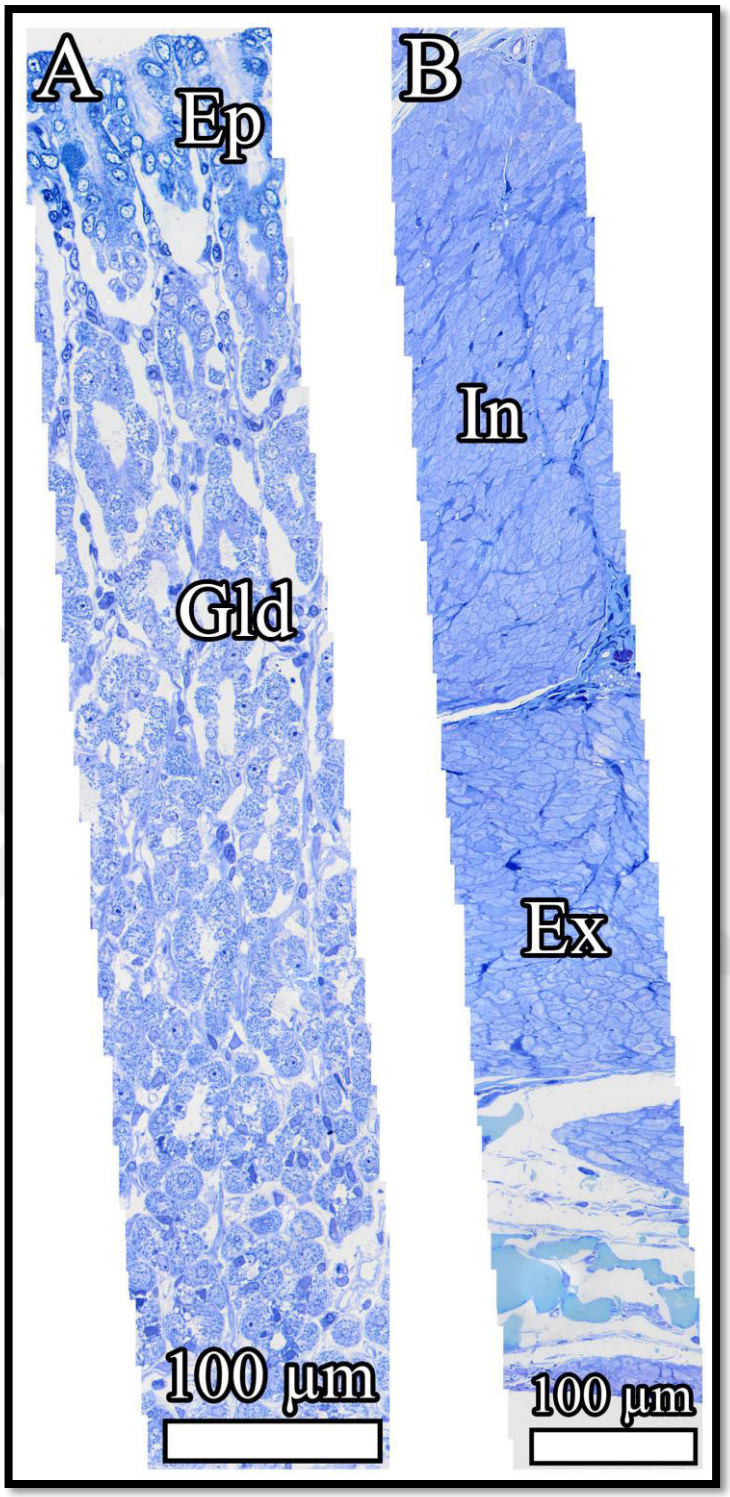

Figure 4. 12. (A, B) A high magnification of the stomach layers is seen. The whole layers of the stomach have a well-protected structure. A simple columnar epithelium (Ep) and glandular structures (Gld), found at the bottom, are observed. Two layers of muscularis externa, externa (Ex) and interna (In), are intact. Semithin section of resin embedded tissue (0.5 µm thickness) and stained with toluidine blue

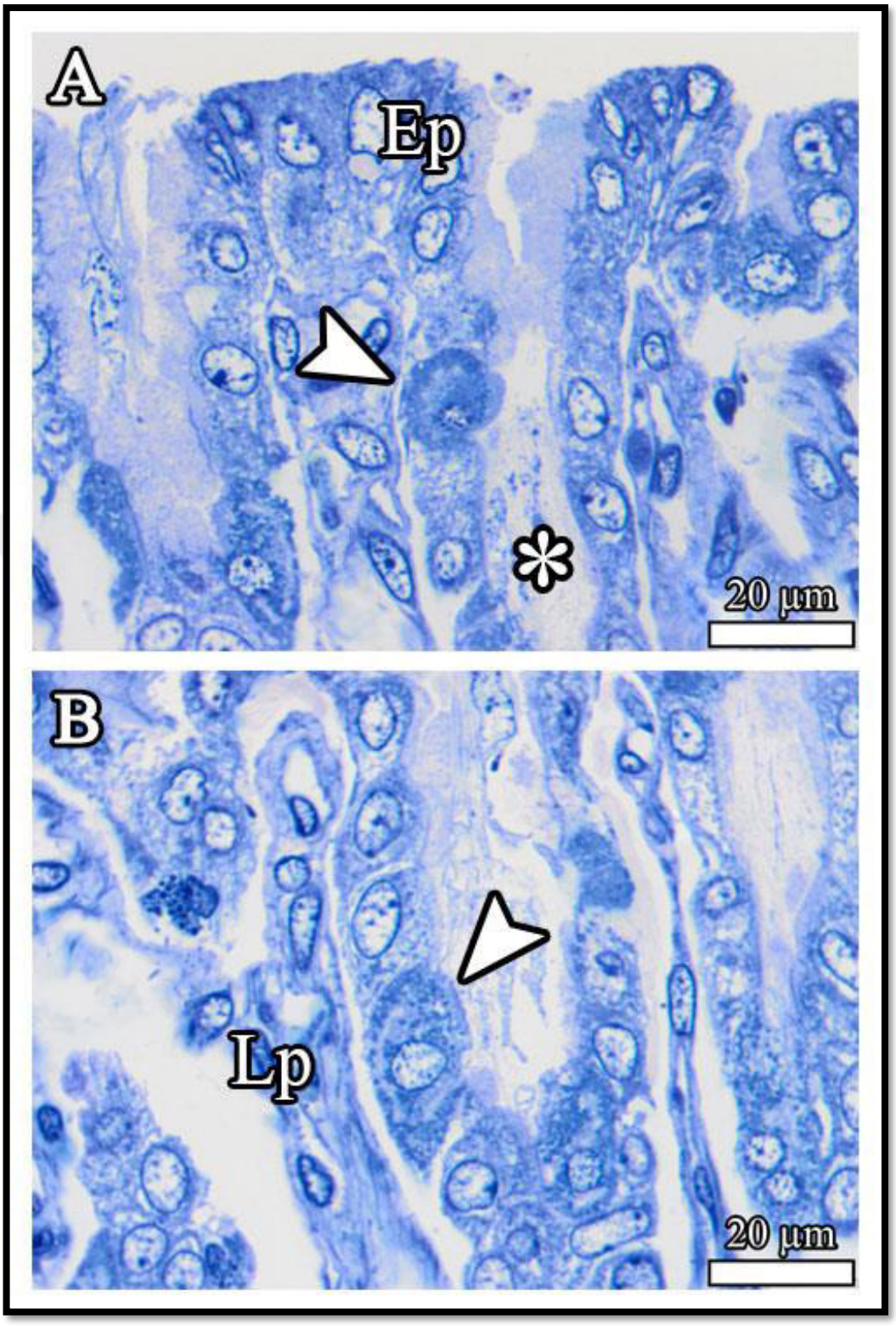

Figure 4. 13. (A, B) High magnification of the stomach layers, the epithelium (Ep) and lamina propria (Lp), are seen. The simple columnar epithelium layer of the stomach looks a healthy structure. Parietal cells of the stomach gland have a large size (arrowhead). The opening of the stomach gland is shown (*). **(B)** Intracellular canaliculi in the parietal cell are pointed by an arrowhead. Semithin section of resin embedded tissue (0.5 µm thickness) and stained with toluidine blue

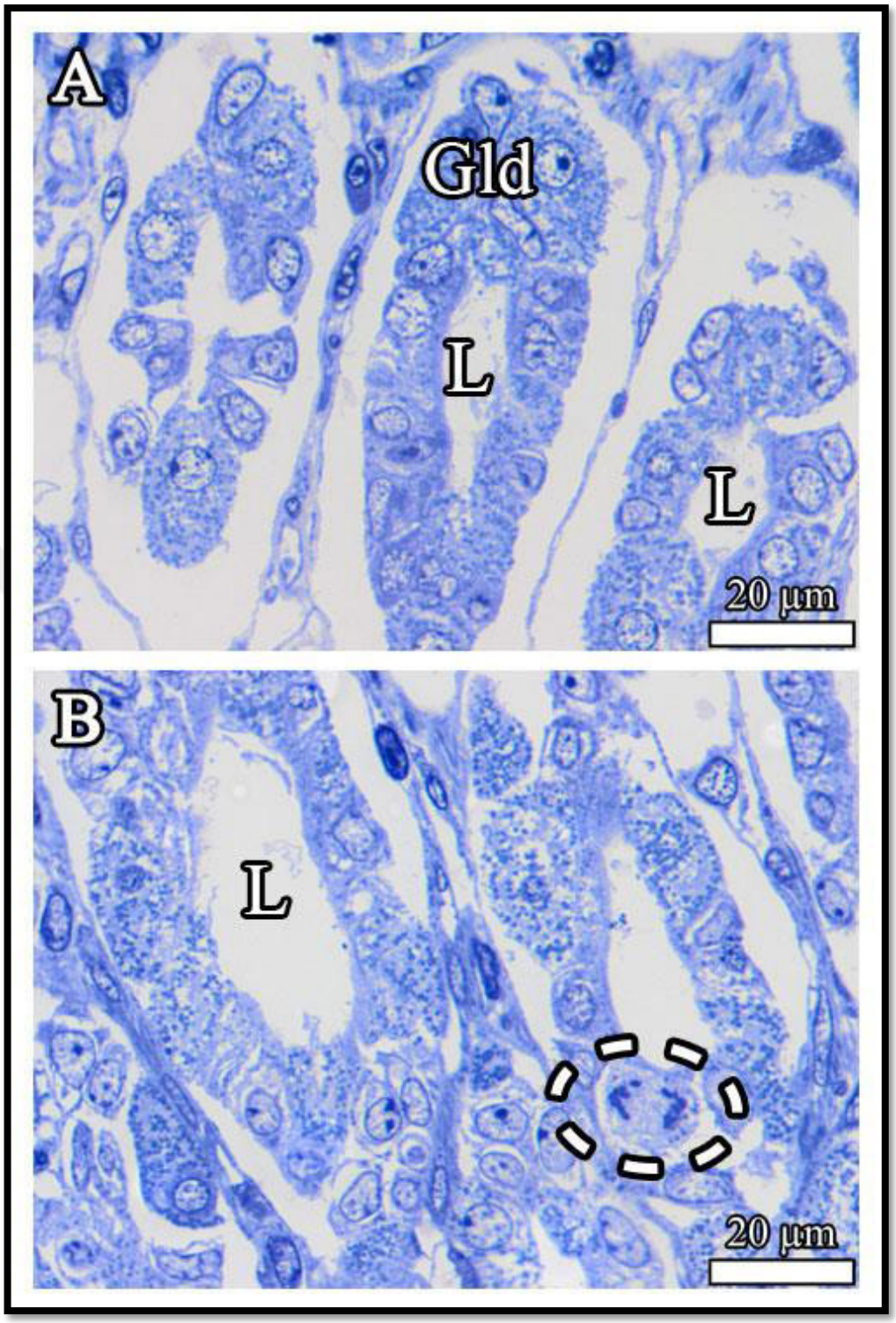

Figure 4. 14. (A, B) High magnification of the glands (Gld) in the stomach, the epithelium (Ep), and lamina propria (Lp) are seen. The lumens of glands (L) are partly large size. The connective tissue around the glands is very loose. Cells in the glands and connective tissue have a healthy morphology. Large-sized cells in the glands are the parietal cells. A mitotic cells division is seen in the gland epithelium (dashed circled area). Semithin section of resin embedded tissue (0.5 µm thickness) and stained with toluidine blue

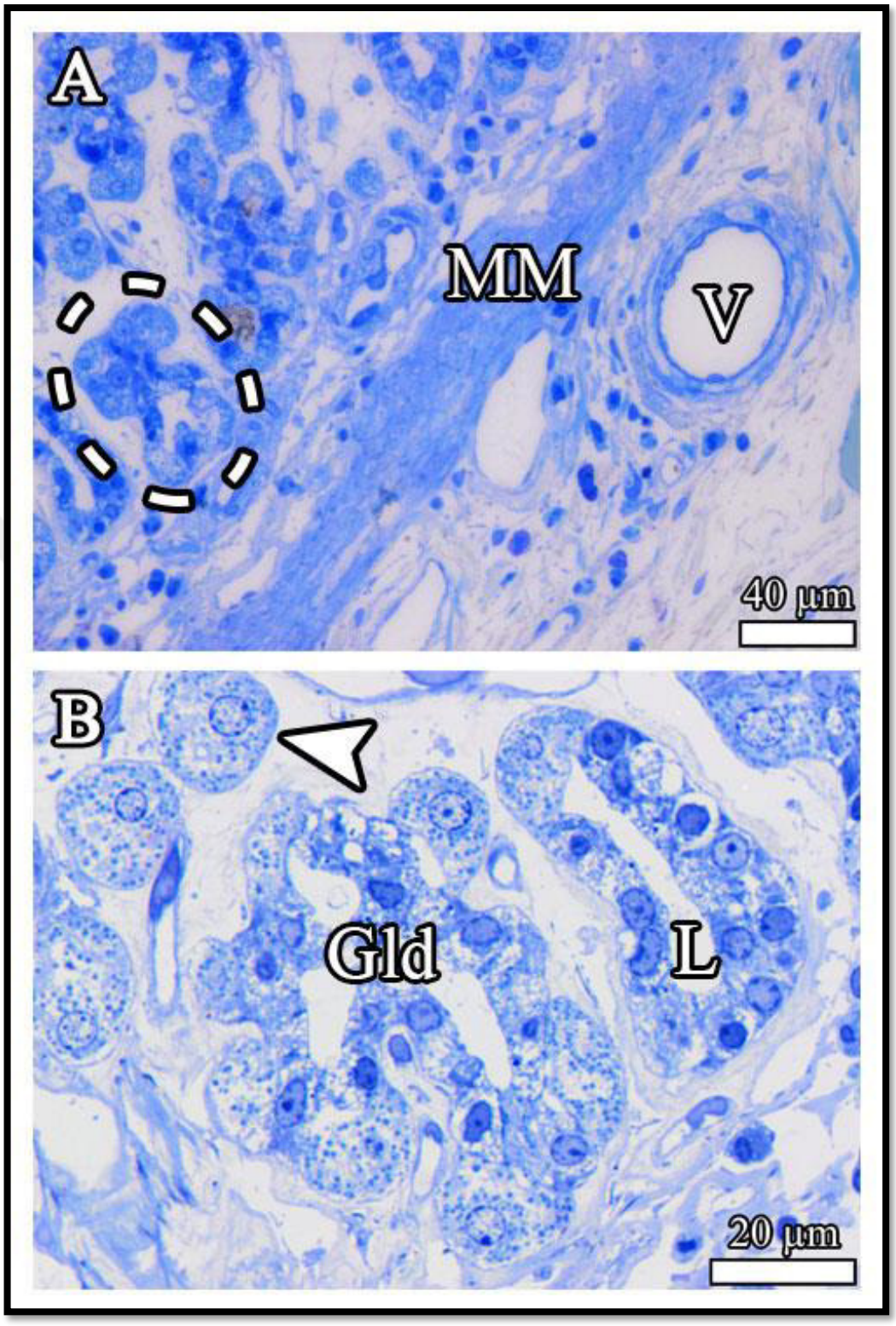

Figure 4. 15. (A, B) High magnification of the glands (Gld), muscularis mucosae (MM), and submucosa layers in the stomach are seen. The lumens of glands (L) are partly large in size. The connective tissue around the glands is very loose. Cells in the glands and connective tissue have a healthy morphology. Large-sized cells in the glands are the parietal cells (arrowhead). A base of gland section (dashed circled area) is seen. (V), vessel. Semithin section of resin embedded tissue (0.5 µm thickness) and stained with toluidine blue

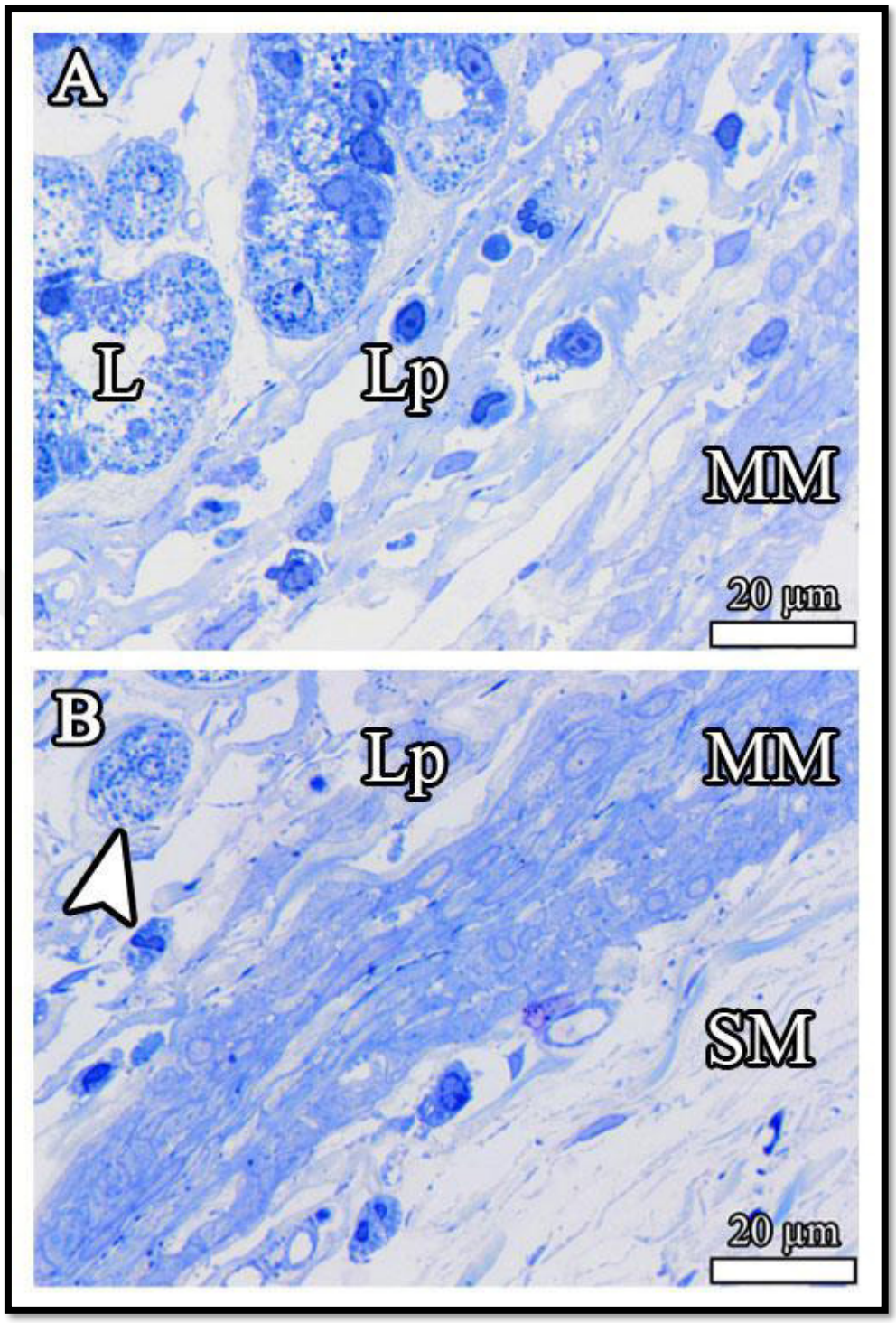

Figure 4. 16. (A, B) High magnification images of the lower part of glands, lamina propria (Lp), and muscularis mucosae layers (MM) of the stomach are observed. The lumens of glands (L) are partly large in size and connective tissue around glands is very loose. All structures in the glands and connective tissue have a healthy morphology. Large-size cells in the glands are the parietal cells (arrowhead). (SM), submucosa; (V), vessel. Semithin section of resin embedded tissue (0.5 µm thickness) and stained with toluidine blue

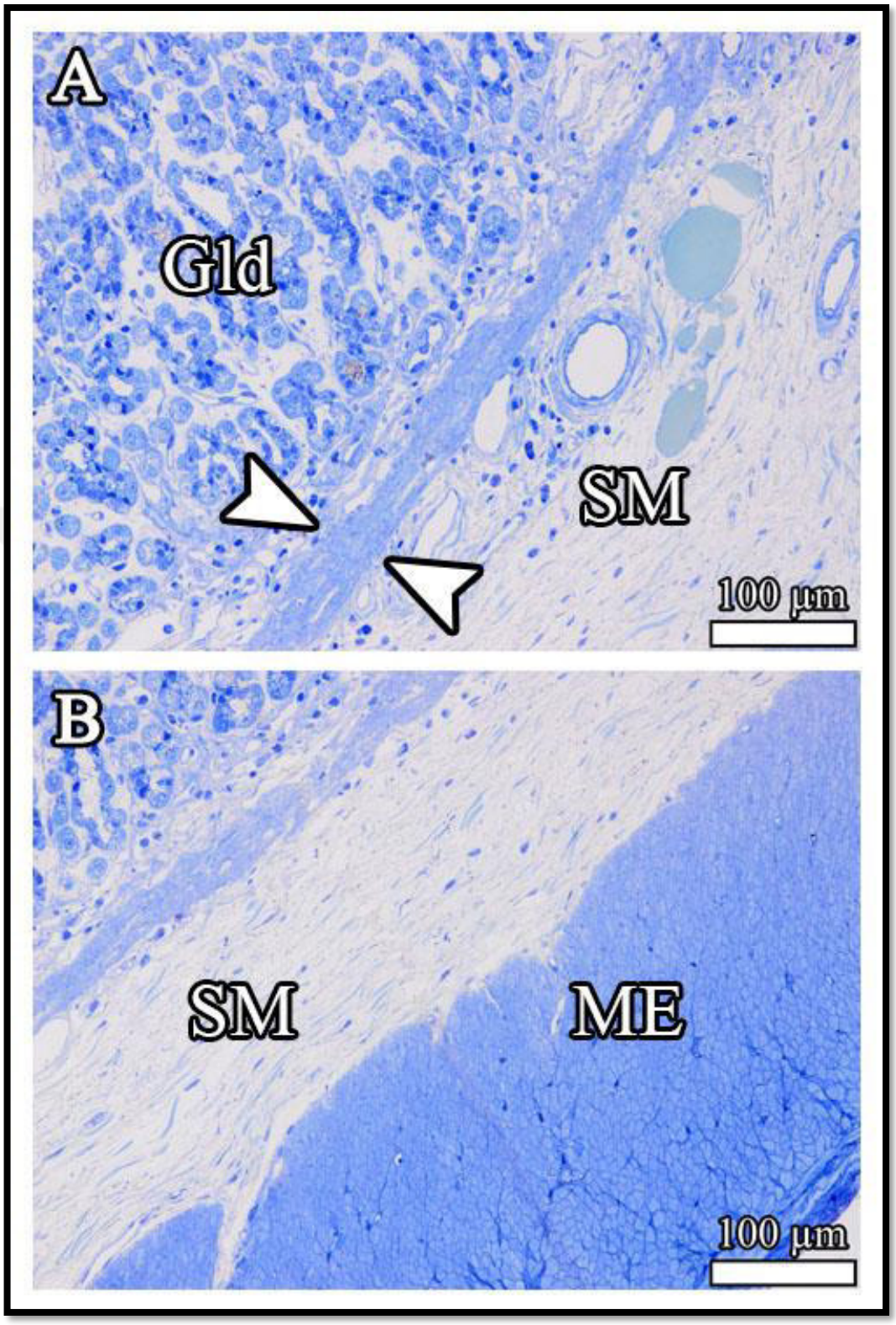

Figure 4. 17. (A, B) The images of the lower part of glands (Gld) lamina propria, muscularis mucosae layers (between arrowheads), and submucosa (SM) of the stomach are observed. All structures in these layers look healthy. The lumens of glands (L) are partly enlarged and connective tissue around glands is very loose. (ME), muscularis externa. Semithin section of resin embedded tissue (0.5 µm thickness) and stained with toluidine blue

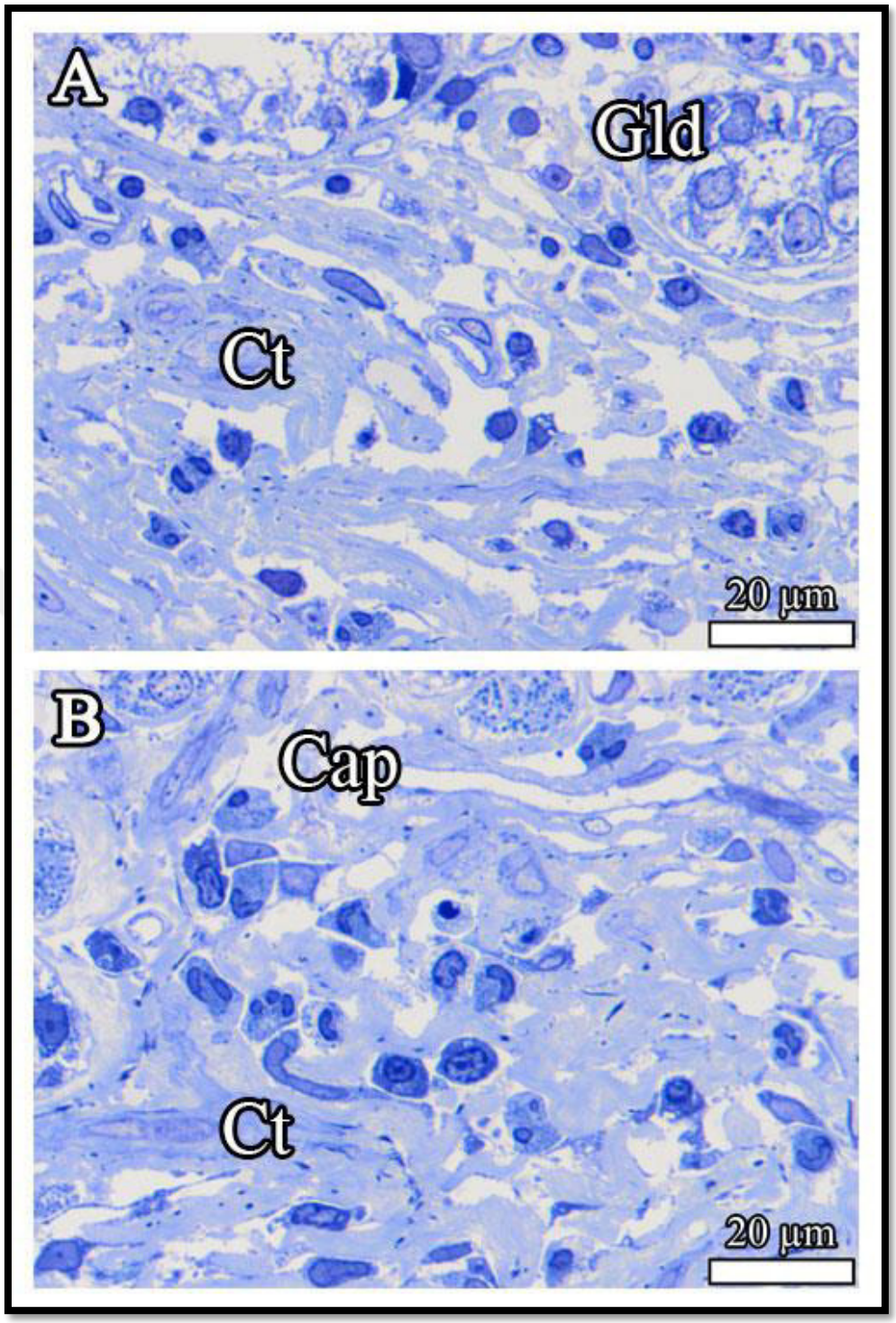

Figure 4. 18. **(A, B)** The images of the lower part of glands (Gld) and connective tissue of the lamina propria are observed. Cells and other elements of connective tissue (Ct) look healthy. Vascular and fibrillar arrangements have a normal organization. (Cap), capillary. Semithin section of resin embedded tissue (0.5 µm thickness) and stained with toluidine blue

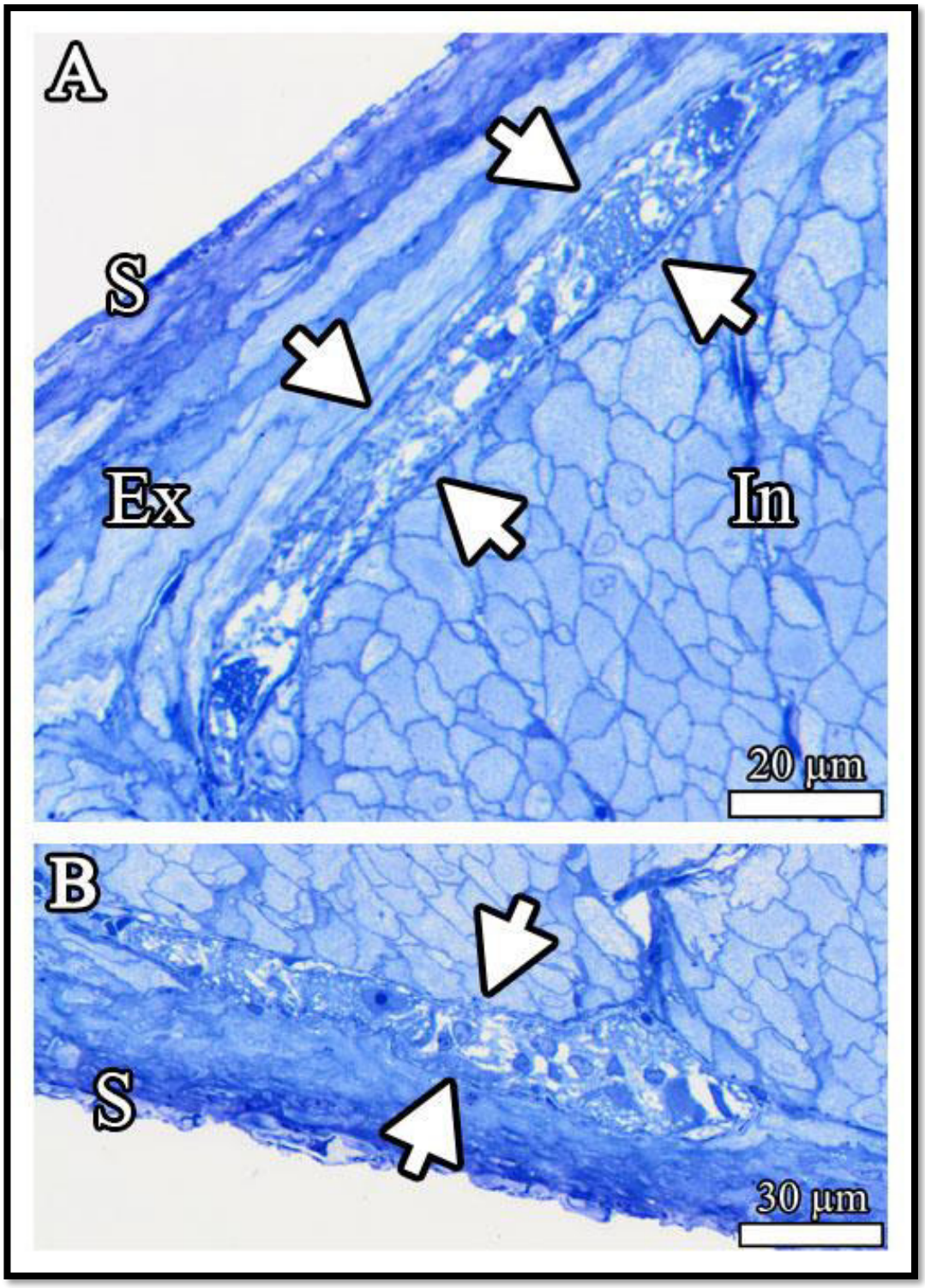

Figure 4. 19. (A, B) The images of muscularis externa that consists of two layers, interna (In) and externa (Ex) of the stomach are observed. This layer is covered by tunica serosa (S). A myenteric plexus between layers of smooth muscles is seen (between arrows). All structures in these layers look healthy. Each muscle cell is covered by a basal membrane (dark lines around muscle cells). Semithin section of resin embedded tissue (0.5 µm thickness) and stained with toluidine blue

4.1.2.1.2. Diclofenac Sodium Group

The apical poles of the cells in the epithelium of this group are densely stained, and such staining is also observed in the gastric pits. There was an enlarged lumen of stomach pits and poor cell structure, with no obvious delineation of cell boundaries and has a smaller nucleus. The boundaries of glands and their lamina propria are difficult to distinguish. Mucosal epithelial erosion is a common occurrence. The apical poles of epithelial cells were frequently shortened, and the gland's lumen was expanded as a result of epithelial erosion. The loss of cytoplasm and the unclear delineation of epithelial cell boundaries are common. The form of nuclei in the epithelium was harmed because spherical/oval nuclei in cells are difficult to see. The connective tissue of the lamina propria is densely stained. The neck mucous cells with a foamy apical region and strongly stained cytoplasm have seen. The nuclei of parietal cells are tiny, even though the cell body is enormous. The majority of these were lightly stained. The glands are surrounded by very loose connective tissue. There are a small number of principal cells with several darkly stained granules near the apical pole of these cells. In the majority of the gland, the parietal cells that were seen lightly/empty structures were dominant. The glandular cells' integrity was severely harmed. In the lamina propria, there are numerous empty spaces and lymphocytic infiltration. The majority of cells in the lamina propria connective tissue were highly dark, and these cells may have lost their function. Architectures of the smooth muscle cells were severely impaired; the boundaries of muscle cells and the basal membrane surrounding them were difficult to see. The ganglionic cells in the myenteric plexus have shrunk significantly, and several vacuoles can be found in this structure. Although several transverse sections of smooth muscle cells were seen in this muscularis externa, only a small proportion of them have nuclei, which could be due to diminishing nuclear size (Figures 4.20-4.30).

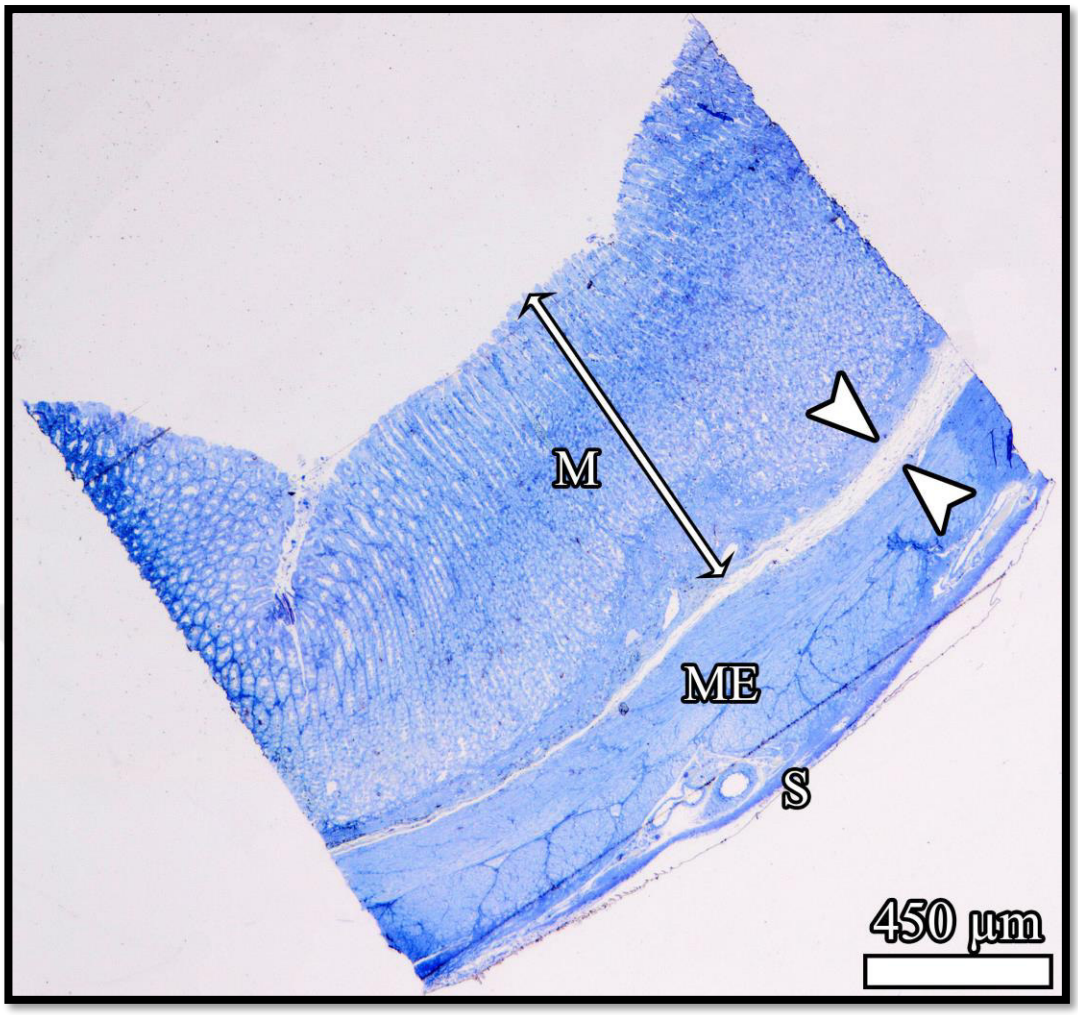

Figure 4. 20. General structure of stomach layers belonging to the diclofenac sodium (DS) group is seen. The mucosa of organ (M), submucosa (arrowheads), muscularis externa (ME), and serosa (S) are observed. Semithin section of resin embedded tissue (0.5 µm thickness) and stained with toluidine blue

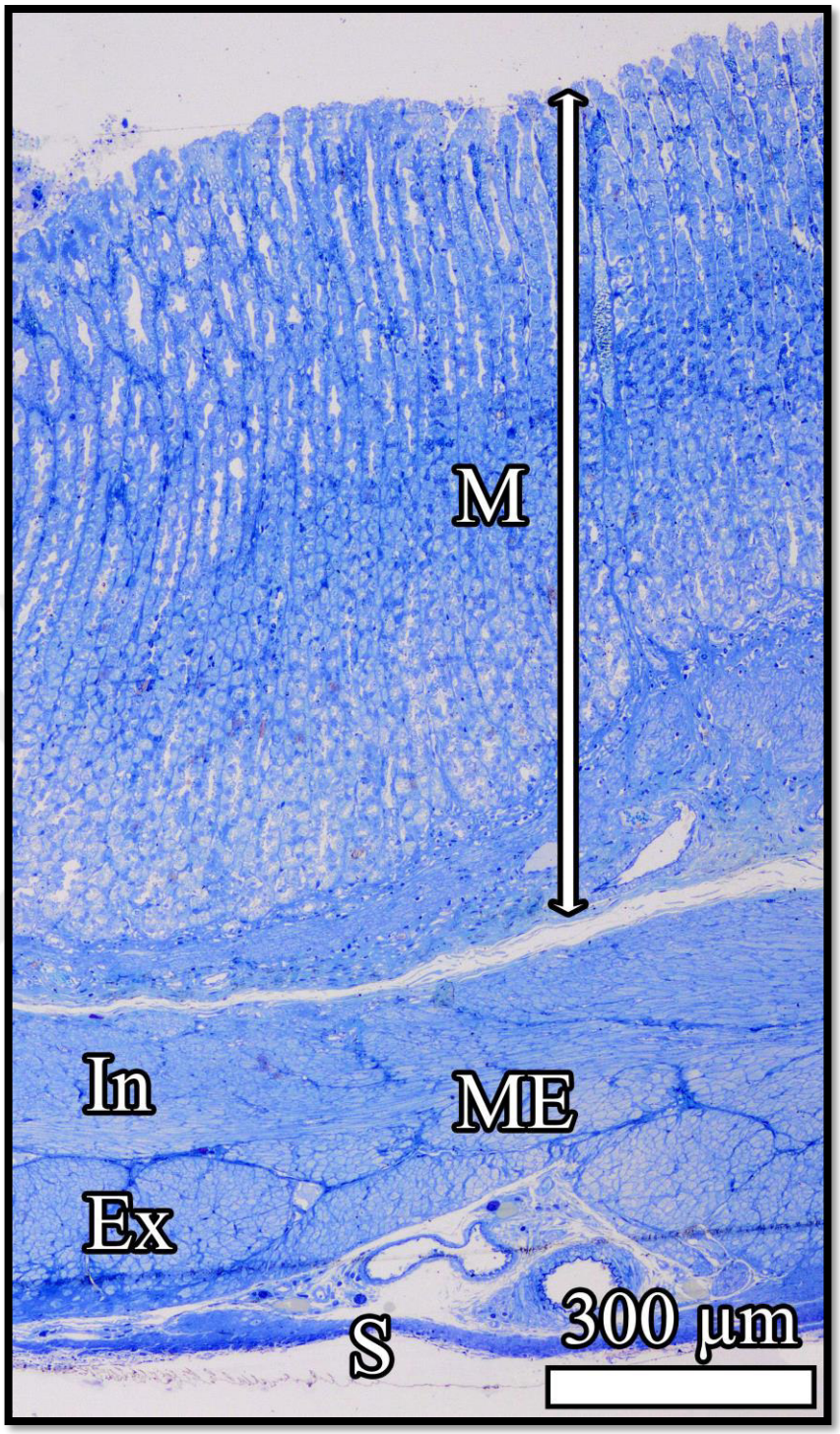

Figure 4. 21. A high magnification of the general structure of stomach layers belonging to the diclofenac sodium group is seen. The mucosa of organ (M), submucosa (arrowheads), muscularis externa (ME), and serosa (S) are observed. Extrinsic (Ex) and intrinsic (In) layers of muscularis externa (ME) can be delineated. Increased lumens of the gastric glands are seen. Semithin section of resin embedded tissue (0.5 µm thickness) and stained with toluidine blue

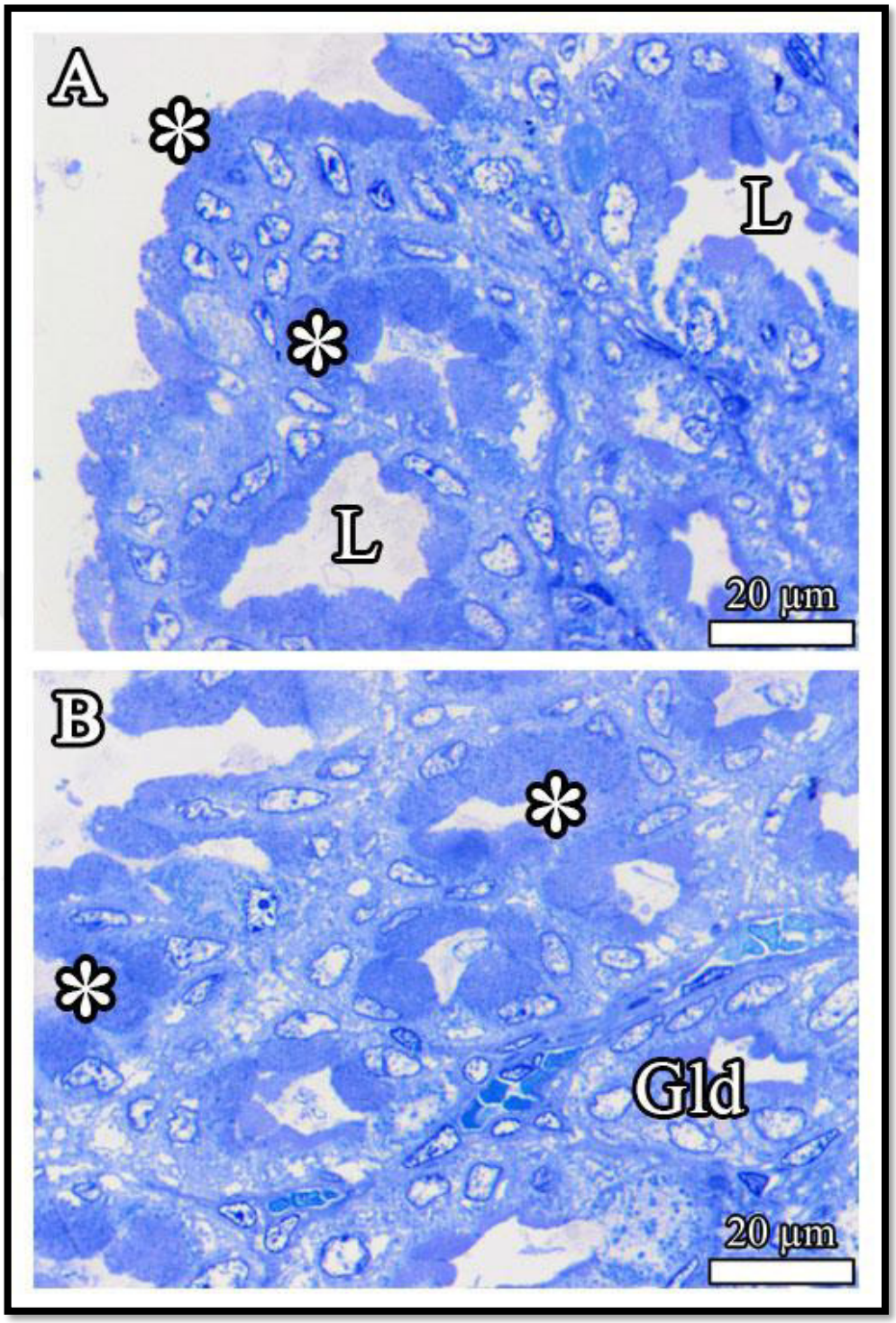

Figure 4. 22. (A, B) A high magnification of the surface epithelium in the stomach belonging to the diclofenac sodium (DS) group is seen. Apical poles of the cells in the epithelium are densely stained (*), and the staining intensity was seen in the gastric pits. An increased lumen (L) of gastric pits (Gld) and impaired cells structure, no clear demarcation of cells borders, and decreased size of nucleus, were observed. It is hard to delineate the borders of glands and their lamina propria. Epithelial erosion in the mucosa is commonly observed. Semithin section of resin embedded tissue (0.5 µm thickness) and stained with toluidine blue

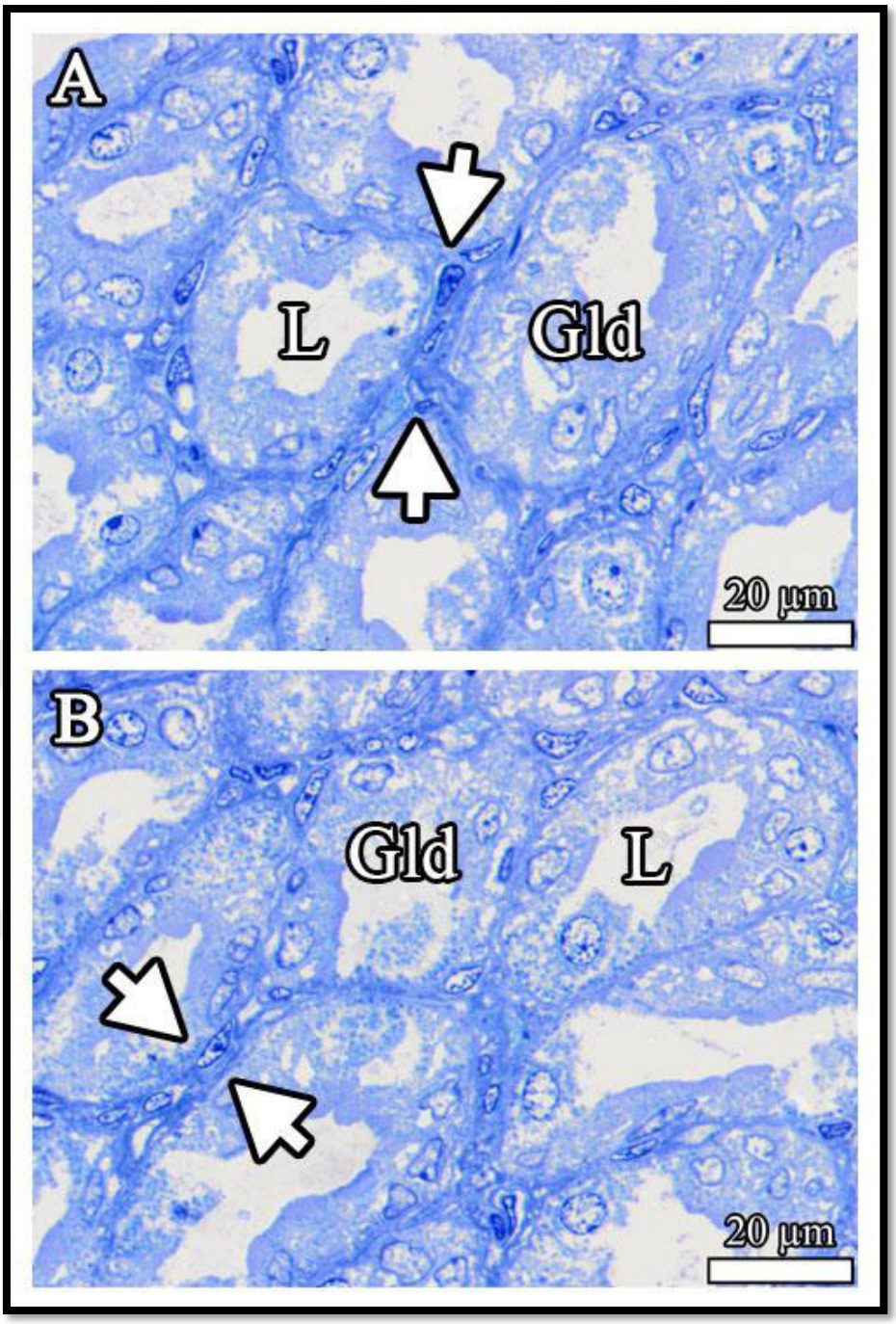

Figure 4. 23. (A, B) A high magnification of transverse sections of the gastric pits (Gld) in the stomach belonging to the diclofenac sodium (DS) group is seen. Apical poles of the cells in the epithelium were commonly truncated as a result of epithelial erosion. Because of apical erosion, the lumen of the gland was increased. Delineation of epithelial cells borders and loss of cytoplasm are commonly observed. The shape of nuclei in the epithelium was impaired since it is hard to see the spherical/oval shape of the nucleus in the cells. The densely stained connective tissue of lamina propria (arrows) is shown. It is hard to delineate the borders of glands and their lamina propria. Epithelial erosion in the mucosa is commonly observed. Semithin section of resin embedded tissue (0.5 µm thickness) and stained with toluidine blue

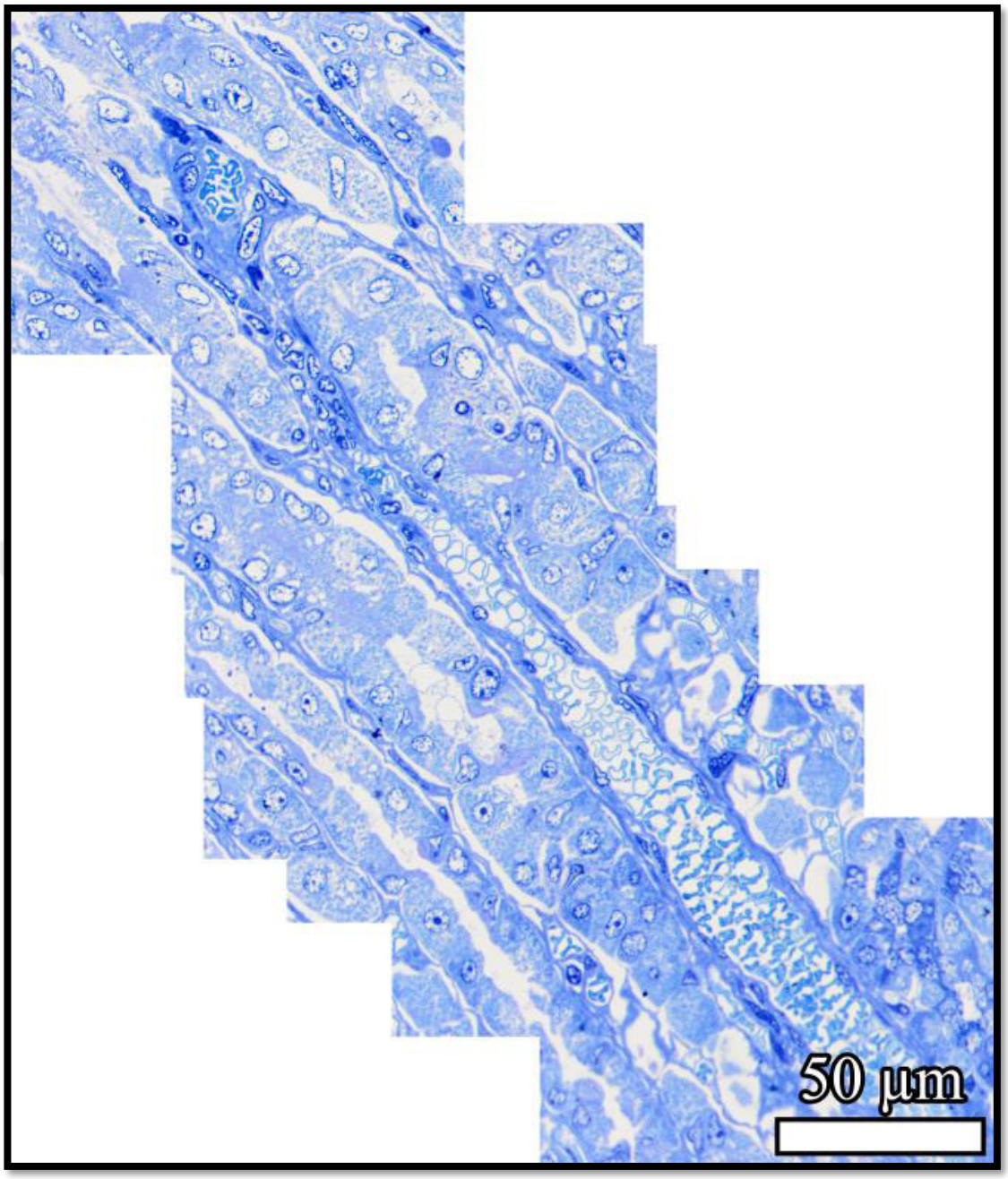

Figure 4. 24. A high magnification of the longitudinal section of the gastric mucosa from the stomach belonging to the diclofenac sodium (DS) group is seen. Because of apical poles of the cells in the epithelium were commonly truncated as a result of it, glands have increased the size of the gland lumen. Although nuclei of glandular cells can be observed, the delineation of epithelial cells borders is hardly seen. Intensely staining of the connective tissue in the lamina propria is seen. Semithin section of resin embedded tissue (0.5 µm thickness) and stained with toluidine blue

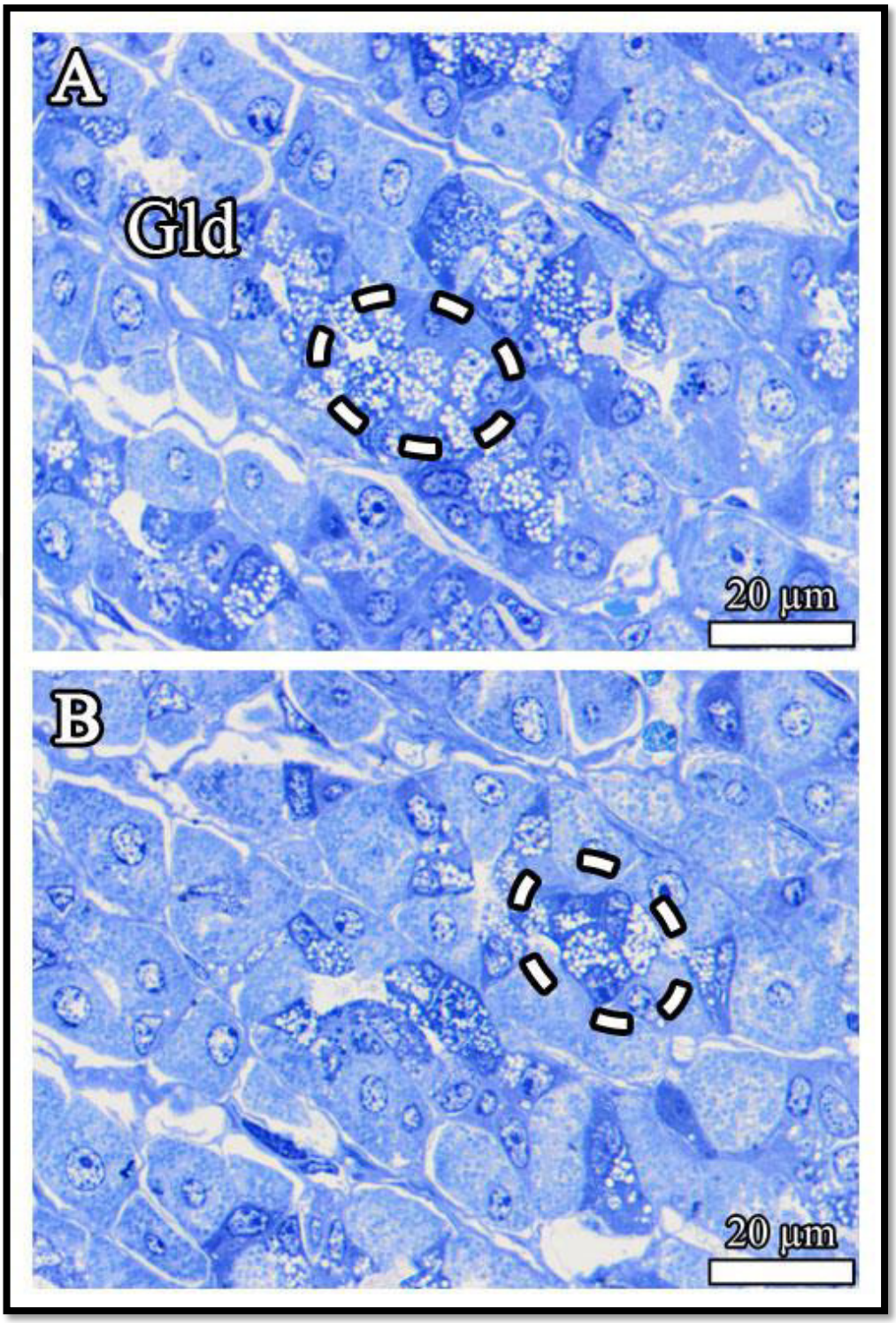

Figure 4. 25. (A, B) High magnification images of a longitudinal section of the gastric glands (Gld) from the stomach belonging to the diclofenac sodium (DS) group are seen. Augmentation of neck mucous cells (dashed circled area) that have a foamy apical part and densely stained cytoplasm are observed. Although having a large size of cell body but the small size of nuclei is found in the parietal cells. Most of these were stained lightly. A very loose connective tissue is found around the glands. Semithin section of resin embedded tissue (0.5 µm thickness) and stained with toluidine blue

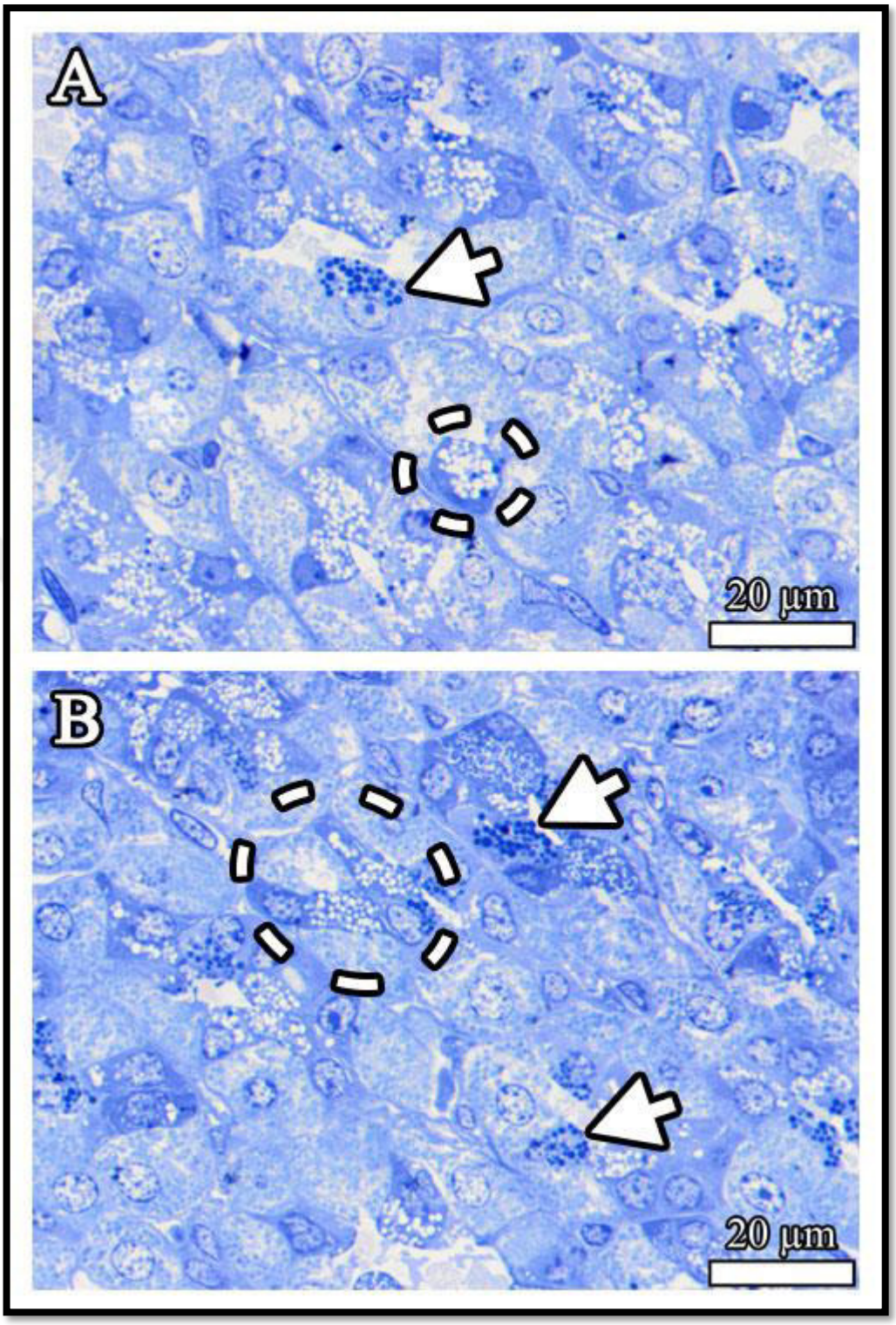

Figure 4. 26. (A, B) Images of the gastric glands from the stomach belonging to the diclofenac sodium (DS) group are observed. In some areas of the gland, augmentations of neck mucous cells (dashed circled area) that have a foamy apical part and densely stained cytoplasm are seen. Although having a large size of cell body but the small size of nuclei is found in the parietal cells. Most of these were stained lightly. Enlarged lumens of glands are also seen. Few numbers of the chief cells that have many darkly stained granules at the apical pole of these cells are observed. Semithin section of resin embedded tissue (0.5 µm thickness) and stained with toluidine blue

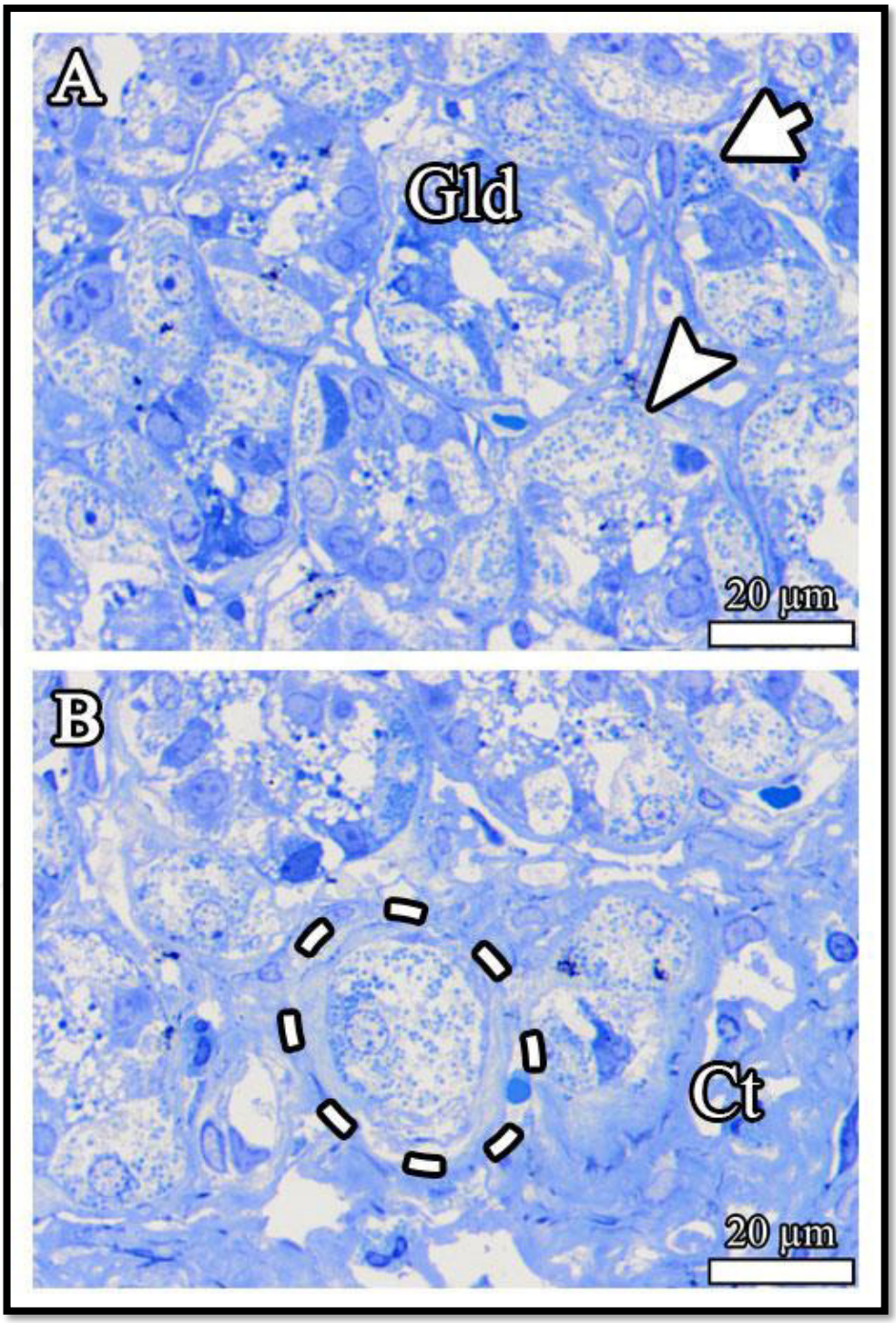

Figure 4. 27. (A, B) Transverse sections from the base of gastric glands (Gld) group are observed. The dominancy of the parietal cells that were seen lightly/empty structures was observed in most areas of the gland (arrowhead). The huge size of the parietal cell is shown (dashed circled area). The integrity of glandular cells was seriously impaired. It is hard to see the chief cells. The elements of connective tissue (Ct) cannot be seen clearly. Semithin section of resin embedded tissue (0.5 µm thickness) and stained with toluidine blue

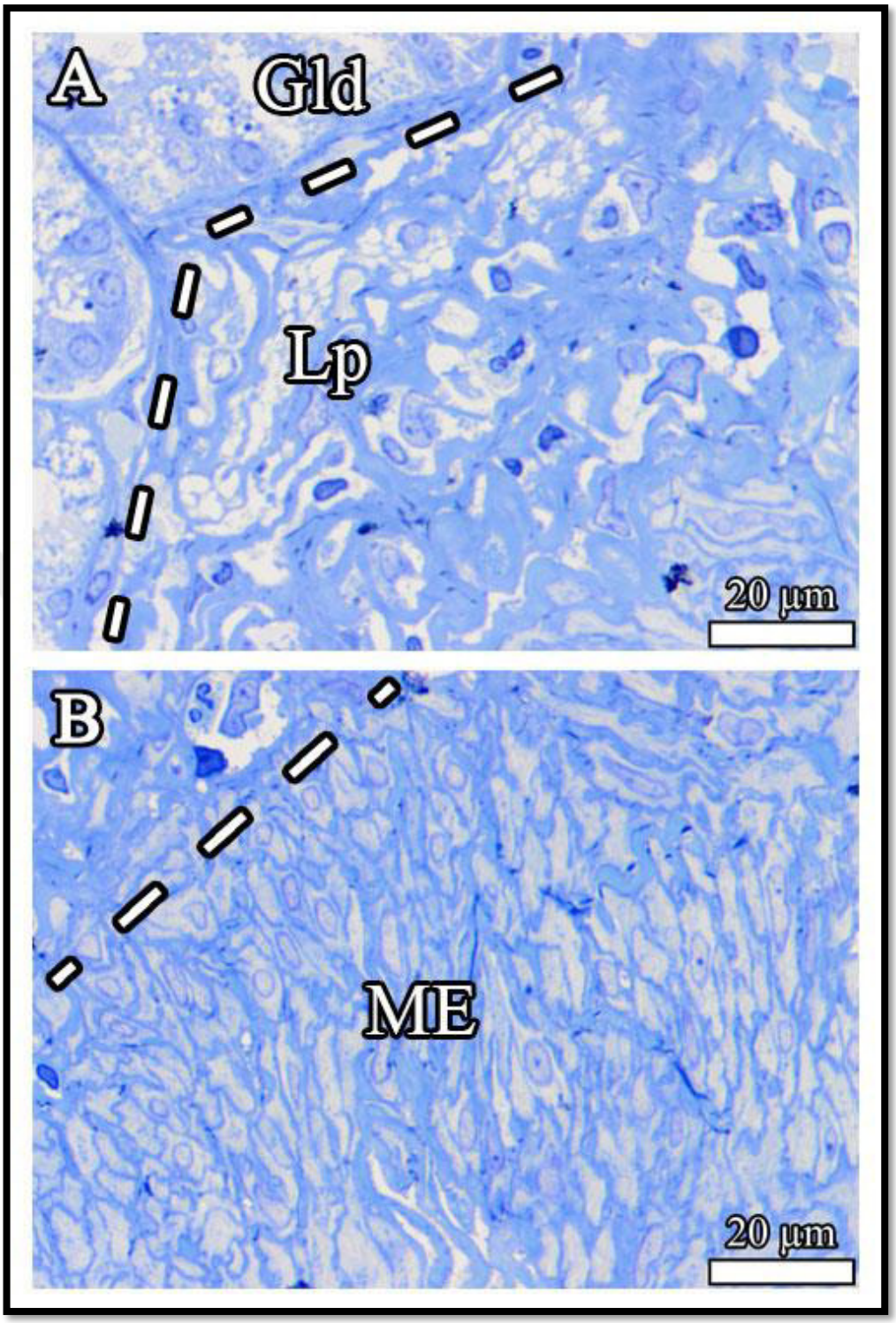

Figure 4. 28. (A) A transverse section from the base of gastric glands (Gld) and lamina propria (Lp) in the stomach belonging to the diclofenac sodium (DS) group is seen. There are many empty spaces and lymphocytic infiltration in this layer. Most of the cells in the connective tissue of lamina propria (Lp) were densely stained and these cells might lose their function. **(B)** Smooth muscle cells of the muscularis externa (ME) are seen. The structures of these cells were seriously impaired; it is hard to see the borders of muscle cells and the basal membrane around them. Semithin section of resin embedded tissue (0.5 µm thickness) and stained with toluidine blue

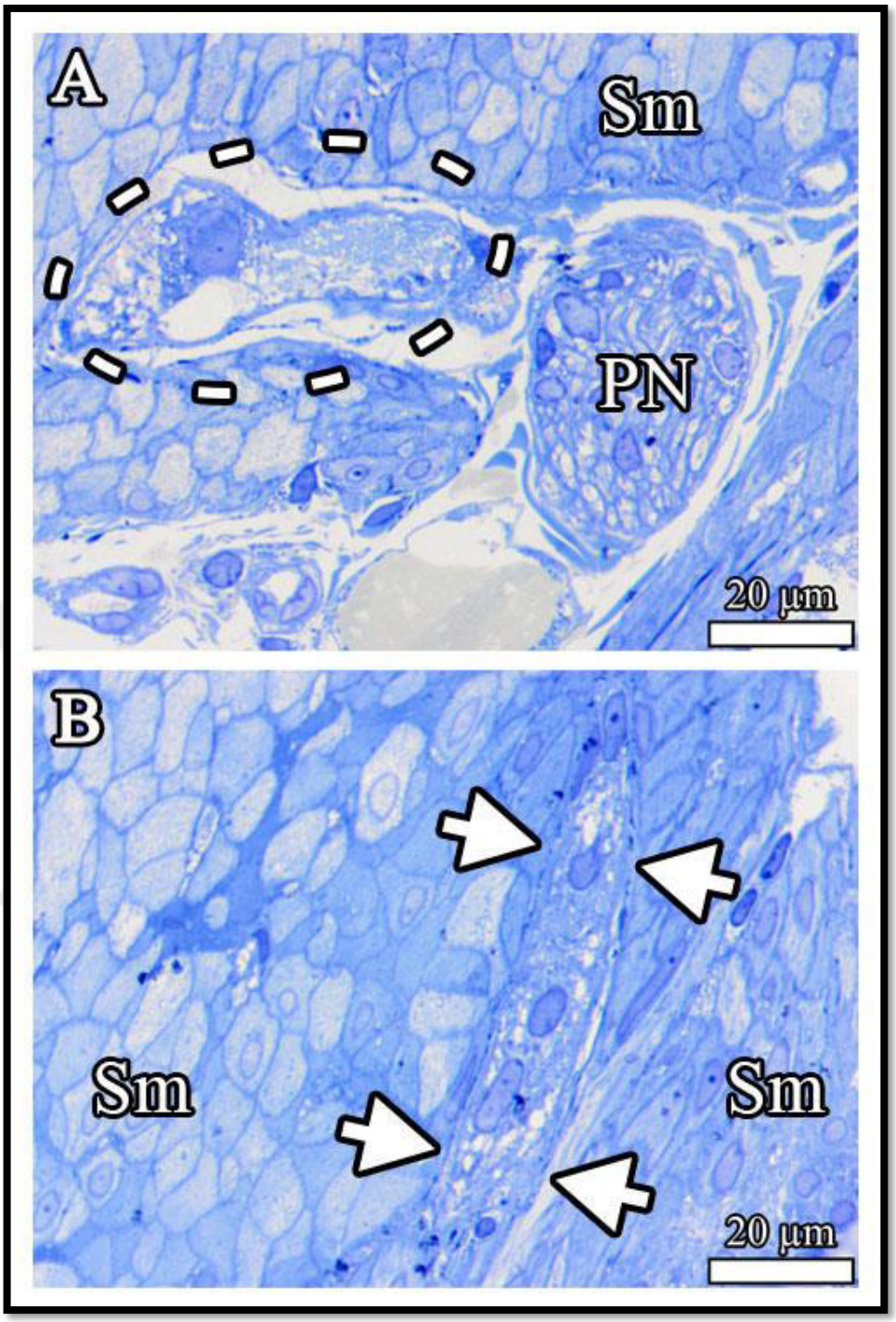

Figure 4. 29. (A) A transverse section from the muscularis externa of the stomach belonging to the diclofenac sodium (DS) group is seen. Sections of the myenteric plexus (dashed circled area) and peripheral nerve (PN) in the muscle layer are observed. Ganglionic cell in the plexus was seriously shrinkage and there are many vacuoles are seen in this structure. Although there are many transverse sections of muscle cells (Sm) in this section were observed, a few numbers of them have a nucleus, this might be a result of decreasing nuclear size. **(B)** A cross-section of muscularis externa, between smooth muscle cells (Sm), ganglionic cells in the partly protected myenteric plexus are shown (arrows). Semithin section of resin embedded tissue (0.5 µm thickness) and stained with toluidine blue

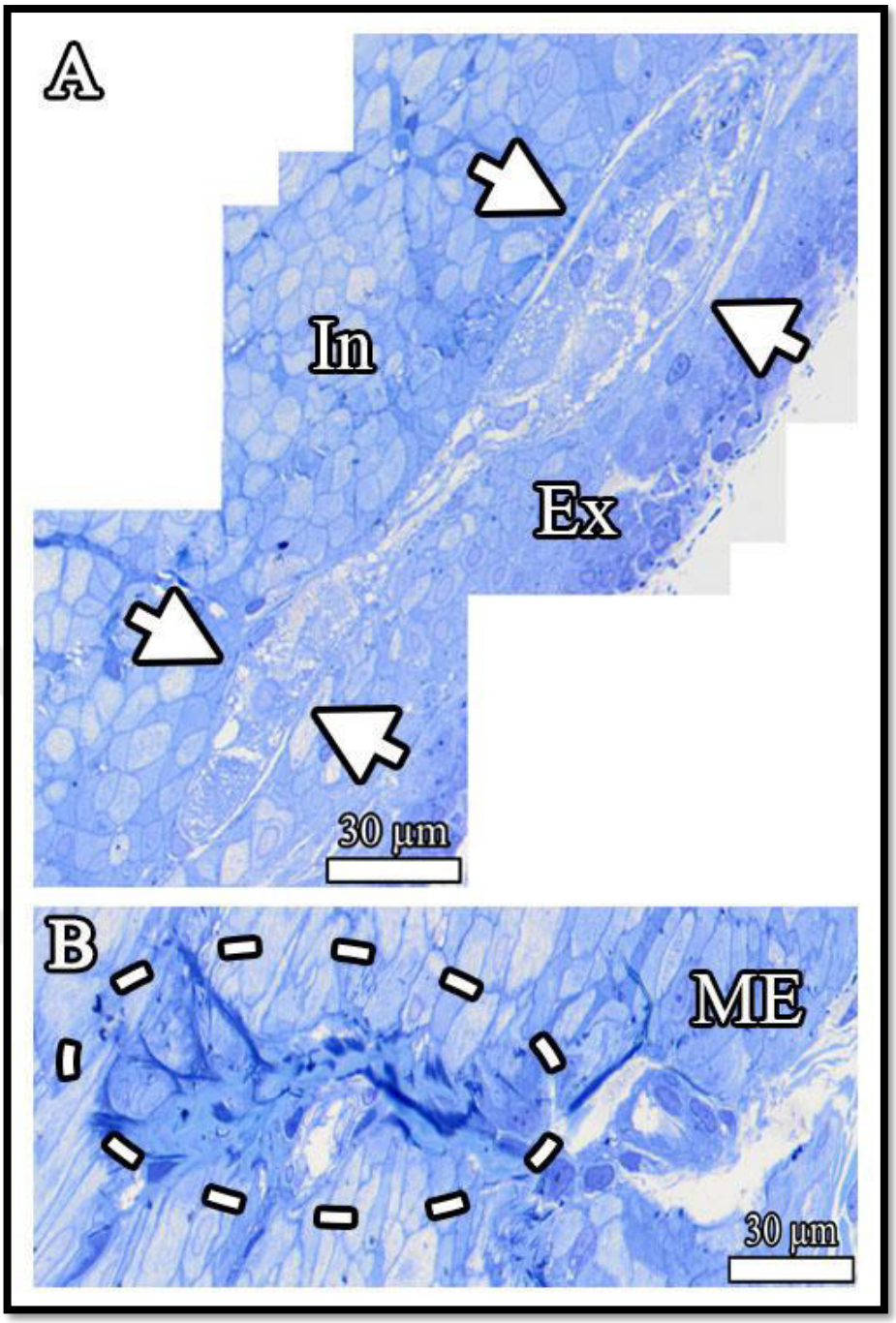

Figure 4. 30. (A) A transverse section from the muscularis externa of the stomach belonging to the diclofenac sodium (DS) group is seen. A very long section of the myenteric plexus (arrows) is observed between the internal and external layers of the muscle layer are observed. Ganglionic cells in the plexus were seriously shrinkage and there are many vacuoles are found in the plexus. Although there are many transverse sections of muscle cells (Sm) in this image were observed, a few numbers of them have a nucleus, this might be a result of decreasing nuclear size. **(B)** Peripheral nerve section (darkly stained) in muscularis externa, is shown (dashed elliptical area). Semithin section of resin embedded tissue (0.5 µm thickness) and stained with toluidine blue

4.1.2.1.3. Diclofenac Sodium + Gum Arabic Group

The glands in the organ mucosa, submucosa, and muscularis externa are seen intact in this group. All layers can be distinguished and appear to be healthy. The muscularis mucosae are observed to be intact. Although the surface epithelium is somewhat shielded, densely stained apical poles of the epithelial cells are visible, and the staining intensity was also seen in the stomach pits. Although parietal cells had a normal appearance, the gland's principal cells were extensively stained. These cells may lose the majority of their functionality. The neck mucous cells with a foamy apical region and darkly stained cytoplasm have augmented in some regions in the gastric gland. The lumens of gastric gland have been partially expanded. The parietal cells of the gastric gland are healthy and have a big cell body size. The majority of these cells were weakly stained. In the glands, it's difficult to tell the difference between the principal cells. Around the glands lies a lamina propria, which has a very loose connective tissue. It's difficult to find the difference between the chief cells and the neck mucous cells in the glands; a dense clump of cells could be chief cells, but some of them could also be neck mucous cells. The submucosa, muscularis mucosae, and lamina propria layers are all in good morphology. The lamina propria has a very loose connective tissue. All layers of the stomach, including the lamina propria, muscularis mucosae, submucosa, muscularis externa, and serosa, are healthy in this group (Figures 4.31-4.40).

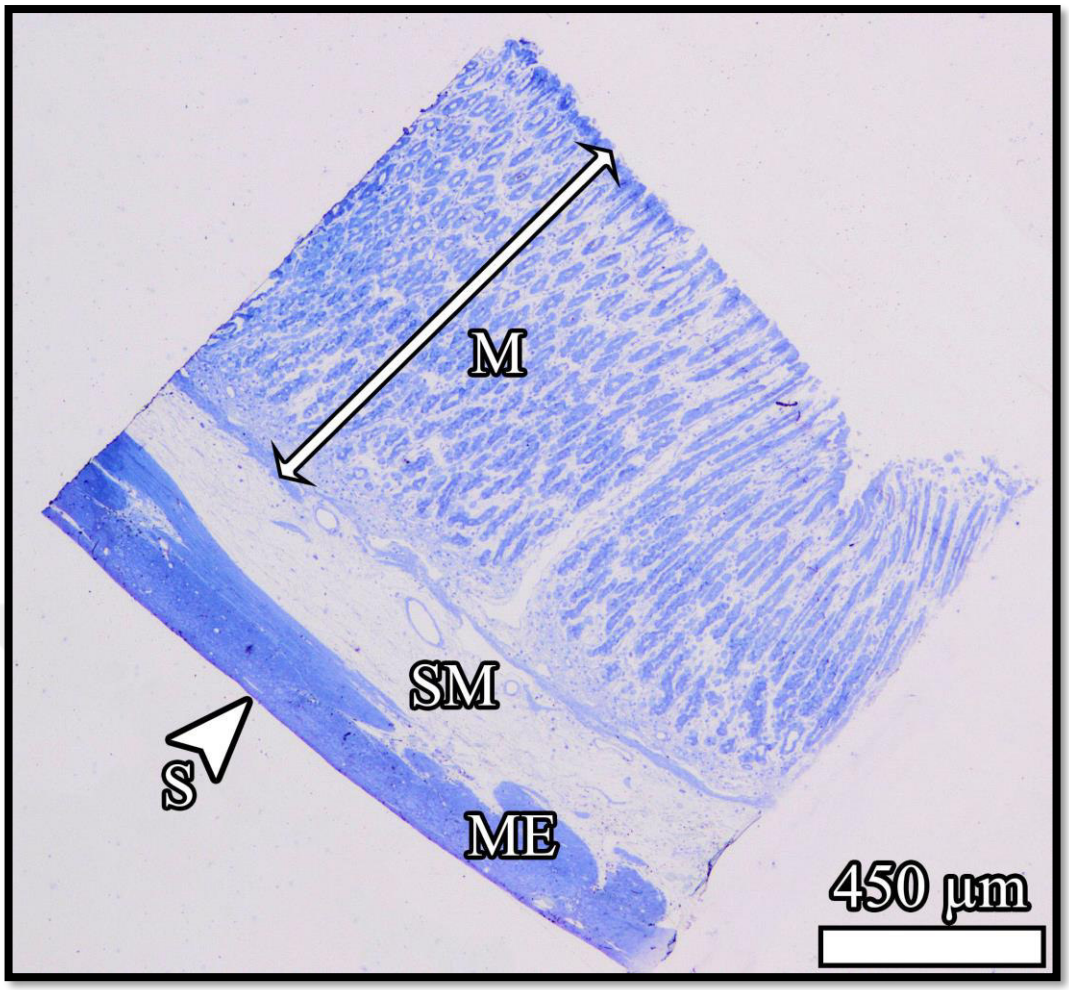

Figure 4. 31. General structure of stomach layers belonging to the diclofenac sodium + gum Arabic (DS + GA) group is seen. The mucosa of organ (M), submucosa (SM), muscularis externa (ME) and serosa (S) are observed. Semithin section of resin embedded tissue (0.5 µm thickness) and stained with toluidine blue

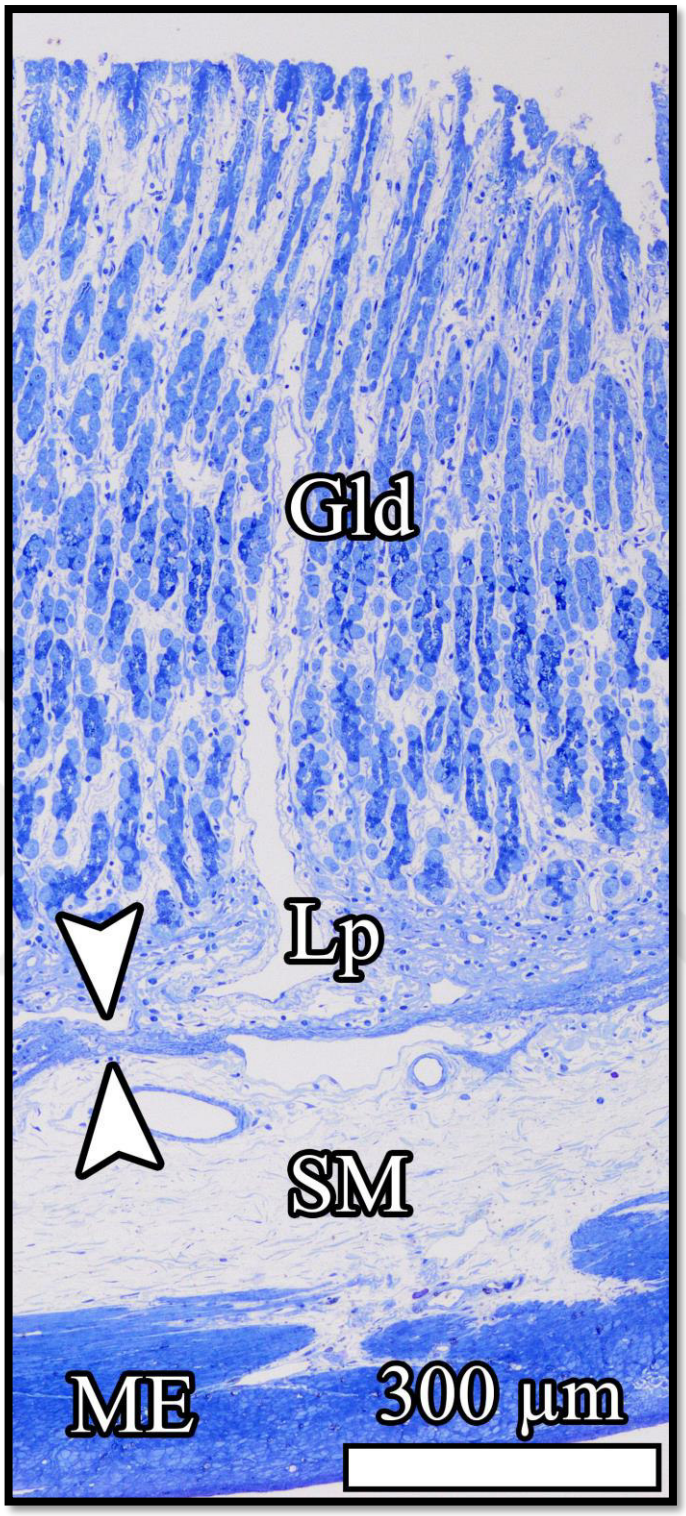

Figure 4. 32. A high magnification of the general structure of stomach layers belonging to the diclofenac sodium + gum Arabic (DS + GA) group is seen. The glands in the mucosa of the organ (Gld), submucosa (SM), and muscularis externa (ME) are observed. All layers can be delineated and look healthy. Intact muscularis mucosae are seen (arrowheads). (Lp) Lamina propria. Semithin section of resin embedded tissue (0.5 µm thickness) and stained with toluidine blue

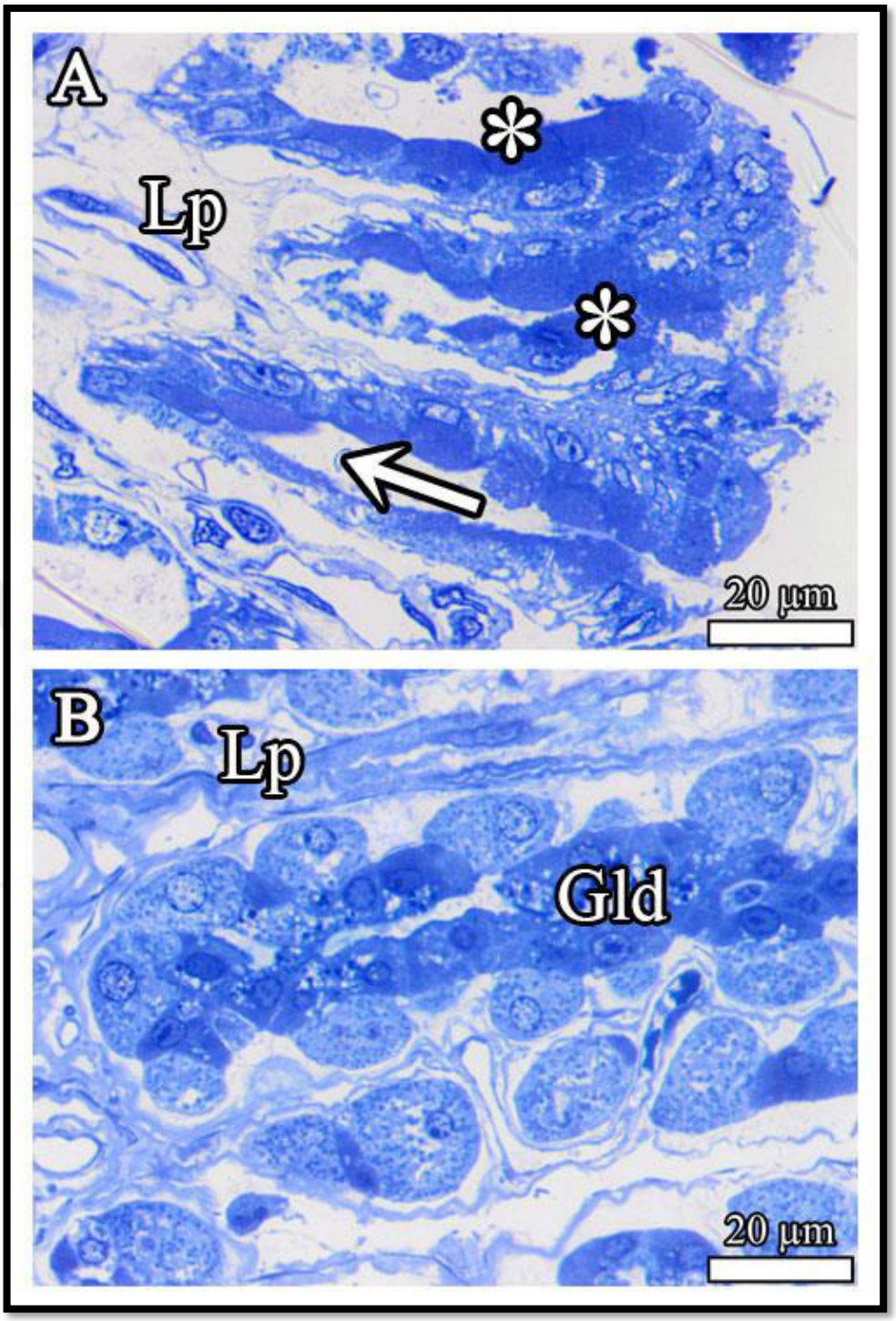

Figure 4. 33. **(A, B)** High magnification images of the general structure of stomach mucosal layers belonging to the diclofenac sodium + gum Arabic (DS + GA) group are seen. Although partly protected surface epithelium is observed, densely stained apical poles of the cells in the epithelium are seen (*), and the staining intensity was also seen in the gastric pits (arrow). **(B)** Gastric glands (Gld) and connective tissue of lamina propria (Lp) look healthy, although parietal cells have normal morphology, most of the chief cells in the gland were densely stained. These cells might lose most of their function. Semithin section of resin embedded tissue (0.5 µm thickness) and stained with toluidine blue

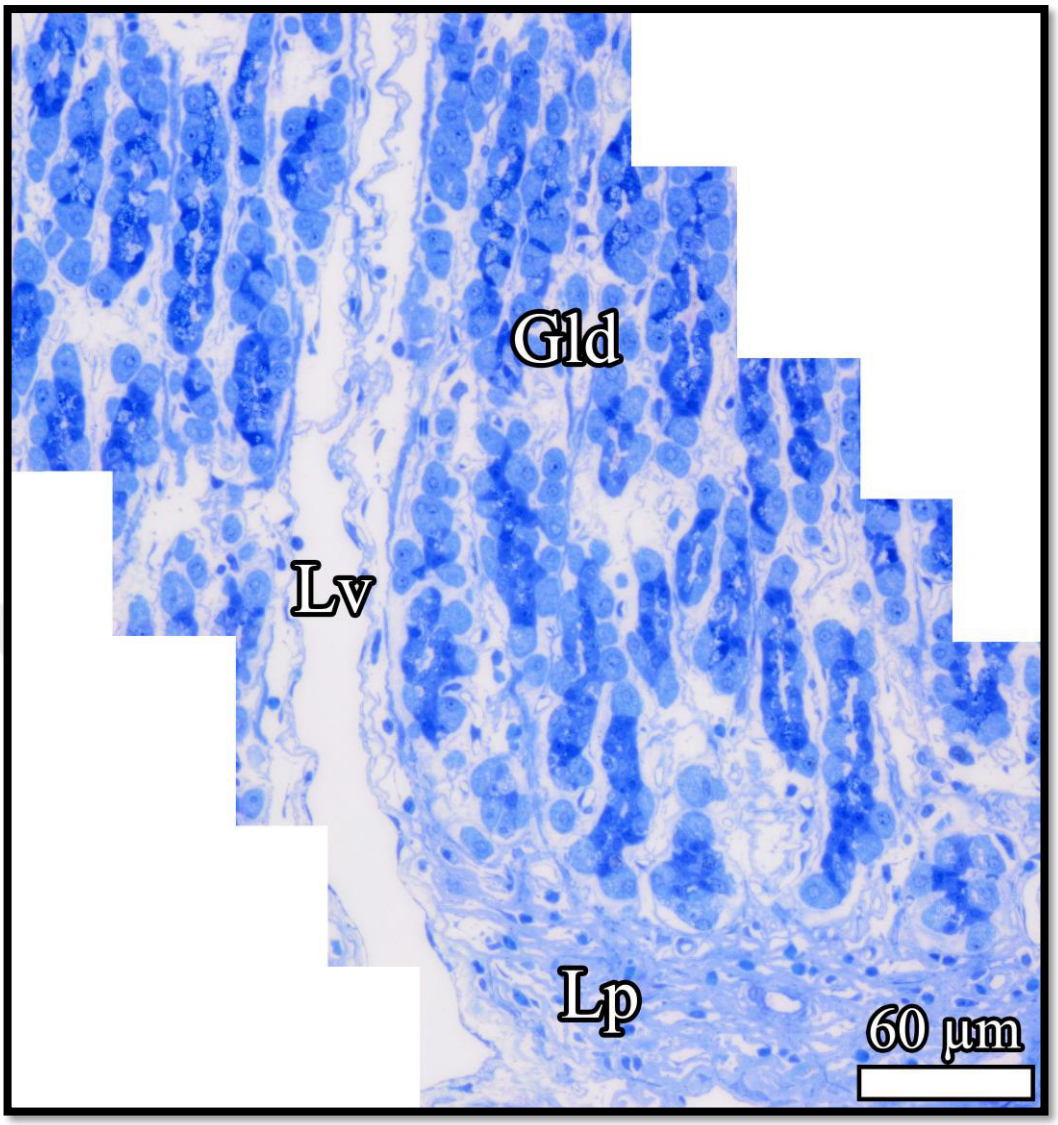

Figure 4. 34. High magnification image of the general structure of stomach mucosal layers belonging to the diclofenac sodium + gum Arabic (DS + GA) group is seen. Although most of the structures in this region have a protected structures but densely stained cells in the glands (Gld). Increased size of the gland lumen can be observed in some glands. A large size lymphatic vessel (Lv) is seen in the lamina propria (Lp). Semithin section of resin embedded tissue (0.5 µm thickness) and stained with toluidine blue

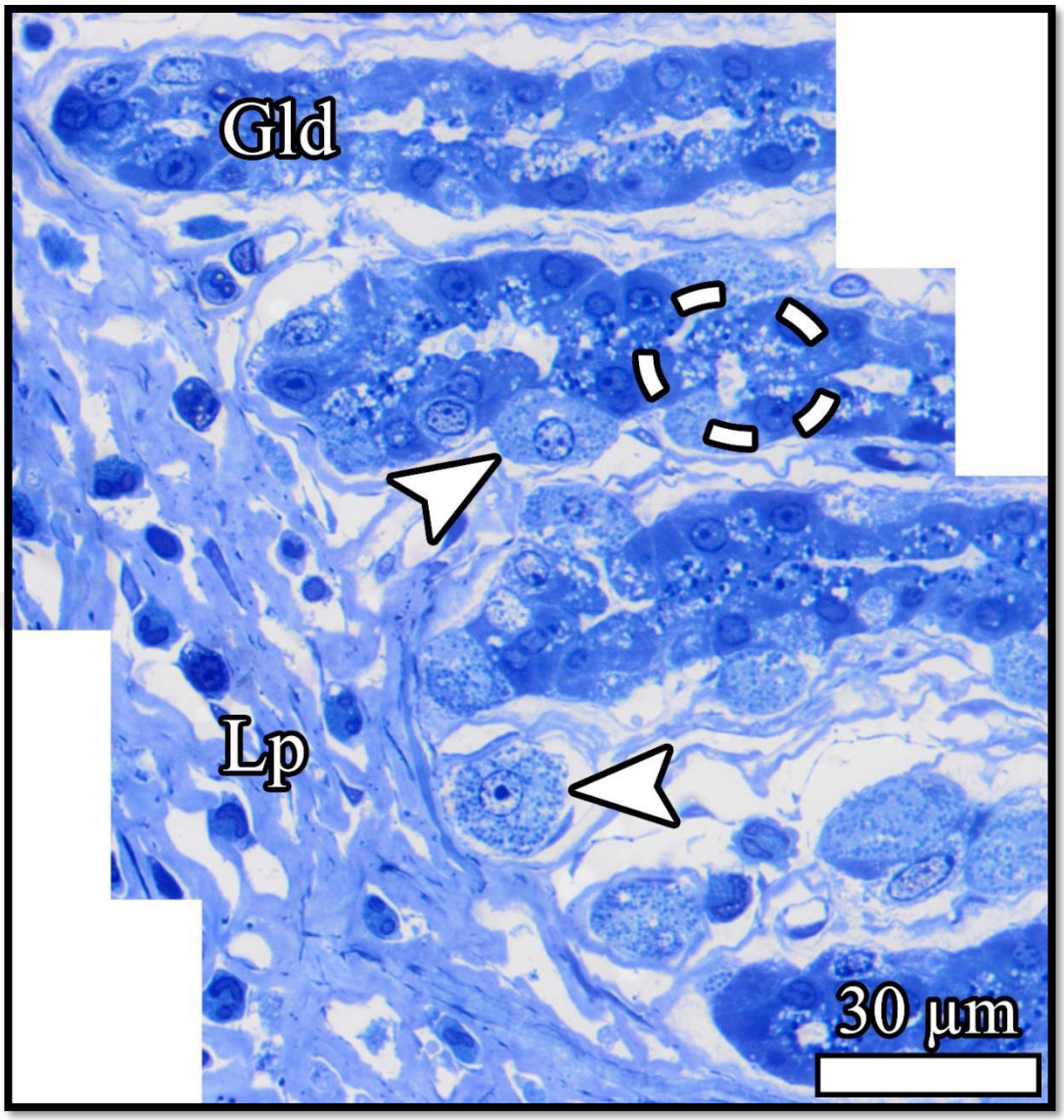

Figure 4. 35. A high magnification image of the general structure of the stomach mucosal layer belonging to the diclofenac sodium + gum Arabic (DS + GA) group is seen. Augmentation of neck mucous cells (dashed circled area) that have a foamy apical part and densely stained cytoplasm are observed. The lumens of gastric glands are partly increased. The parietal cells (arrowhead) of the gastric gland have a healthy structure and have a large size of the cell body. Most of these cells were stained lightly. It is hard to differentiate chief cells in the glands. A very loose connective tissue (Lp) is found around the glands (Gld). Semithin section of resin embedded tissue (0.5 µm thickness) and stained with toluidine blue

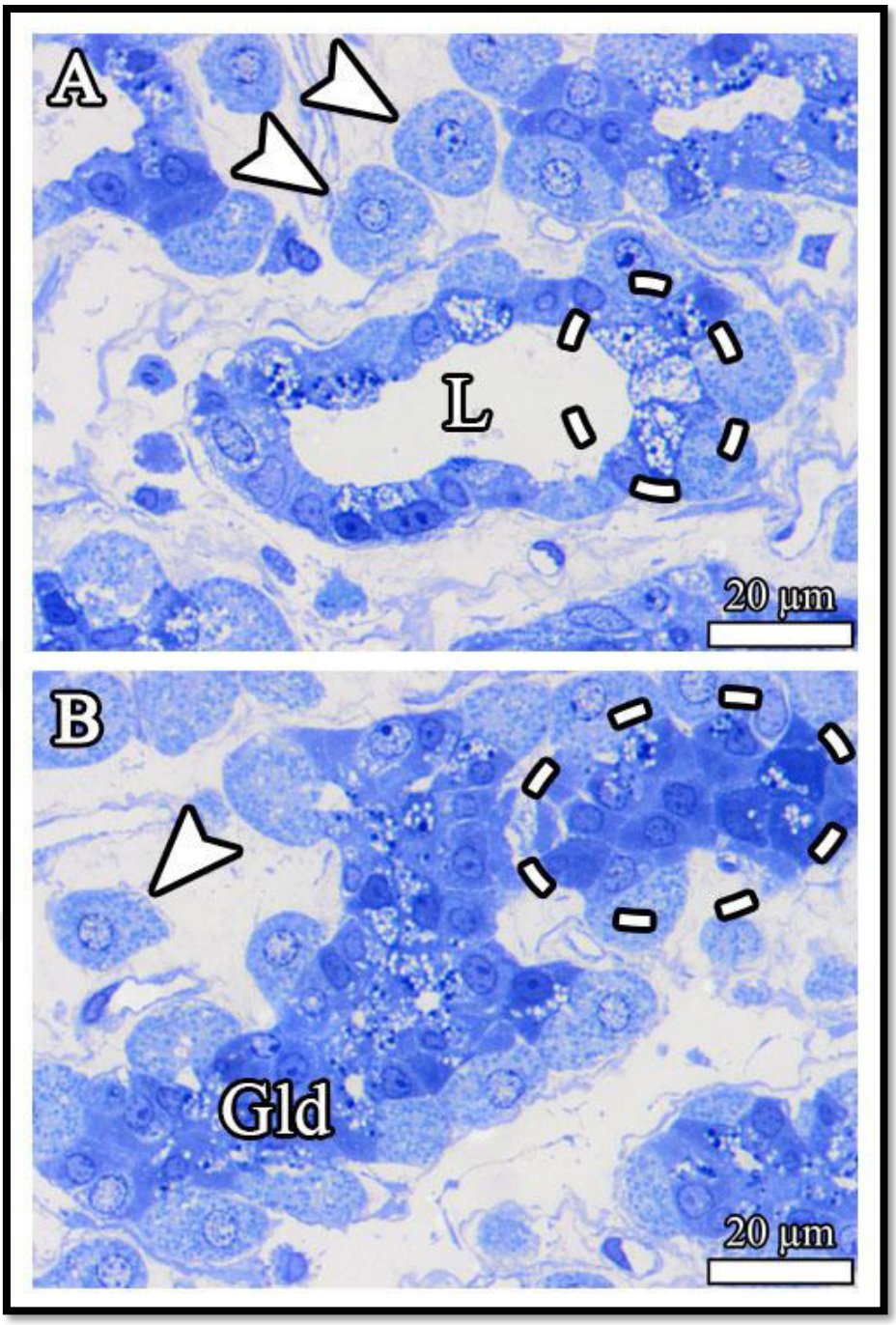

Figure 4. 36. (A, B) High magnified images of the glands (Gld) in the stomach belonging to the diclofenac sodium + gum Arabic (DS + GA) group are seen. **(A)** Augmentation of neck mucous cells (dashed circled area) that have a foamy apical part and densely stained cytoplasm are observed. The lumen of the gland (L) was seriously increased. The parietal cells (arrowhead) in the gastric gland have a healthy structure and have a large size of the cell body. Most of these cells were stained lightly. **(B)** A gastric gland (Gld) is seen, and a big size of parietal cells locates at the periphery of the gland. It is hard to differentiate the chief cells in the glands, a dark accumulation of the cells group might be chief cells and some of them might be also neck mucous cells (dashed circled area). A very loose connective tissue is found around the glands. Semithin section of resin embedded tissue (0.5 µm thickness) and stained with toluidine blue

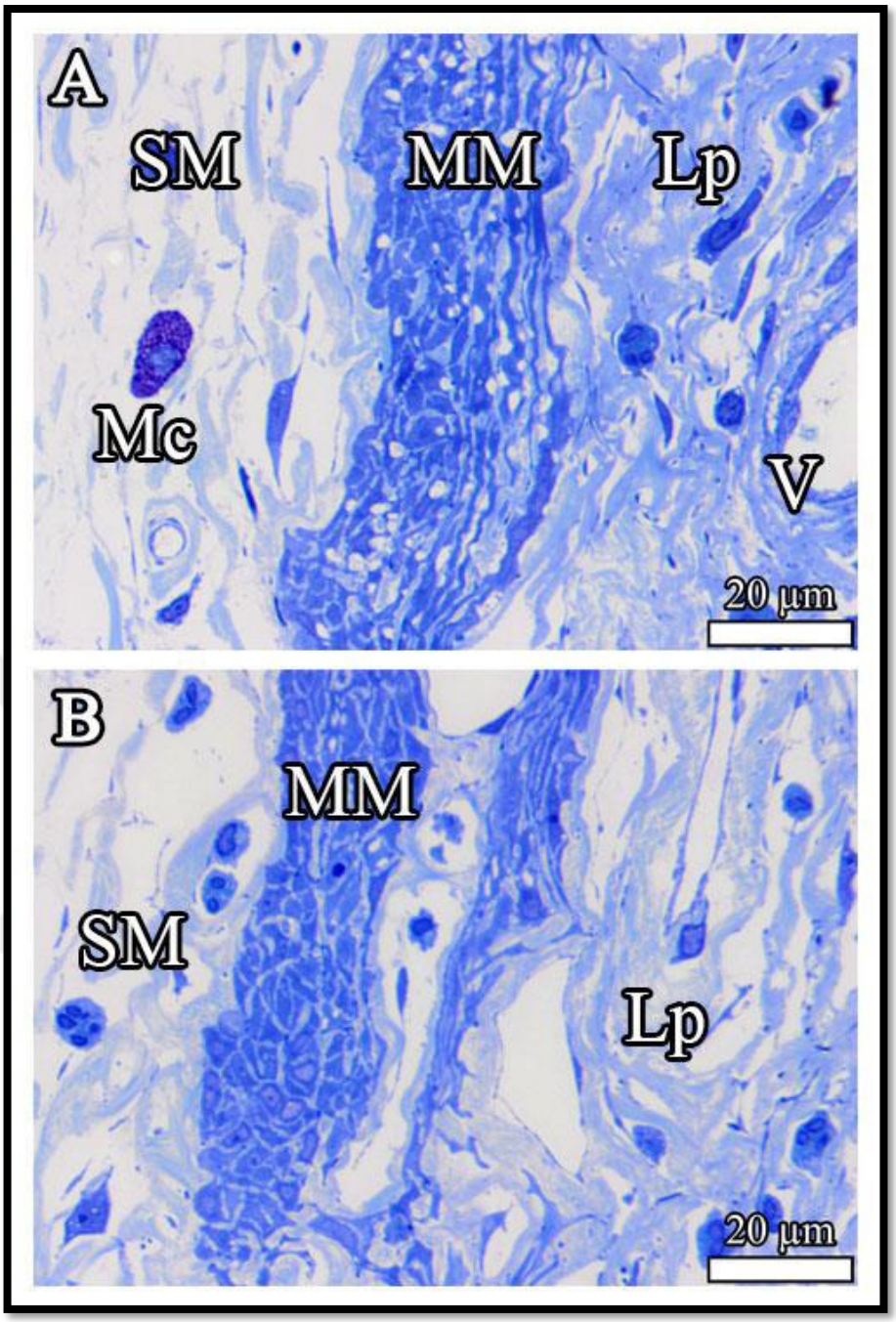

Figure 4. 37. (A, B) Images of the stomach layers belonging to the diclofenac sodium + gum Arabic (DS + GA) group are seen. At the center of the images, the muscularis mucosae (MM) of the mucosa layer is observed. Submucosa (SM), MM, and lamina propria (Lp) layers have a healthy structure. A very loose connective tissue is found in the (Lp). (Mc), mast cell; (V), vessel. Semithin section of resin embedded tissue (0.5 µm thickness) and stained with toluidine blue

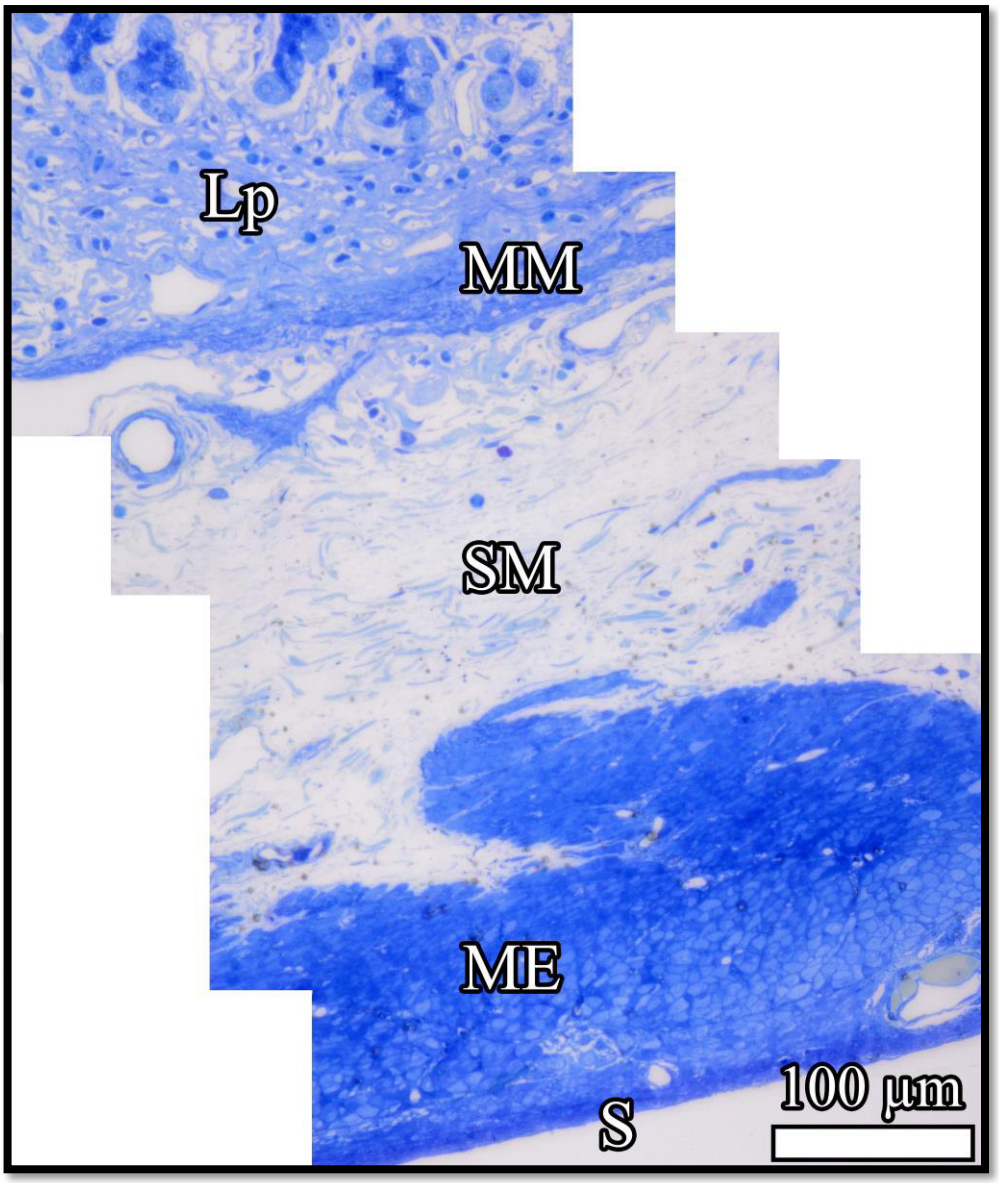

Figure 4. 38. An image of the stomach wall layers belonging to the diclofenac sodium + gum Arabic (DS + GA) group is seen. All of the layers of the stomach, including lamina propria (Lp), muscularis mucosae (MM), submucosa (SM), muscularis externa (ME), and serosa (S) are observed healthy. Semithin section of resin embedded tissue (0.5 µm thickness) and stained with toluidine blue

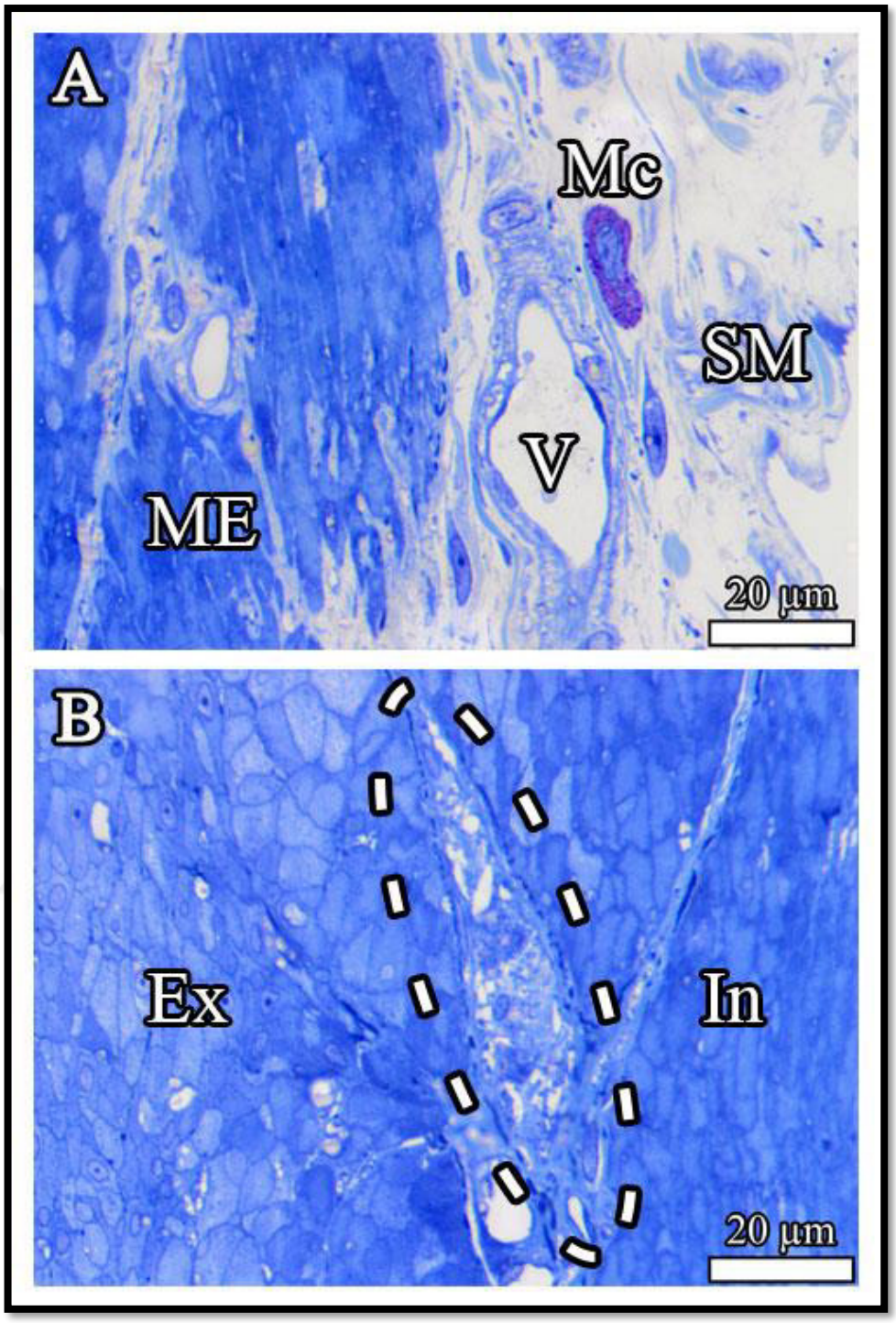

Figure 4. 39. (A, B) Images of the stomach wall layers that are submucosa (SM) and muscularis externa (ME) belonging to the diclofenac sodium + gum Arabic (DS + GA) group are seen. Both layers are found healthy. A large size of mast cells (Mc) and vessel (V) are observed in the submucosa. A part of the myenteric plexus is found between the externa (Ex) and interna (In) layers of muscularis externa (dashed elliptical area). Semithin section of resin embedded tissue (0.5 µm thickness) and stained with toluidine blue

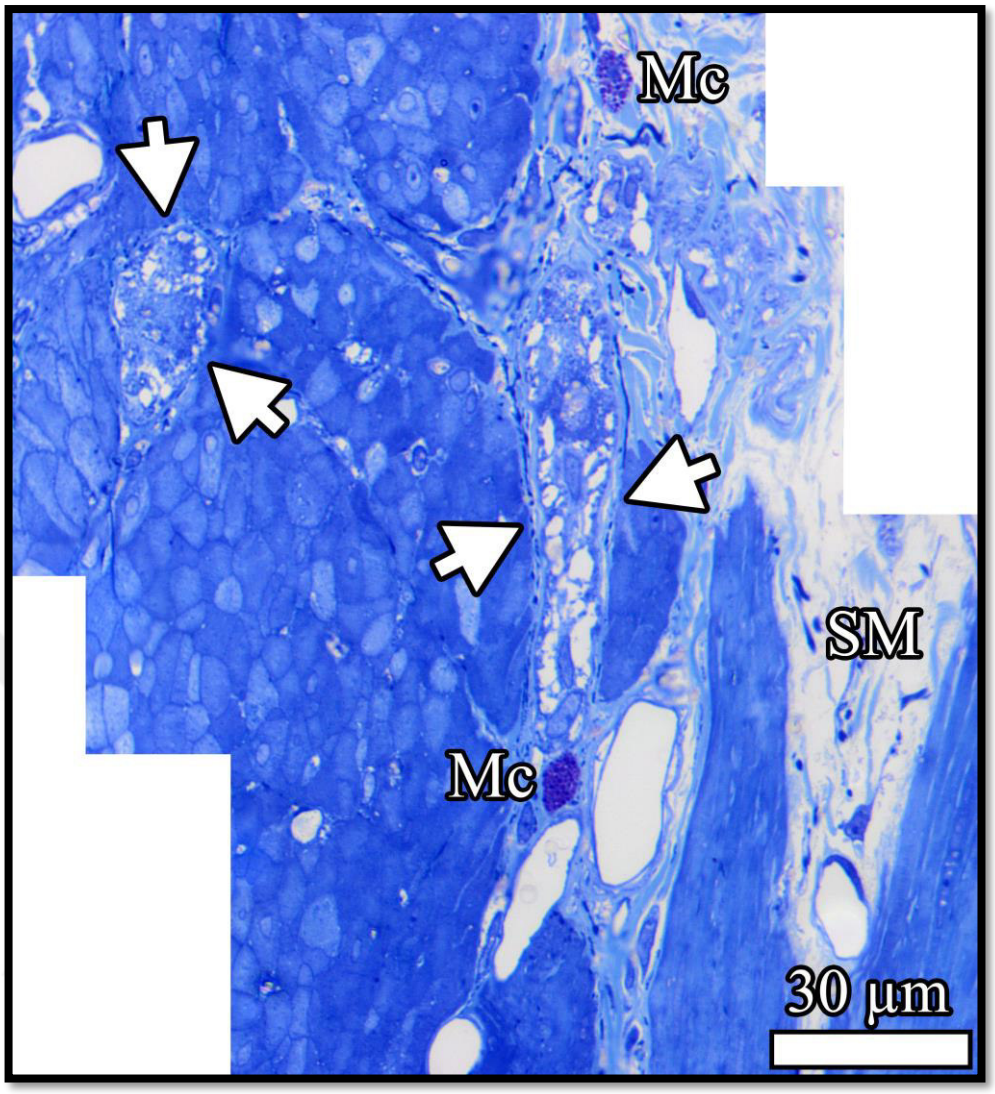

Figure 4. 40. An image of the stomach layers that are submucosa (SM) and muscularis externa (ME) belonging to the diclofenac sodium + gum Arabic (DS + GA) group is seen. Although both layers look healthy, but in some areas, densely stained transected muscle fibers are observed. Mast cells (Mc) and vessels are observed in the submucosa. A part of the myenteric plexus is found between the layers of muscularis externa (arrows). Semithin section of resin embedded tissue (0.5 µm thickness) and stained with toluidine blue

4.1.2.1.4. Gum Arabic Group

The entire structure of the stomach of this group is healthy and well protected. The glandular layer of the organ remains intact, including a portion of the mucosa, submucosa, and muscularis externa. The morphology of the muscularis mucosae is normal. Although the surface epithelium and glandular cells appear healthy but the apical aspect of the epithelium has intense staining. The pits in the stomach are likewise well protected. The lumen of some gastric glands is dilated. Whereas the glandular cells appear healthy, the lumen of several gastric glands is swollen. Large size parietal cells can be easily identified, and some of the darkly stained cells appear to be the neck mucosa cells due to the numerous foamy granules at the apical pole of them. The loose connective tissue of the lamina propria surrounds each gastric gland. The arteries, surrounding connective tissue, and smooth muscles all appear to be in good shape. Because each layer of the vessel can be seen clearly, vessels of all diameters have a normal shape. Smooth muscle cells have a well-structured basement membrane surrounding them, and a transverse section of the nucleus can be seen near the cell's center in some muscle cells. A myenteric plexus is visible between smooth muscles (Figures 4.41-4.49).

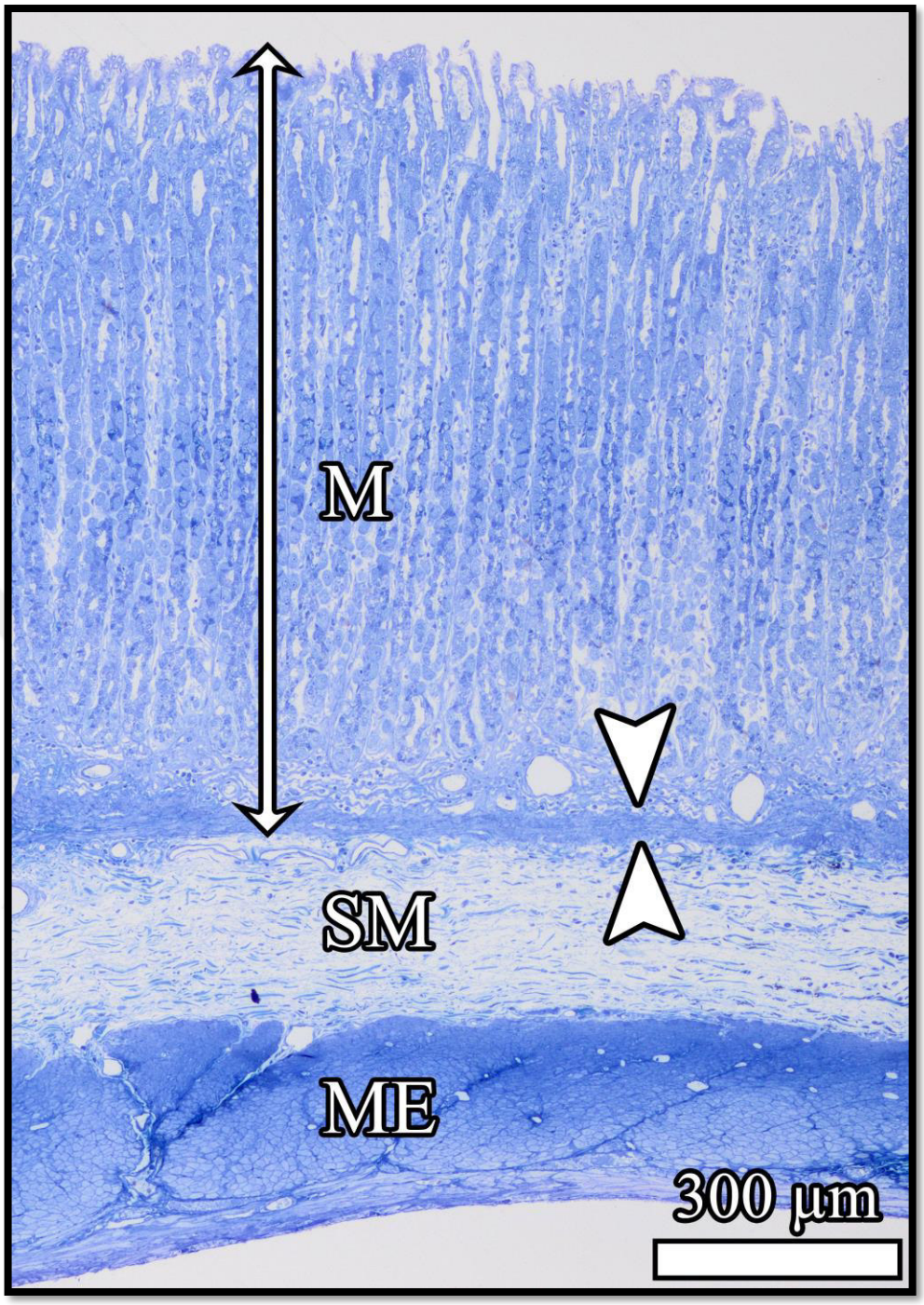

Figure 4. 41. General structures of the stomach belonging to the gum Arabic (GA) group are seen. The whole layers in the wall of the stomach have a healthy and well-protected structure. Glandular layer of organ (arrow) i.e. a part of mucosa (M), submucosa (SM) and muscularis externa (ME) are intact. Muscularis mucosae have a healthy morphology (between arrowheads). Semithin section of resin embedded tissue (0.5 µm thickness) and stained with toluidine blue

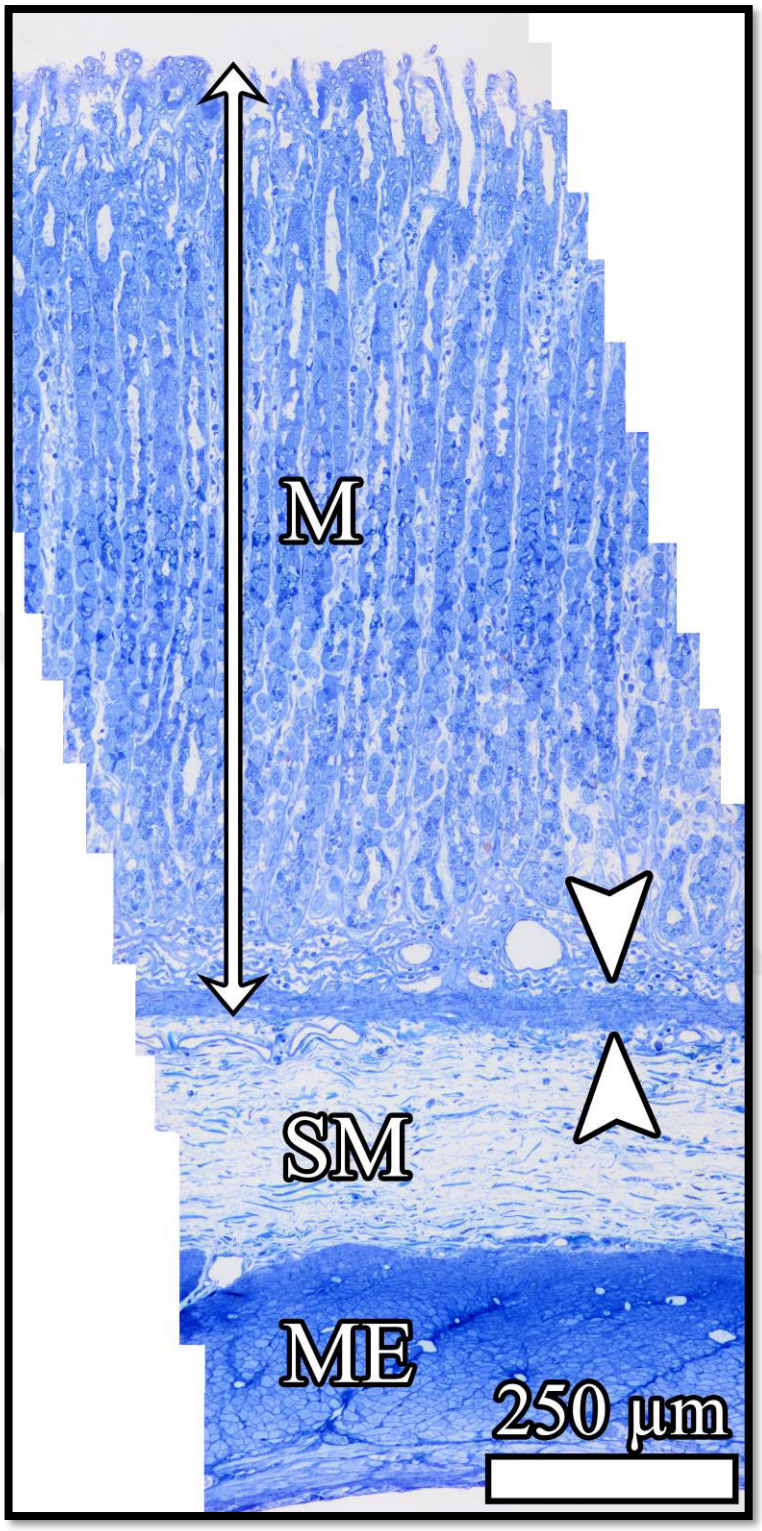

Figure 4. 42. Whole layers in the wall of the stomach belonging to the gum Arabic (GA) group are seen. All of them look healthy and well-protected structures at this magnification. Glandular layer of organ (arrow) i.e. a part of mucosa (M), submucosa (SM) and muscularis externa (ME) are intact. Muscularis mucosae have a healthy morphology (between arrowheads). Semithin section of resin embedded tissue (0.5 µm thickness) and stained with toluidine blue

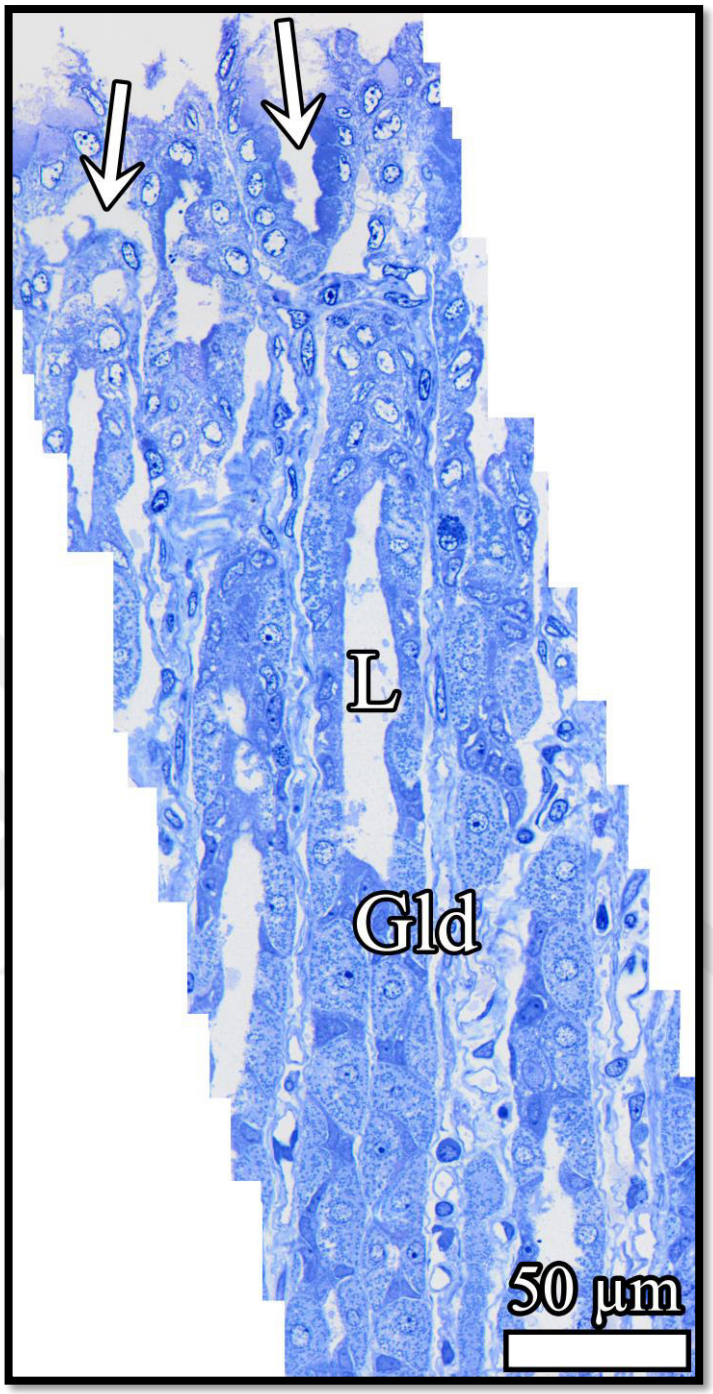

Figure 4. 43. A part of mucosal layer in the wall of the stomach belonging to the gum Arabic (GA) group is seen. Although the surface epithelium and glandular cells (Gld) look healthy, densely staining on the apical side of the epithelium is observed. Gastric pits are also well protected (arrows). Some parts of gastric glands have a distended lumen (L). Semithin section of resin embedded tissue (0.5 µm thickness) and stained with toluidine blue

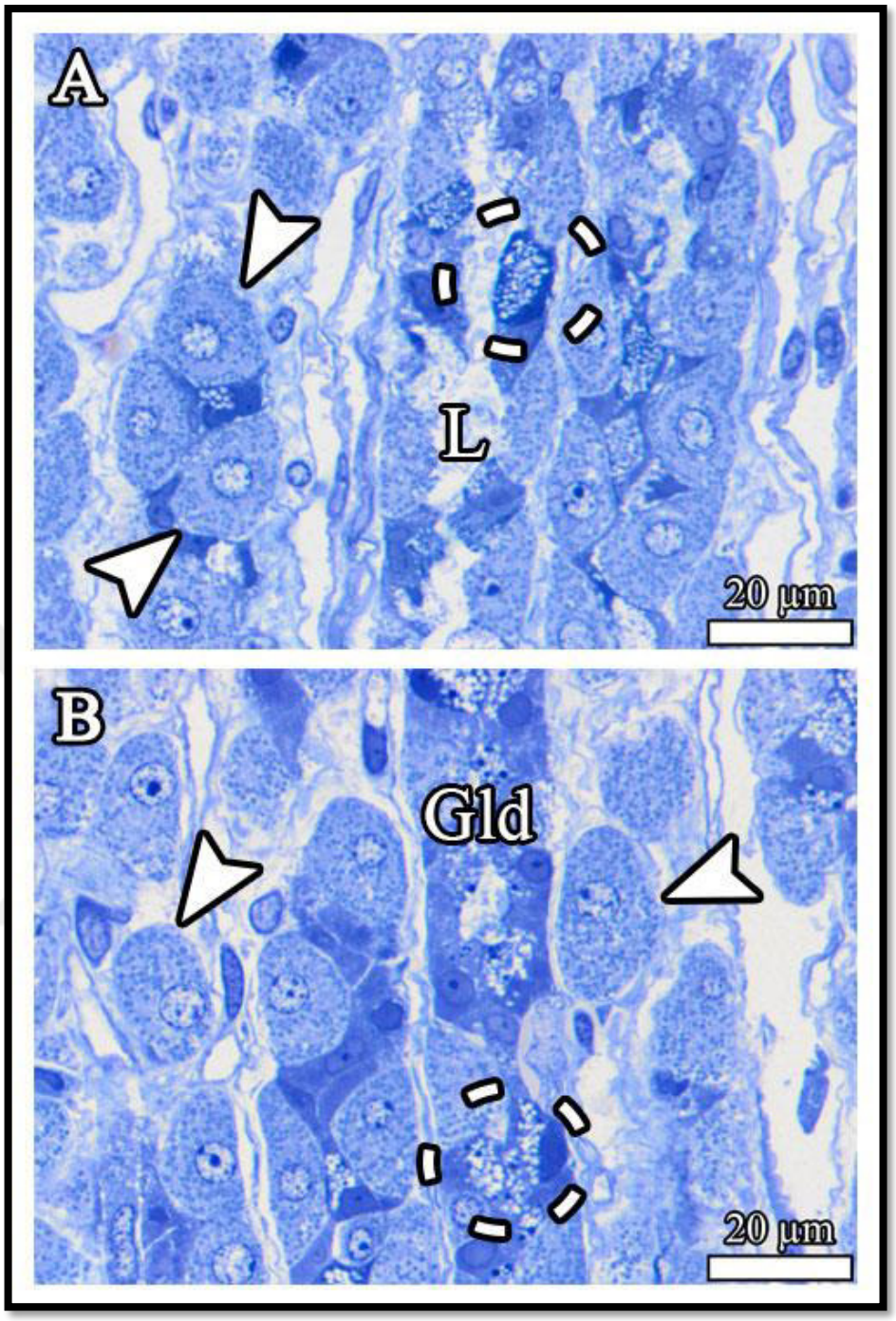

Figure 4. 44. (A, B) Magnified images of a glandular part in the tunica mucosa of the stomach wall belonging to the gum Arabic (GA) group are seen. Although the glandular cells (Gld) look healthy, some parts of gastric glands have a distended lumen (L). Large-sized parietal cells can be recognized easily (arrowheads), some darkly stained cells look to be neck mucosa cells since there are many foamy granules at the apical pole of cells (dashed circled area). Semithin section of resin embedded tissue (0.5 µm thickness) and stained with toluidine blue

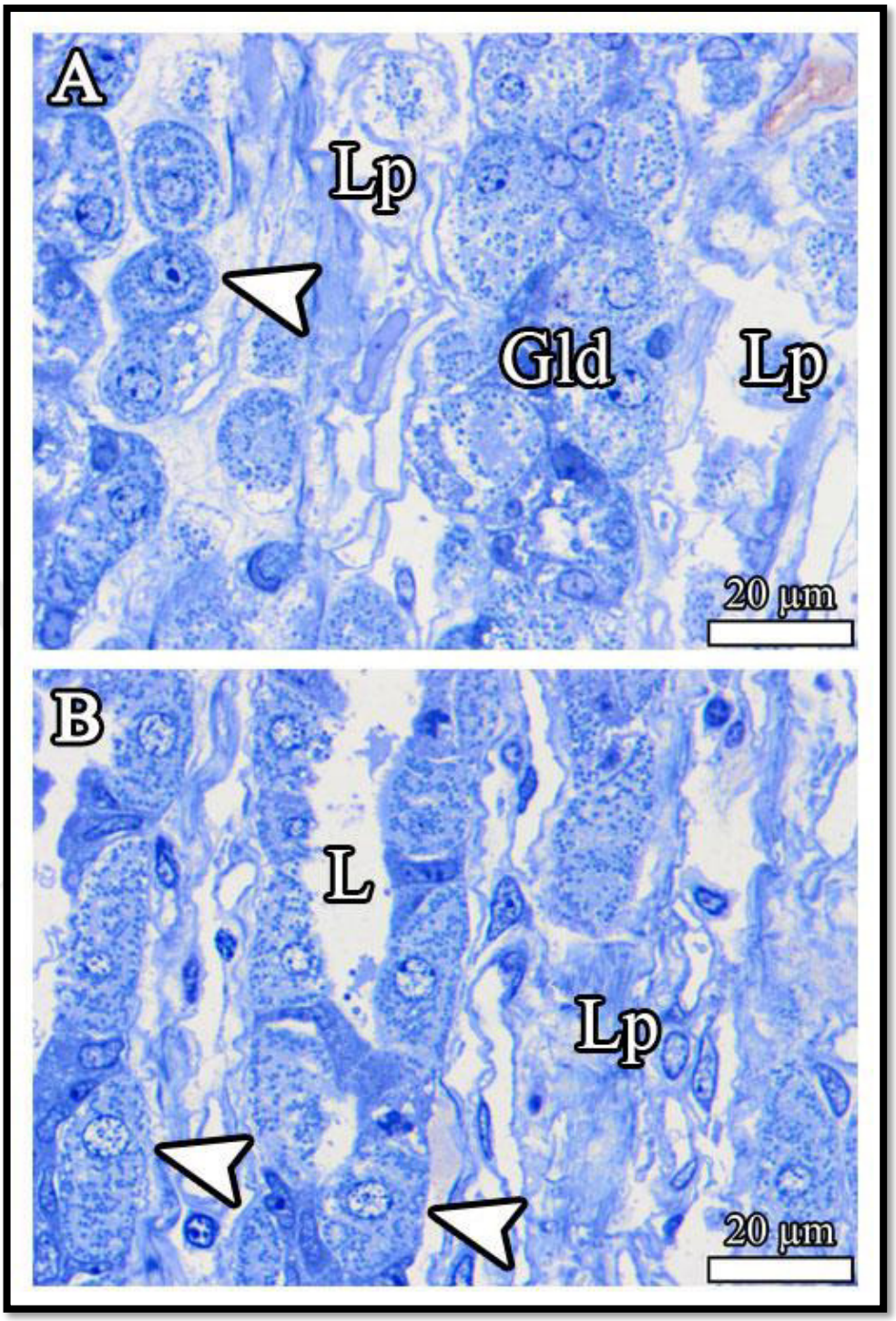

Figure 4. 45. (A, B) Magnified images of a glandular part in the wall of stomach belonging to the gum Arabic (GA) group are seen. Although the gastric glandular cells (Gld) look healthy, some parts of them have a distended lumen (L). Large-sized parietal cells can be recognized easily (arrowheads). Each gastric gland is surrounded by the loose connective tissue of the lamina propria (Lp). Semithin section of resin embedded tissue (0.5 µm thickness) and stained with toluidine blue

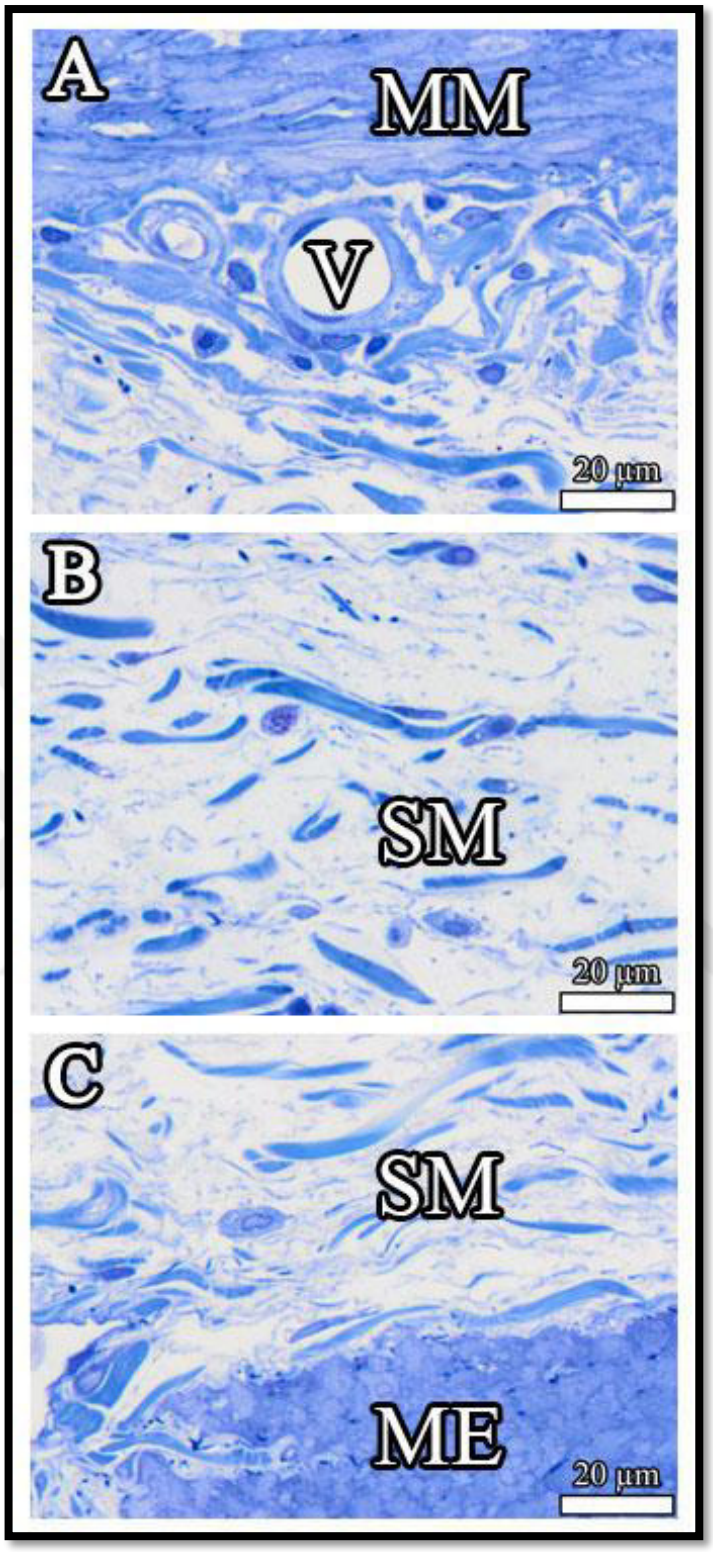

Figure 4. 46. (A, B, C) Magnified images of the stomach layers belonging to the gum Arabic (GA) group are seen. All layers have healthy structures. (MM), muscularis mucosae; (SM), submucosa; (ME), muscularis externa; (V), vessel. Semithin section of resin embedded tissue (0.5 µm thickness) and stained with toluidine blue

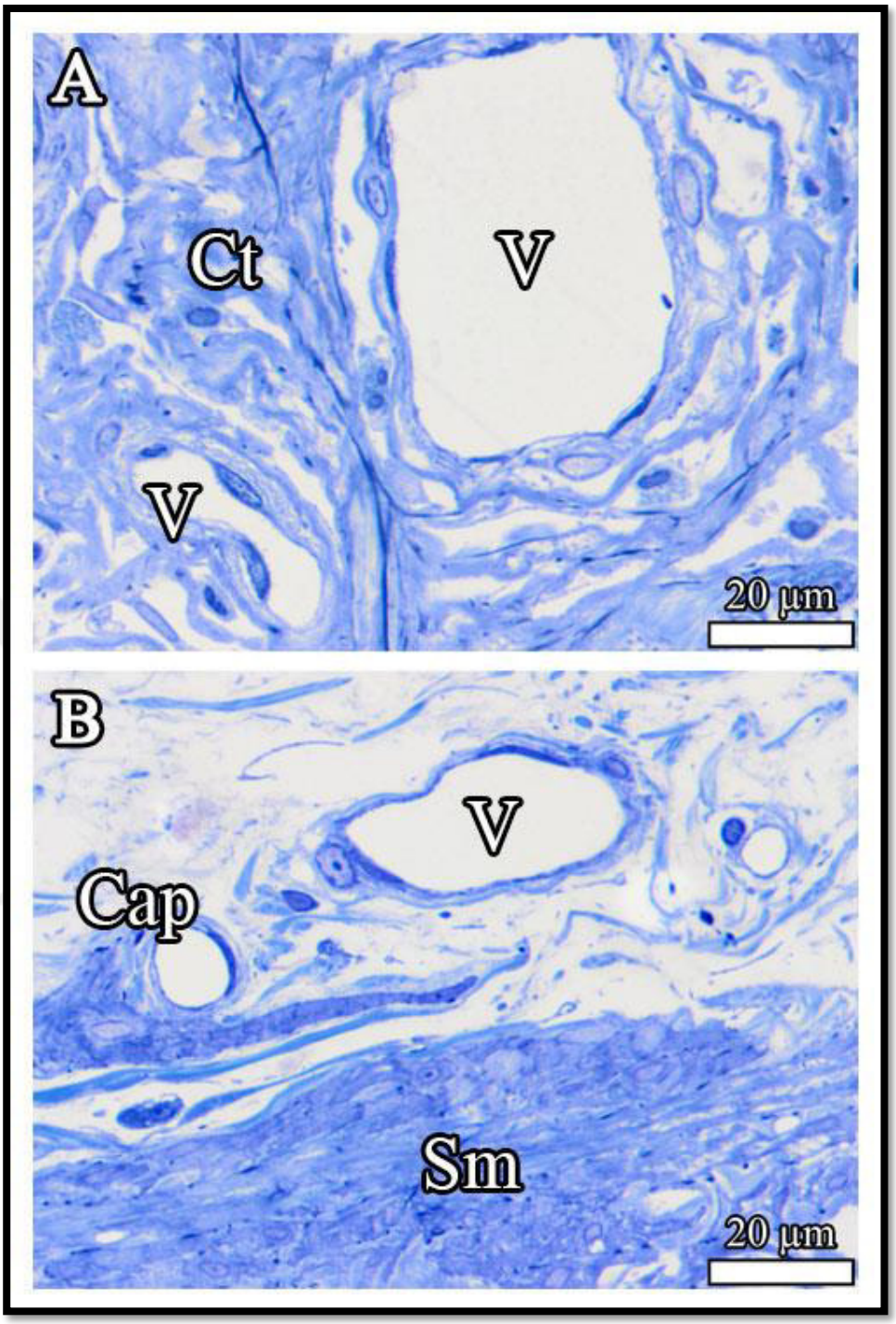

Figure 4. 47. (A, B) Magnified images of the vessels in the submucosa layer in the wall of the stomach belonging to the gum Arabic (GA) group are seen. The structures of vessels, surrounding connective tissue, and smooth muscles look very healthy. Large and small sizes of vessels have a normal morphology since each layer of the vessel can be observed clearly. (Ct), connective tissue; (Cap), capillary; (V), vessel. Semithin section of resin embedded tissue (0.5 µm thickness) and stained with toluidine blue

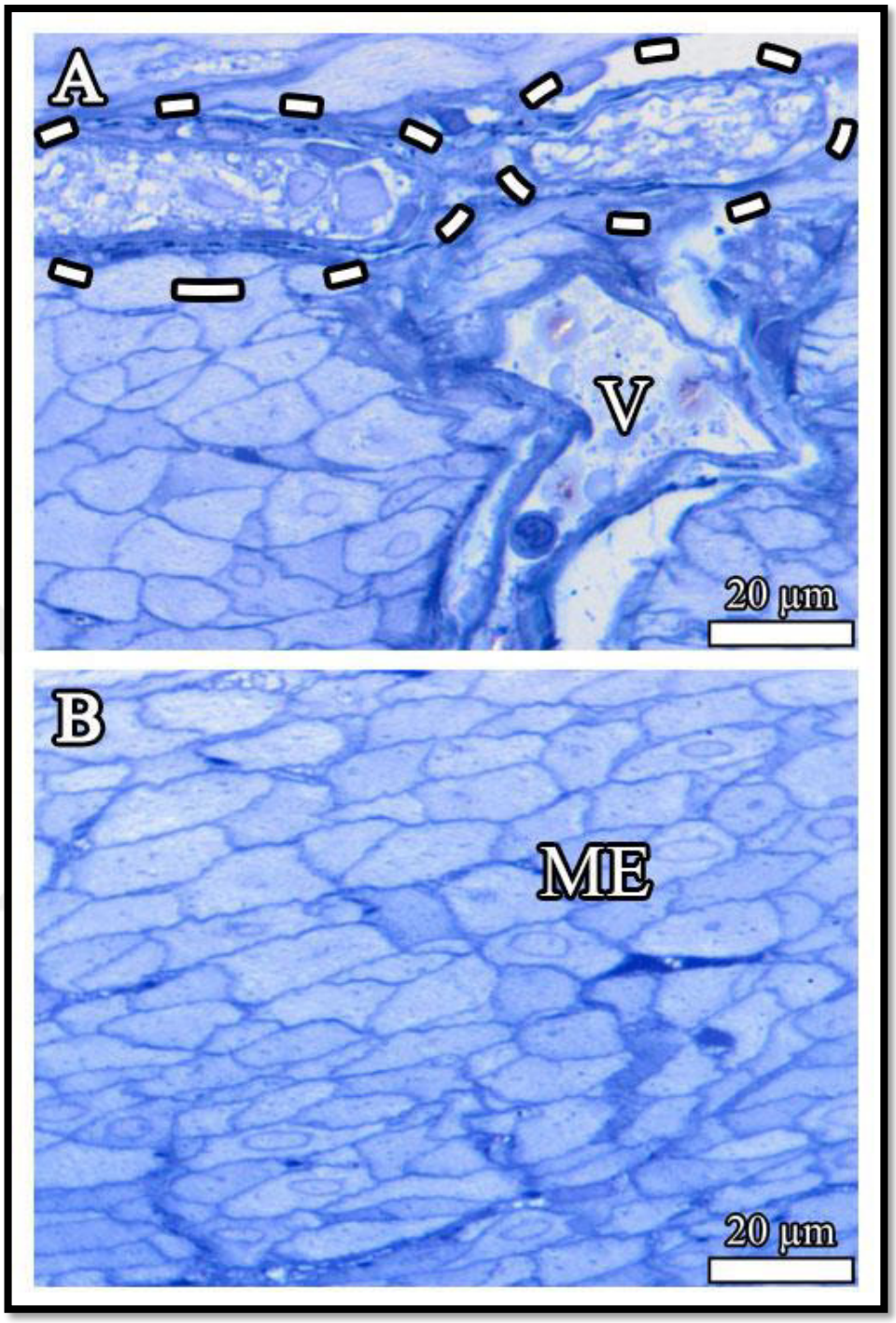

Figure 4. 48. (A, B) Magnified images of the muscularis externa in the wall of the stomach belonging to the gum Arabic (GA) group are seen. The transverse section images of smooth muscle cells in the muscularis externa of the stomach are observed. These cells have a well-structured basement membrane around them (dark lines around muscle cells); a transverse section of a nucleus in some muscle cells can be seen at the center of cells. A myenteric plexus between smooth muscles is observed (dashed elliptical area). (ME), muscularis externa; (V), vessel. Semithin section of resin embedded tissue (0.5 µm thickness) and stained with toluidine blue

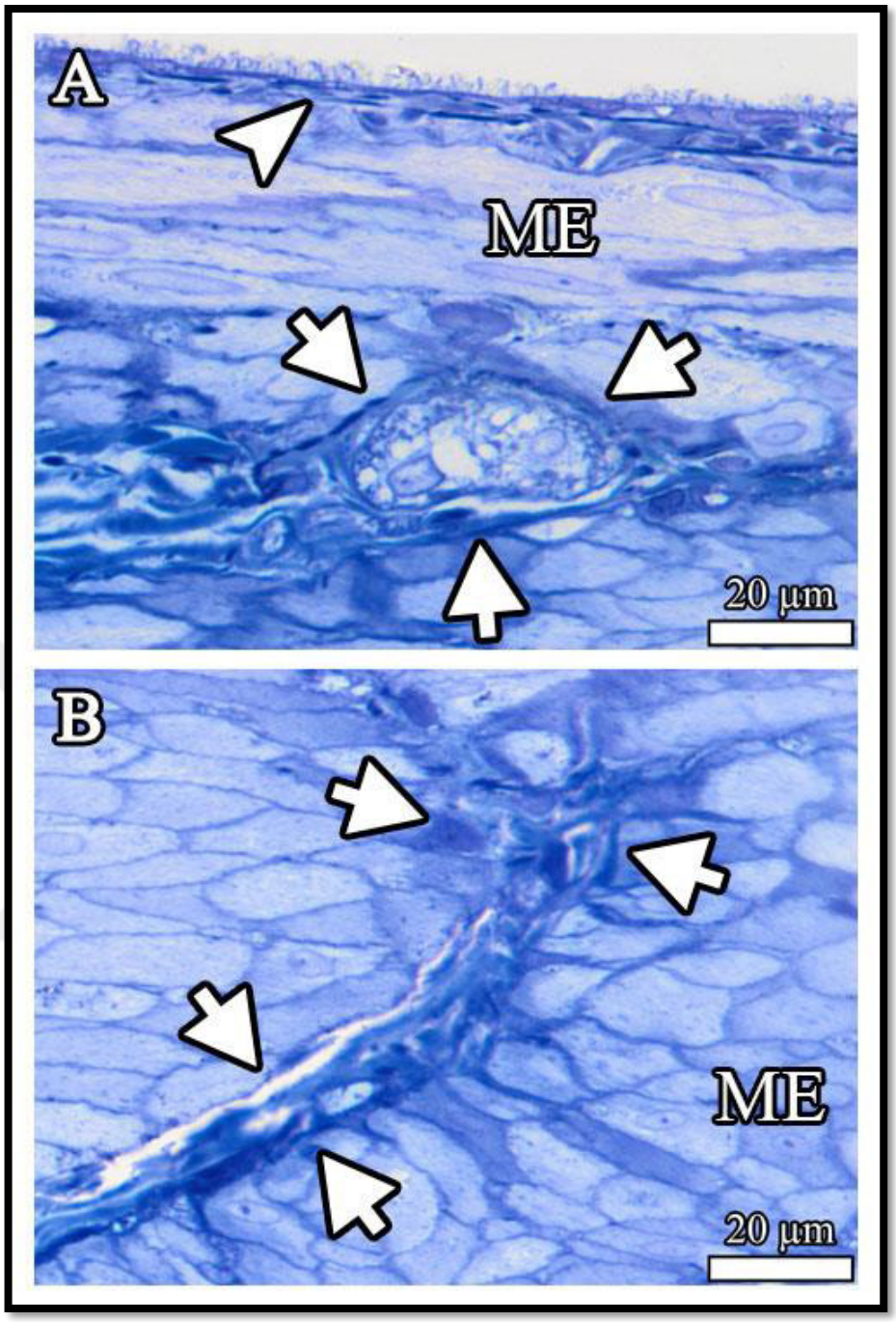

Figure 4. 49. (A, B) Magnified images of the muscularis externa (ME) in the wall of the stomach belonging to the gum Arabic (GA) group are seen. The transverse and longitudinal sections of smooth muscle cells in the muscularis externa in this wall are observed. A thin layer of tunica serosa is shown (arrowhead). Smooth muscle cells have a well-structured basement membrane around them (dark lines around muscle cells); a transverse section of a nucleus in some muscle cells can be seen at the center of cells. **(A)** A myenteric plexus between smooth muscles is seen (between arrows). **(B)** The peripheral nerve of the myenteric plexus between smooth muscles is observed (between arrows). (ME), muscularis externa; (V), vessel. Semithin section of resin embedded tissue (0.5 µm thickness) and stained with toluidine blue

4.1.2.2. Small Intestine

4.1.2.2.1. Control Group

The entire layer of small intestine structure in the control group is well protected. The villus, Lieberkühn crypts (glands) and connective tissue of the lamina propria are all intact. The surface epithelium and its lamina propria appear to be in good structure. Brush margins and Goblet cells are determined to be in good morphology. An abundance of Paneth cells can be seen near the base of the intestinal gland. These pyramidal-shaped cells have a large number of dens granules with electron-dense centers and haloes. The nuclei of these cells are found at the cell's base. All of the elements in the sections of small intestine are well structured. There is a lot of connective tissue and submucosal ganglionic cells in the submucosa. Ganglionic cells in the myenteric plexus are found between two layers of muscular externa, and the tunica serosa is observed healthy (Figures 4.50-4.60).

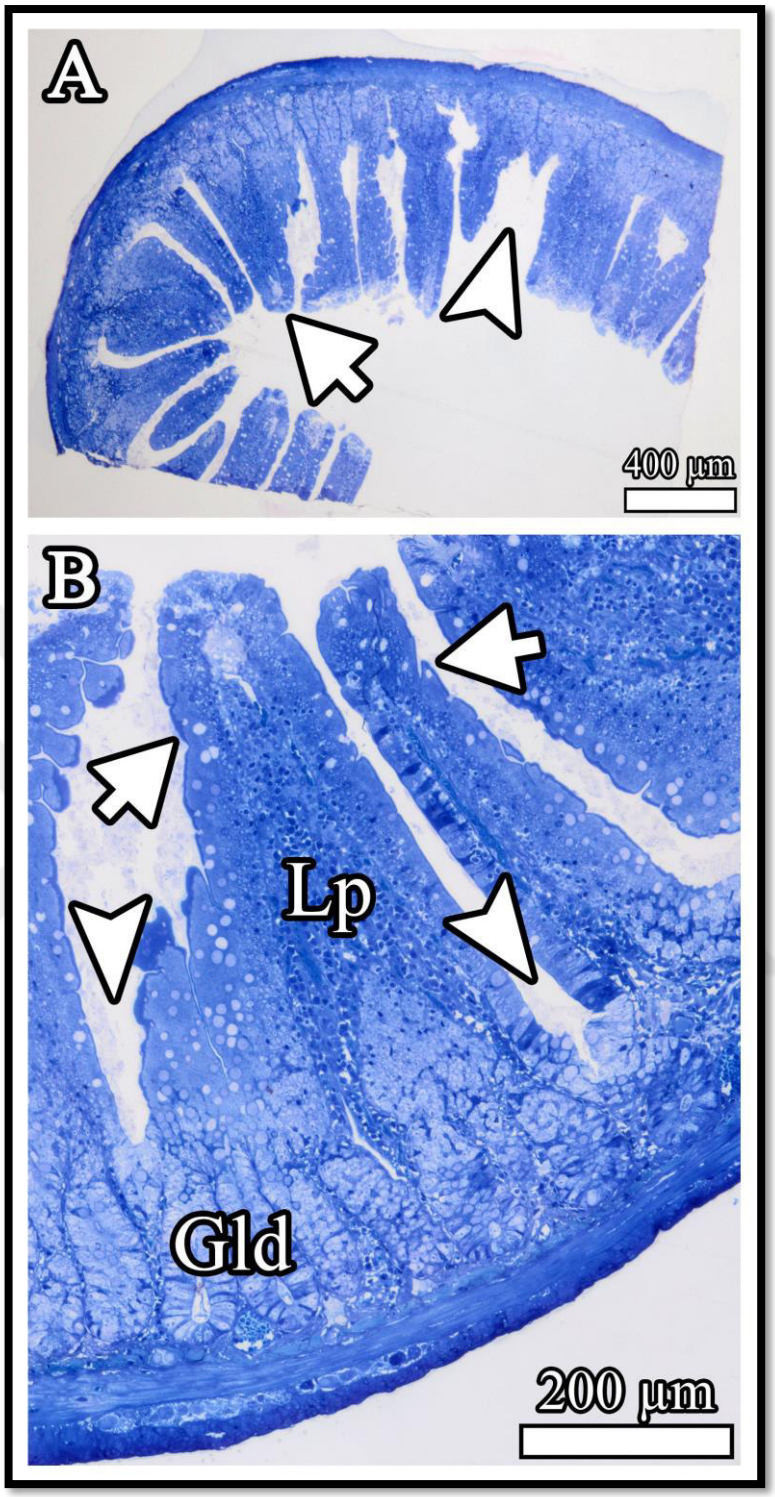

Figure 4. 50. **(A, B)** General structures of the small intestine belonging to the control group are seen. The whole layers of the intestine have a well-protected structure. Finger-like villus (arrows), crypts of Lieberkühn (arrowheads), glands (Gld), and connective tissue of lamina propria (Lp) are intact. Semithin section of resin embedded tissue (0.5 µm thickness) and stained with toluidine blue

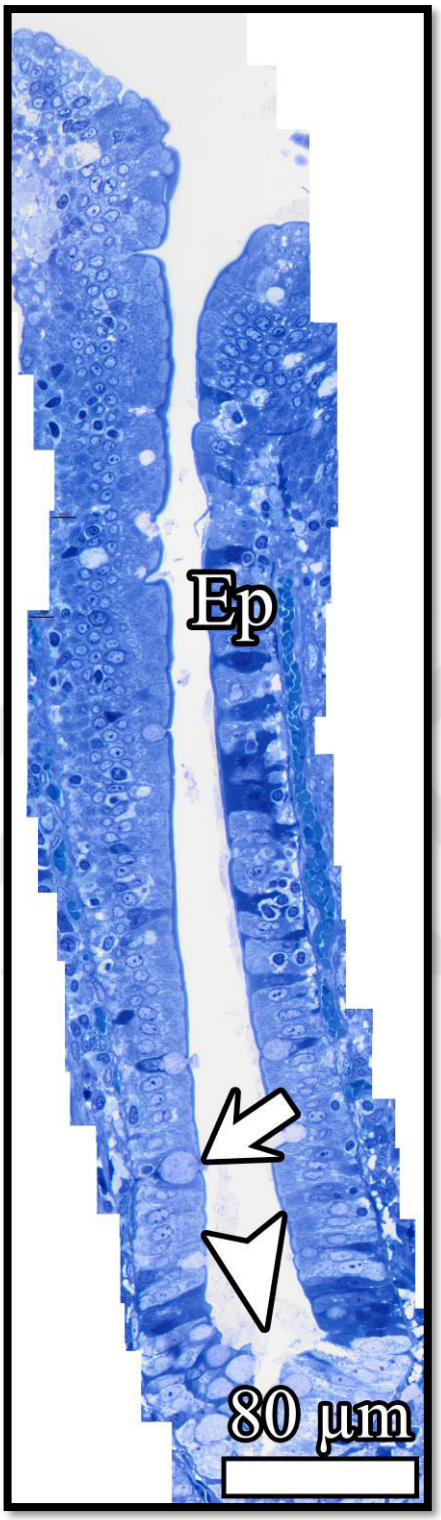

Figure 4. 51. General structures of the tubular gland in the small intestine belonging to the control group are seen. The cells in the gland have a well-protected structure. Epithelium (Ep) and its Goblet cells (arrow) and crypt of Lieberkühn (arrowhead) are clearly observed. Semithin section of resin embedded tissue (0.5 µm thickness) and stained with toluidine blue

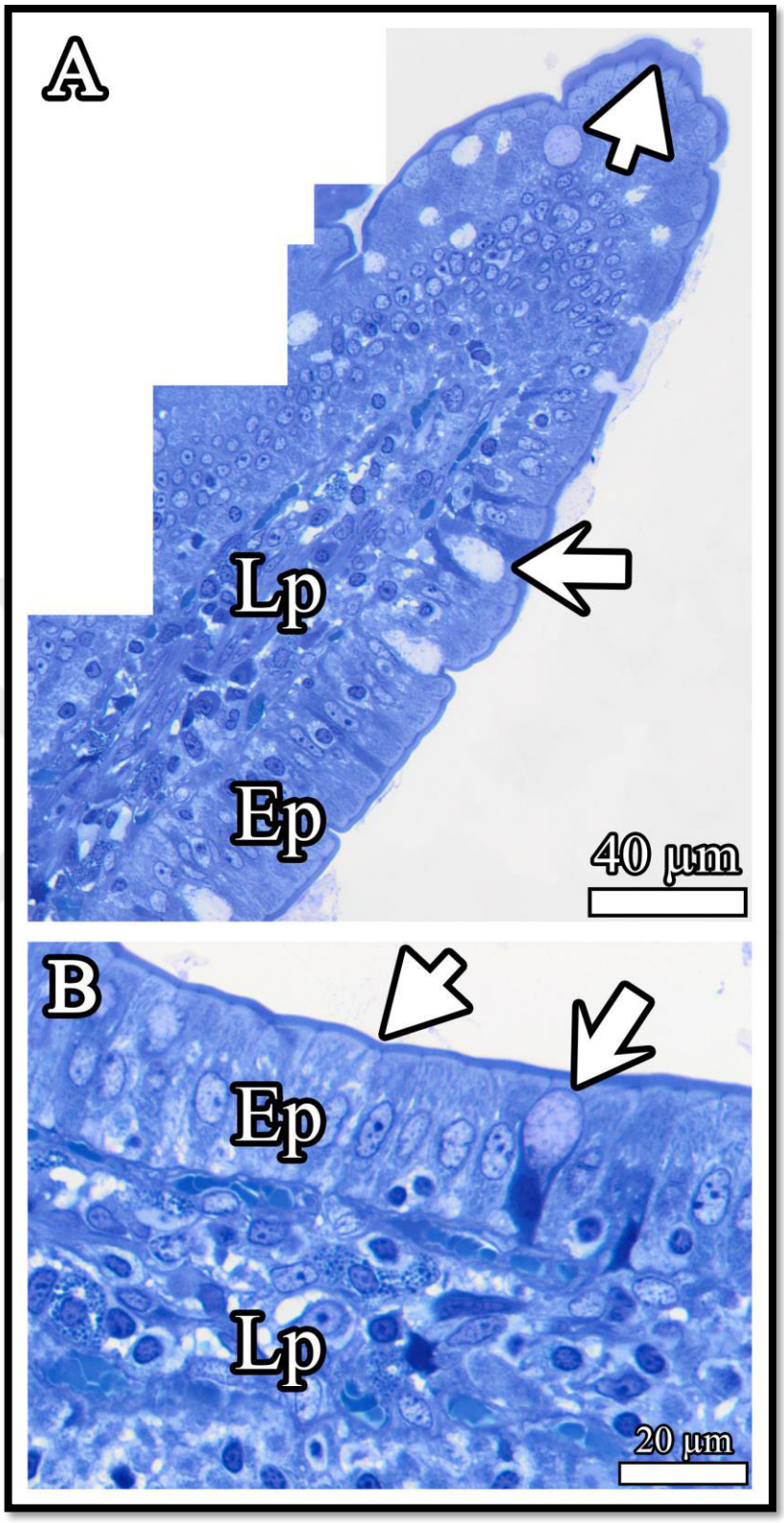

Figure 4. 52. (A, B) High magnification of the small intestine images belonging to the control group is seen. The surface epithelium (Ep) and its lamina propria (Lp) look healthy. Brush borders (blunt arrow) and Goblet cells (sharp arrows) are found normal. Semithin section of resin embedded tissue (0.5 µm thickness) and stained with toluidine blue

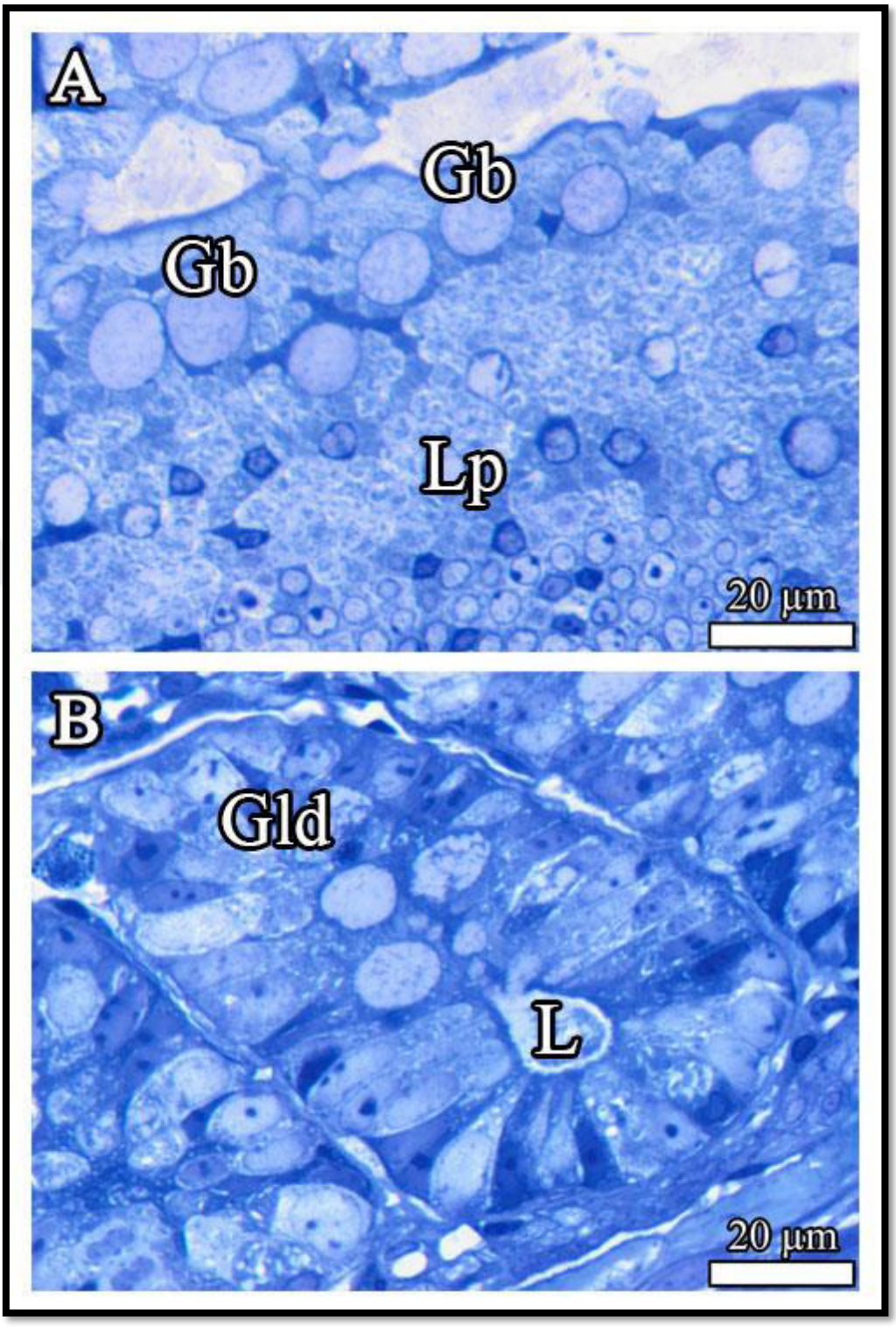

Figure 4. 53. **(A)** A high magnification of the surface epithelium belonging to the small intestine image from the control group is seen. In most parts of the section, it was cut to parallel to the surface, for this reason, most Goblet cells (Gb) have been seen as circular. Transversely sectioned nuclei of cells in the lamina propria (Lp) also are observed as circular. **(B)** The longitudinal section of intestinal glands (Gld) looks healthy. A visible lumen (L) and Paneth cell are seen near the bottom of the gland. Semithin section of resin embedded tissue (0.5 µm thickness) and stained with toluidine blue

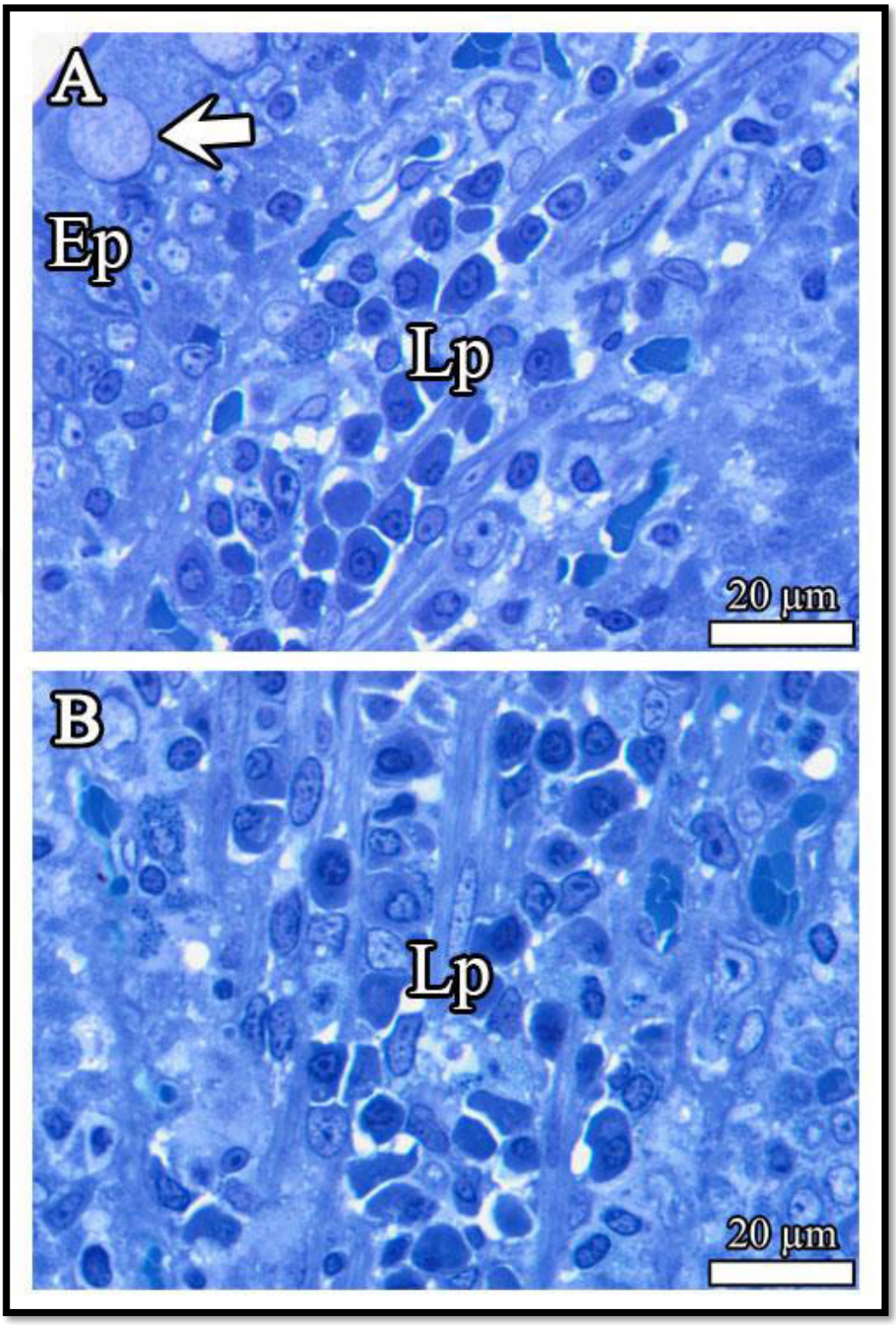

Figure 4. 54. (A, B) High magnification of the surface epithelium (Ep) and its lamina propria (Lp) belonging to the small intestine image from the control group is seen. The Goblet cells (arrow) in the epithelium look healthy. Each element of tissue has a well-protected structure. A longitudinal section of the smooth muscle cells can be seen at the center of the lamina propria. Semithin section of resin embedded tissue (0.5 µm thickness) and stained with toluidine blue

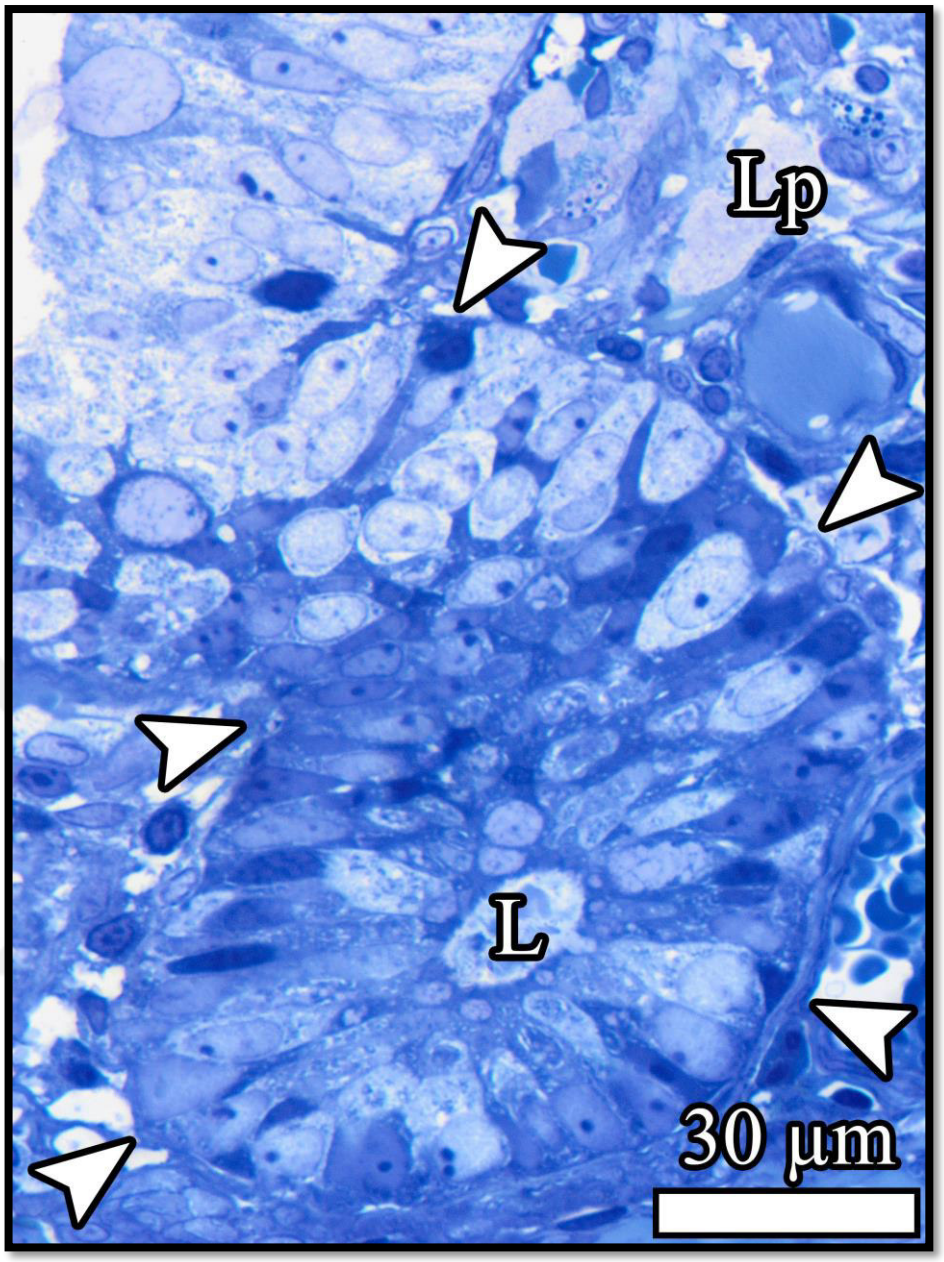

Figure 4. 55. A high magnification of the surface epithelium, its lamina propria (Lp), and intestinal gland with a lumen (L) belonging to the small intestine from the control group is seen. Arrowheads delineate the borders of the gland. All elements in the section have a healthy structure. Semithin section of resin embedded tissue (0.5 µm thickness) and stained with toluidine blue

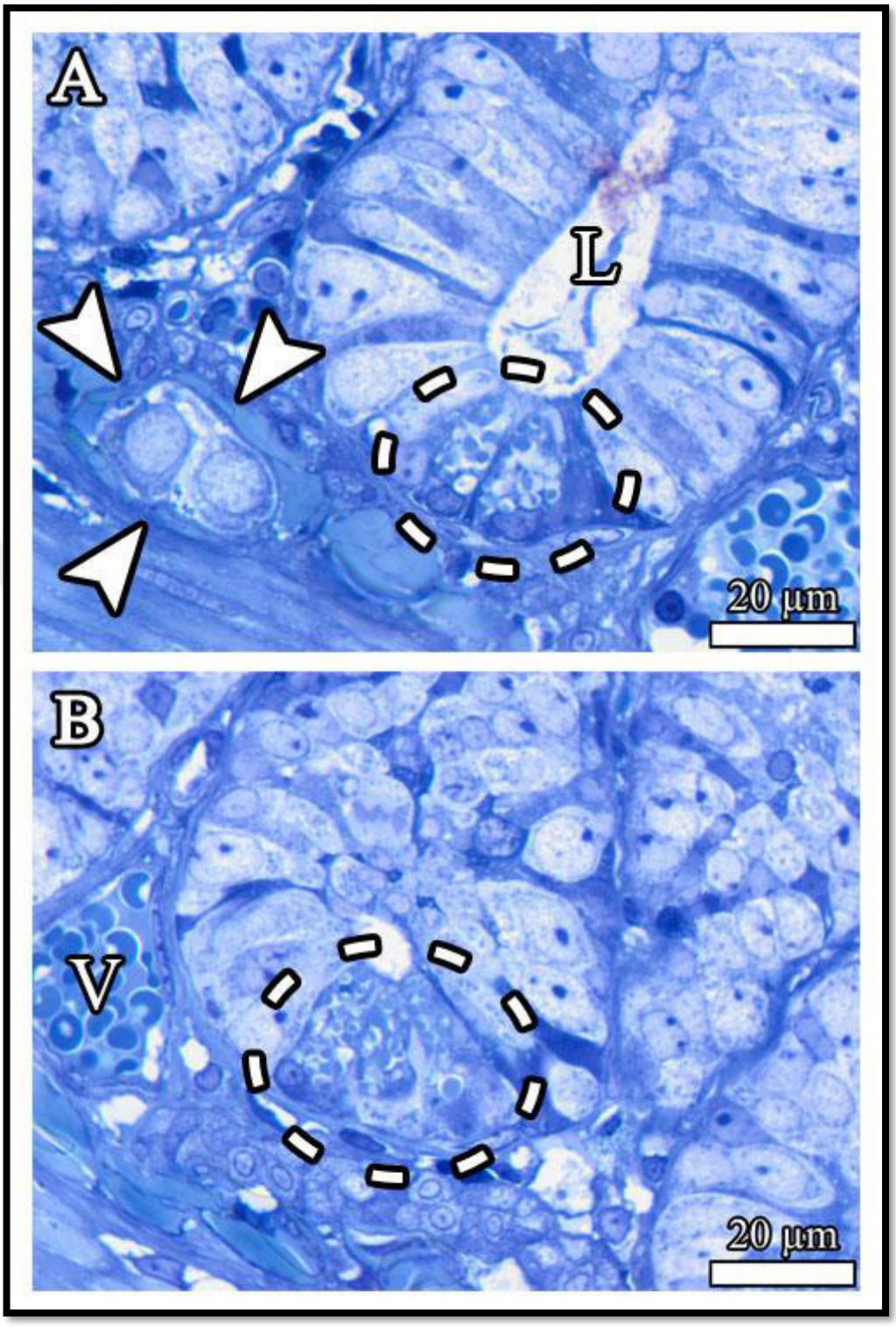

Figure 4. 56. (A) A longitudinal section of the intestinal gland with a lumen (L), at the base of it, an accumulation of the Paneth cells from the control group is observed (dashed circled area). These cells, pyramidal-shaped, have many dens granules with highly electron-dense cores and haloes. The nuclei of them located at the base of the cells. Arrowheads show pair of ganglionic cells. Well develop connective tissue around these cells is seen. **(B)** A transfer section of the intestinal gland is observed, and an accumulation of the Paneth cells (dashed circled area) is seen at the base of the gland. (V), vessel. Semithin section of resin embedded tissue (0.5 µm thickness) and stained with toluidine blue

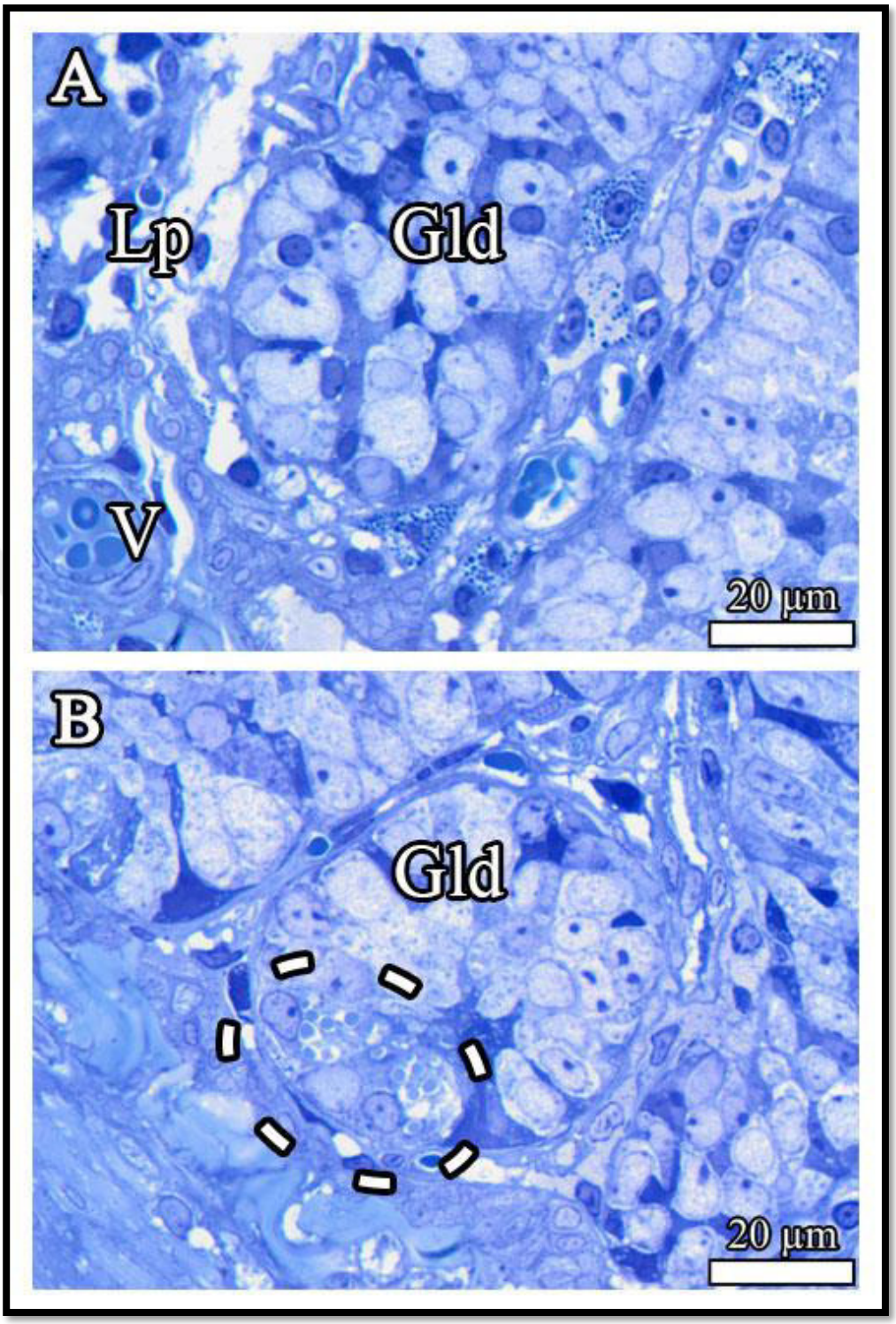

Figure 4. 57. (A, B) Longitudinal and transverse sections of the intestinal glands (Gld) from the control group are seen. **(A)** The longitudinal section of the gland is covered by a connective tissue (Lp) that has many mast cells. A rich capillary network is seen in this connective tissue. **(B)** A transverse section of the intestinal gland (Gld) is observed, and an accumulation of the Paneth cells is found in the bottom of the gland (dashed circled area). (V), vessel. Semithin section of resin embedded tissue (0.5 µm thickness) and stained with toluidine blue

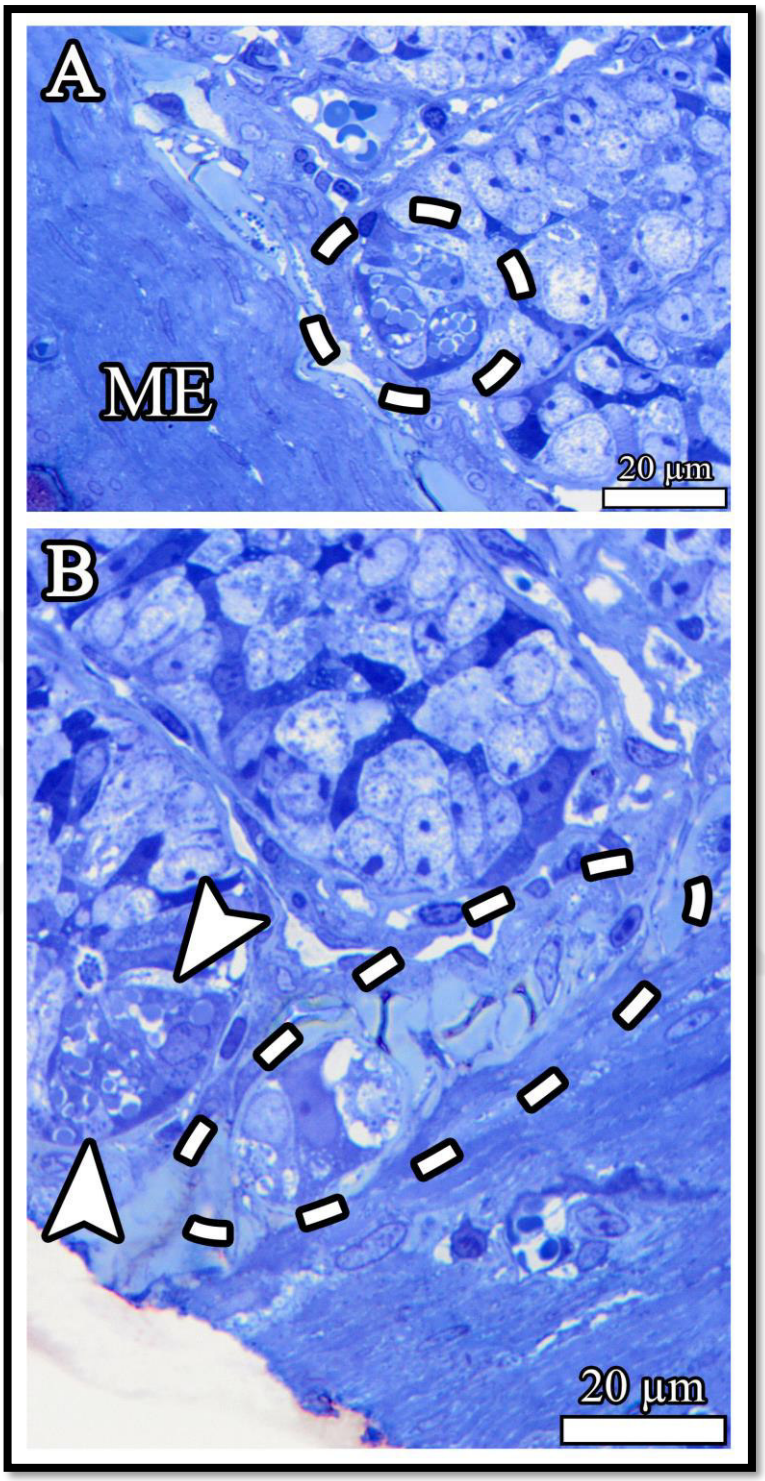

Figure 4. 58. (A, B) Longitudinal sections of the intestinal glands (Gld) from the control group are seen. (A) An accumulation of the Paneth cells at the base of the gland (dashed circled area) is observed. This part of the intestine has a narrow submucosa since muscularis externa (ME) commences. Nuclei and nucleoli of the glandular cells are easily visible. **(B)** Longitudinal sections of two intestinal glands (Gld) are observed, and an accumulation of the Paneth cells (arrowheads) is found in the bottom of the gland (dashed circled area). A submucosal ganglionic cells accumulation is seen in the submucosa (dashed elliptic area). Semithin section of resin embedded tissue (0.5 µm thickness) and stained with toluidine blue

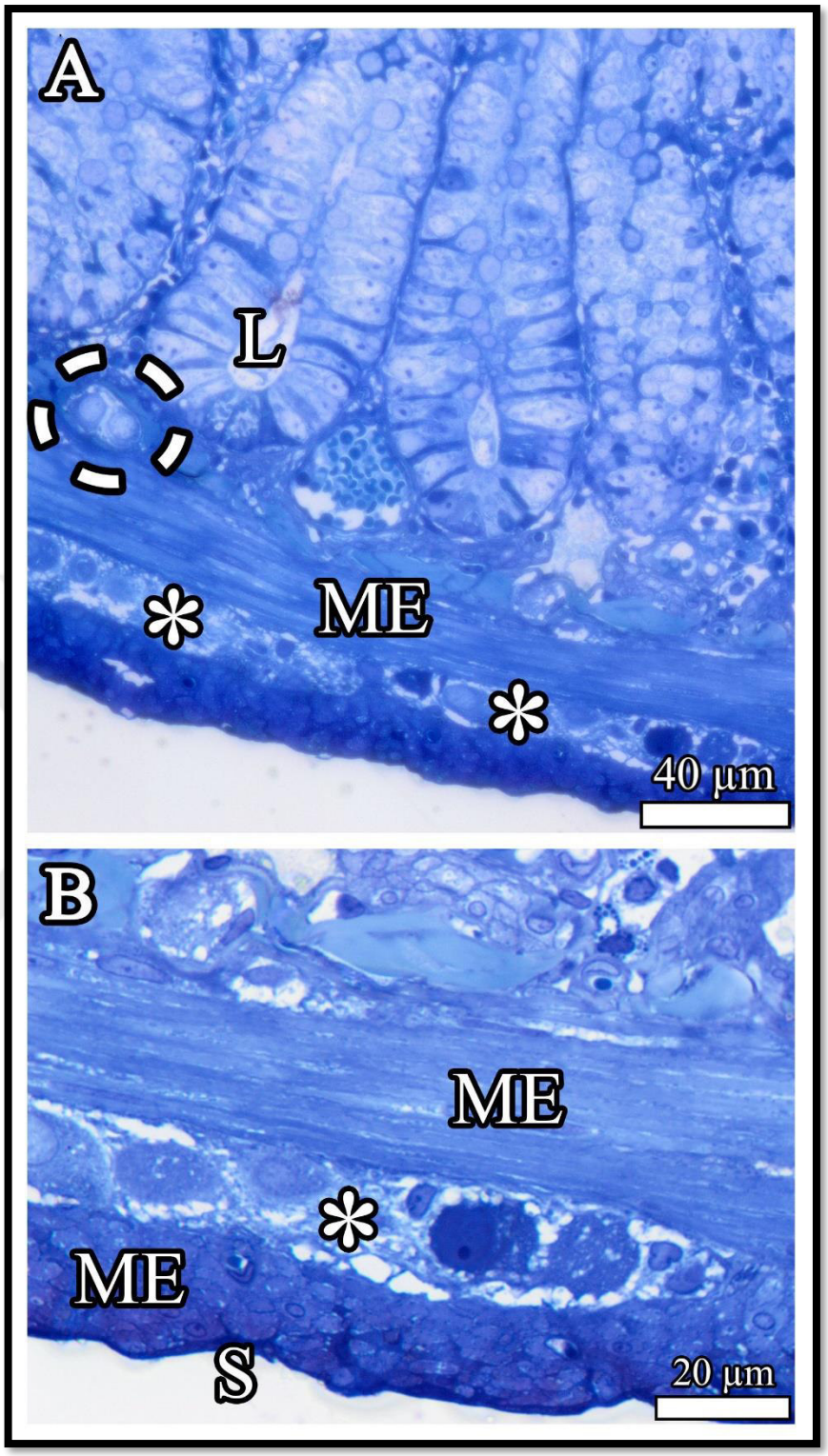

Figure 4. 59. (A) Longitudinal sections of the intestinal glands (Gld) from the control group are seen. A rich and well-developed connective tissue and submucosal ganglionic cells (dashed circled area) are visible. Some glands have lumen (L); ganglionic cells augmentation (*) is seen between two layers of muscularis externa (ME). **(B)** High magnification of some parts of the picture is shown. Ganglionic cells (*) of myenteric plexus localized between two layers of muscular externa (ME) are observed. (S), tunica serosa. Semithin section of resin embedded tissue (0.5 µm thickness) and stained with toluidine blue

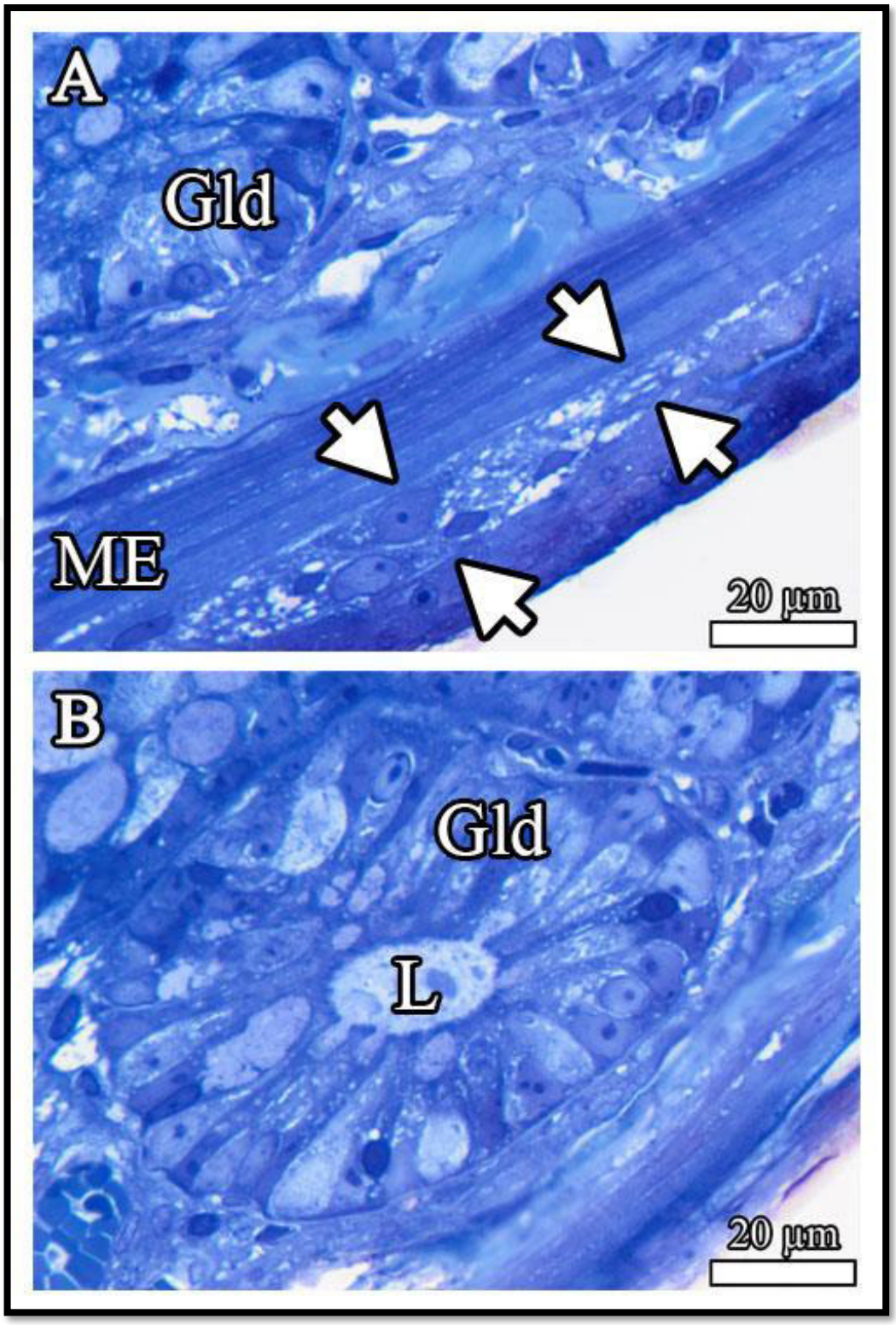

Figure 4. 60. (A) A section of the intestinal glands (Gld), lamina propria, muscularis mucosae, submucosa, and muscularis externa (ME) belonging to the control group are seen. Ganglionic cells of the myenteric plexus (arrows) are observed between the inner and outer smooth muscle layers of ME. **(B)** A transverse section of the intestinal gland (Gld) is shown; it has a large lumen (L). Semithin section of resin embedded tissue (0.5 µm thickness) and stained with toluidine blue

4.1.2.2.2. Diclofenac Sodium Group

In this group, the basal membrane of the epithelium in the small intestine is somewhat thicker. In the lamina propria, there are several vacuolization of various sizes. The brush boundary of microvilli appears to be very thin, making it difficult to distinguish. Some of the dens structures within the epithelium may be apoptotic bodies of cells that have died. The lamina propria of mucosa is visible, and the epithelium's basal membrane demarcates the connective tissue's borders. The lamina propria has a lot of vacuolization. The basal membrane has thickened to some extent. There is a lot of lymphocyte infiltration into the epithelium and an increased number of plasma cells are seen. There were no Paneth cells found (Figures 4.61-4.74).

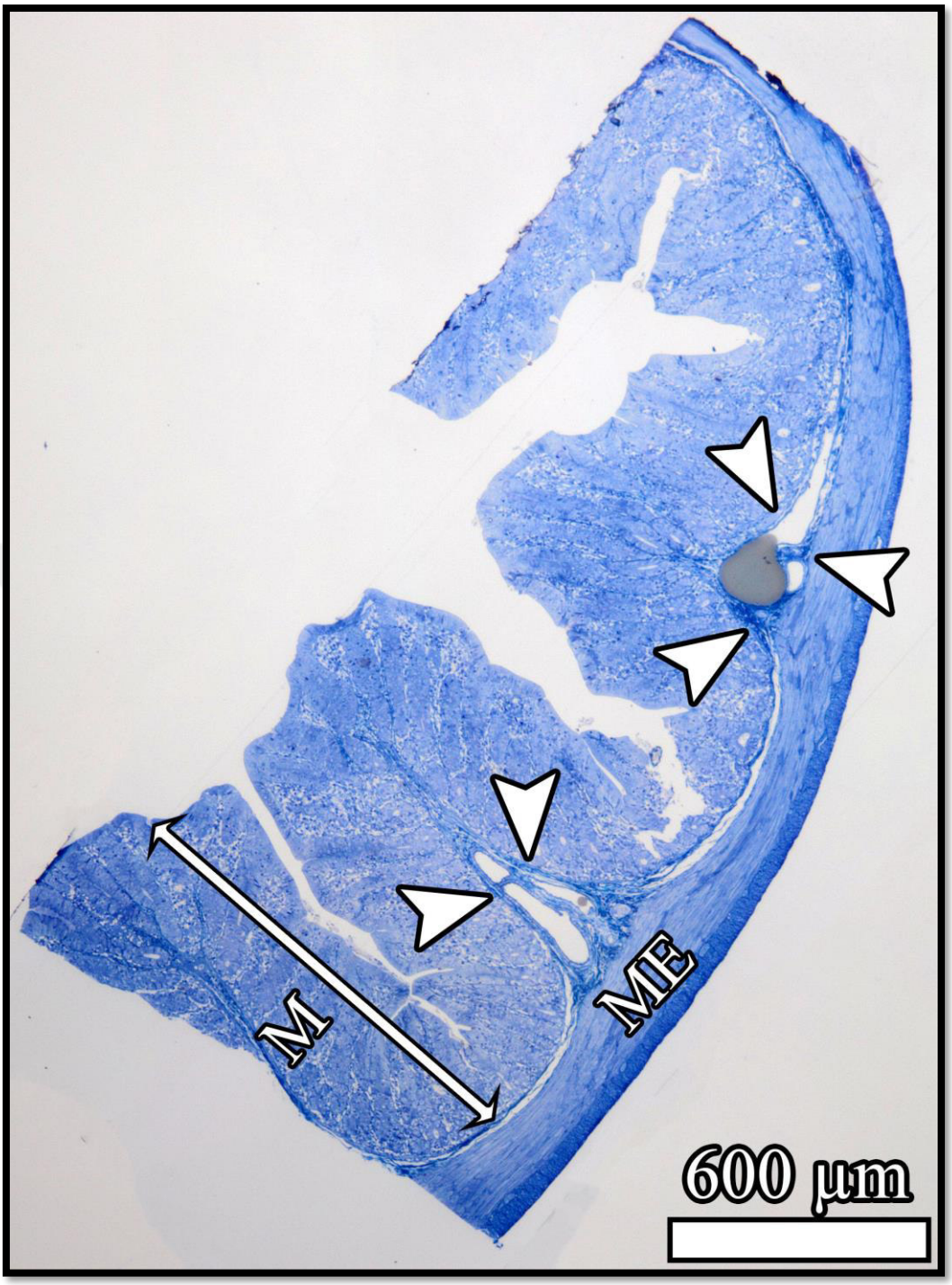

Figure 4. 61. A general view of the small intestine belongs to the diclofenac sodium (DS) group. All layers of the organ are seen. Enlarged vessels and lipid droplets (arrowheads) are observed. (M), mucosa; (ME), muscularis externa. Semithin section of resin embedded tissue (0.5 µm thickness) and stained with toluidine blue

Figure 4. 62. A high magnification of the general view of the small intestine belongs to the diclofenac sodium (DS) group. All layers of the organ are seen intact at this magnification. (Ep), simple columnar epithelium; (Lp), a loose connective tissue of lamina propria; (Gld), intestinal gland; (ME), muscularis externa. Semithin section of resin embedded tissue (0.5 µm thickness) and stained with toluidine blue

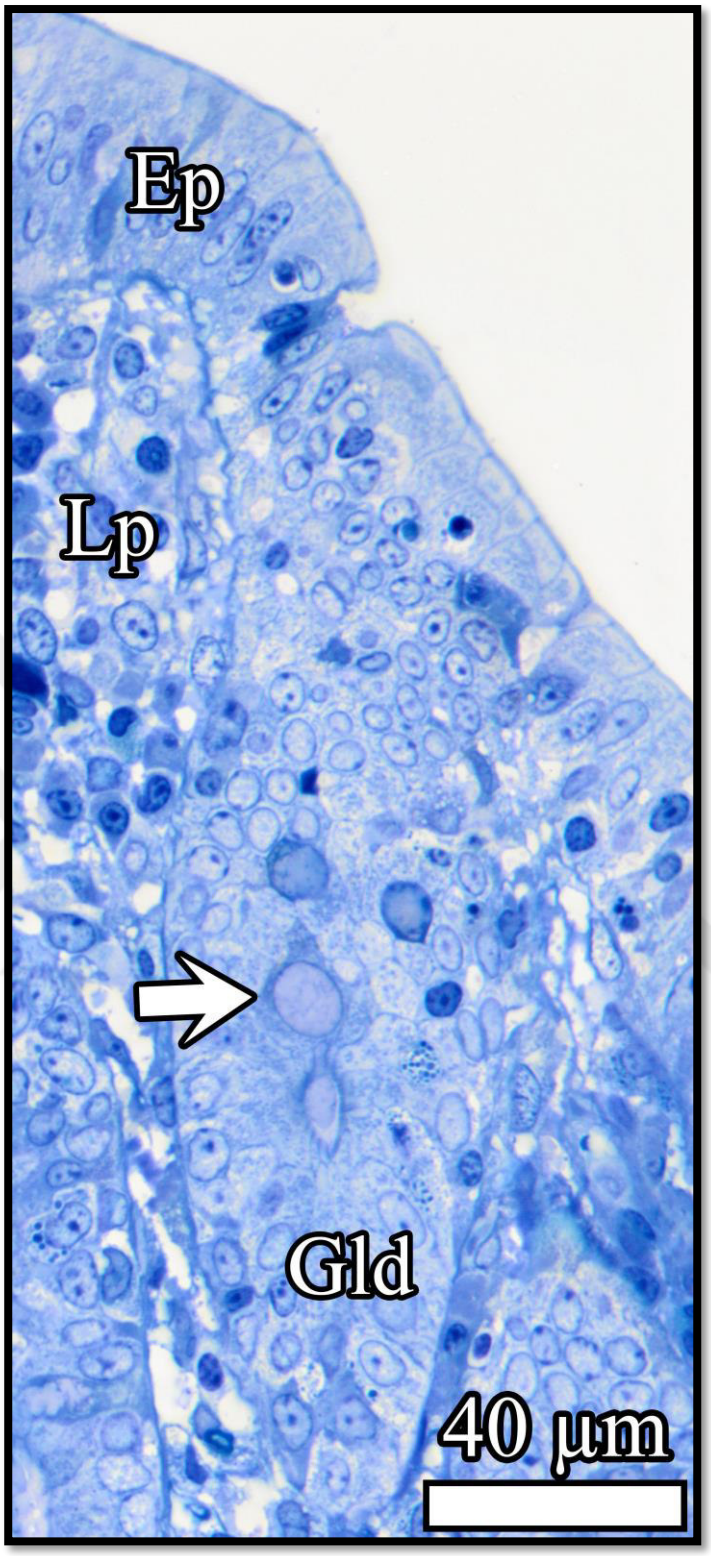

Figure 4. 63. A high magnification of simple columnar epithelium of the small intestine belongs to the diclofenac sodium (DS) group. Although two layers of the mucosa are seen intact at this magnification, a slight thickened basal membrane is observed. Many different size vacuolization is found in the lamina propria (Lp). (Ep), simple columnar epithelium; (Gld), intestinal gland; (arrow), Goblet cell. Semithin section of resin embedded tissue (0.5 µm thickness) and stained with toluidine blue

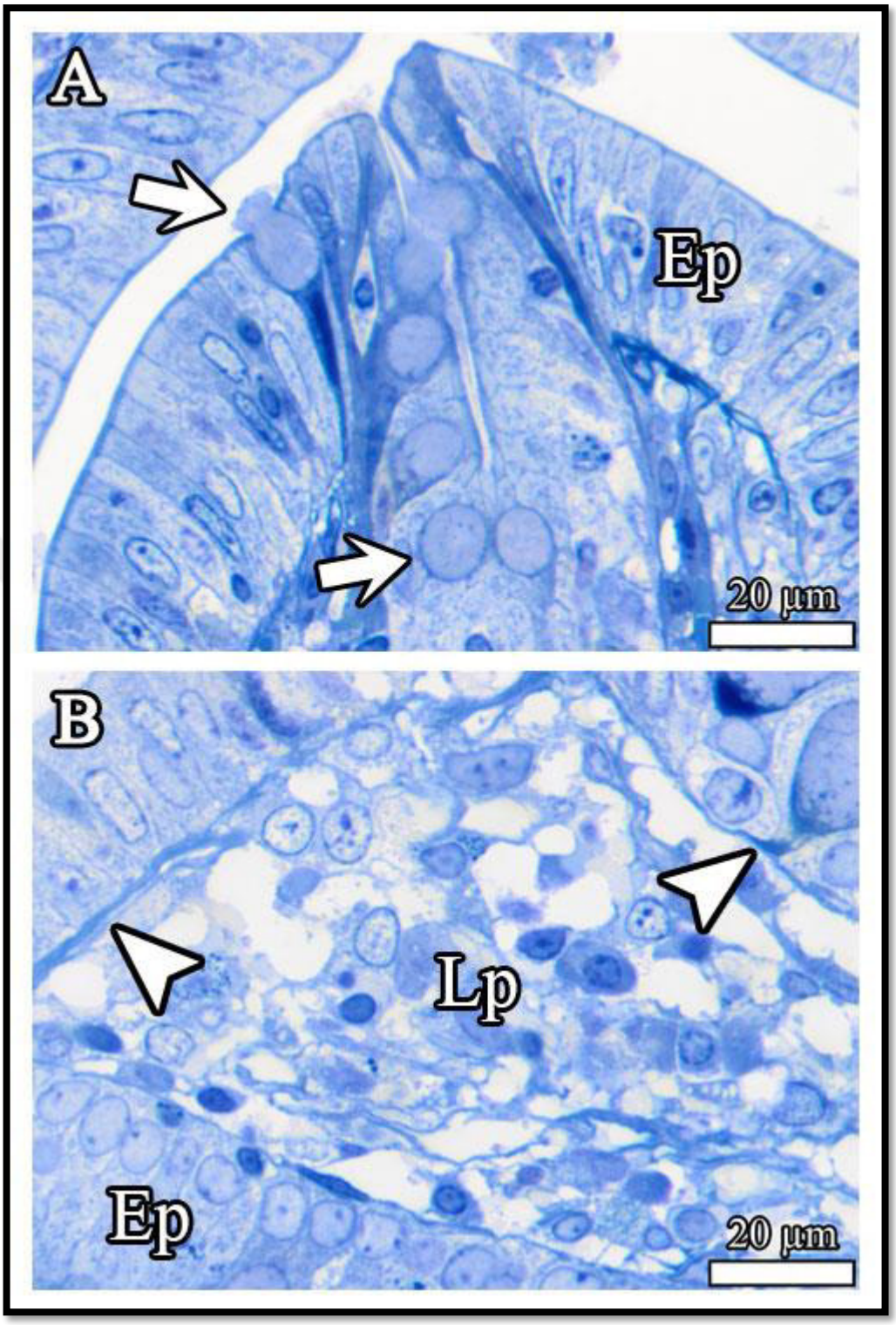

Figure 4. 64. **(A)** A high magnification of simple columnar epithelium (Ep) of the small intestine belongs to the diclofenac sodium (DS) group. It has many Goblet cells; one of them is discharging its secretion (arrow). The brush border of microvilli is seen as very thin and so difficult to recognize. Some of the dens structures inside of the epithelium might be an apoptotic body of destroyed cells. **(B)** Lamina propria (Lp) of the mucosa is seen, and the basal membrane of epithelium delineates the borders of this connective tissue (arrowheads). Many vacuolization in the tissue are a prominent feature of lamina propria. The basal membrane was partly thickened. Semithin section of resin embedded tissue (0.5 µm thickness) and stained with toluidine blue

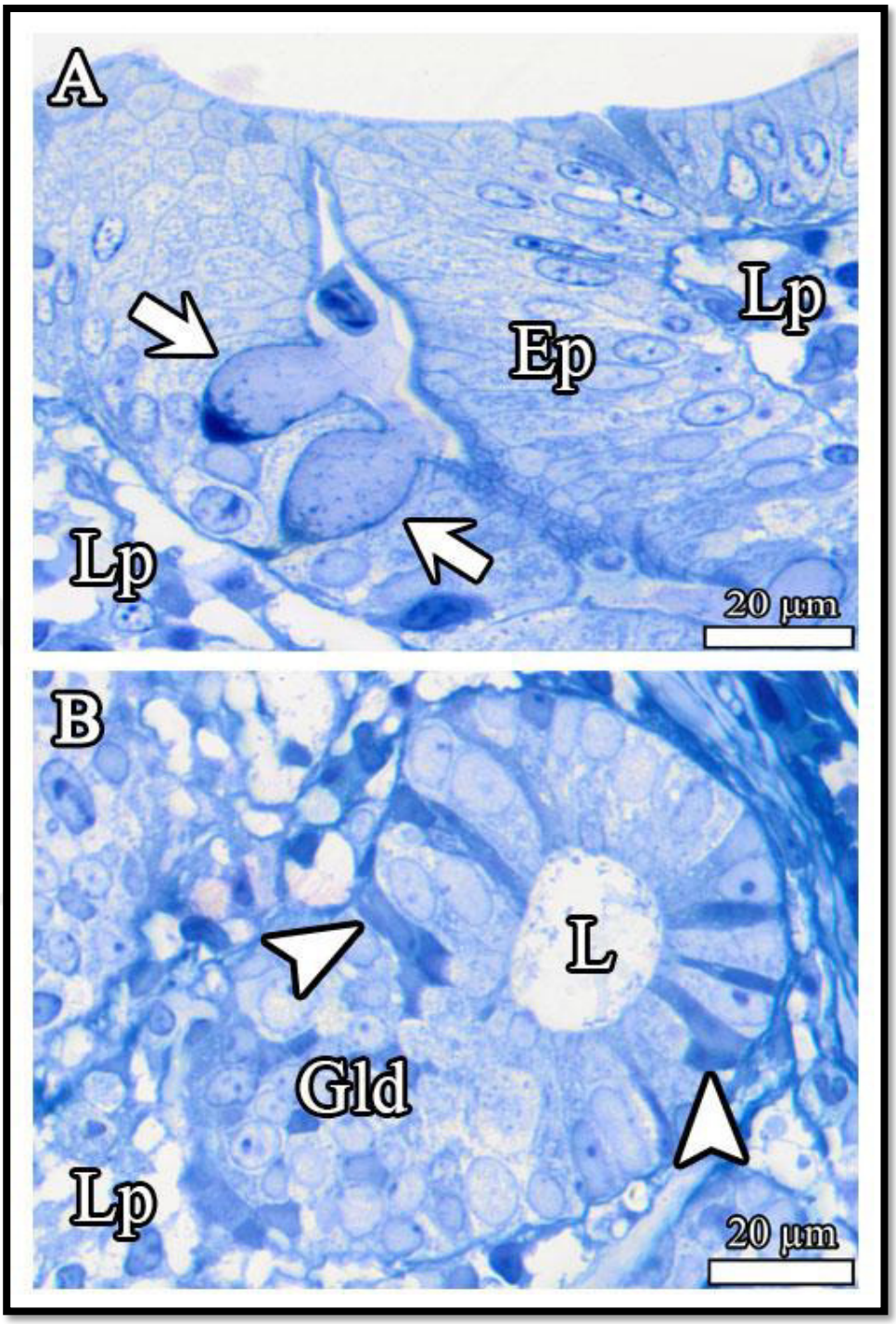

Figure 4. 65. **(A)** A high magnification of simple columnar epithelium (Ep) of the small intestine belongs to the diclofenac sodium (DS) group. Two Goblet cells are seen (arrows); both of them are discharging their secretion (arrow). The brush border of microvilli is very thin and so difficult to recognize. Some of the dens structures inside and outside of the epithelium might be an apoptotic body of impaired cells. Lamina propria (Lp) of the mucosa is seen, and the basal membrane of epithelium delineates the borders of this connective tissue (arrowheads). **(B)** An intestinal gland (Gld) and its lumen (L) are observed. Many vacuolization in the tissue are a prominent feature of Lp. The basal membrane is partly thickened. Many densely stained cells in the gland are found. Those might be non-functional cells. Semithin section of resin embedded tissue (0.5 µm thickness) and stained with toluidine blue

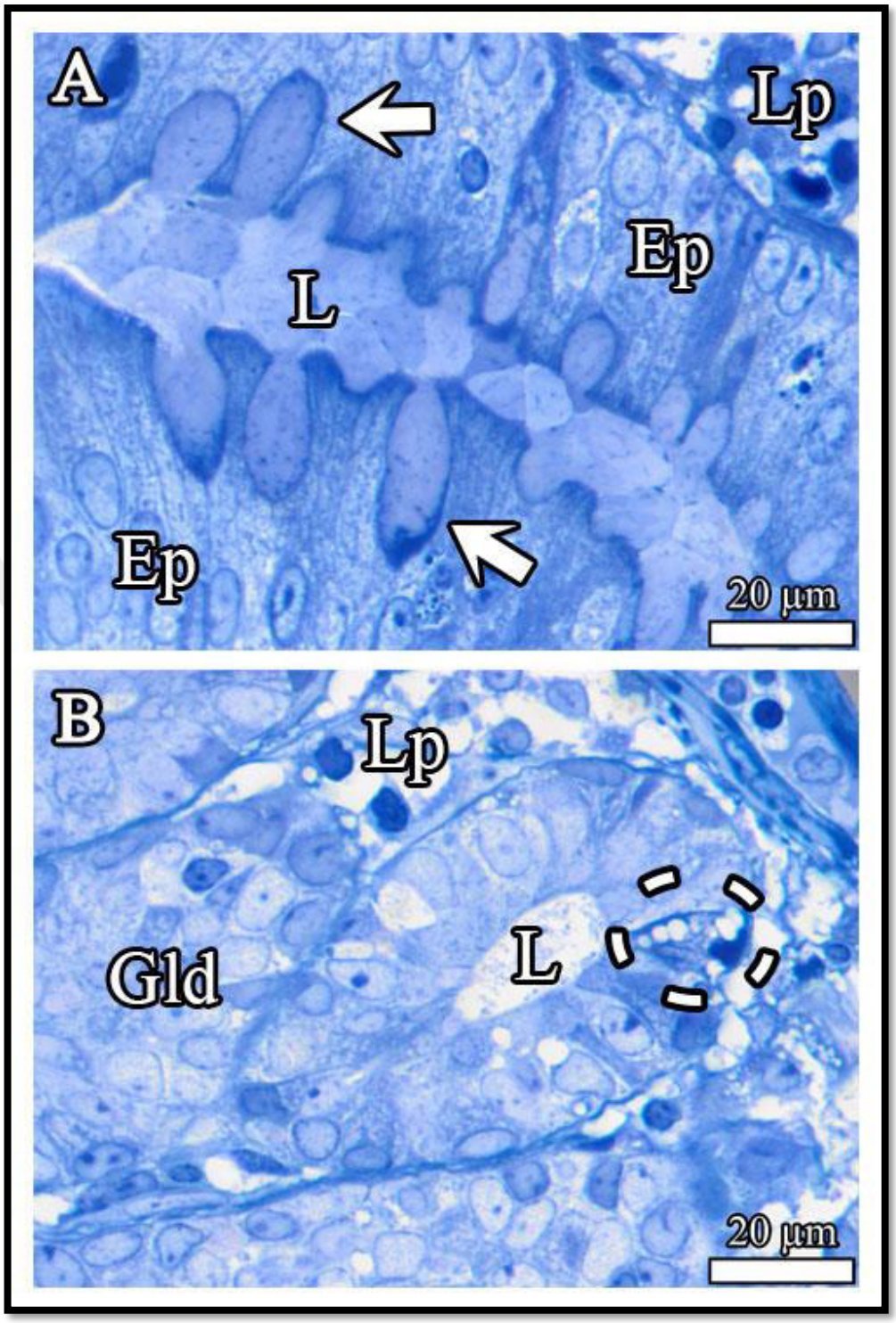

Figure 4. 66. (A) A high magnification of intestinal gland, it is lined by simple columnar epithelium (Ep) that has many Goblet cells (arrows) that belongs to the diclofenac sodium (DS) group. Two Goblet cells are seen (arrows); both of them are discharging their secretion (arrow). **(B)** An intestinal gland (Gld), transverse sectioned, and its lumen (L) is observed. A cell-like structure is seen in the epithelium, this might be an intermediate cell, a transition of a cell from Goblet to Paneth cell (dashed circled area). A high number of vacuolization in the (Lp) is observed. Semithin section of resin embedded tissue (0.5 µm thickness) and stained with toluidine blue

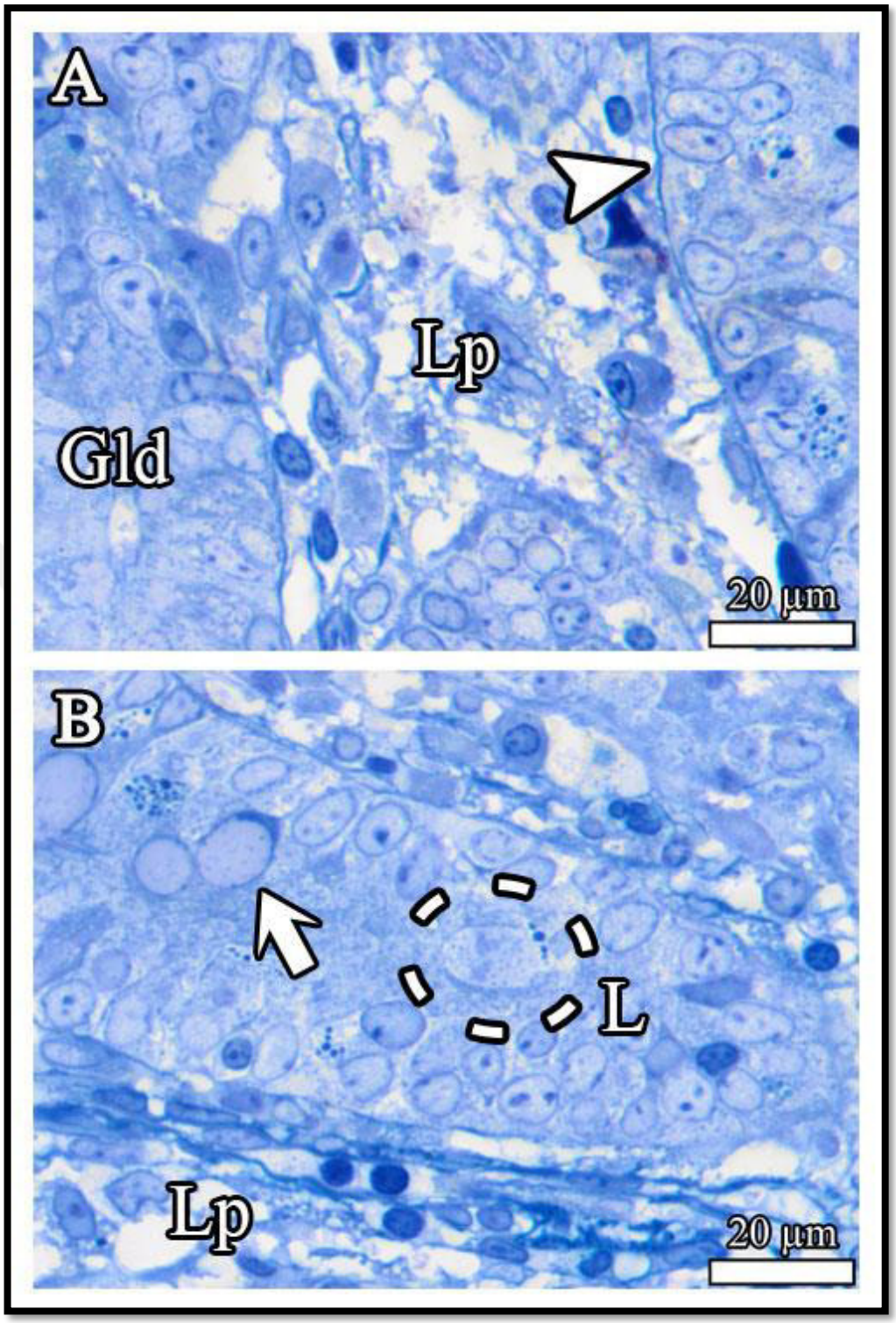

Figure 4. 67. (A) A high magnification of lamina propria (Lp) and glandular epithelium of the small intestine belongs to the diclofenac sodium (DS) group. Many different size vacuoles are a prominent feature of this group. A thick basal membrane (arrowhead) and many small size dense granules might be an apoptotic body of impaired cells in the epithelium. **(B)** A longitudinal section of the gland, its lumen (dashed lined area), and Goblet cells (arrow) are observed. Many dense granular structures are seen in the different parts of epithelium, they might be apoptotic bodies. Semithin section of resin embedded tissue (0.5 µm thickness) and stained with toluidine blue

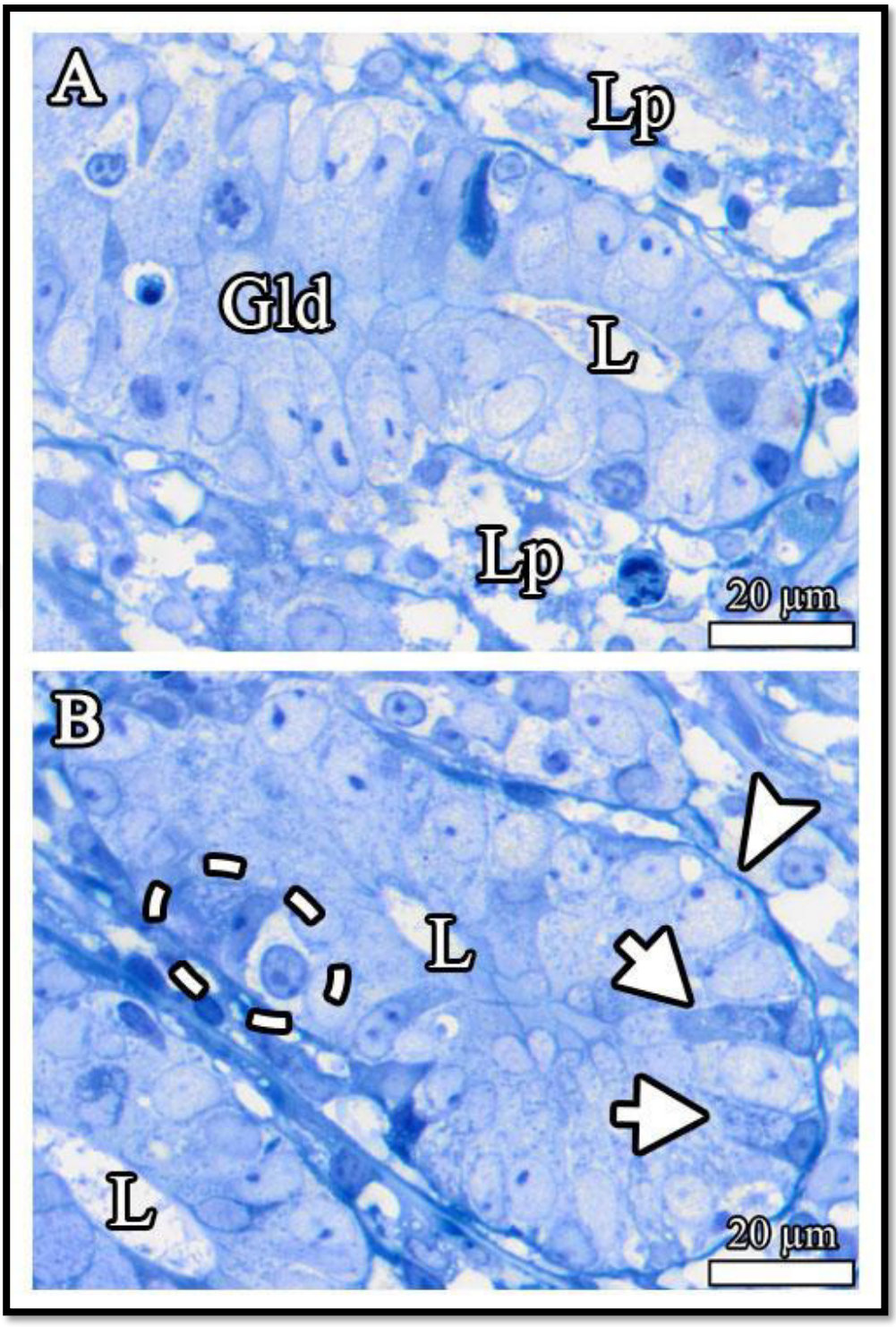

Figure 4. 68. **(A, B)** Longitudinally sectioned intestinal glands (Gld) with a lumen (L) belonging to the diclofenac sodium (DS) group is seen. Each gland is surrounded by lamina propria (Lp) that has many different sizes of vacuoles. A thick basal membrane (arrowhead) surrounds the glandular epithelium. Many lymphocytes infiltration into the epithelium (dashed circle area) is seen. **(B)** Darkly stained cells might be Paneth cells (arrow). Semithin section of resin embedded tissue (0.5 µm thickness) and stained with toluidine blue

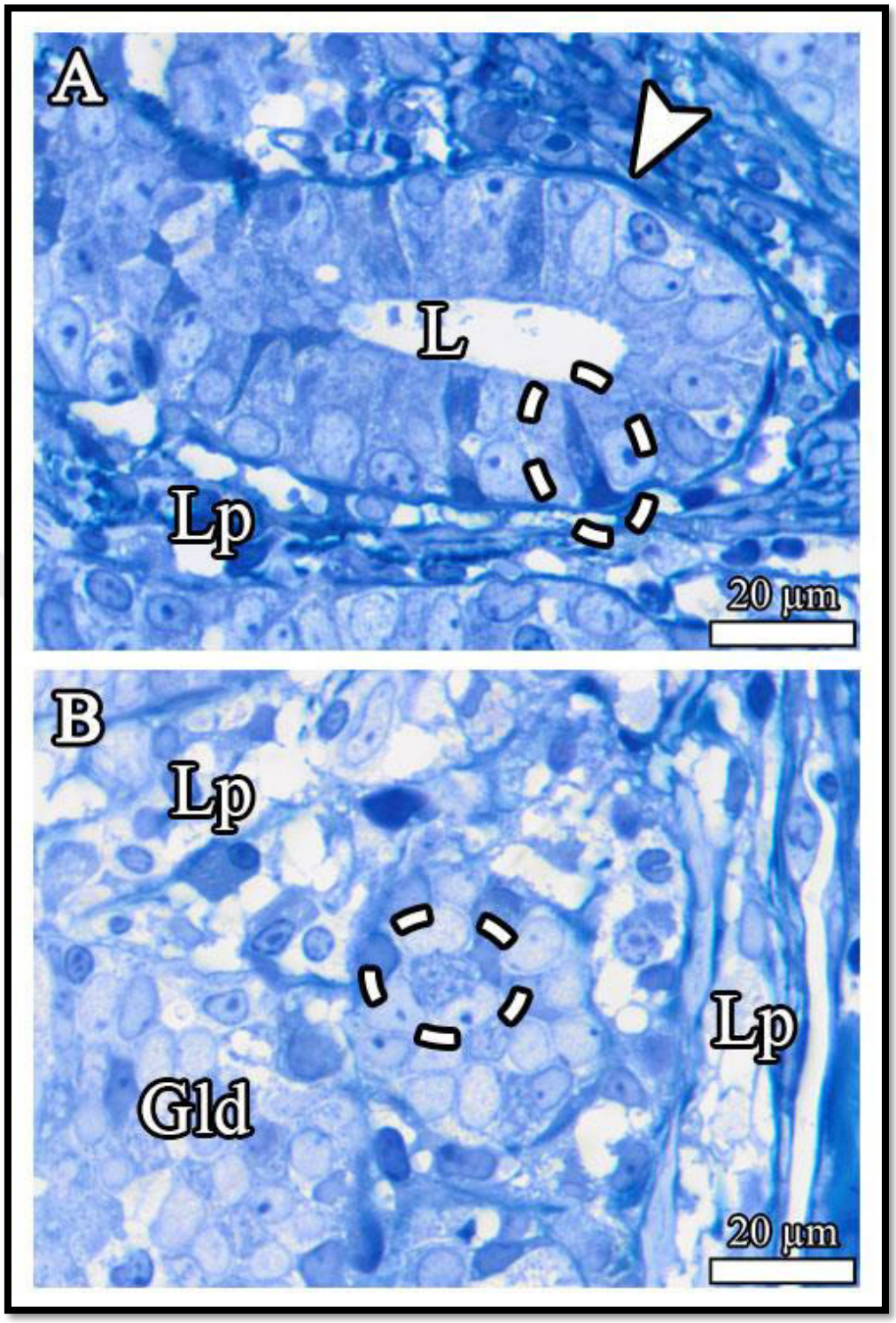

Figure 4. 69. (A) A longitudinal section of the intestinal gland with a thick basal membrane (arrowhead) belonging to the diclofenac sodium (DS) group is seen. The gland has a large size lumen (L) and many darkly stained cells (dashed circled area) in the glandular epithelium are observed. The density of connective tissue of the lamina propria (Lp) is also clearly seen. **(B)** A small size/transverse section of the intestinal gland (Gld) is observed, and a section was not passed from the lumen of it. A granular structure may be a small part of the Paneth cell is delineated (dashed circled area). Many different size vacuoles are found in the (Lp). Semithin section of resin embedded tissue (0.5 µm thickness) and stained with toluidine blue

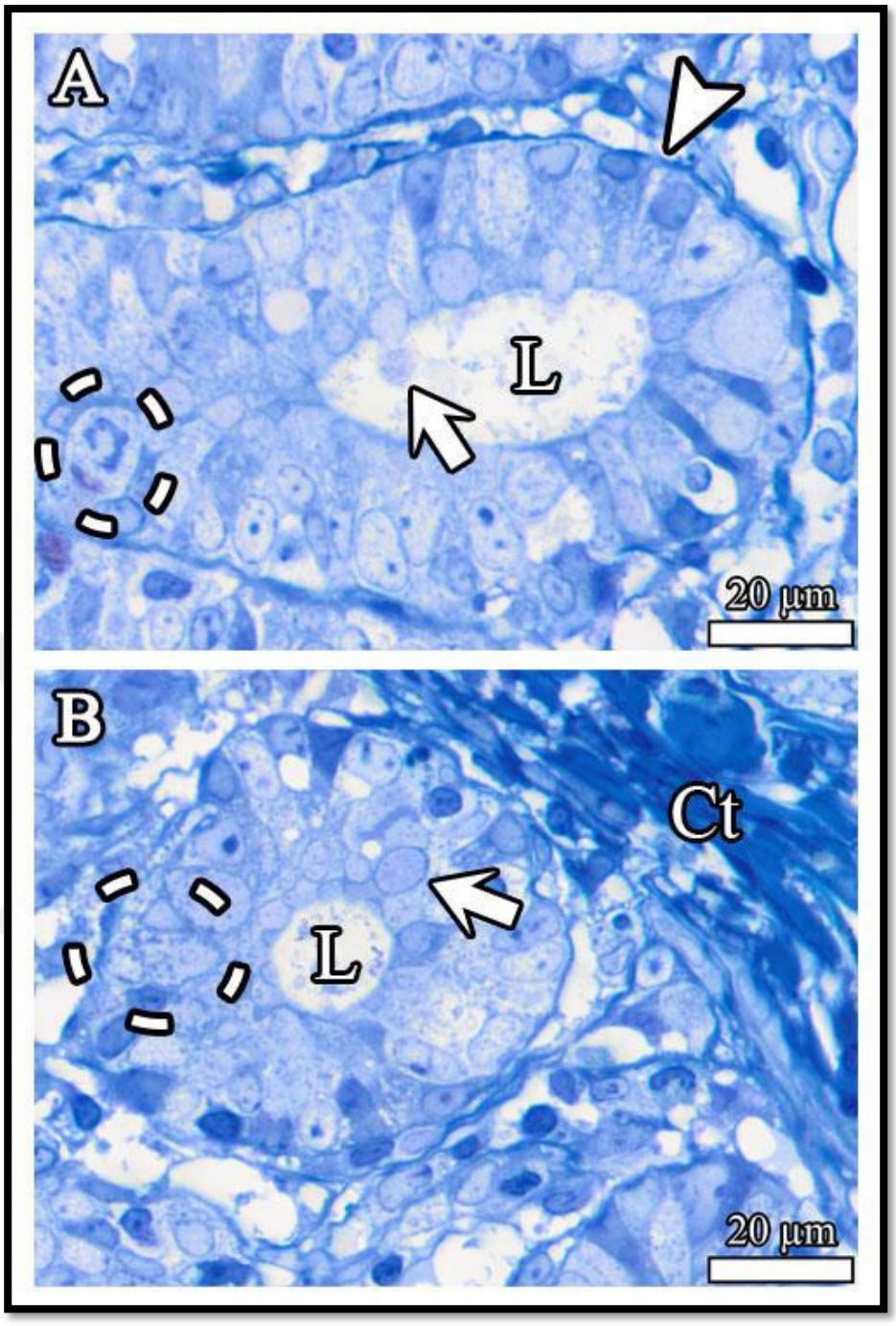

Figure 4. 70. (A) A longitudinal section of the intestinal gland with a thick basal membrane (arrowhead) belonging to the diclofenac sodium (DS) group is observed. The gland has a large size lumen (L) and a mitotic figure (dashed circled area) in the glandular epithelium is observed. Goblet cells are discharging (arrow) their secretion into the lumen. **(B)** A small size/transverse section of the intestinal gland with a small size lumen (L) is observed. A granular structure might be a remnant of Paneth cells that is delineated by a dashed circled area. Goblet cell is shown (arrow). Many different size vacuoles in the connective tissue (Ct) of lamina propria are seen. Semithin section of resin embedded tissue (0.5 µm thickness) and stained with toluidine blue

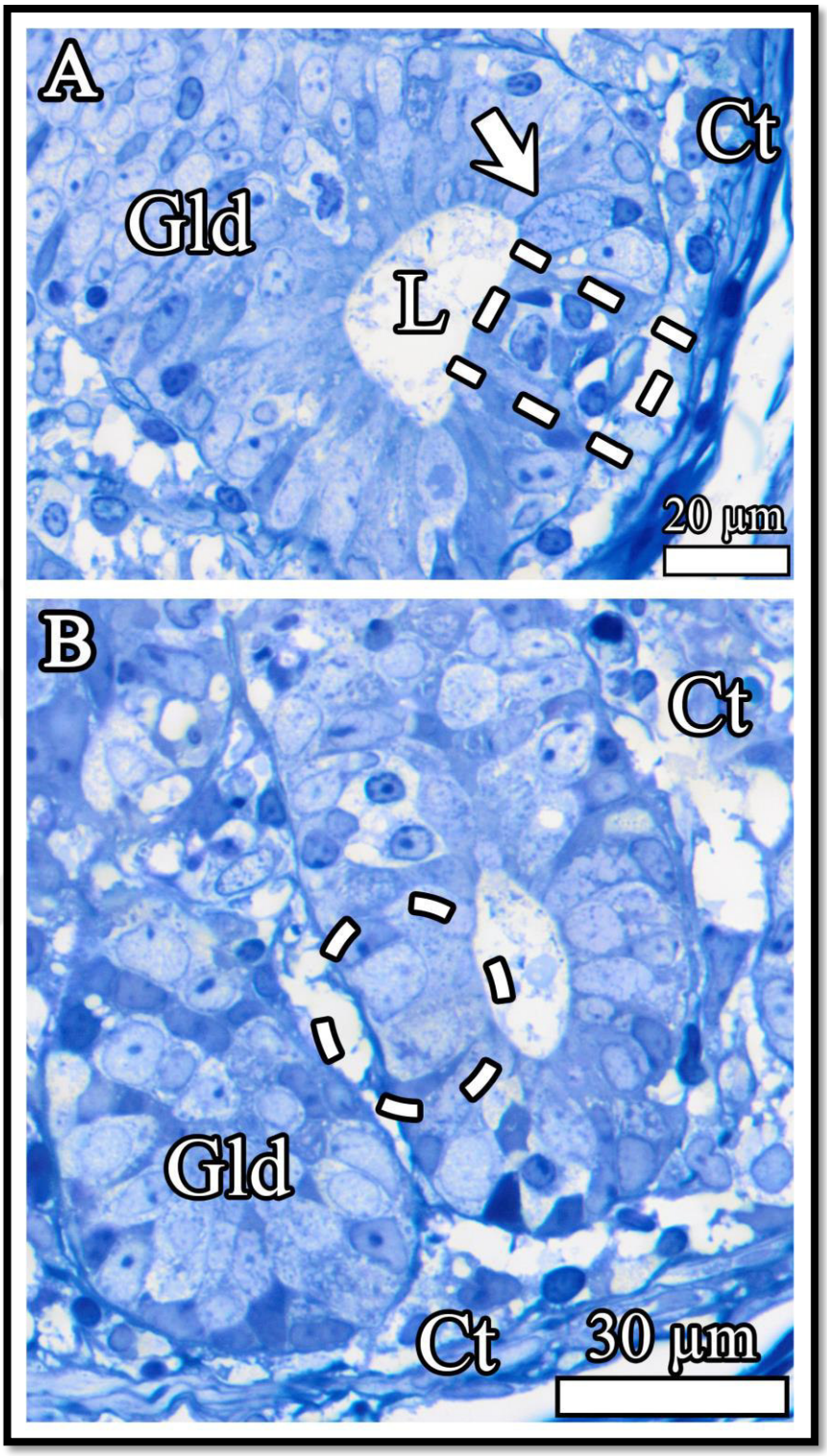

Figure 4. 71. (A, B) Longitudinal sections of intestinal glands (Gld) with a thick basal membrane (arrowhead) belonging to the diclofenac sodium (DS) group are observed. These glands have large size lumens (L) and many Goblet cells (arrow) in the glandular epithelium as well as many cells infiltration into the epithelium (dashed squared area) is observed. Goblet cells are discharging (arrow) their secretion into the lumen. **(B)** Enlarged Goblet cells accumulation is observed. Many different size vacuoles in the connective tissue (Ct) of lamina propria are seen. Semithin section of resin embedded tissue (0.5 µm thickness) and stained with toluidine blue

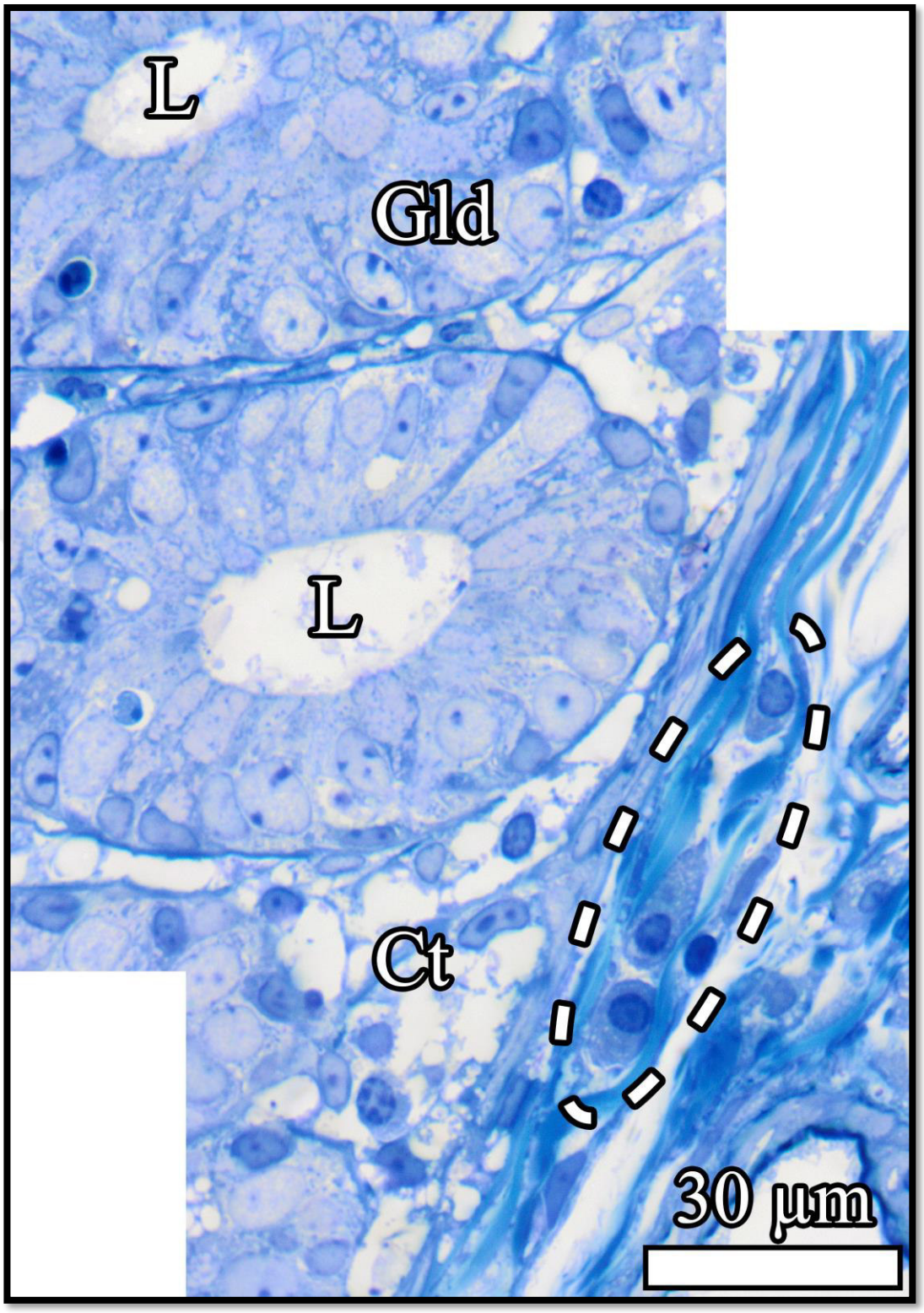

Figure 4. 72. A unified image of sections belonging to the small intestinal glands (Gld) with a thick basal membrane to the diclofenac sodium (DS) group is observed. It has a large size lumen (L). Connective tissue (Ct) of lamina propria has many different sizes of vacuoles. An augmentation of plasma cells (dashed elliptical area) is seen. Semithin section of resin embedded tissue (0.5 µm thickness) and stained with toluidine blue

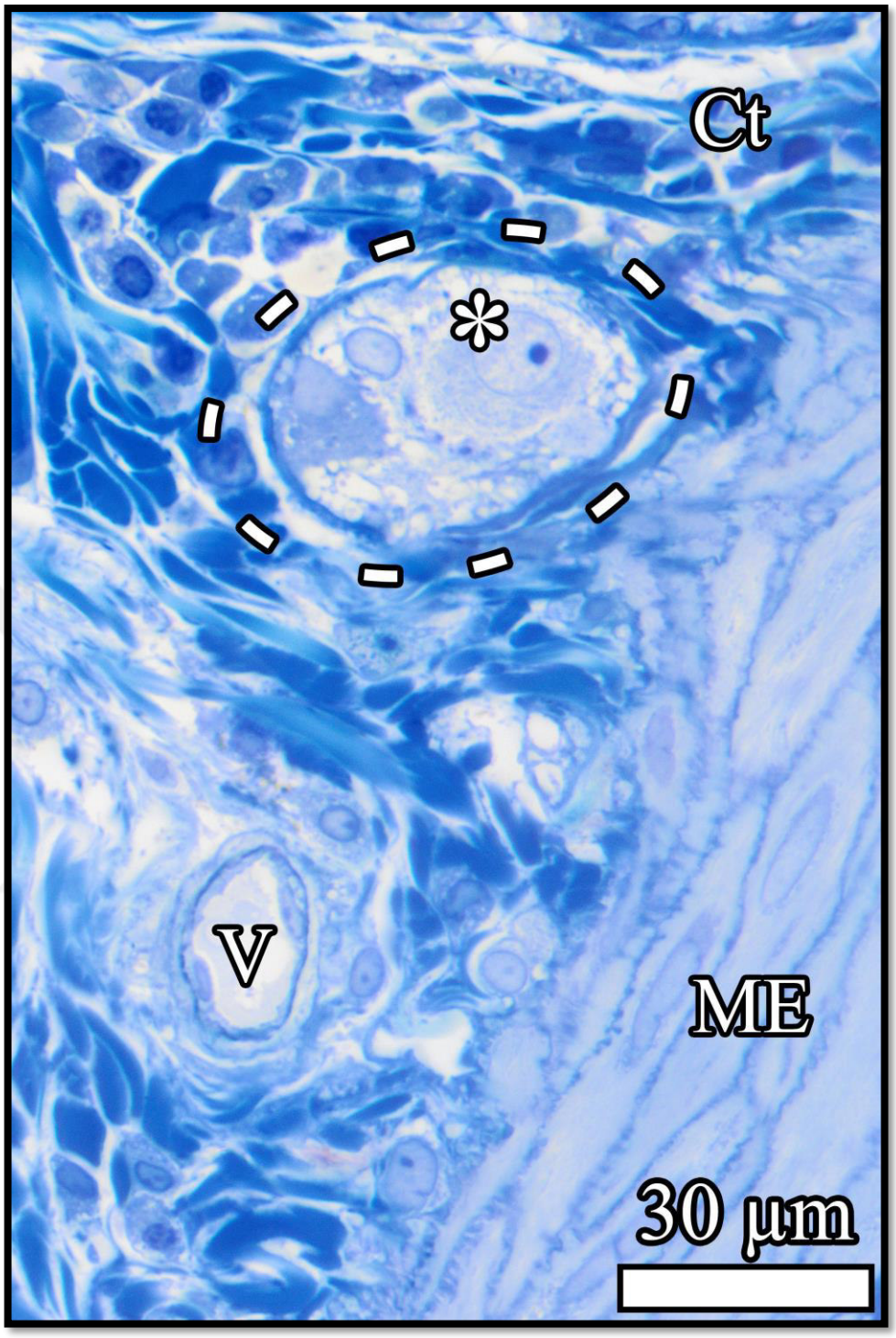

Figure 4. 73. A submucosal ganglion that is surrendered by a connective tissue capsule (dashed circled area) belonging to the diclofenac sodium (DS) group is observed. A ganglionic cell is shown by (*). Vessel (V) in the densely stained connective tissue (Ct) is seen. Muscle cells, covered by a thick basal membrane, of tunica muscularis externa (ME) are observed. Semithin section of resin embedded tissue (0.5 µm thickness) and stained with toluidine blue

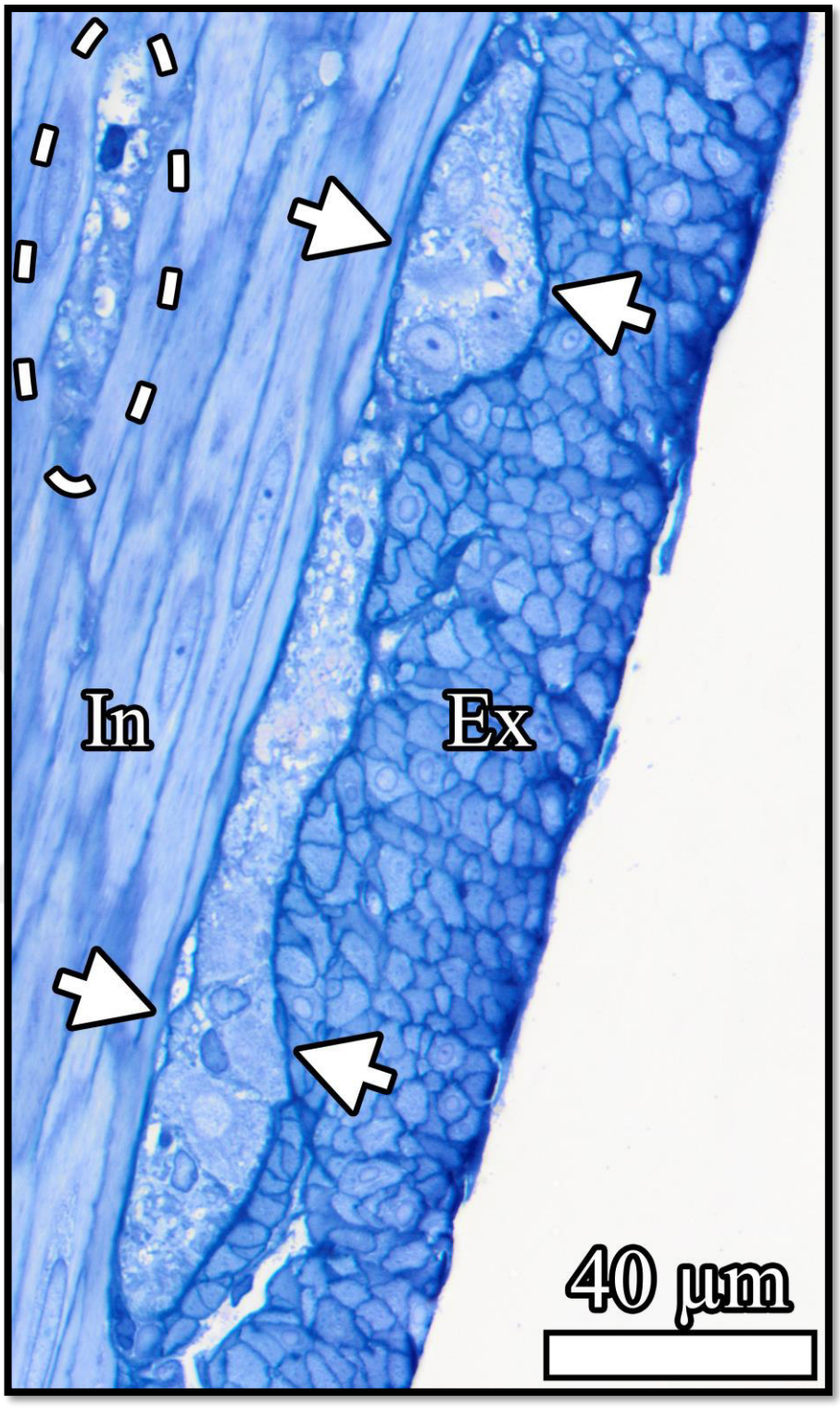

Figure 4. 74. A longitudinal section of muscularis externa that has internal and external layers of muscle belonging to the diclofenac sodium (DS) group is observed. Arrows show ganglionic cells of the myenteric plexus. A densely stained capsule has covered this structure. The dashed elliptical area shows another ganglionic cells accumulation in the inner circular layer (In) of smooth muscle cells. (Ex), the external layer of the muscularis externa. Semithin section of resin embedded tissue (0.5 µm thickness) and stained with toluidine blue

4.1.2.2.3. Diclofenac Sodium + Gum Arabic Group

The small intestine in this group, as a result of the extension, the villus grew in size and in the lamina propria, there is a significant lymphocyte infiltration. The intestinal glands' lumen was partially enlarged. Except for a significant density of lymphocytes in the lamina propria, all of the small intestinal layers appear to be healthy. The epithelium contains a high number of Goblet cells. There are several tiny vacuoles at the epithelium's base, as well as lymphocyte infiltration. In the lamina propria, lymphatic capillary and mast cells can be observed. At the base of the gland, Paneth cells accumulation is seen. The tunica mucosa, submucosa, muscularis externa, and tunica serosa are visible. There is a submucosal ganglionic plexus with a neuron (Figures 4.75-4.85).

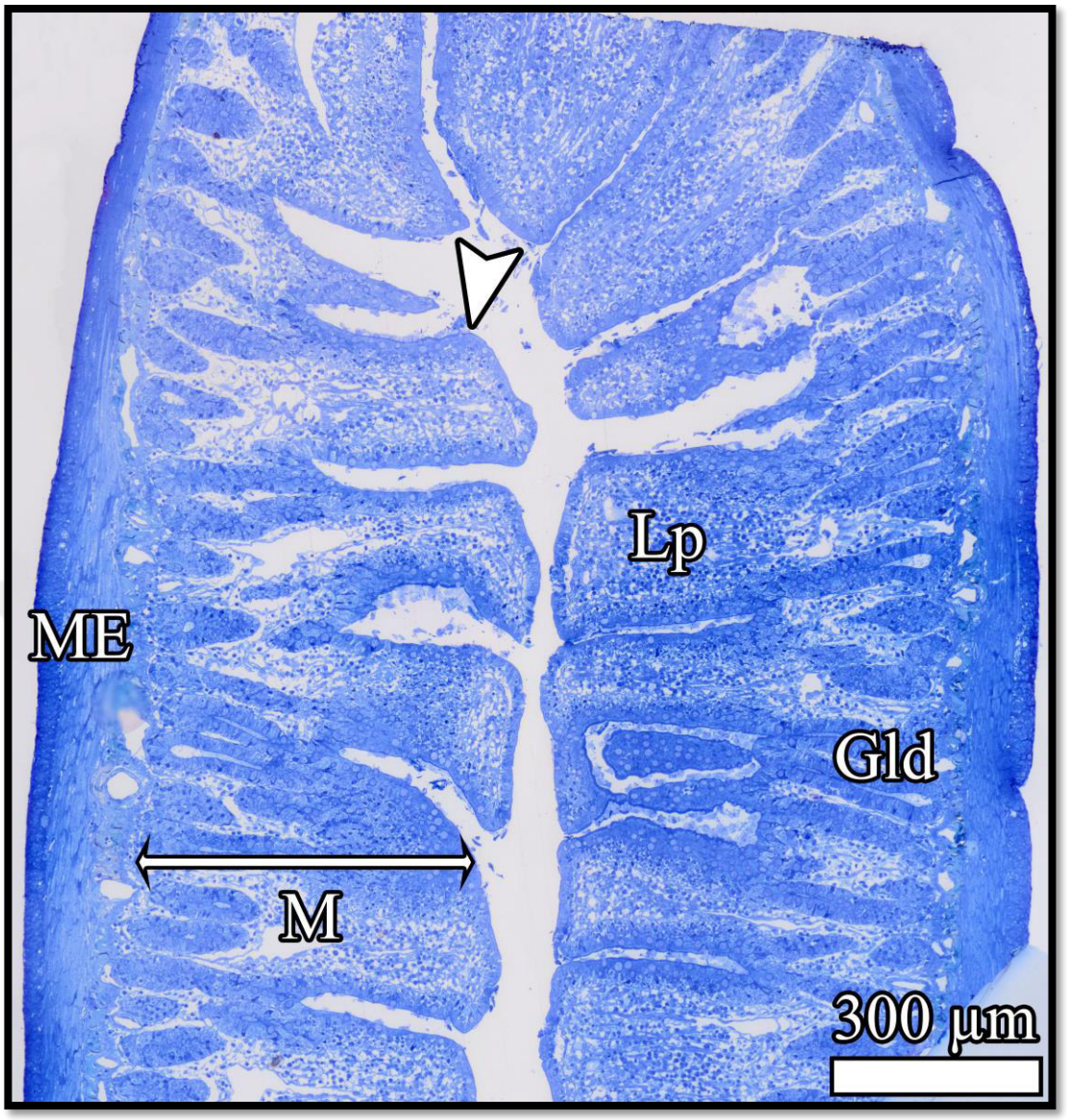

Figure 4. 75. A general view of the small intestine belonging to the DS + GA group. The size of the villus (arrowhead) was increased as a result of the extension. Pronounced lymphocyte infiltration in lamina propria (Lp) is seen. The lumen of the intestinal glands (Gld) was partly increased. (M), mucosa; (ME), muscularis externa. Semithin section of resin embedded tissue (0.5 µm thickness) and stained with toluidine blue

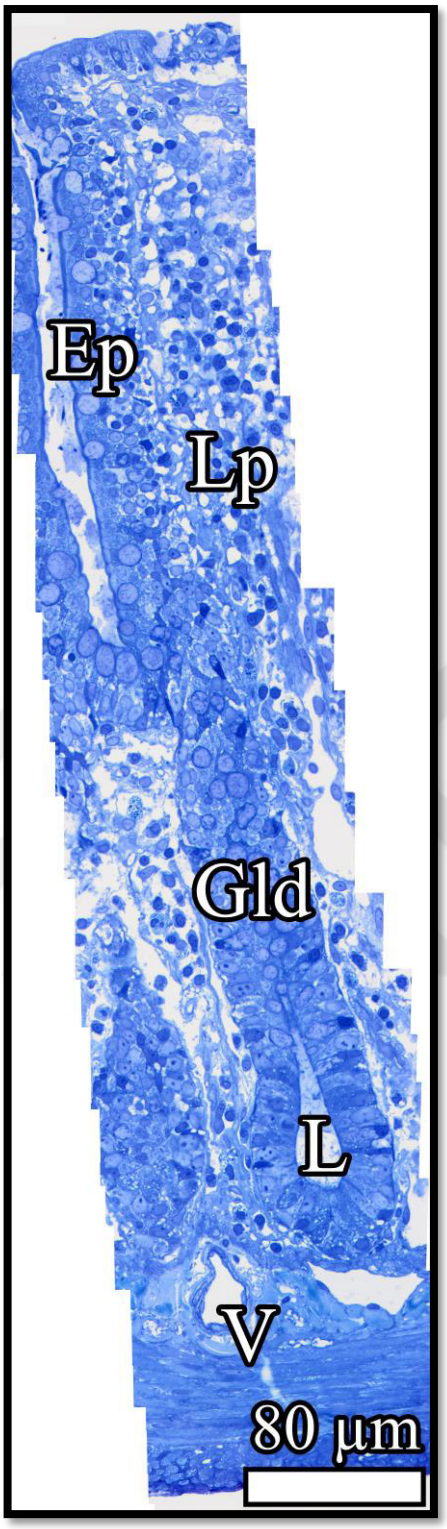

Figure 4. 76. A high magnification of the small intestine belonging to the DS + GA group is seen. All of the small intestine layers look healthy, except for a high density of lymphocytes in the lamina propria (Lp). The lumen (L) of the gland (Gld) is partly enlarged. Many Goblet cells can be seen in the epithelium (Ep). (V), vessel. Semithin section of resin embedded tissue (0.5 µm thickness) and stained with toluidine blue

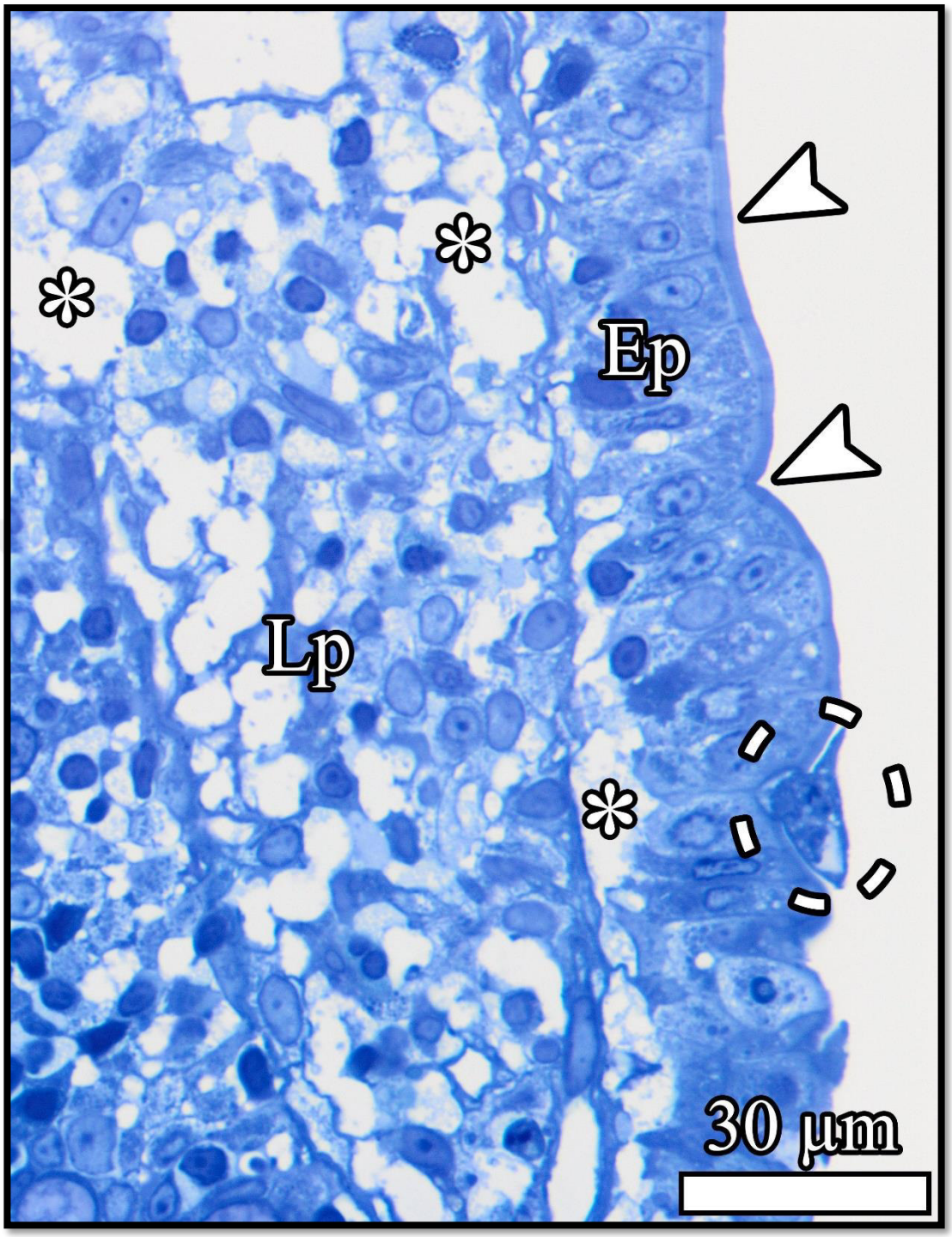

Figure 4. 77. A high magnification of epithelium (Ep) and lamina propria (Lp) of the small intestine belonging to the DS + GA group is seen. Most of both layers of the small intestine look healthy, except for a high density of lymphocytes in the lamina propria as well as in the epithelium that has a brush border (arrowheads) on it. A high number of vacuoles in the lamina propria are observed. Debris of cells is found on the epithelium surface (dashed circled area). Semithin section of resin embedded tissue (0.5 µm thickness) and stained with toluidine blue

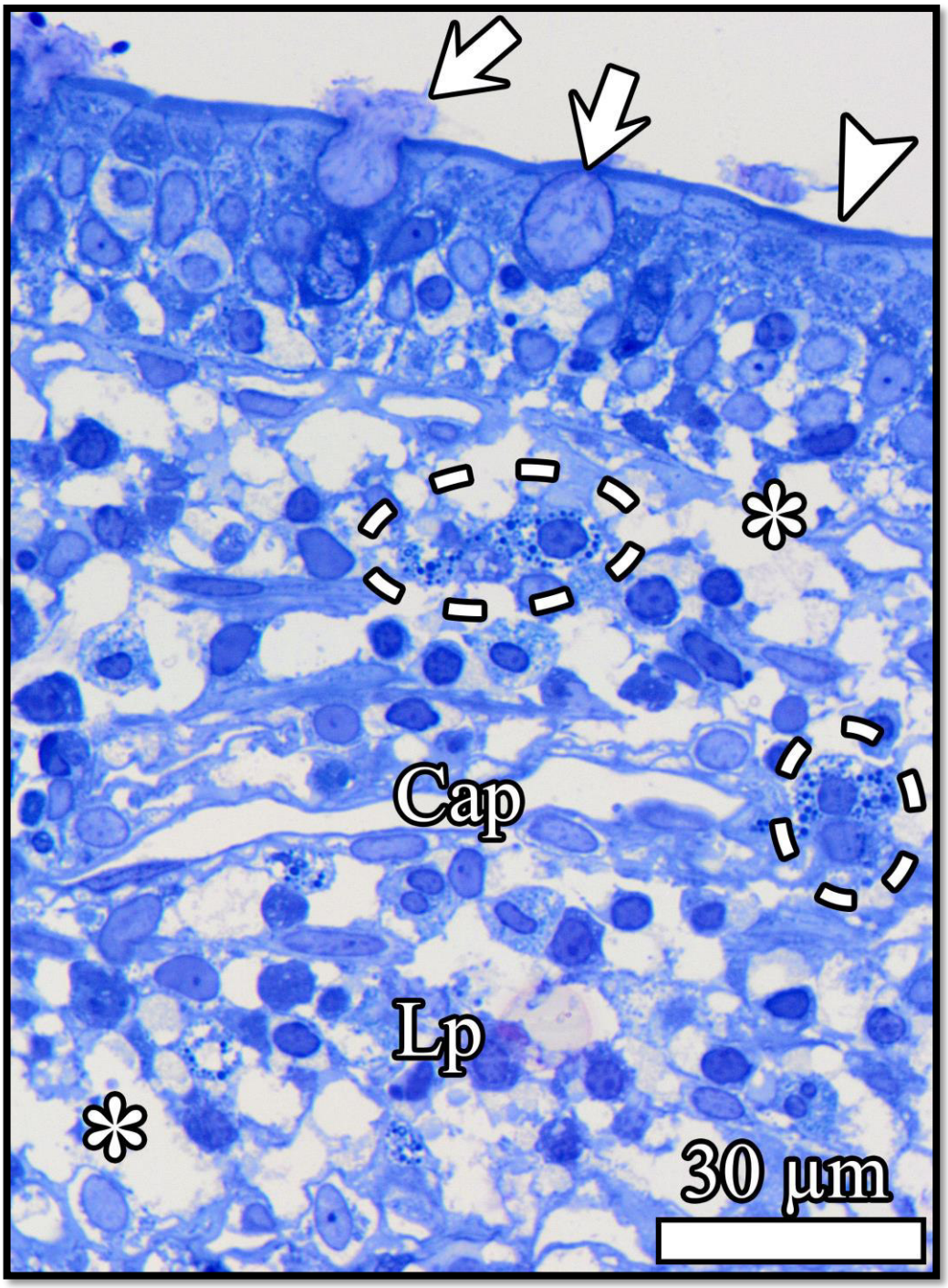

Figure 4. 78. A high magnification of epithelium (Ep) and lamina propria (Lp) of the small intestine belonging to the DS + GA group is observed. Most of these layers of the small intestine look healthy, except for a high density of lymphocytes in the lamina propria as well as in the epithelium that has a brush border (arrowheads) on it. Goblet cells in the epithelium are discharging their secretion (arrows). Many numbers of small size vacuoles at the base of the epithelium (*) and lymphocyte infiltration are observed. A lymphatic capillary (Cap) and mast cells (dashed lined area) in the lamina propria are seen. Semithin section of resin embedded tissue (0.5 µm thickness) and stained with toluidine blue

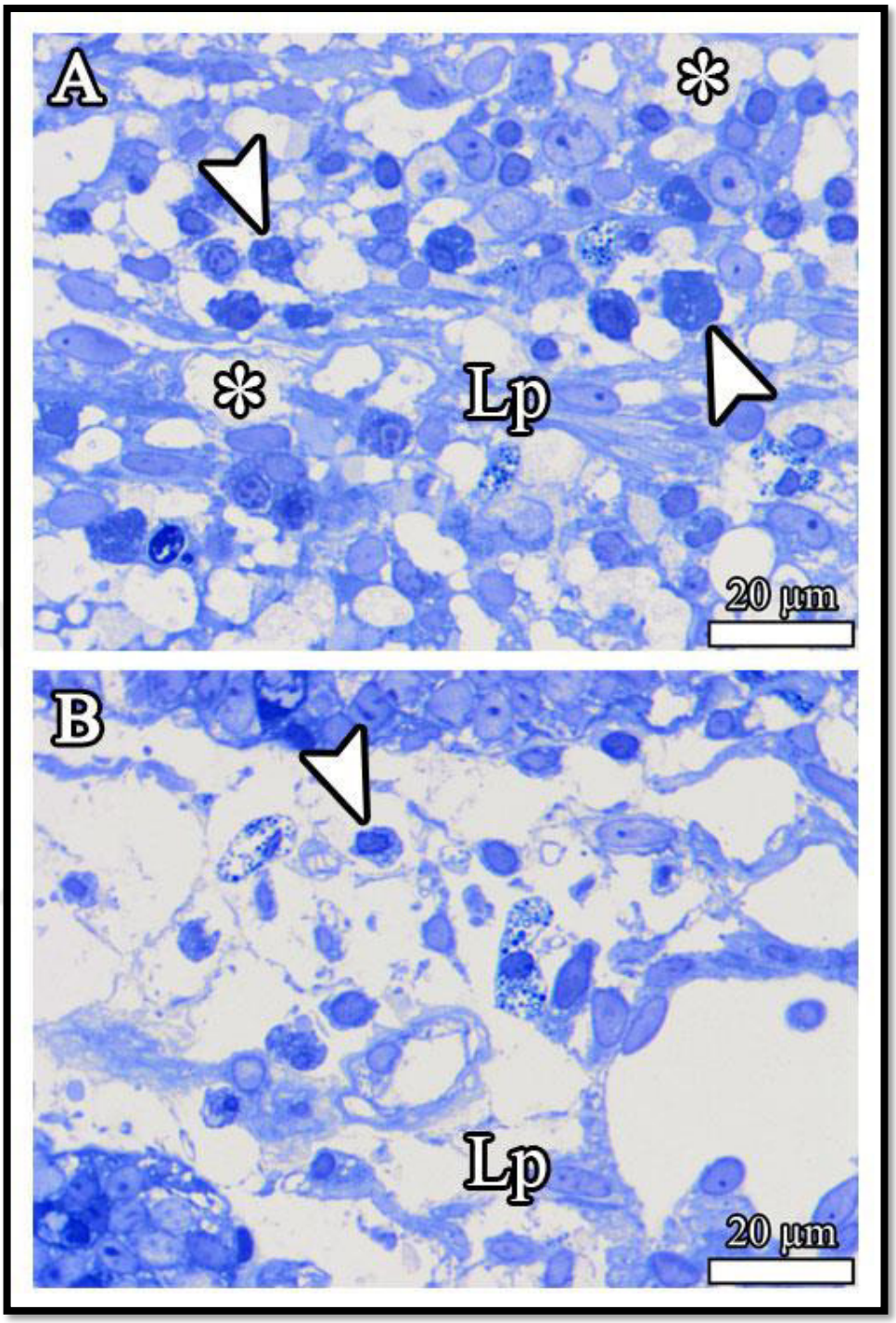

Figure 4. 79. (A, B) High magnification of lamina propria (Lp) of the small intestine belonging to the DS + GA group are observed. This layer of mucosa looks healthy, except for a high density of lymphocytes infiltration. Many numbers of different size vacuoles are observed (*). Darkly stained and large size cells (arrowheads) might be macrophages. Some of the granular structures may be mast cells. Semithin section of resin embedded tissue (0.5 µm thickness) and stained with toluidine blue

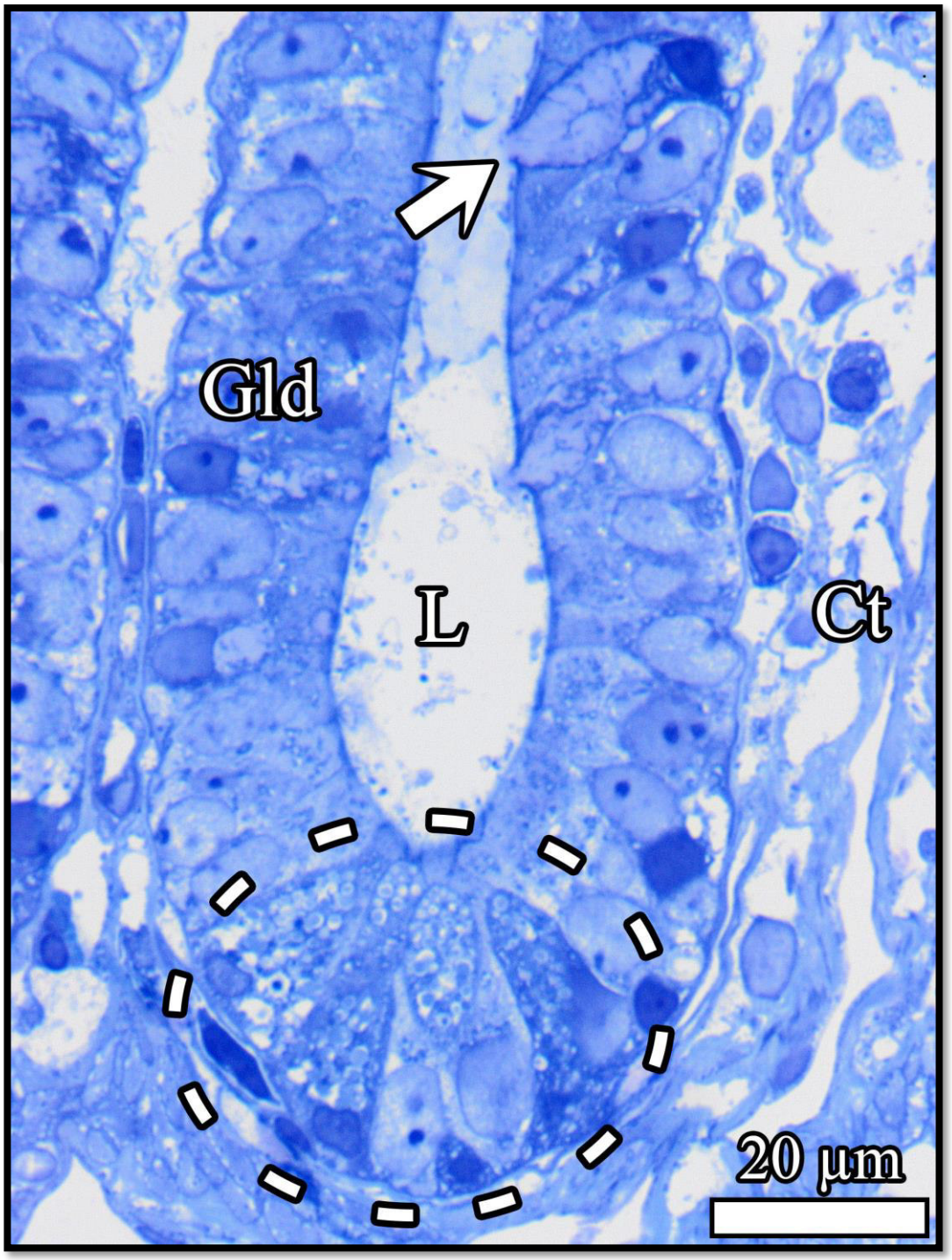

Figure 4. 80. A high magnification of an intestinal gland (Gld) and surrounding connective (Ct) in the small intestine belonging to the DS + GA group is seen. Glandular epithelium looks healthy and an enlarged Goblet cell that is discharging its content into the lumen is seen (arrow). The lumen (L) of the gland (Gld) is partly large in size. A Paneth cells accumulation is observed at the base of the gland (dashed circular area). Semithin section of resin embedded tissue (0.5 µm thickness) and stained with toluidine blue

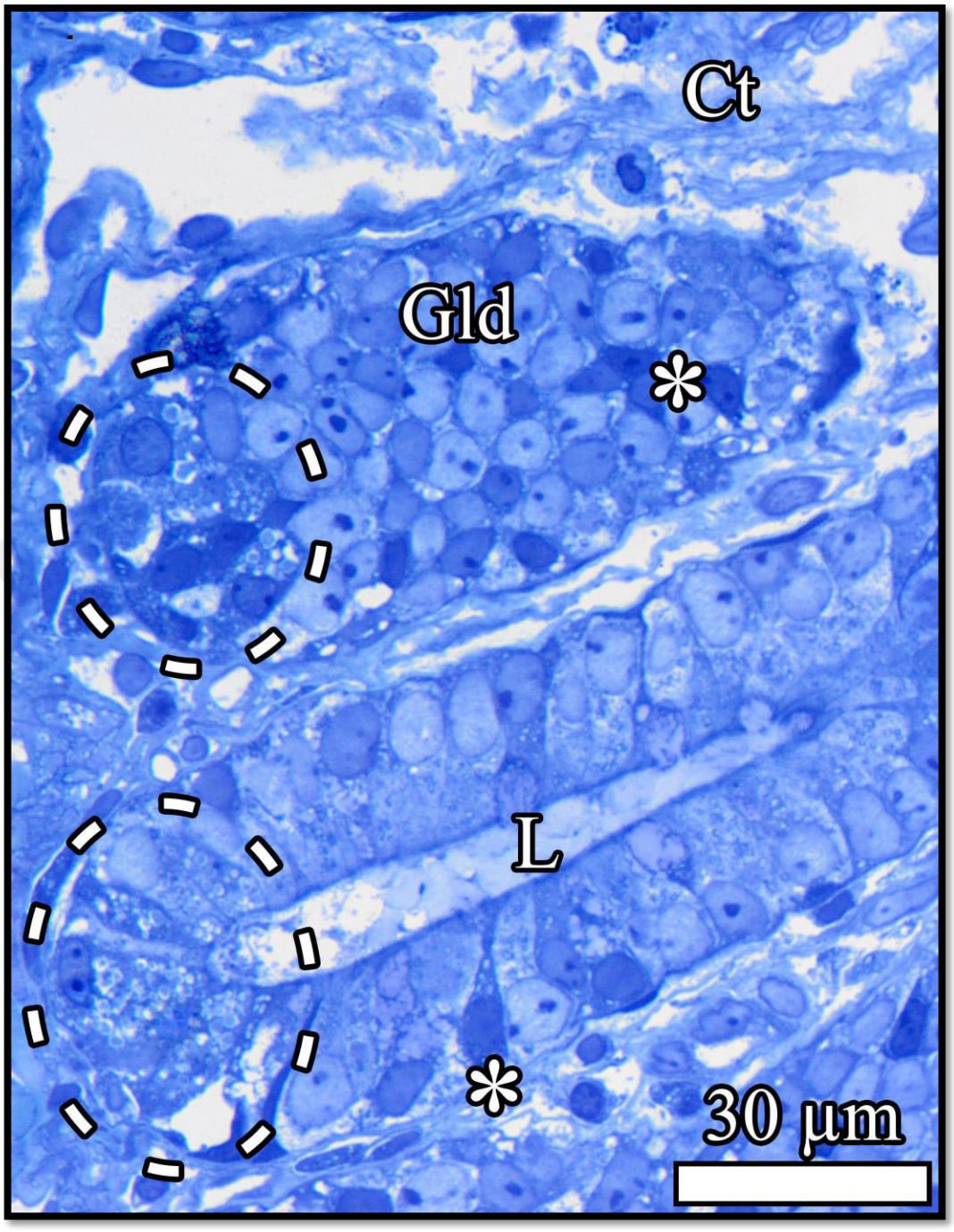

Figure 4. 81. A high magnification of two intestinal glands (Gld) that were cut longitudinally belonging to the DS + GA group is seen. At the base of them, accumulations of Paneth cells are observed (dashed circled line). Although most of the glandular cells have a healthy structure, some of them were darkly stained which may be lost their function (*). Pyramidal-shaped Paneth cells have densely stained granules; their nucleus is located at the base of the cells. The lumen (L) of the gland has partly a large size. Semithin section of resin embedded tissue (0.5 µm thickness) and stained with toluidine blue

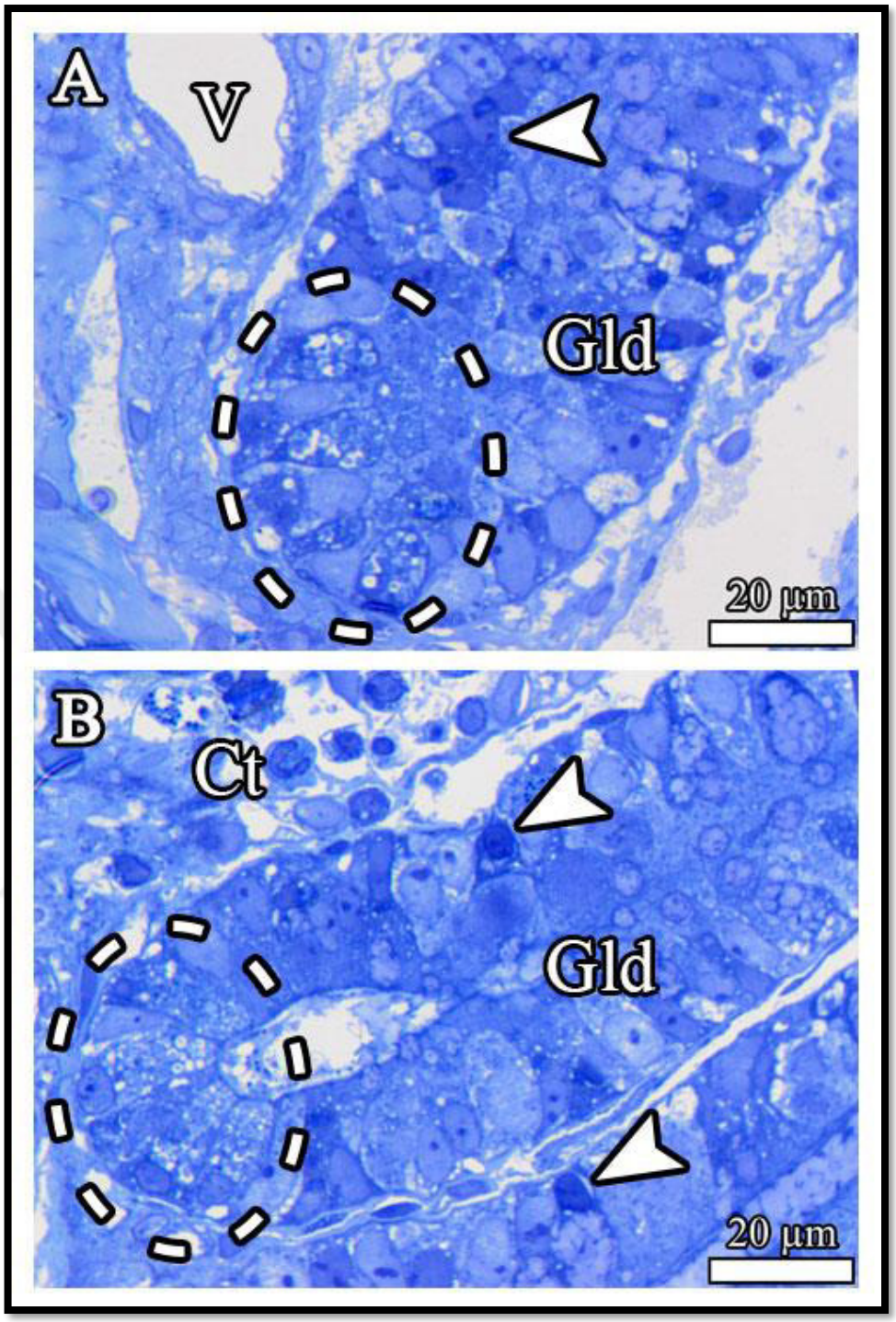

Figure 4. 82. **(A, B)** High magnification of two intestinal glands (Gld) that were cut longitudinally belonging to the DS + GA group are seen. At the base of them, accumulations of Paneth cells are found (dashed circled line). Although most of the glandular cells have a healthy structure, some of them were darkly stained which may be lost their function (arrowheads). Pyramidal-shaped Paneth cells have densely stained granules; their nucleus is located at the base of the cells. The lumen (L) of the gland has partly a large size and connective tissue (Ct) covers intestinal glands. Semithin section of resin embedded tissue (0.5 µm thickness) and stained with toluidine blue

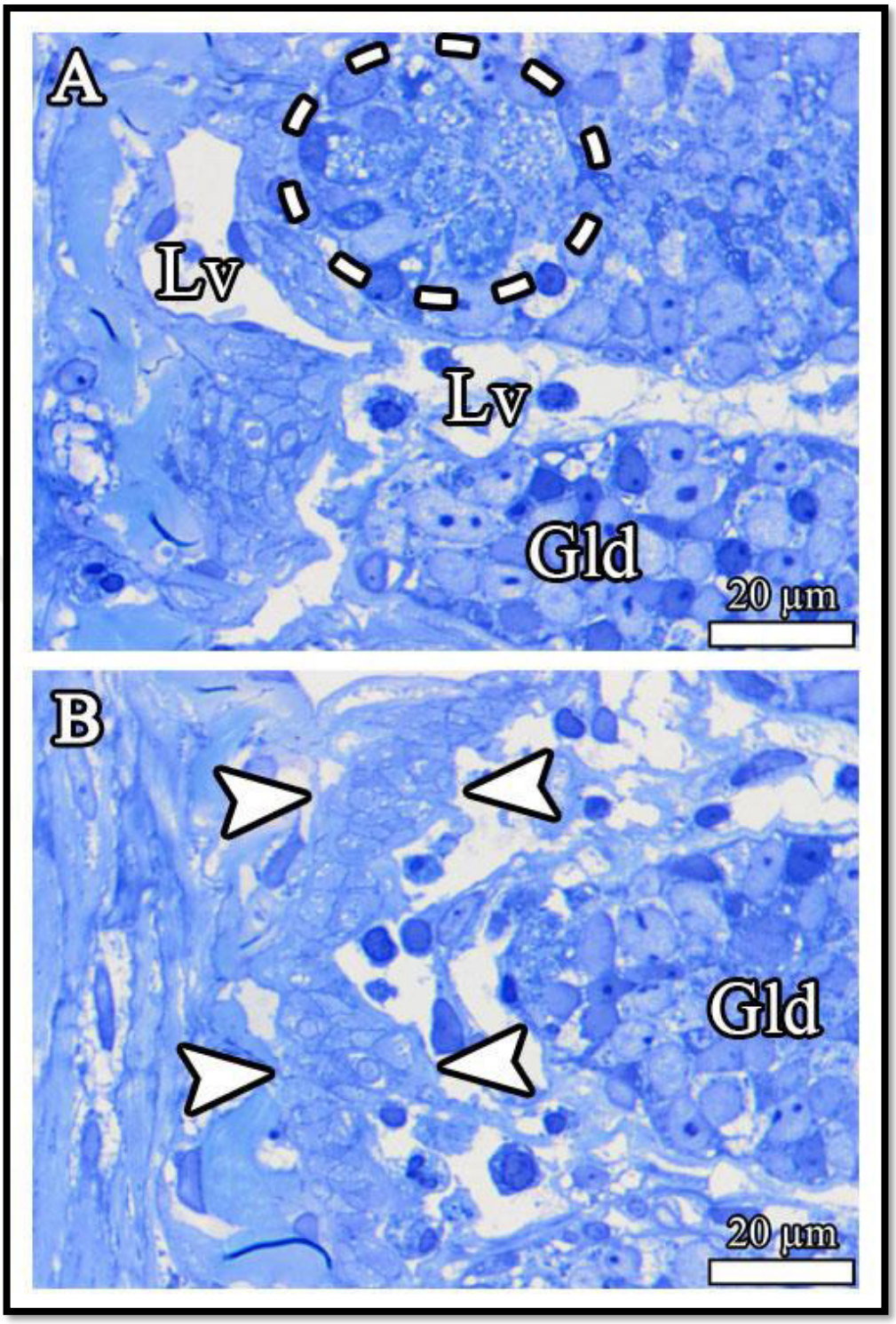

Figure 4. 83. (A) A high magnification of two intestinal glands (Gld) belonging to the DS + GA group is seen. At the base of one of them, an accumulation of Paneth cells is found (dashed circled line). Although most of the glandular cells have a healthy structure, some of them were very darkly stained which may lose their function. An enlarged size of the lymphatic vessel (Lv) is observed near the base of the gland. **(B)** The borders of a well-developed muscularis mucosae layer are shown by arrowheads. Lamina propria of mucosa has many vacuoles. Semithin section of resin embedded tissue (0.5 µm thickness) and stained with toluidine blue

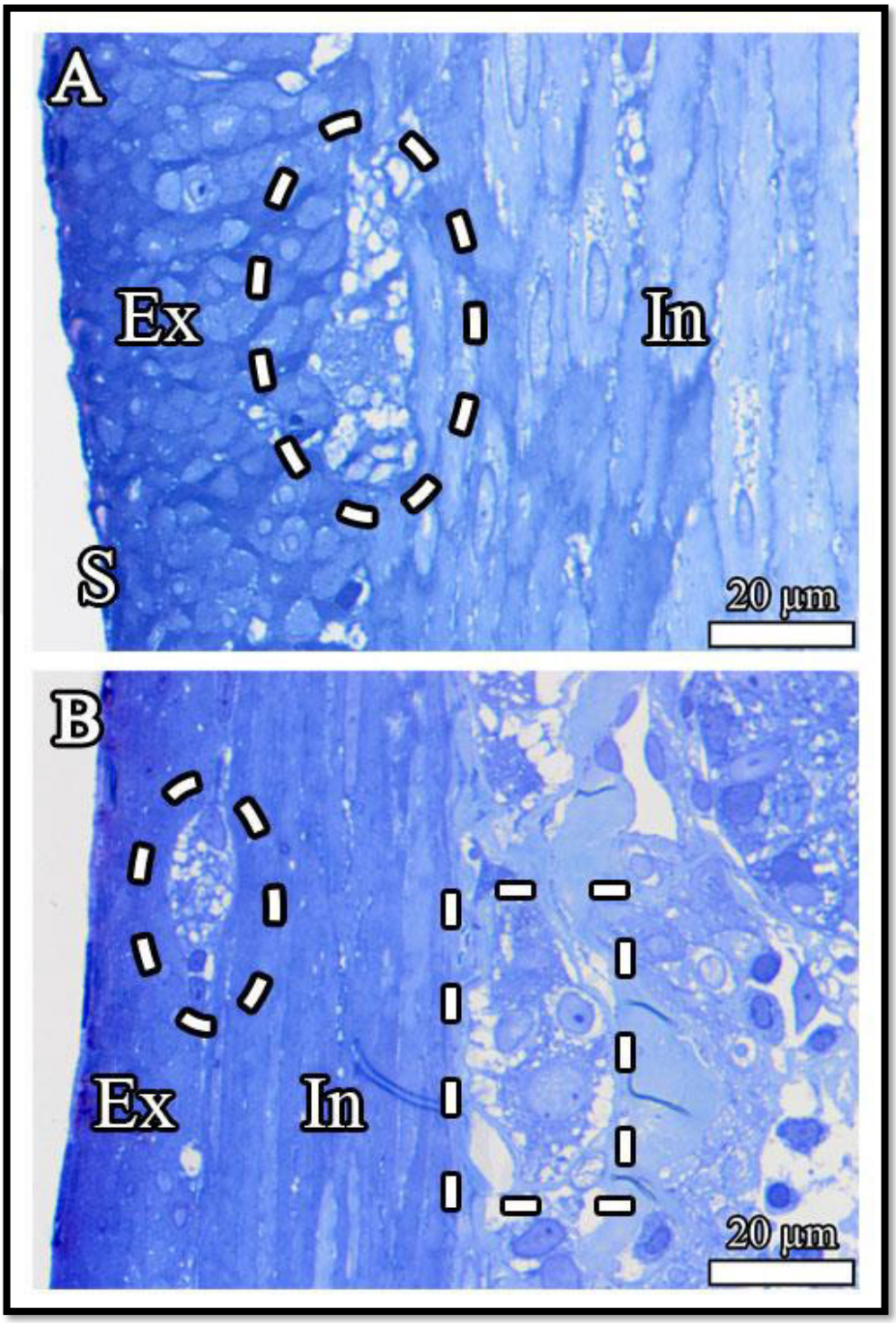

Figure 4. 84. (A) A high magnification of muscularis externa that consists of an inner (In) and external (Ex) layer belonging to the DS + GA group is seen. Between two layers of muscularis externa, a myenteric plexus is observed (dashed elliptic area). **(B)** Muscularis mucosae layer of tunica mucosa, submucosa, muscularis externa and tunica serosa are seen healthy. A submucosal ganglionic plexus with neuron is seen (dashed rectangular area). (Ex), external layer; (In), internal layer; (S), serosa. Semithin section of resin embedded tissue (0.5 µm thickness) and stained with toluidine blue

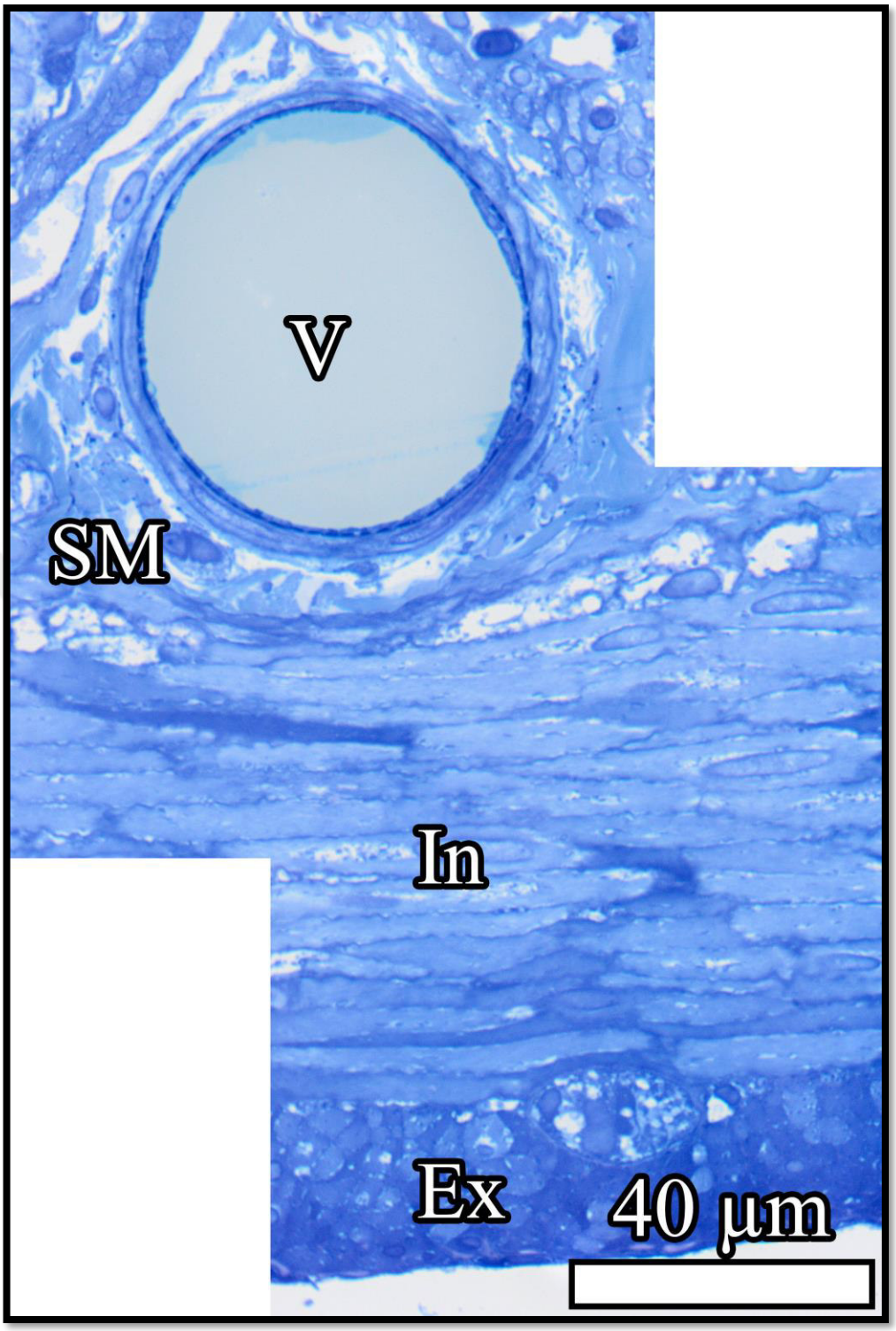

Figure 4. 85. (A) A high magnification of muscularis externa that consists of an inner (In) and external (Ex) and submucosa layer (SM) belonging to the DS + GA group is seen. The large size of the vessel is observed. (S), serosa. Semithin section of resin embedded tissue (0.5 µm thickness) and stained with toluidine blue

4.1.2.2.4. Gum Arabic Group

The whole layers of the small intestine in this group are well protected. The villus, Lieberkühn crypts, glands, epithelium, and connective tissue of the lamina propria are all intact. The surface epithelium and its lamina propria appear to be in good condition. Brush borders of epithelium and Goblet cells are found to be normal. The lamina propria's connective tissue and arteries have a well-protected structure. There is a small amount of lymphocyte infiltration in the epithelium. The nuclei of simple columnar epithelium, as well as their brush borders and Goblet cells, are visible and look healthy. The connective tissue has a dense capillary network. The apical cytoplasm of each Goblet cell is quite big. The Paneth cell can be seen in the intestinal gland's wall. A thick muscularis mucosae and submucosal plexus can be found beneath the gland. Myenteric plexus is observed between the inner and outer layers of the muscularis externa (Figures 4.86-4.95).

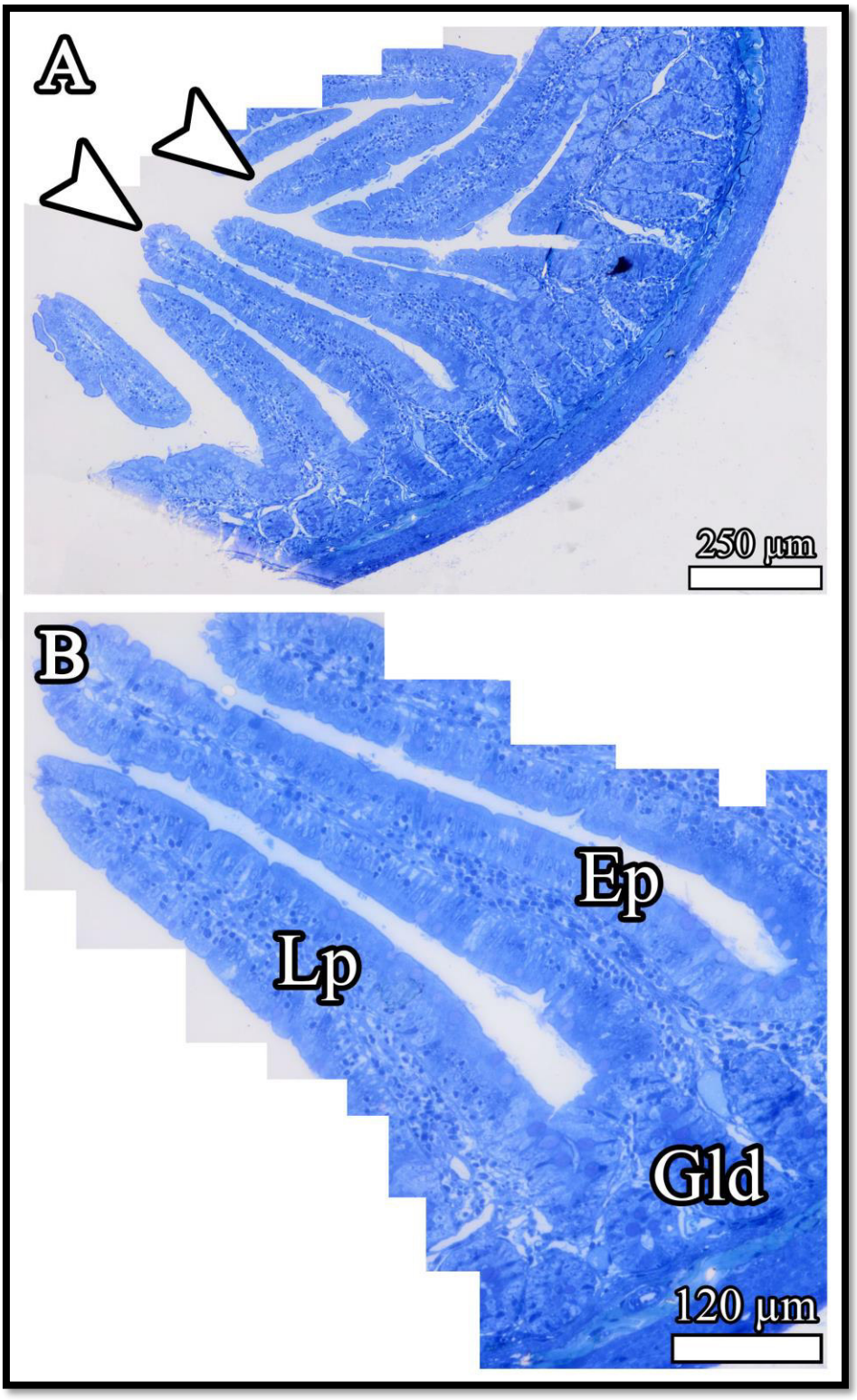

Figure 4. 86. (A, B) General structure of the small intestine belonging to the GA group is seen. The whole layers of the small intestine have a well-protected structure. Finger-like villus (arrows), crypts of Lieberkühn (arrowheads), glands (Gld), the epithelium (Ep), and connective tissue of lamina propria (Lp) are intact. Semithin section of resin embedded tissue (0.5 µm thickness) and stained with toluidine blue

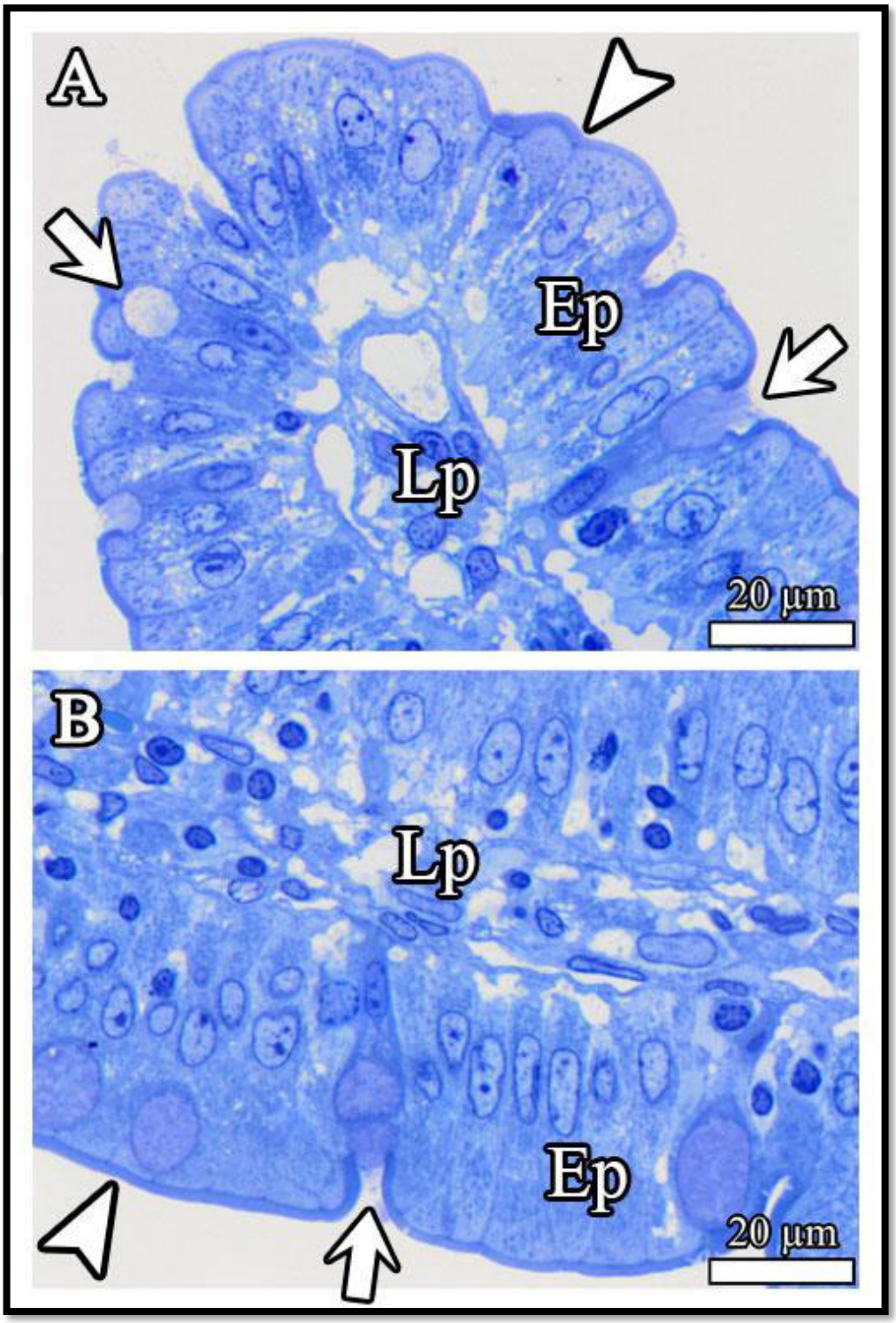

Figure 4. 87. (A, B) High magnification of the small intestine images belonging to the GA group is seen. The surface epithelium (Ep) and its lamina propria (Lp) look healthy. Brush borders (arrowheads) of the epithelium and Goblet cells (arrows) are found normal. Connective tissue in the Lp and its vessels has a well-protected structure. Few lymphocyte infiltrations in the Ep can be seen. Semithin section of resin embedded tissue (0.5 µm thickness) and stained with toluidine blue

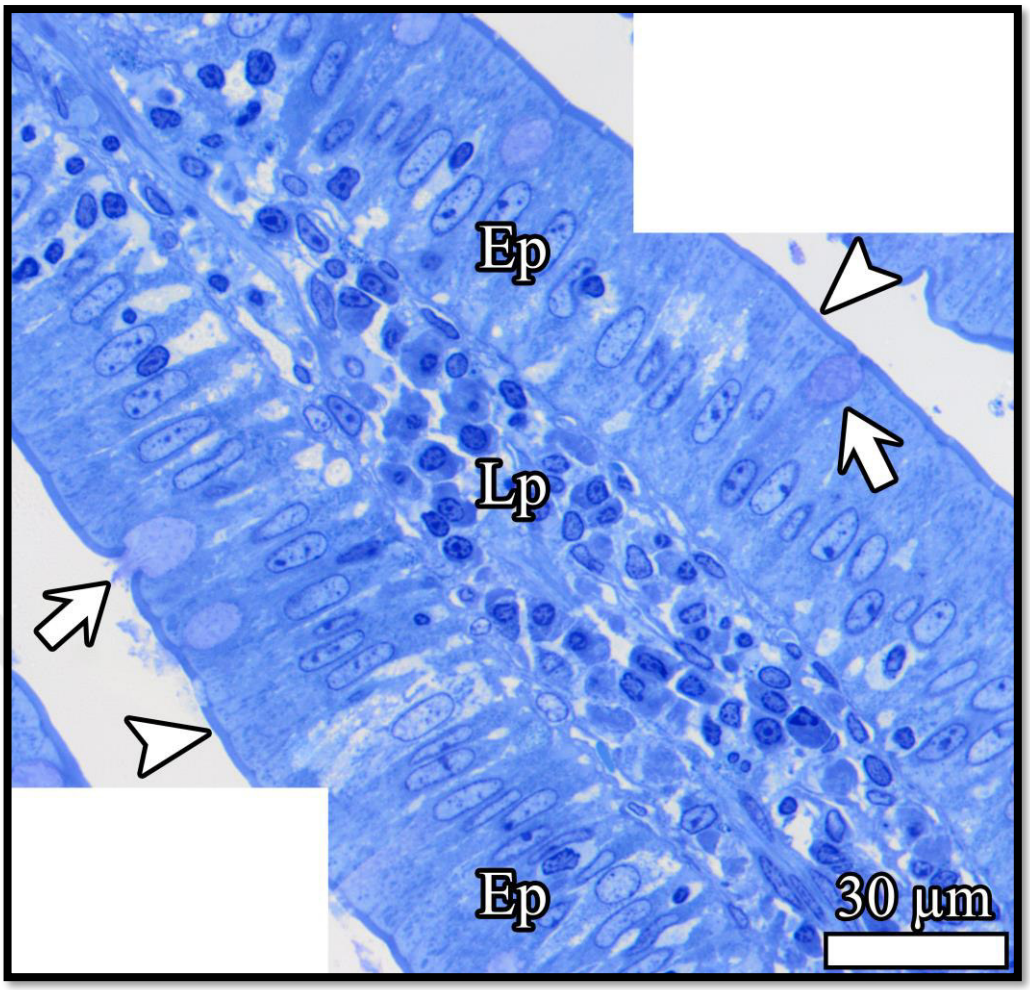

Figure 4. 88. (A, B) General structures of the tubular gland in the small intestine image belonging to the GA group are seen. The epithelial cells as well as the connective tissue of lamina propria (Lp) have a well-protected structure. The borders of nuclei of the simple columnar epithelium (Ep), its brush borders (arrowhead), and Goblet cells (arrow) are clearly observed. Semithin section of resin embedded tissue (0.5 µm thickness) and stained with toluidine blue

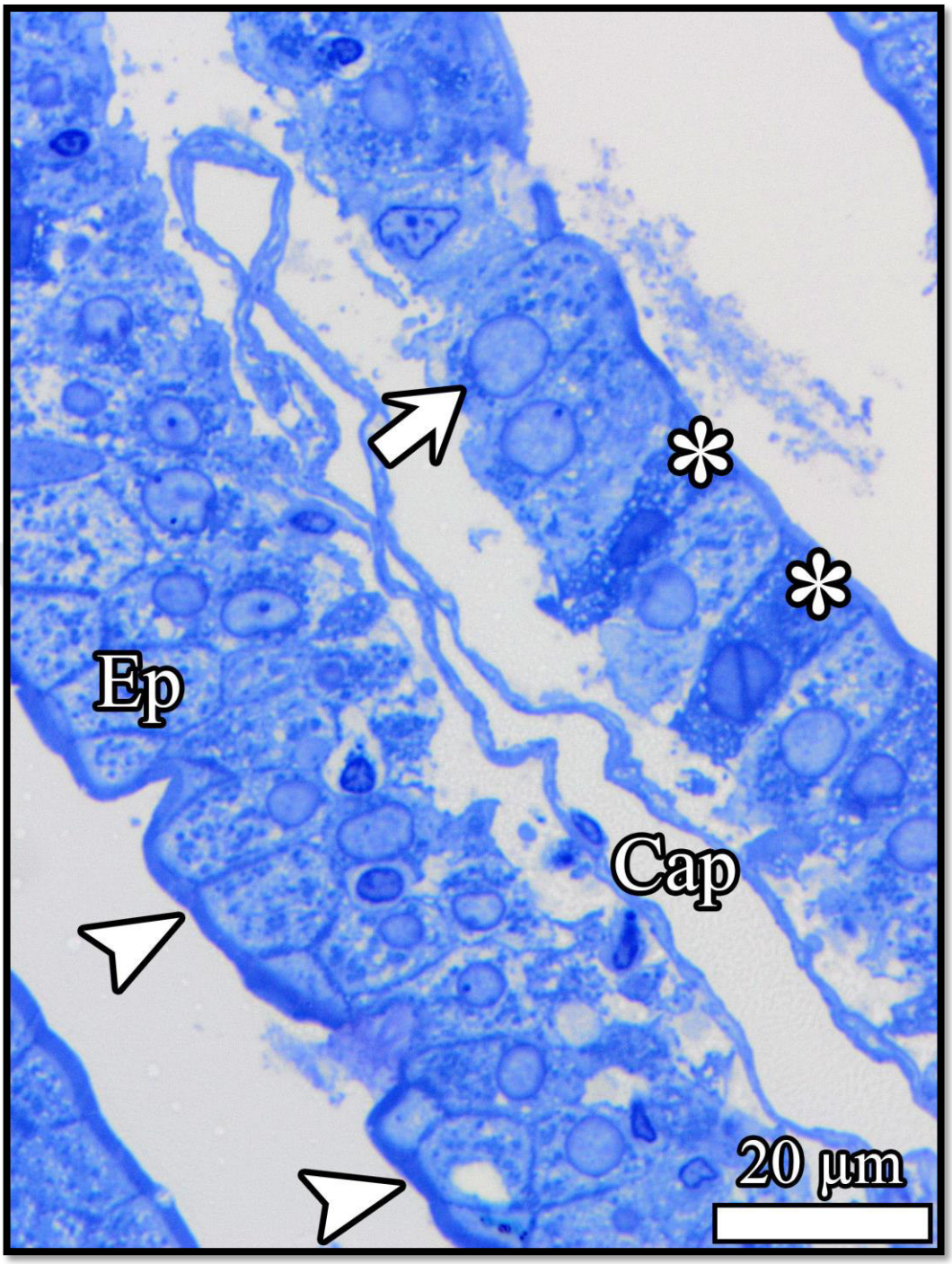

Figure 4. 89. Magnified and unified images of the small intestine belonging to the GA group are observed. As seen that the boards of each cell in the epithelium can be clearly observed. The surface epithelium (Ep) and its lamina propria (Lp) look healthy. Some cells in the epithelium were darkly stained (*), these cells might lose their function. Brush borders (arrowheads) of the epithelium and its enterocyte (arrow) are found normal. Connective tissue in the lamina propria and its vessels (Cap) has a well-protected structure. Semithin section of resin embedded tissue (0.5 µm thickness) and stained with toluidine blue

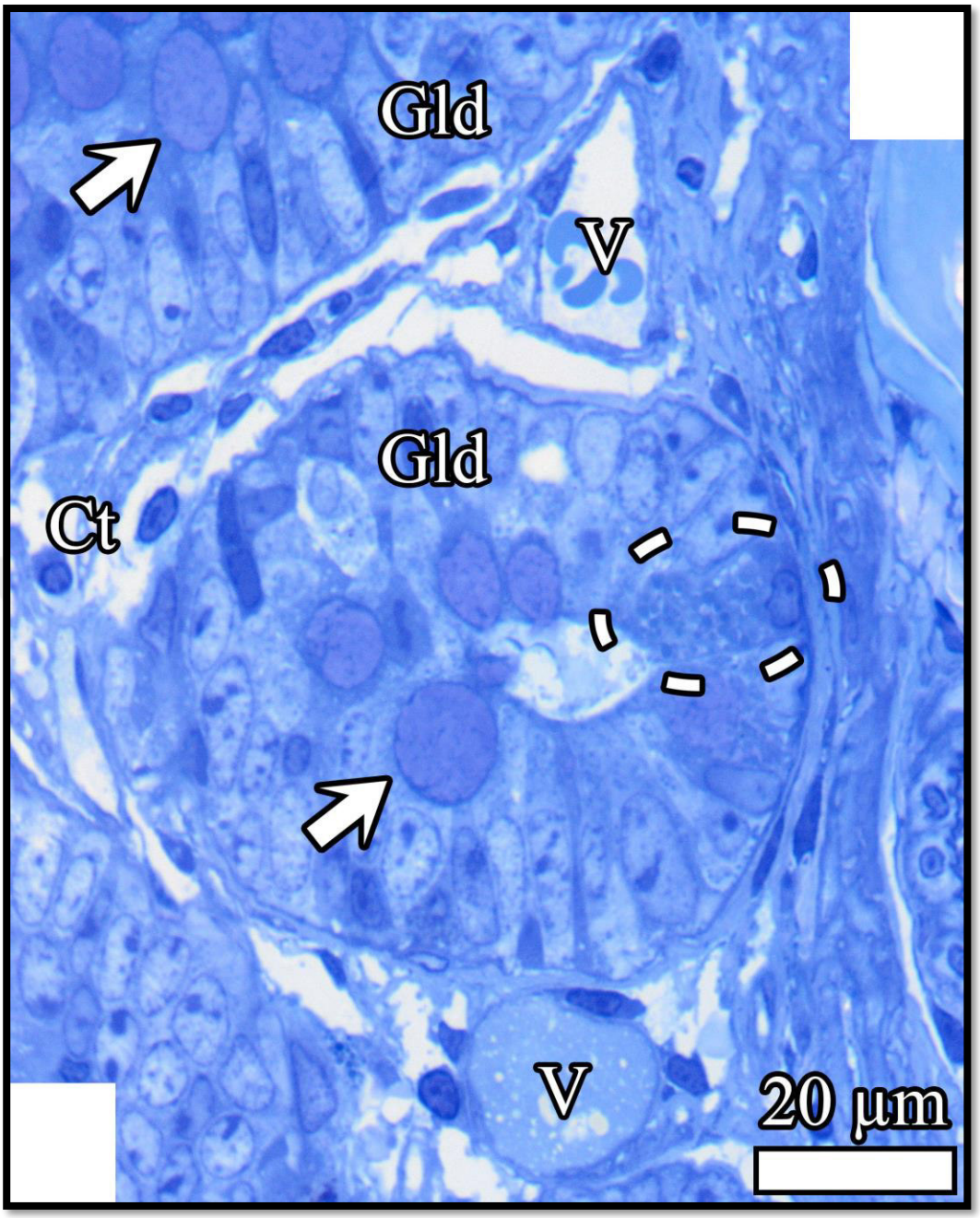

Figure 4. 90. Transverse sections of the intestinal glands (Gld) belonging to the GA group are seen. This gland is covered by a connective tissue that has many small size vacuoles. A rich capillary network is seen in this connective tissue (Ct). Each Goblet cell has a large apical cytoplasm (arrows). A Paneth cell in the wall of the intestinal gland is seen (dashed lined circular area). (V), vessel. Semithin section of resin embedded tissue (0.5 µm thickness) and stained with toluidine blue

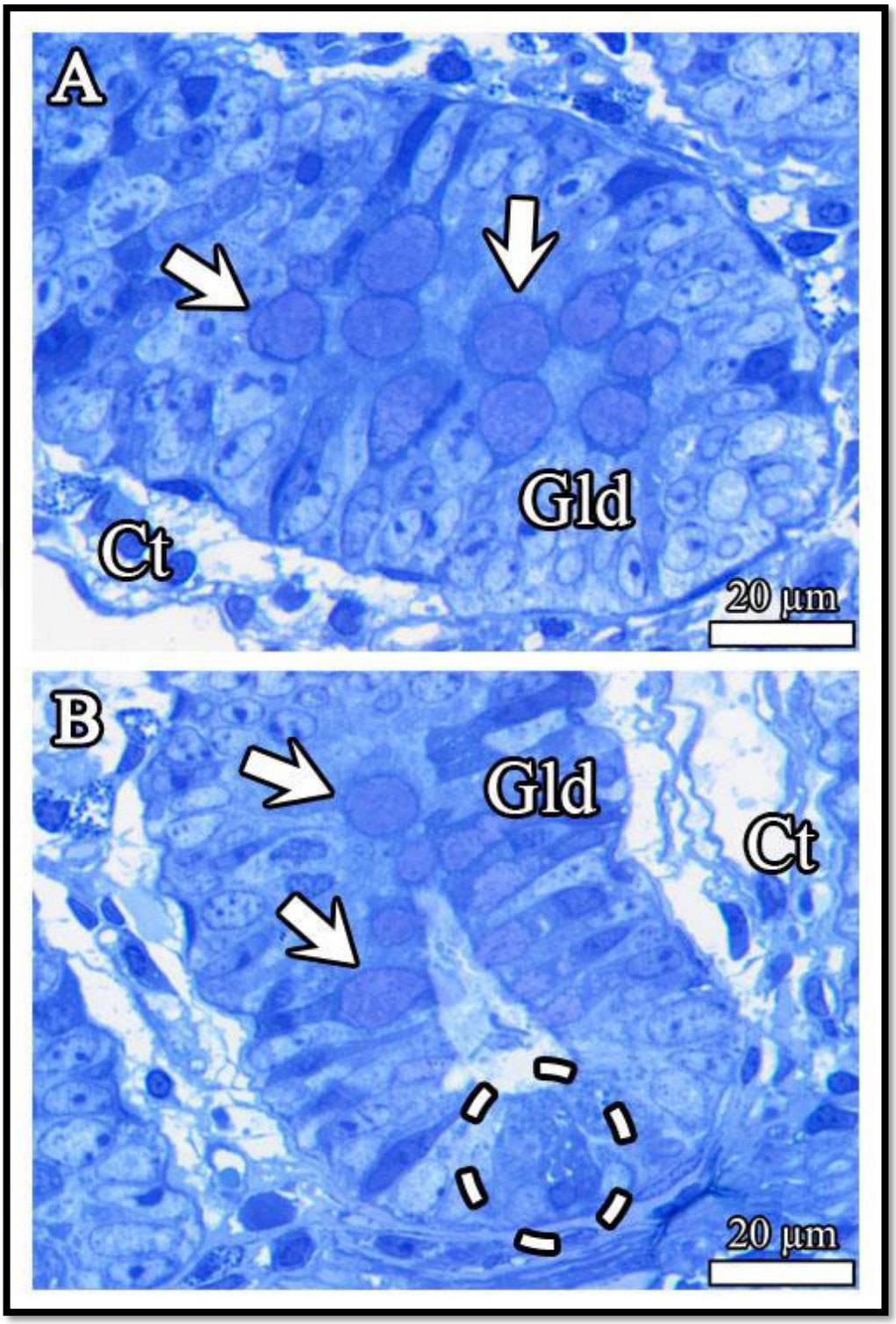

Figure 4. 91. (A, B) A partly longitudinal sections of the intestinal glands (Gld) belonging to the GA group are seen. The glands are covered by a connective tissue (Ct) that has some small size vacuoles. Each Goblet cell has a large apical cytoplasm (arrows). A Paneth cell in the wall of the intestinal gland is seen (dashed lined circular area). Darkly stained cells in the wall of intestinal glands are also found. Semithin section of resin embedded tissue (0.5 µm thickness) and stained with toluidine blue

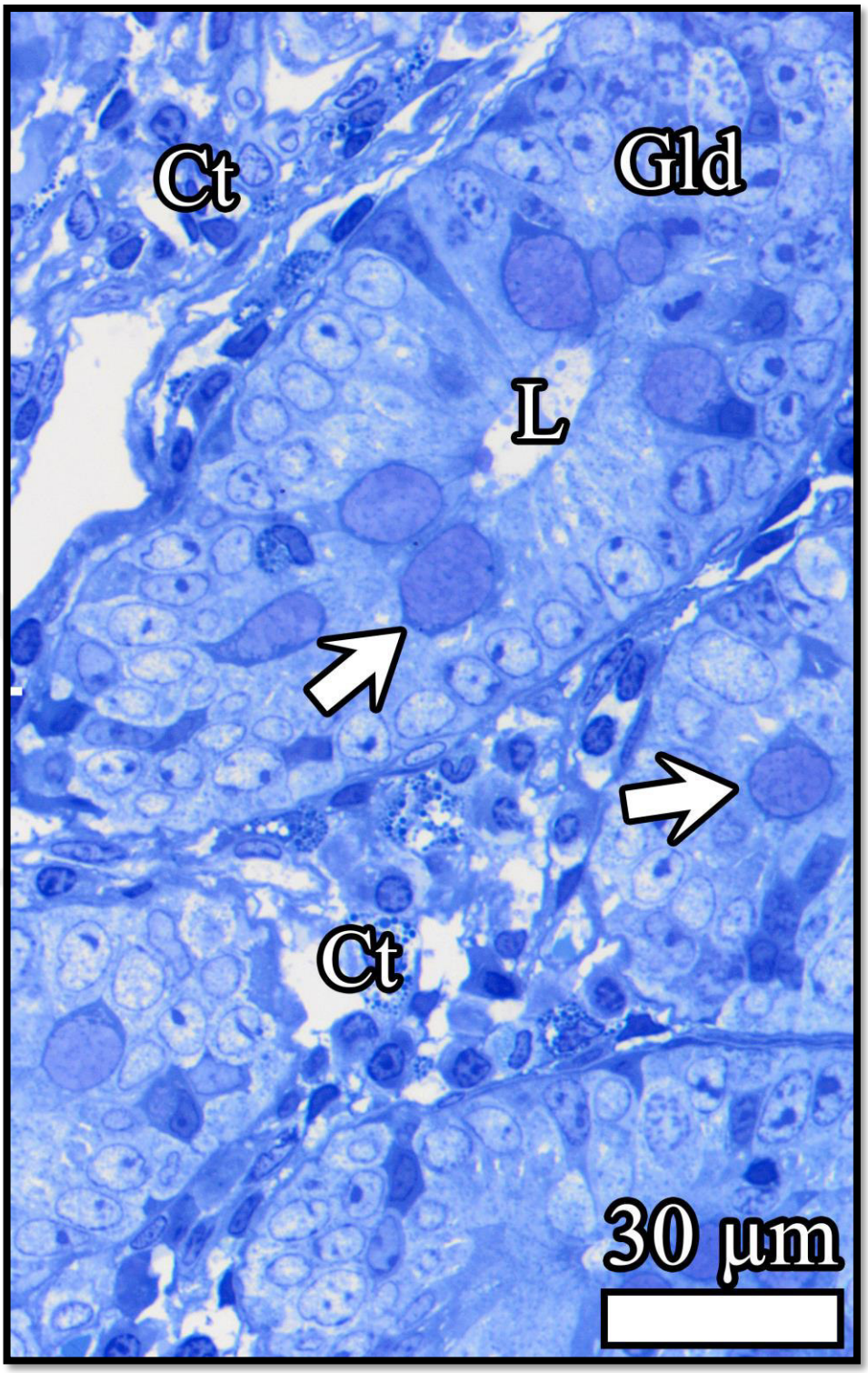

Figure 4. 92. The sections of the intestinal glands (Gld) in the small intestine belonging to the GA group are seen. Glandular cells and their connective tissue (Ct) look healthy. Each gland is covered by a connective tissue that has some small size vacuoles. Each Goblet cell has a large apical cytoplasm that is filled with granules (arrows). Darkly stained cells, pyramidal shape, in the wall of intestinal glands are also observed. Semithin section of resin embedded tissue (0.5 µm thickness) and stained with toluidine blue

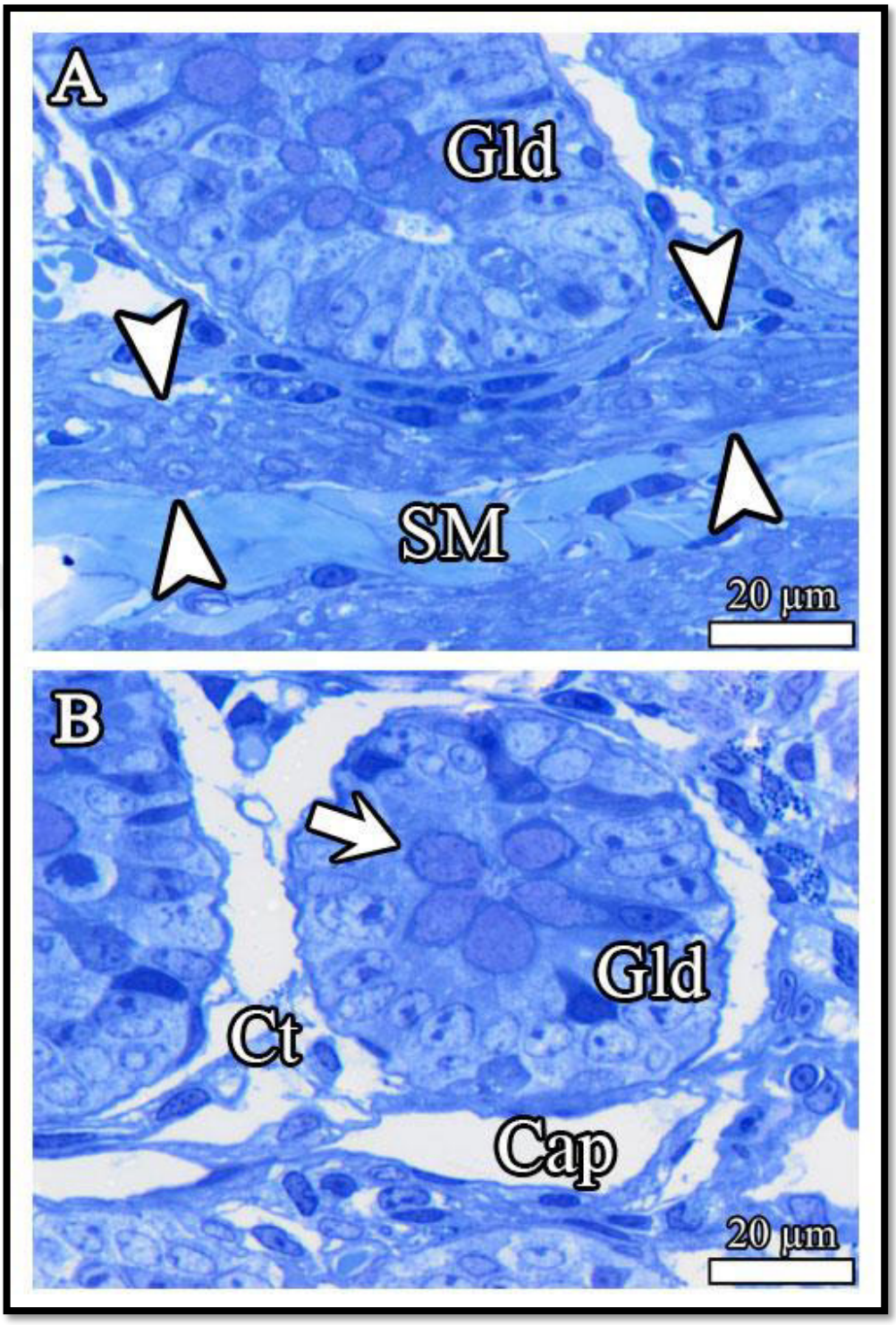

Figure 4. 93. (A, B) The sections of the intestinal glands (Gld) in the small intestine belonging to the GA group are observed. Glandular cells and their connective tissue (Ct) look healthy. Each gland is covered by a connective tissue that has some small size vacuoles. The Goblet cell has a large apical cytoplasm that is filled with granules (arrows). Darkly stained cells, pyramidal shape, in the wall of intestinal glands are also observed. **(A)** A beneath of gland, a thick muscularis mucosae layer is seen (arrowheads). **(B)** A transverse section of the gland surrounded by connective tissue is observed. (Cap), capillary. Semithin section of resin embedded tissue (0.5 µm thickness) and stained with toluidine blue

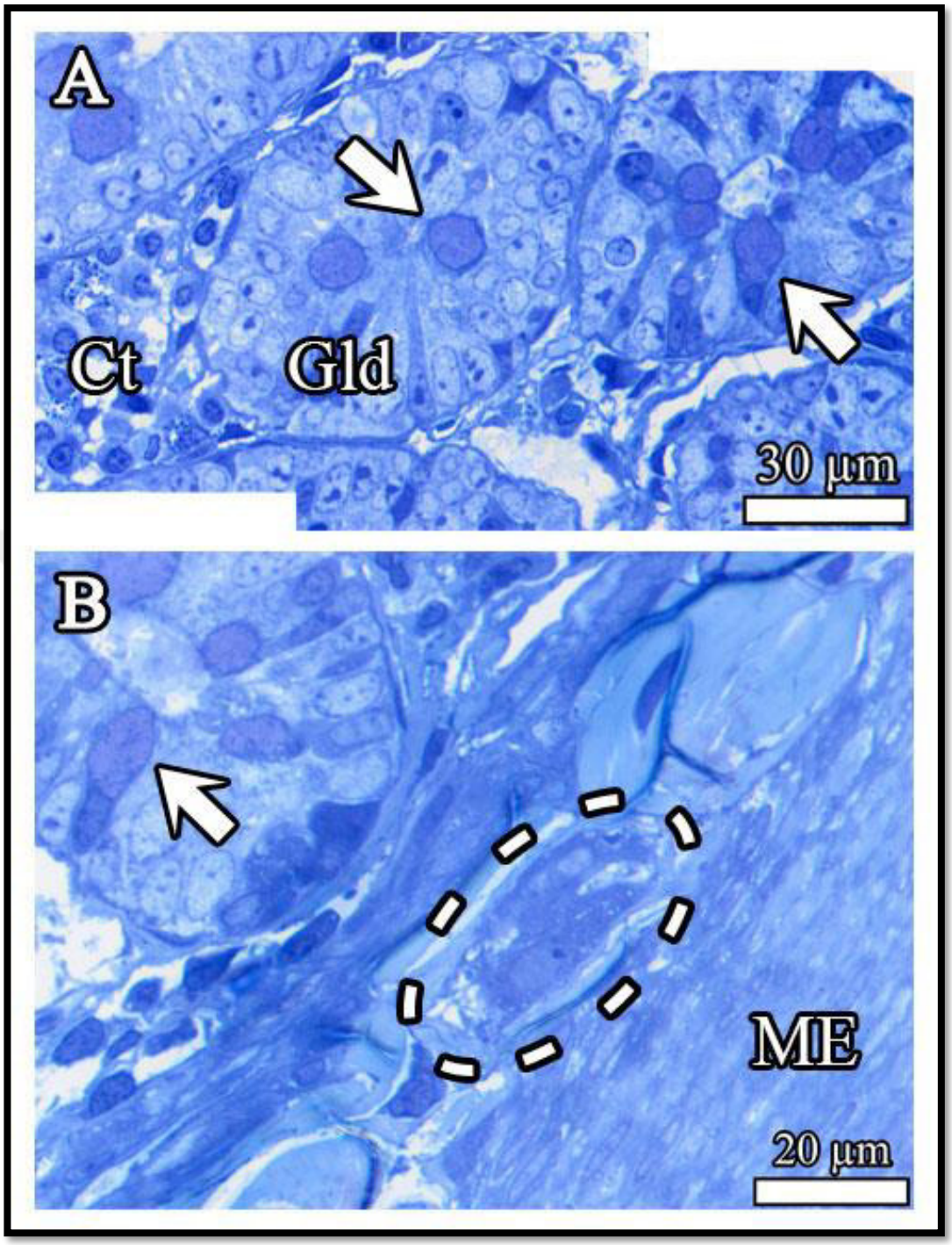

Figure 4. 94. (A, B) The sections of the intestinal glands (Gld) in the small intestine belonging to the GA group are seen. Glandular cells and their connective tissue (Ct) look healthy. Each gland is covered by a connective tissue that has some small size vacuoles. The Goblet cell has a large apical cytoplasm that is filled with granules (arrows). Darkly stained cells, pyramidal shape, in the wall of intestinal glands are also observed. **(B)** Beneath of gland, a thick muscularis mucosae and submucosal plexus (dashed lined elliptic area) are seen. (ME), muscularis externa. Semithin section of resin embedded tissue (0.5 µm thickness) and stained with toluidine blue

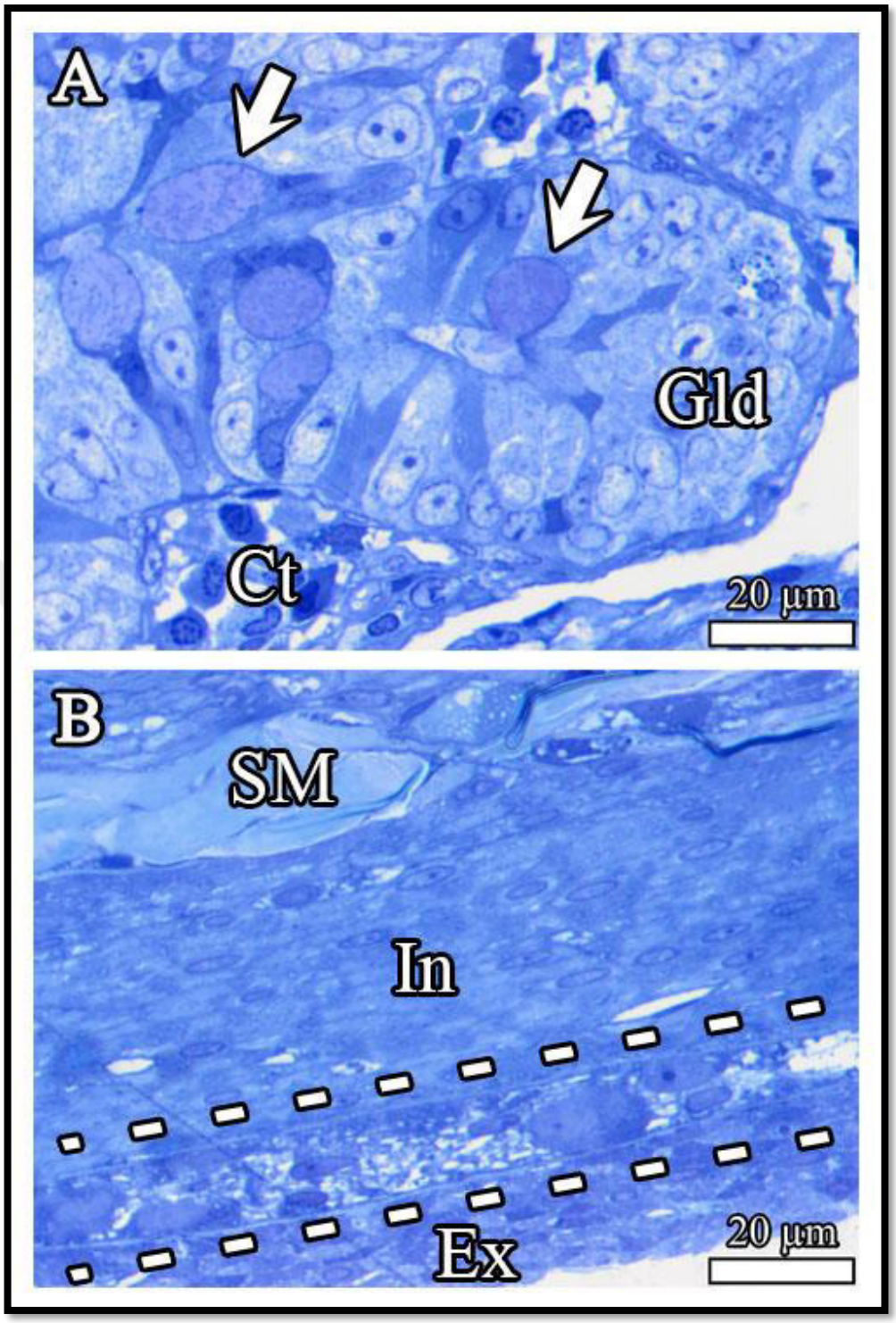

Figure 4. 95. (A) The sections of the intestinal glands (Gld) in the small intestine belonging to the GA group are seen. Glandular cells and their connective tissue (Ct) look healthy. The gland is covered by a connective tissue that has some small size vacuoles. The Goblet cell has a large apical cytoplasm that is filled with granules (arrows). Some darkly stained cells, pyramidal shape, in the wall of intestinal glands are also observed. **(B)** A part of the submucosa (SM) and muscularis externa that has an inner (In) and external (Ex) layer between them myenteric plexus is seen. Semithin section of resin embedded tissue (0.5 µm thickness) and stained with toluidine blue

4.1.2.3. Large Intestine

4.1.2.3.1. Control Group

All of the organ layers in this group look in a good condition. Mucosa with good protection, Lieberkühn crypts (intestinal crypts), submucosa, and muscularis externa are all visible. Many Goblet cells and healthy Lieberkühn crypts can be found in the epithelium of the well-protected mucosa. It is possible to discern a thick muscularis mucosae, submucosa, and muscularis externa. Lamina propria is a well-organized connective tissue that covers the glands. The surface epithelium has few Goblet cells, although augmentations of these cells have been reported in the digestive glands. It's possible to see their nucleus and secretory granules. The muscularis externa is divided into two layers: interna and externa. Both layers appear to be in good morphology and a myenteric plexus may be seen between them (Figures 4.96-4.104).

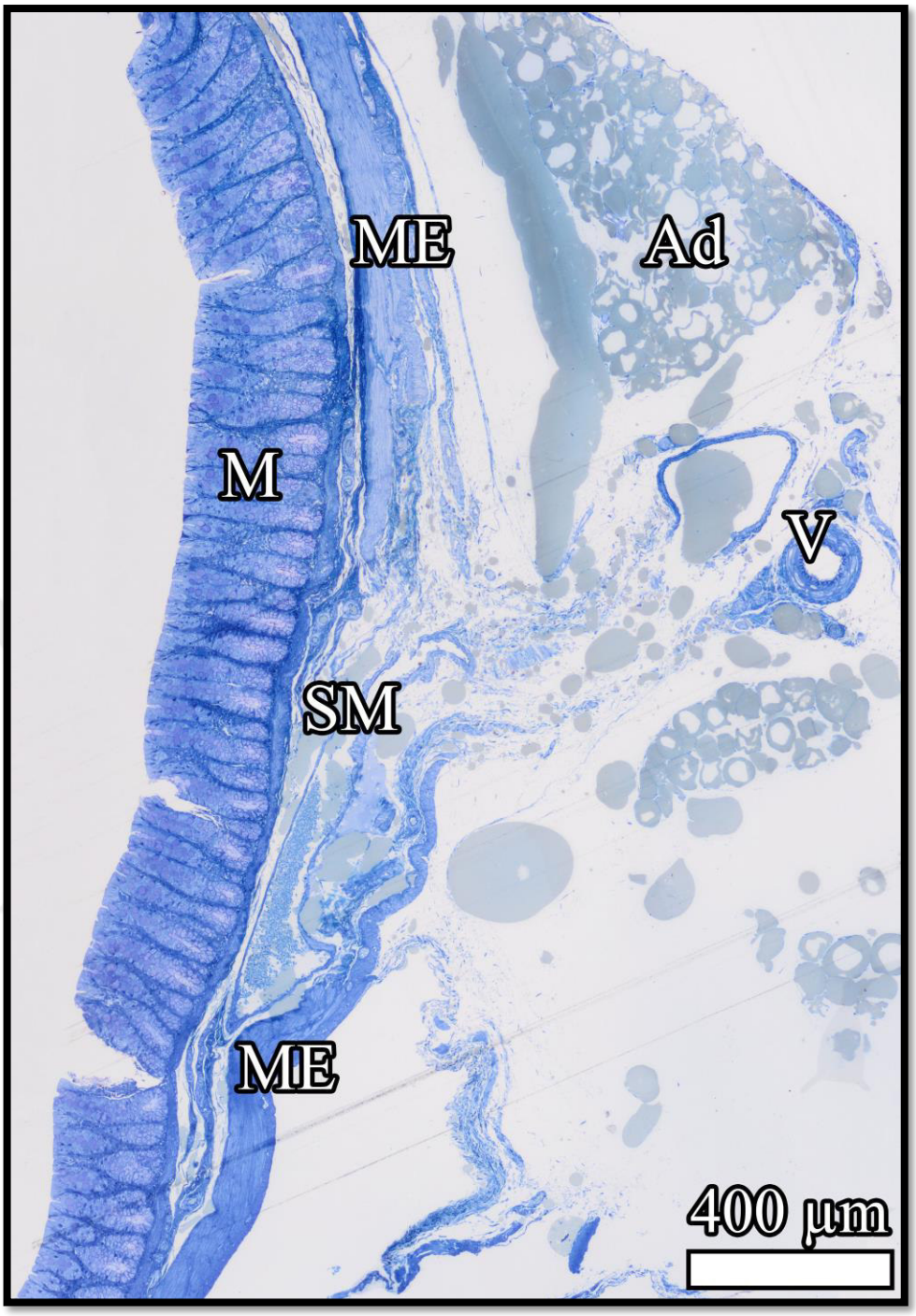

Figure 4. 96. A general view of the large intestine belongs to the control (Cont) group. All layers of the organ are seen as healthy. Well-protected mucosa (M), healthy crypts of Lieberkühn (i.e. intestinal crypt), submucosa (SM), and muscularis externa (ME) are observed. (Ad), adipocytes; (V), vessels. Semithin section of resin embedded tissue (0.5 µm thickness) and stained with toluidine blue

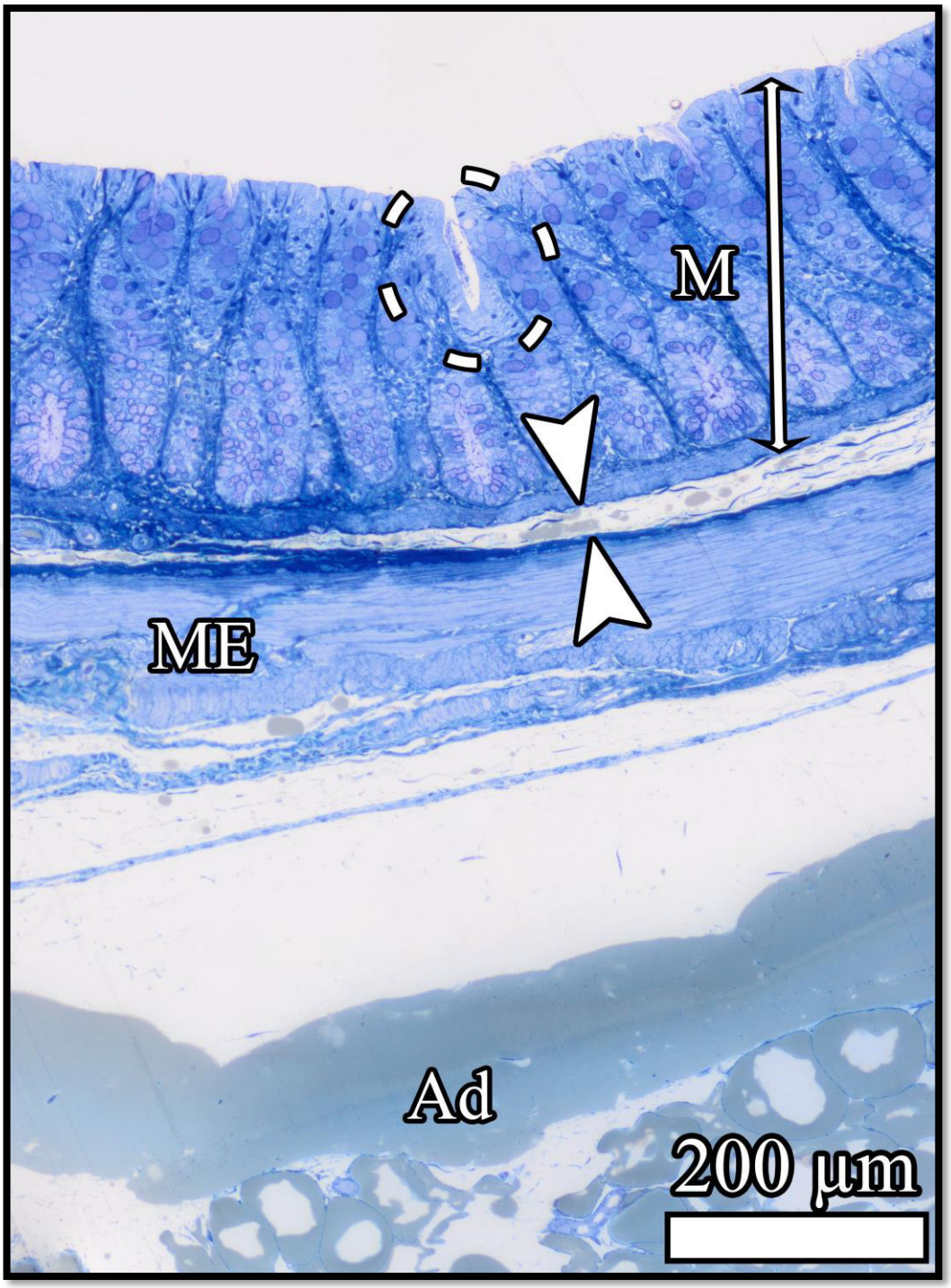

Figure 4. 97. A high magnification of the general view of the large intestine belongs to the control (Cont) group all layers of the organ are found healthy. Well-protected mucosa (M), healthy crypts of Lieberkühn (i.e. intestinal crypt) (dashed circled area), submucosa (between arrowhead), and muscularis externa (ME) are seen. (Ad), adipocytes. Semithin section of resin embedded tissue (0.5 µm thickness) and stained with toluidine blue

Figure 4. 98. A high magnification of the general view of the large intestine belonging to the control (Cont) group is seen. All layers of the organ are observed healthy. Epithelium of the well-protected mucosa has many Goblet cells (arrow) and healthy crypts of Lieberkühn (Gld). A thick muscularis mucosae (MM), submucosa and muscularis externa (ME) are seen. Semithin section of resin embedded tissue (0.5 µm thickness) and stained with toluidine blue

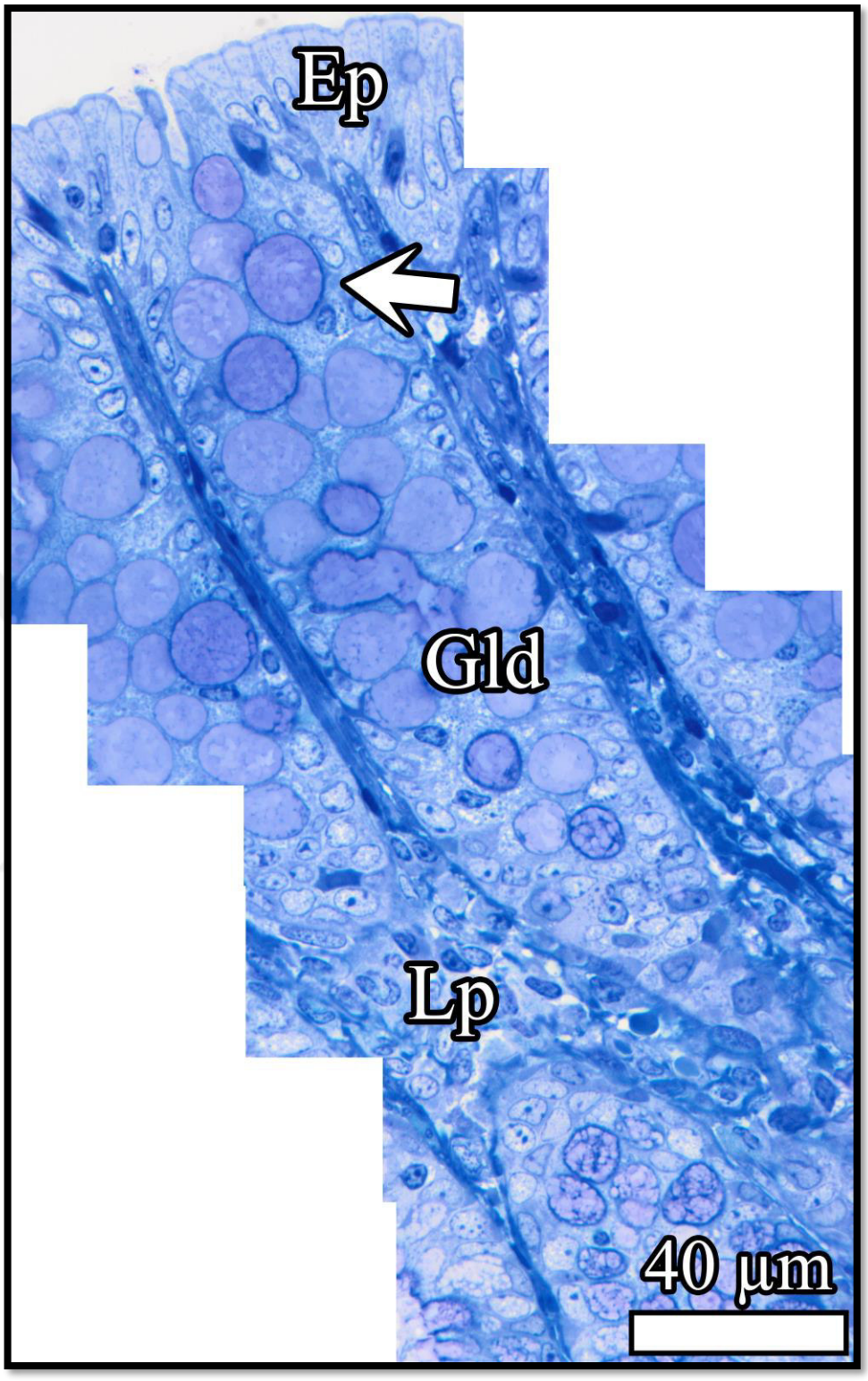

Figure 4. 99. A high magnification of the epithelium (Ep) and lamina propria (Lp) of the large intestine belonging to the control (Cont) group are seen. Although few Goblet cells were seen in the surface epithelium, many of them were found in the intestinal glands (arrow). A well-organized connective tissue of lamina propria covers the glands (Gld). Semithin section of resin embedded tissue (0.5 µm thickness) and stained with toluidine blue

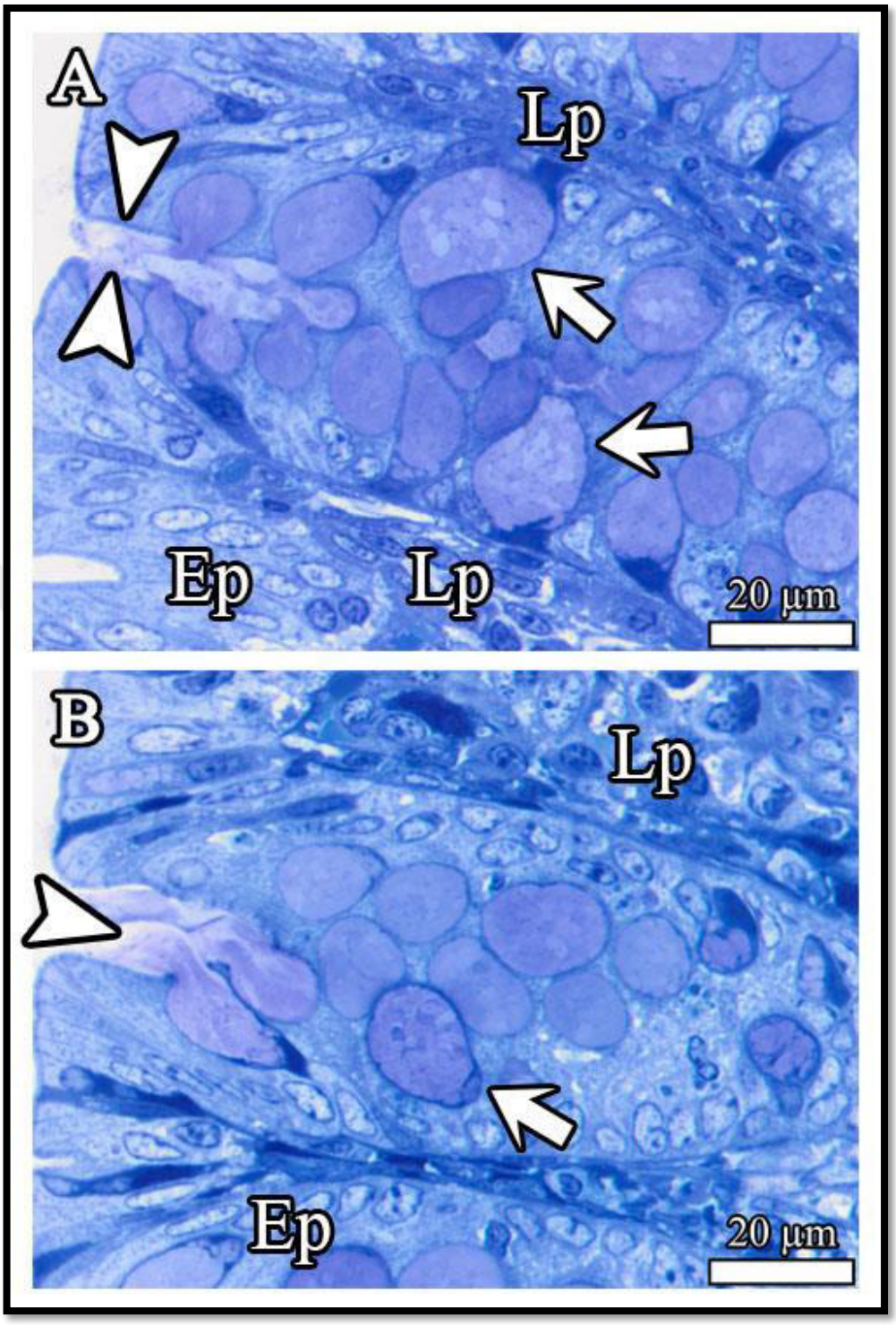

Figure 4. 100. (A, B) A high magnification of the epithelium (Ep) and lamina propria (Lp) of the large intestine belonging to the control (Cont) group are seen. There are few Goblet cells seen in the surface epithelium, but augmentations of these cells were observed in the intestinal glands (arrow). Their nucleus and secretory granules can be clearly observed. Arrowheads show the openings of intestinal glands. A well-organized connective tissue of lamina propria covers the intestinal glands. Semithin section of resin embedded tissue (0.5 µm thickness) and stained with toluidine blue

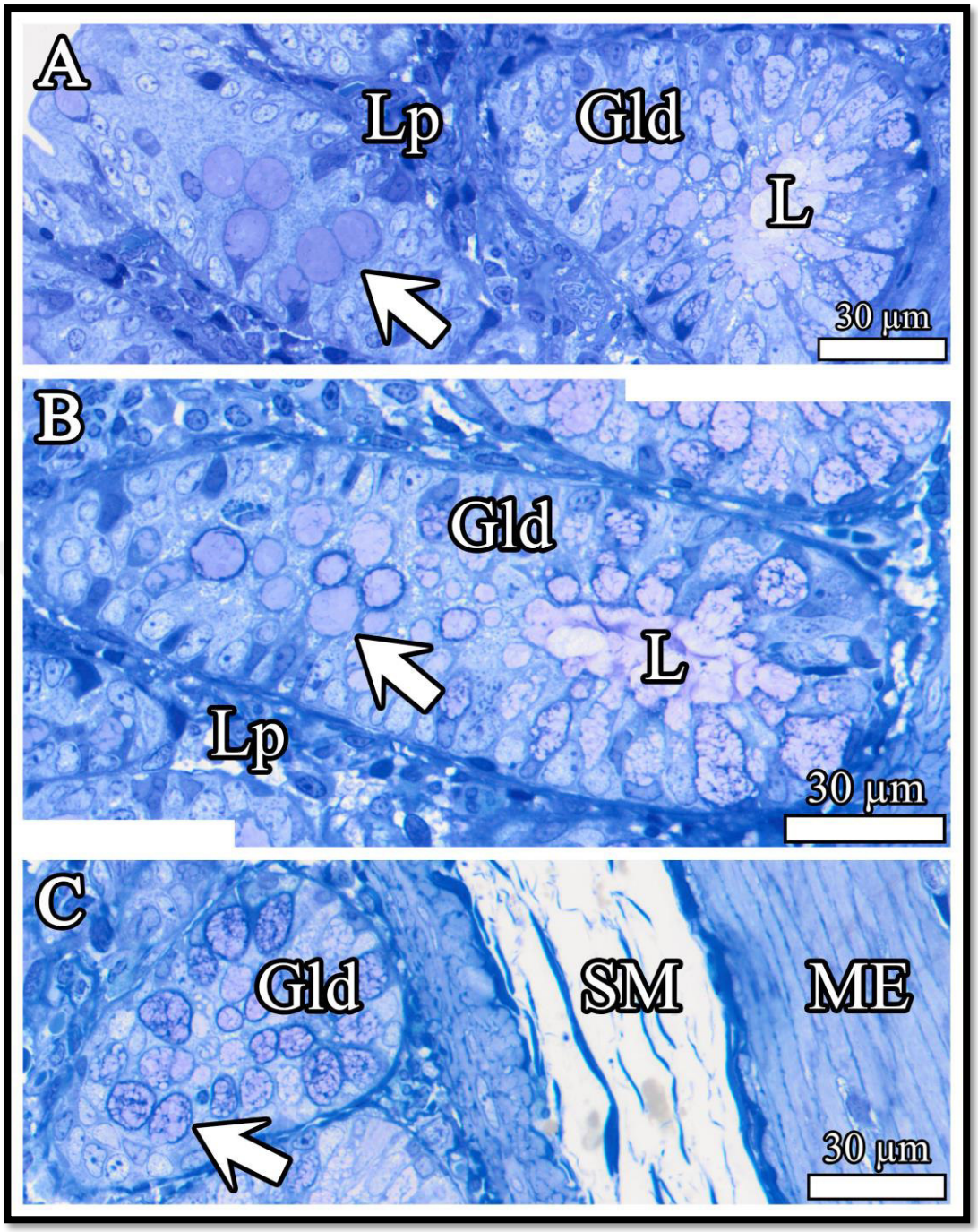

Figure 4. 101. (A, B, C) A high magnification of intestinal glands (Gld) and its lamina propria (Lp) of the large intestine belongs to the control (Cont) group is seen. Few numbers of Goblet cells were seen in the surface epithelium, on the other hand, augmentations of Goblet cells were observed in the intestinal glands (arrows). Their secretory granules can be clearly seen. A well-organized connective tissue of lamina propria covers the intestinal glands. (L), Lumen; (SM), submucosa; (ME), muscularis externa. Semithin section of resin embedded tissue (0.5 µm thickness) and stained with toluidine blue

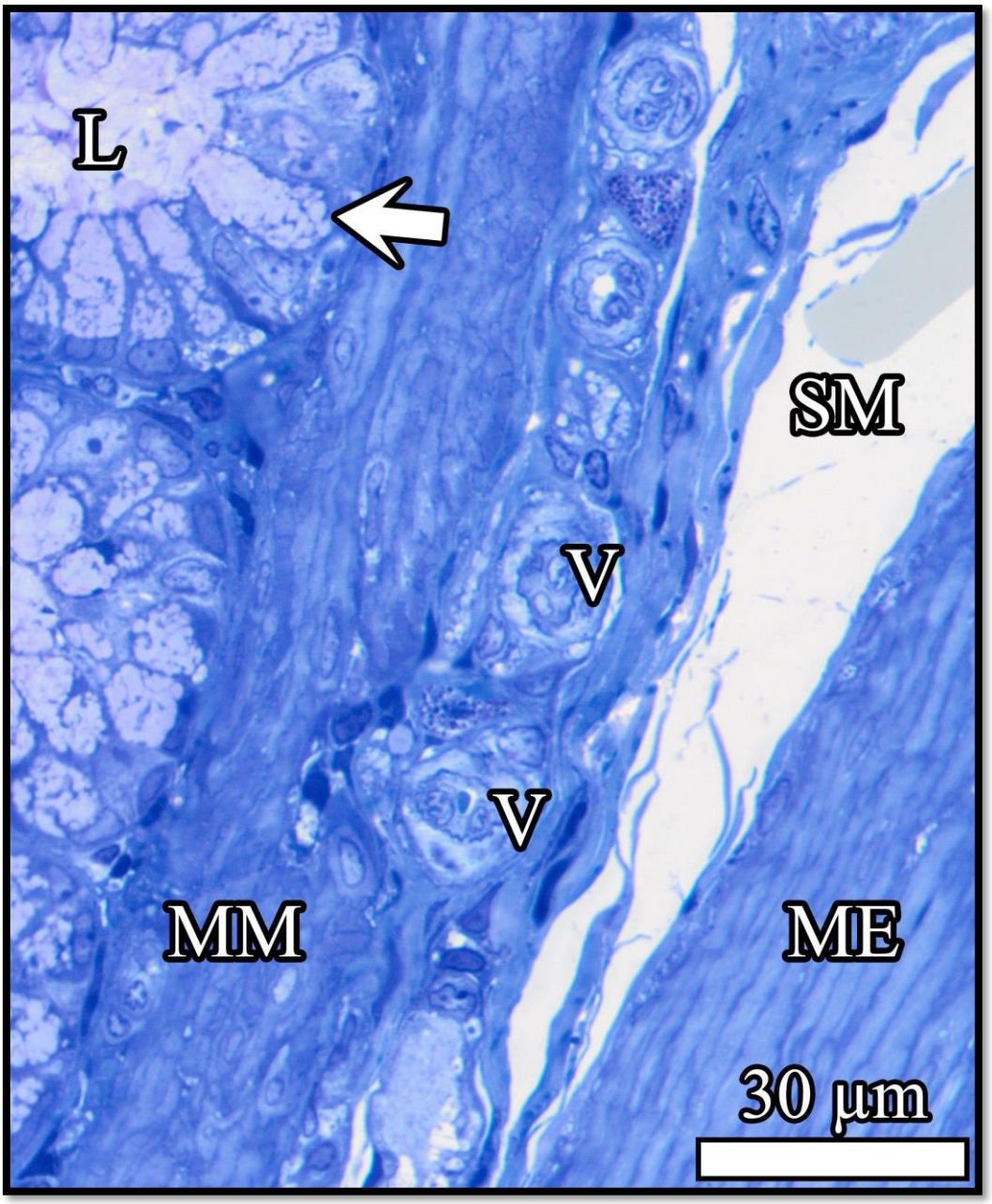

Figure 4. 102. A high magnification of intestinal glands (Gld), its lamina propria, muscularis mucosae (MM), submucosa (SM), and muscularis externa (ME) of the large intestine belong to the control (Cont) group is seen. As seen that a high number of Goblet cells accumulation at the base of the gland is observed (arrow) and its secretory granules can be clearly seen. Submucosa is rich in vessels (V). Lumen (L). Semithin section of resin embedded tissue (0.5 µm thickness) and stained with toluidine blue

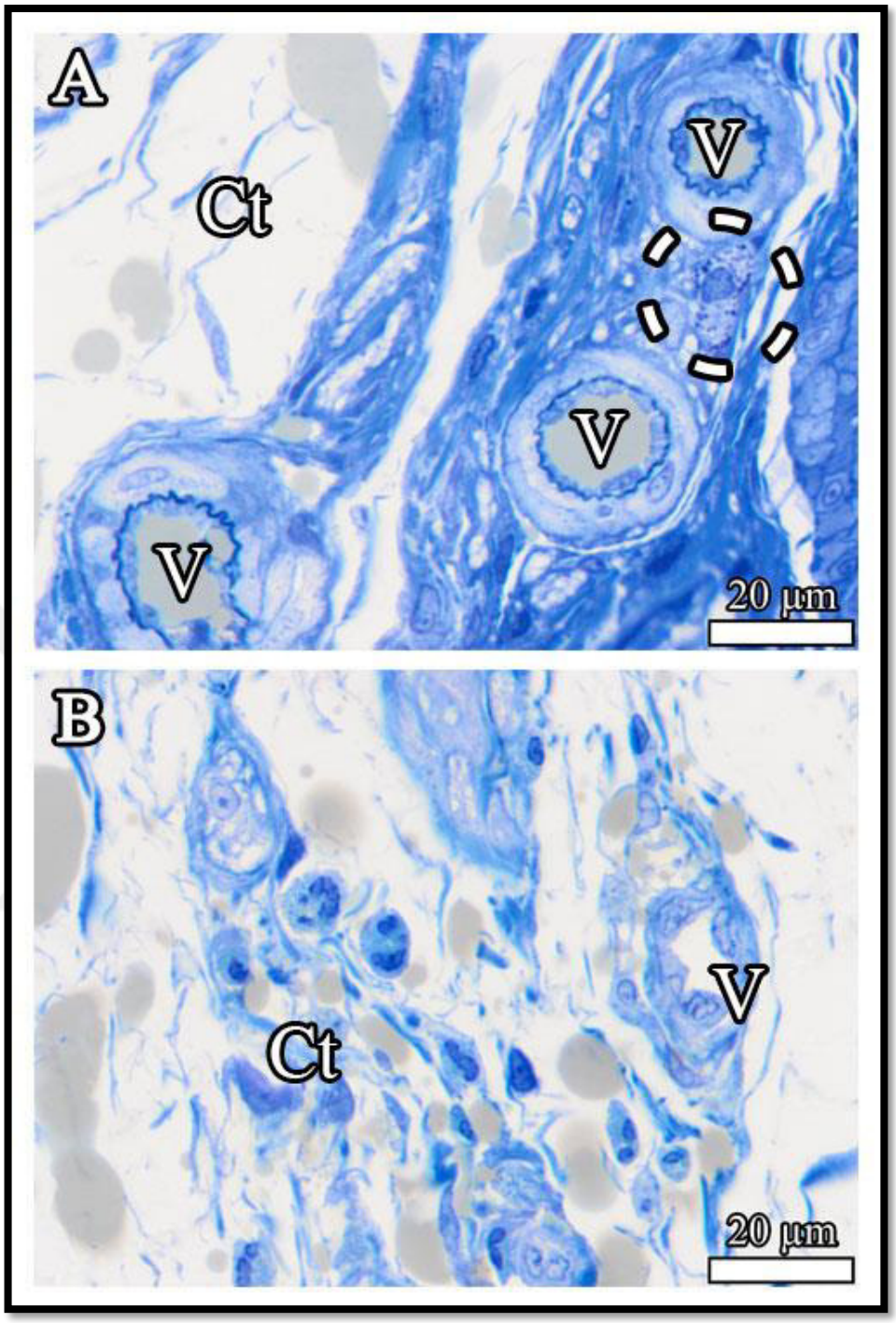

Figure 4. 103. (A, B) A high magnification of connective tissue (Ct) in the submucosa of the large intestine belonging to the control (Cont) group is seen. It has many different sizes of vessels (V), mast cells (dashed circled area), and adipocytes in this tissue. Semithin section of resin embedded tissue (0.5 µm thickness) and stained with toluidine blue

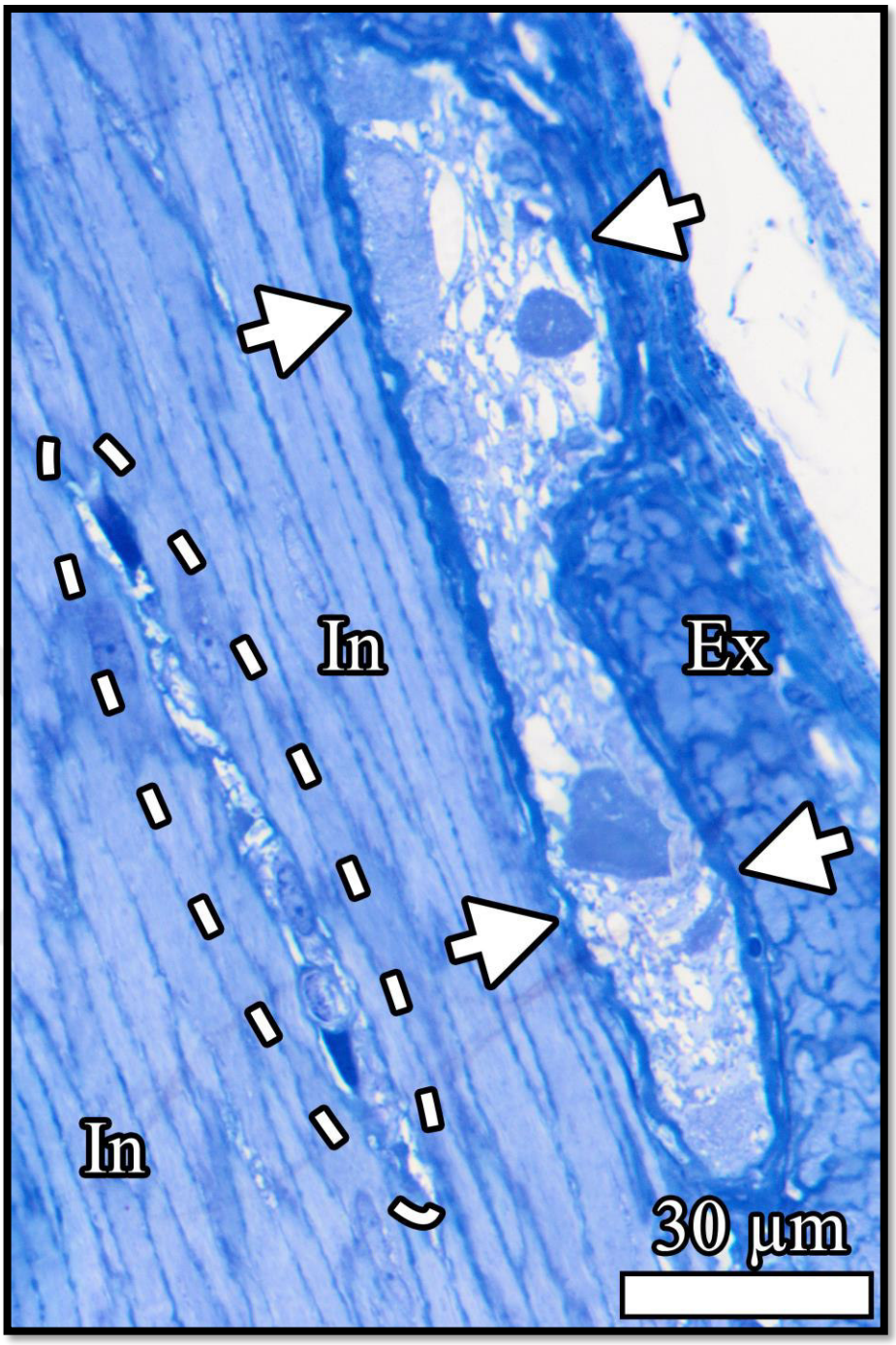

Figure 4. 104. A high magnification of muscularis externa of the large intestine belonging to the control (Cont) group is seen. It has two layers that are named interna (In) and externa (Ex). Both layers look healthy, between them a myenteric plexus is observed, its borders delineated by arrows. A group of cells is seen in the internal layer of muscularis externa (dashed circled area). The smooth muscle of this layer has a healthy structure. Semithin section of resin embedded tissue (0.5 µm thickness) and stained with toluidine blue

4.1.2.3.2. Diclofenac Sodium Group

The large intestine in this group, because of an increased lymphocyte number and other structures, thickness of the mucosa was seriously increased, for this reason it is so difficult to see the intestinal crypt. The brush border of the simple columnar intestinal epithelium is visible, and this layer contains a few numbers of Goblet cells. The ground substance of lamina propria was somewhat discolored. In the intestinal lumen, there is a buildup of cell debris and in the epithelium; there are only a few Goblet cells. The lamina propria, which lies between the intestinal glands, contains a large number of mast cells and numerous tiny vacuoles. The shape and size of glandular cells are severely harmed. Not only does the intestinal gland have a tiny lumen, but it also has a lot of darkly stained and malformed glandular cells. The majority of these cells have lost their ability to function. In the base of the gland, there is an accumulation of Paneth cells. This is not a typical feature of the large intestine morphology; it could be a result of DS exposure (Figures 4.105-4.113).

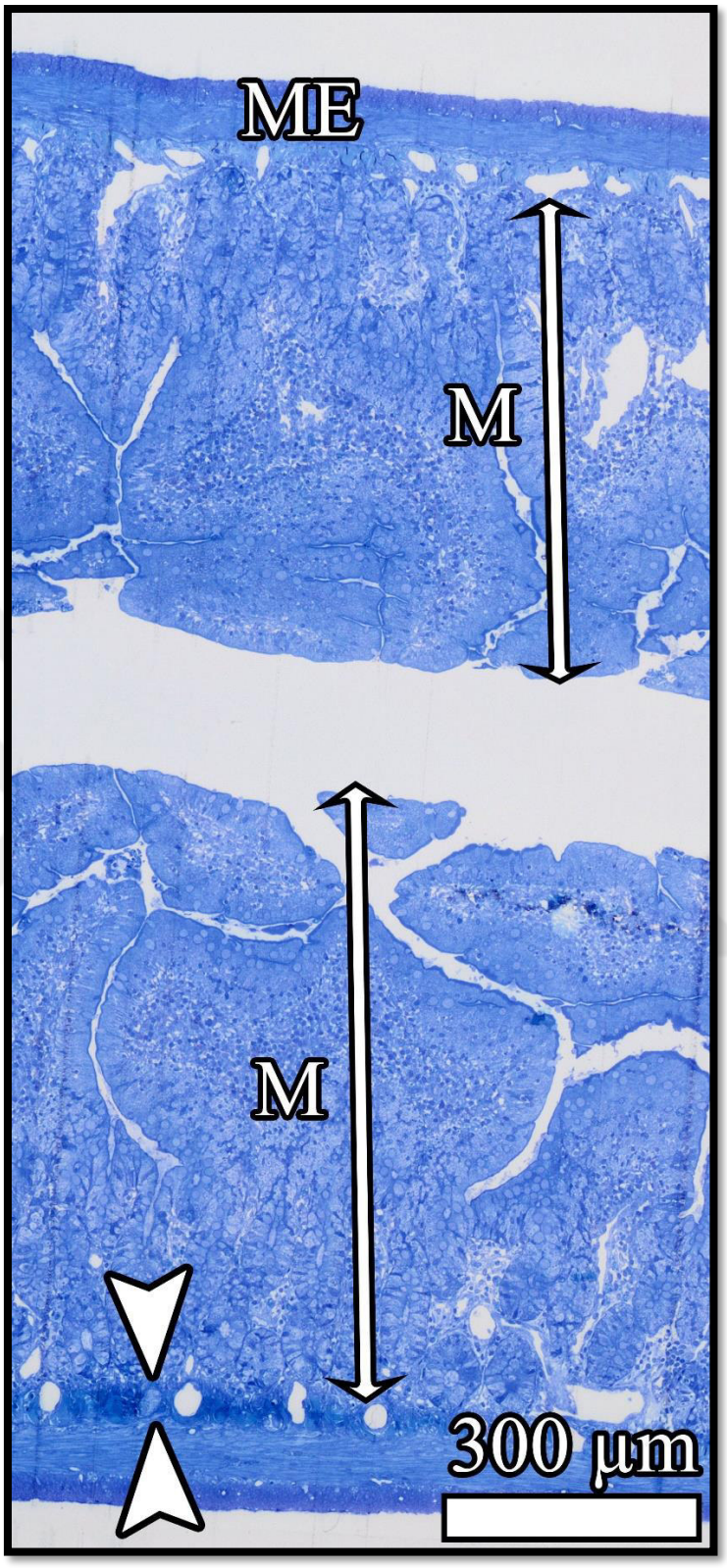

Figure 4. 105. A general view of the large intestine belongs to the diclofenac sodium (DS) group. All layers of the organ are seen. An enlarged mucosa (M) and very large size crypt of Lieberkühn (i.e. intestinal crypt) are observed. Arrowheads show the submucosa. (M), mucosa; (ME), muscularis externa. Semithin section of resin embedded tissue (0.5 µm thickness) and stained with toluidine blue

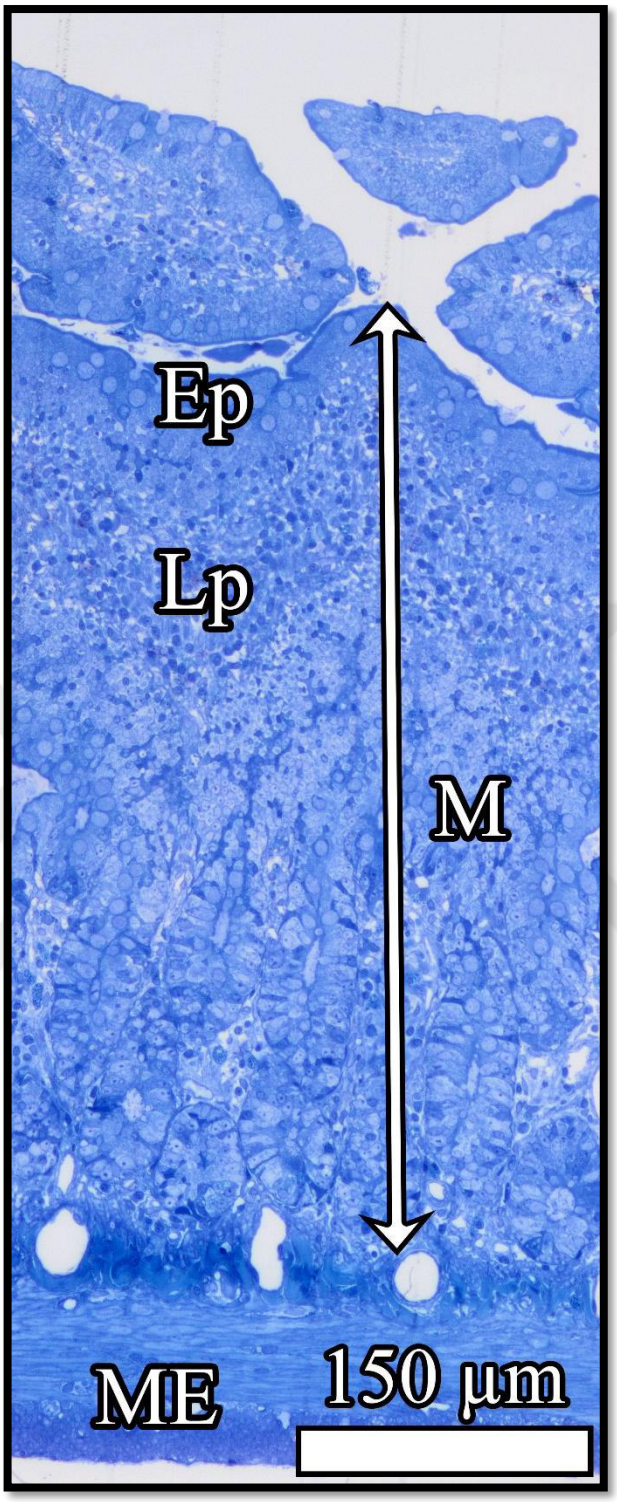

Figure 4. 106. Whole layers of the large intestine wall belonging to the diclofenac sodium (DS) group are seen. Exaggerated lymphocyte number increases the thickness of mucosa, for this reason, it is hard to observe intestinal crypt. Diameters of vessels in the submucosa are also increased. Enlarged mucosa (M) and a very large size crypt of Lieberkühn (i.e. intestinal crypt) are seen. (Ep), epithelium; (Lp), lamina propria; (ME), muscularis externa. Semithin section of resin embedded tissue (0.5 µm thickness) and stained with toluidine blue

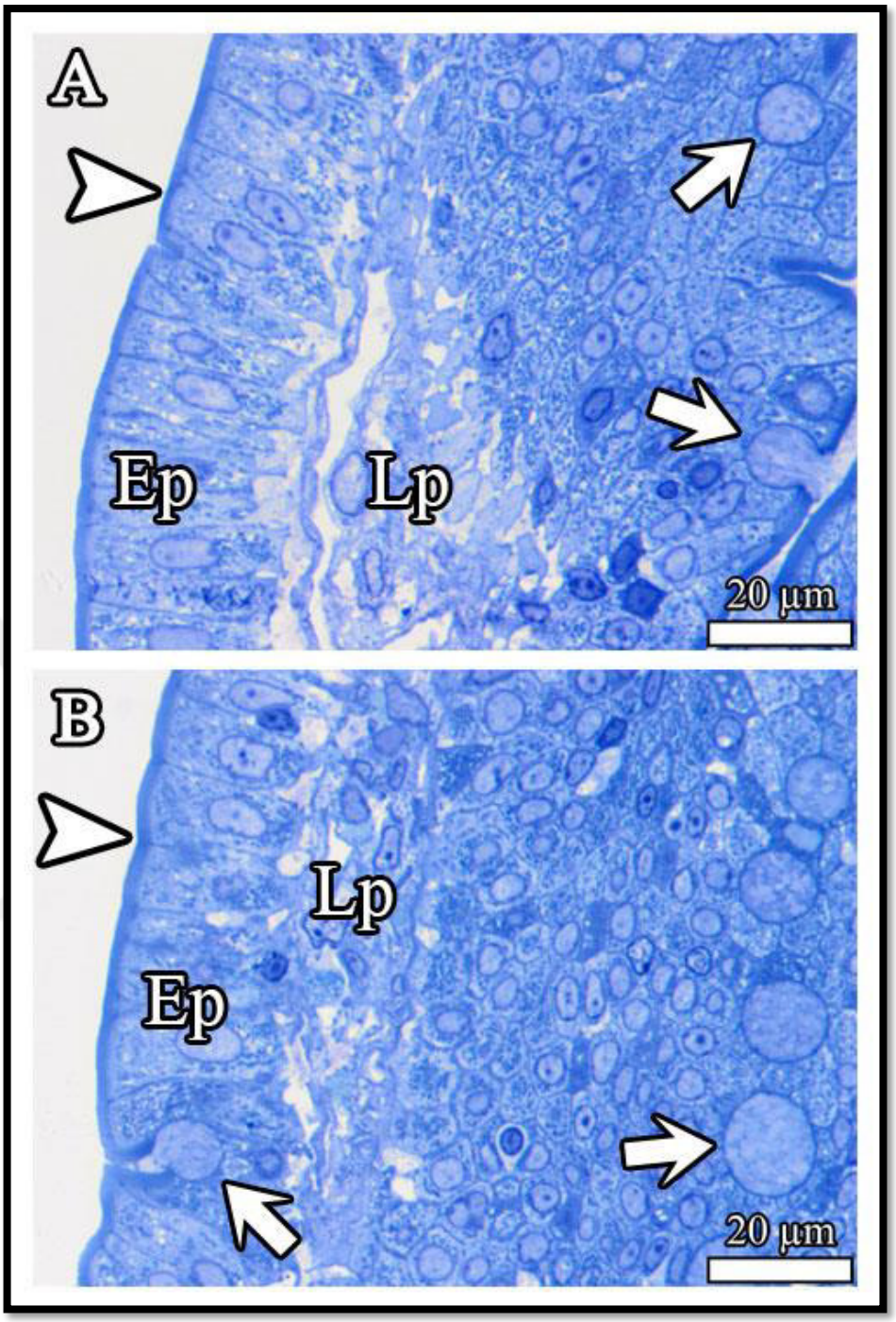

Figure 4. 107. (A, B) Images of the simple columnar epithelium (Ep) and lamina propria (Lp) belonging to the diclofenac sodium (DS) group are seen. The simple columnar epithelium of intestine has a brush border (arrowhead); few numbers of Goblet cells can be found in this layer (arrows). The ground substance of lamina propria was slightly stained. Semithin section of resin embedded tissue (0.5 µm thickness) and stained with toluidine blue

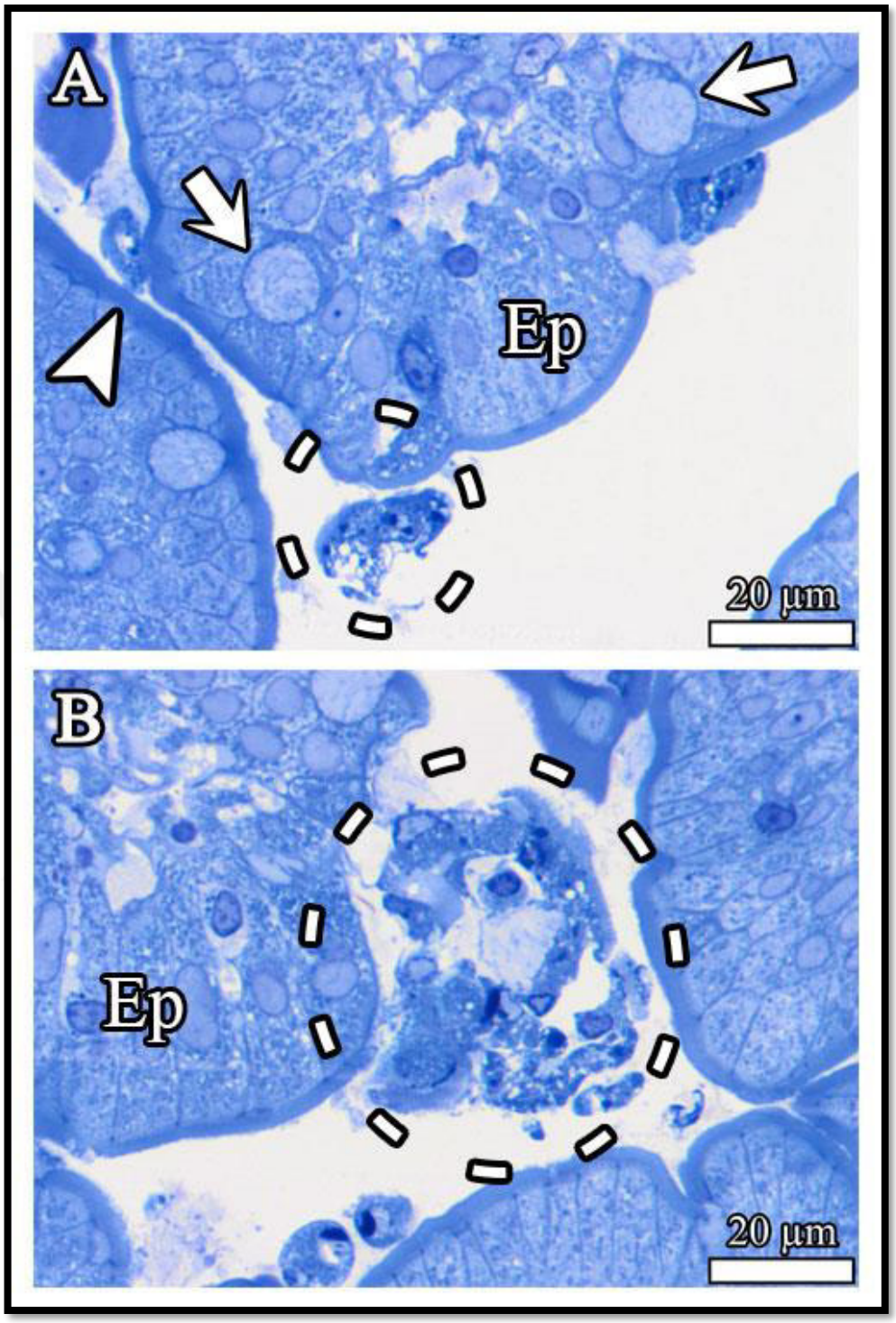

Figure 4. 108. (A, B) The simple columnar epithelium (Ep) and lamina propria belonging to the diclofenac sodium (DS) group is seen. There are few numbers of Goblet cells in the epithelium (arrows). A densely stained and partly thick brush border on the apical part of epithelium is observed (arrowheads). Debris of cells accumulation is found in the intestinal lumen (dashed circled area). Semithin section of resin embedded tissue (0.5 µm thickness) and stained with toluidine blue

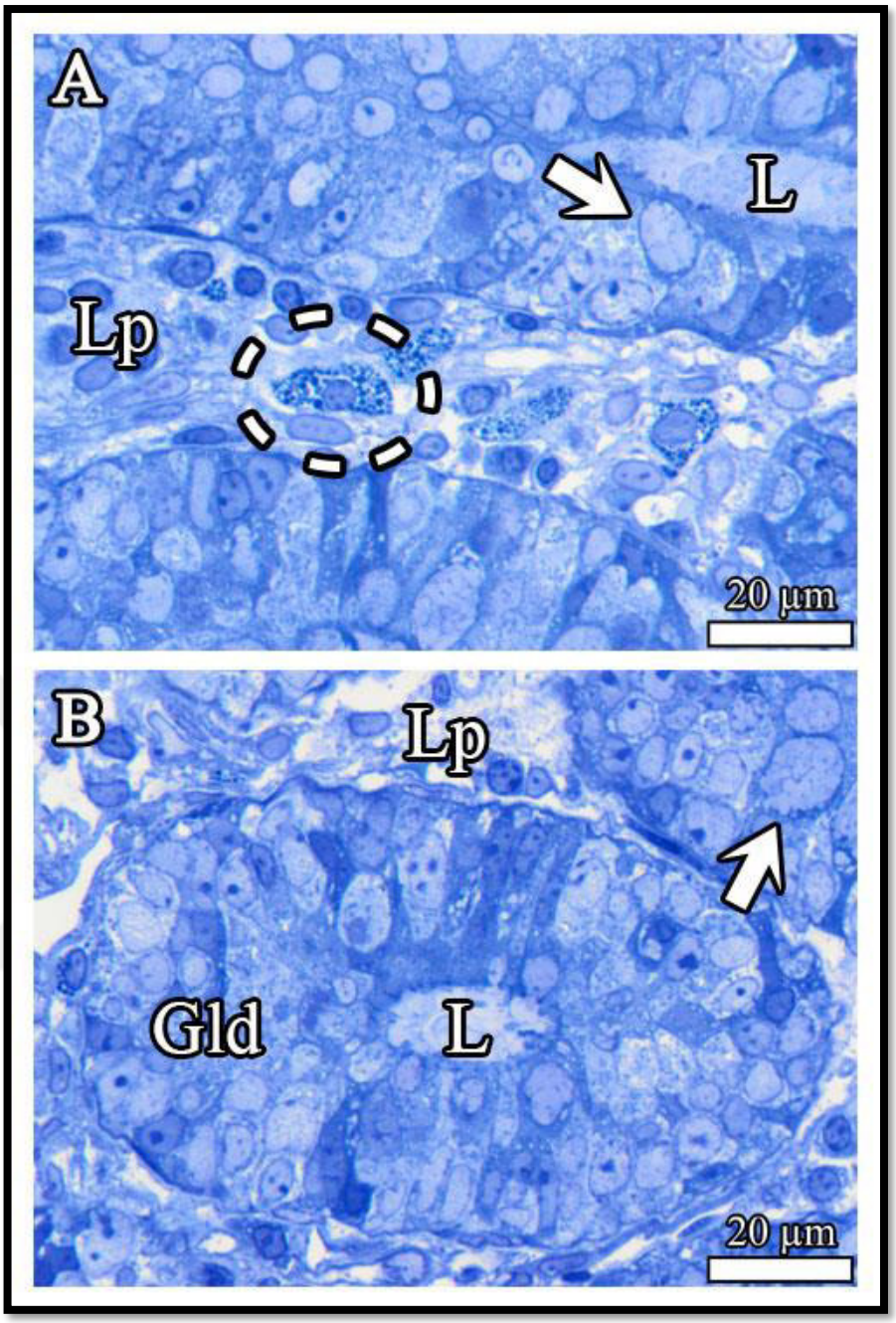

Figure 4. 109. (A, B) Longitudinal sections of intestinal glands belonging to the diclofenac sodium (DS) group are seen. Few numbers of Goblet cells in the epithelium (arrows) are observed. **(A)** Lamina propria (Lp) between intestinal glands has a high number of mast cells (dashed circled area) and many small size vacuoles. The shape and size of glandular cells are seriously affected. **(B)** A transverse section of the intestinal gland (Gld) has not only a small size lumen (L) but also many darkly stained and deformed glandular cells. These cells may be non-functional. Semithin section of resin embedded tissue (0.5 µm thickness) and stained with toluidine blue

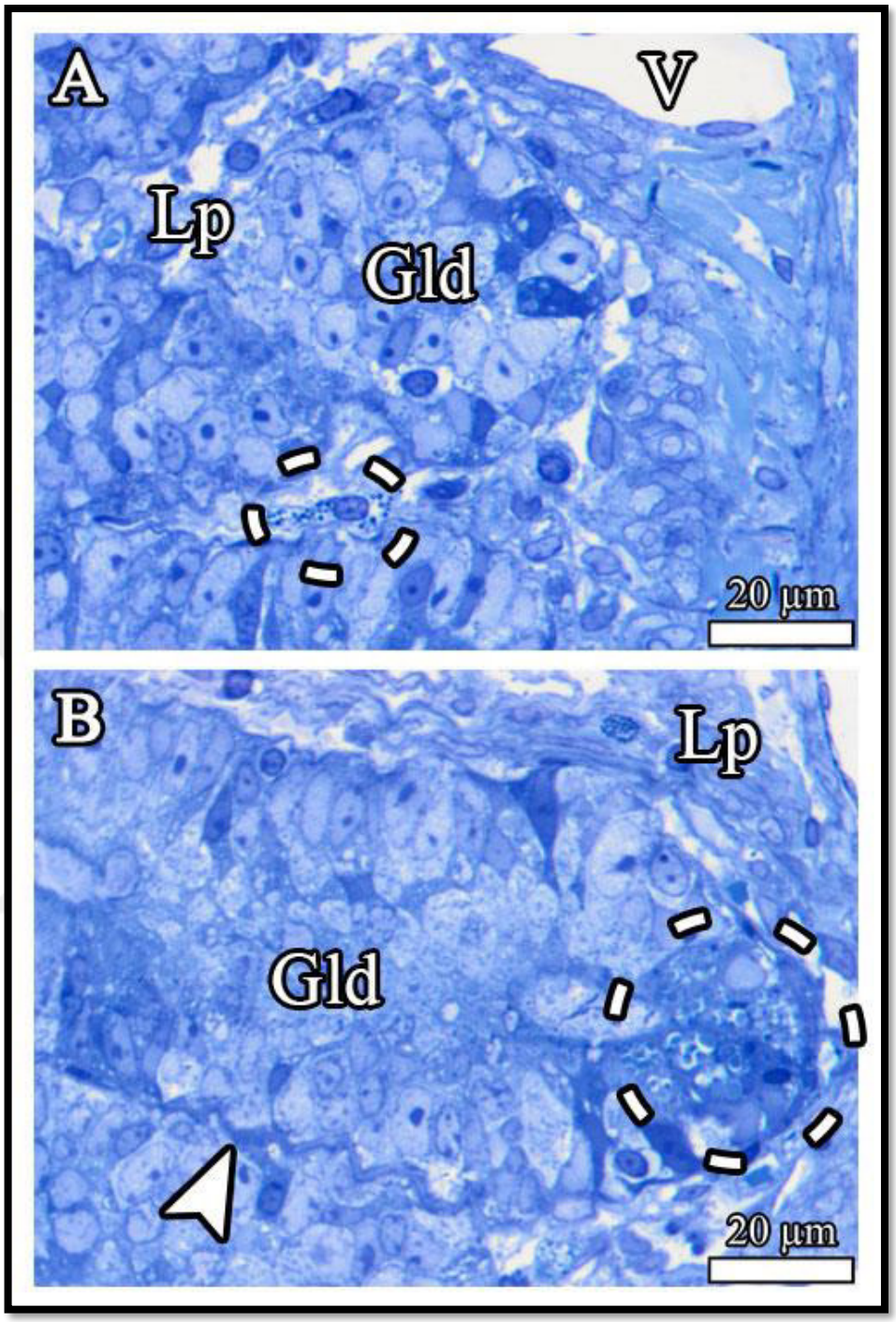

Figure 4. 110. **(A, B)** Intestinal glands belonging to the diclofenac sodium (DS) group are seen. **(A)** Partly sectioned intestinal glands (Gld) and its connective tissue of lamina propria (Lp) between intestinal glands have a mast cell (dashed circled area) and many small size vacuoles. The shape and size of glandular cells are seriously impaired. **(B)** A longitudinal section of the intestinal gland (Gld) has not only a small size lumen (L) but also many darkly stained and deformed glandular cells as well as a thick basal membrane (arrowhead). An accumulation of Paneth cells is found in the base of the gland (dashed line circle area). This structure is not a normal structure for the large intestine; it might be a response to DS exposure. Semithin section of resin embedded tissue (0.5 µm thickness) and stained with toluidine blue

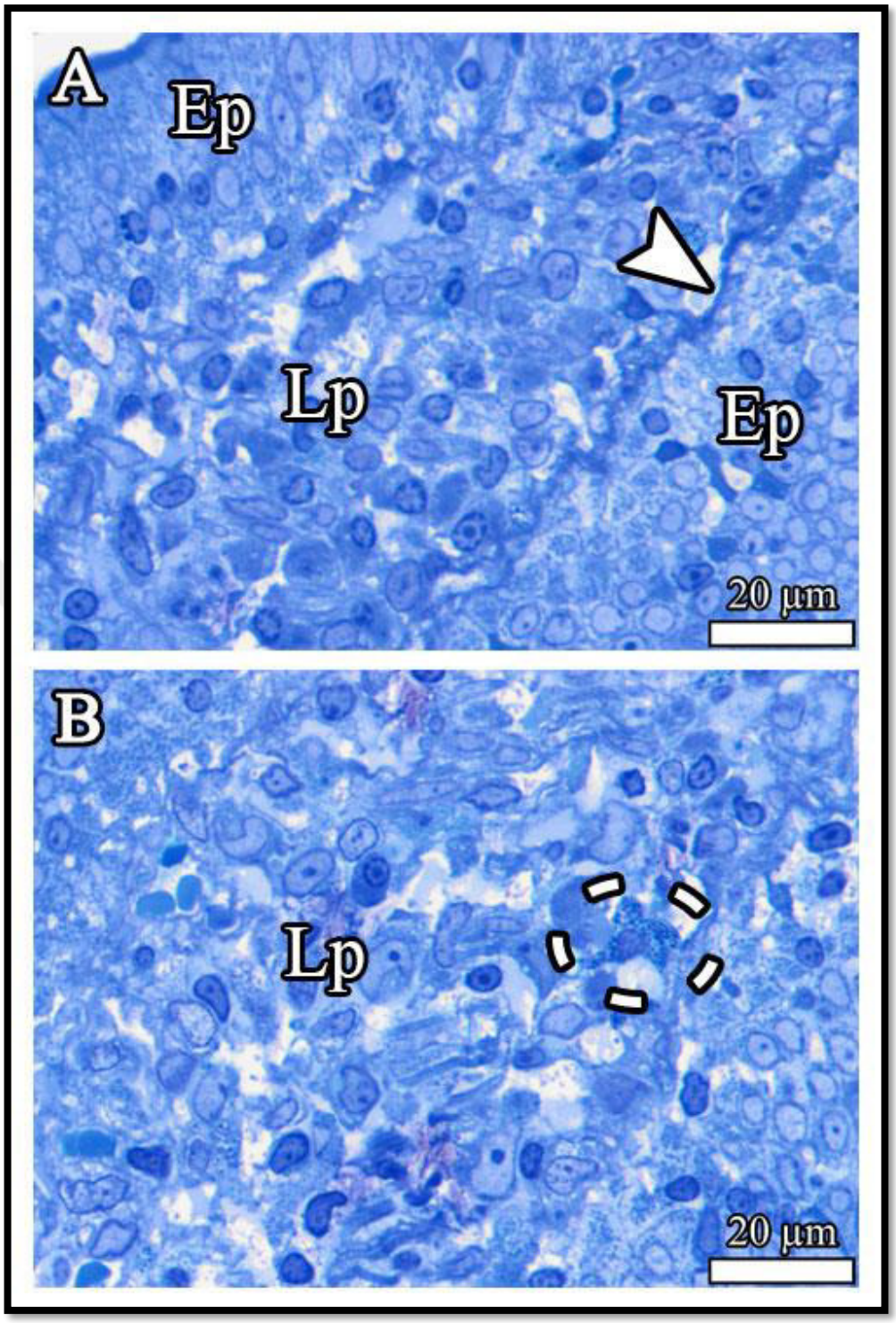

Figure 4. 111. **(A, B)** The images of the epithelium (Ep) and lamina propria (Lp) of intestinal glands belonging to the diclofenac sodium (DS) group are seen. The basal membrane of epithelium is thick (arrowhead) and lamina propria of mucosa was heavily infiltrated by lymphocytes. It is hard to see the borders of epithelial cells. Mast cell (dashed line circle area) is found in the lamina propria. Semithin section of resin embedded tissue (0.5 µm thickness) and stained with toluidine blue

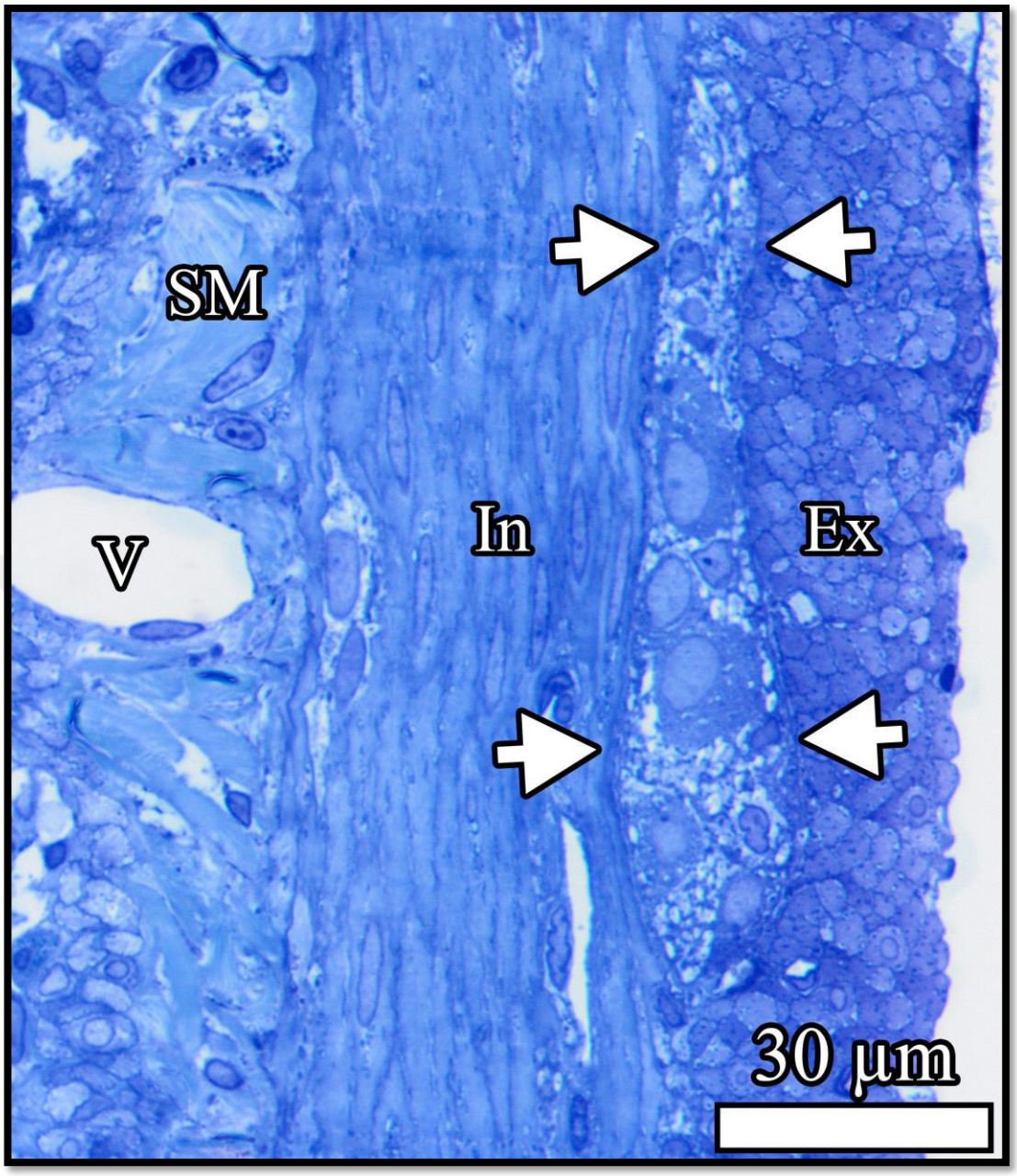

Figure 4. 112. A high magnification of submucosa (SM) and muscularis externa that consists of two layers named interna (In) and externa (Ex) are seen. Between two layers of smooth muscles, a myenteric ganglion is observed (between arrows). The borders and structure of muscle cells cannot be clearly seen. A large size of the vessel in the submucosa is observed (V). Semithin section of resin embedded tissue (0.5 µm thickness) and stained with toluidine blue

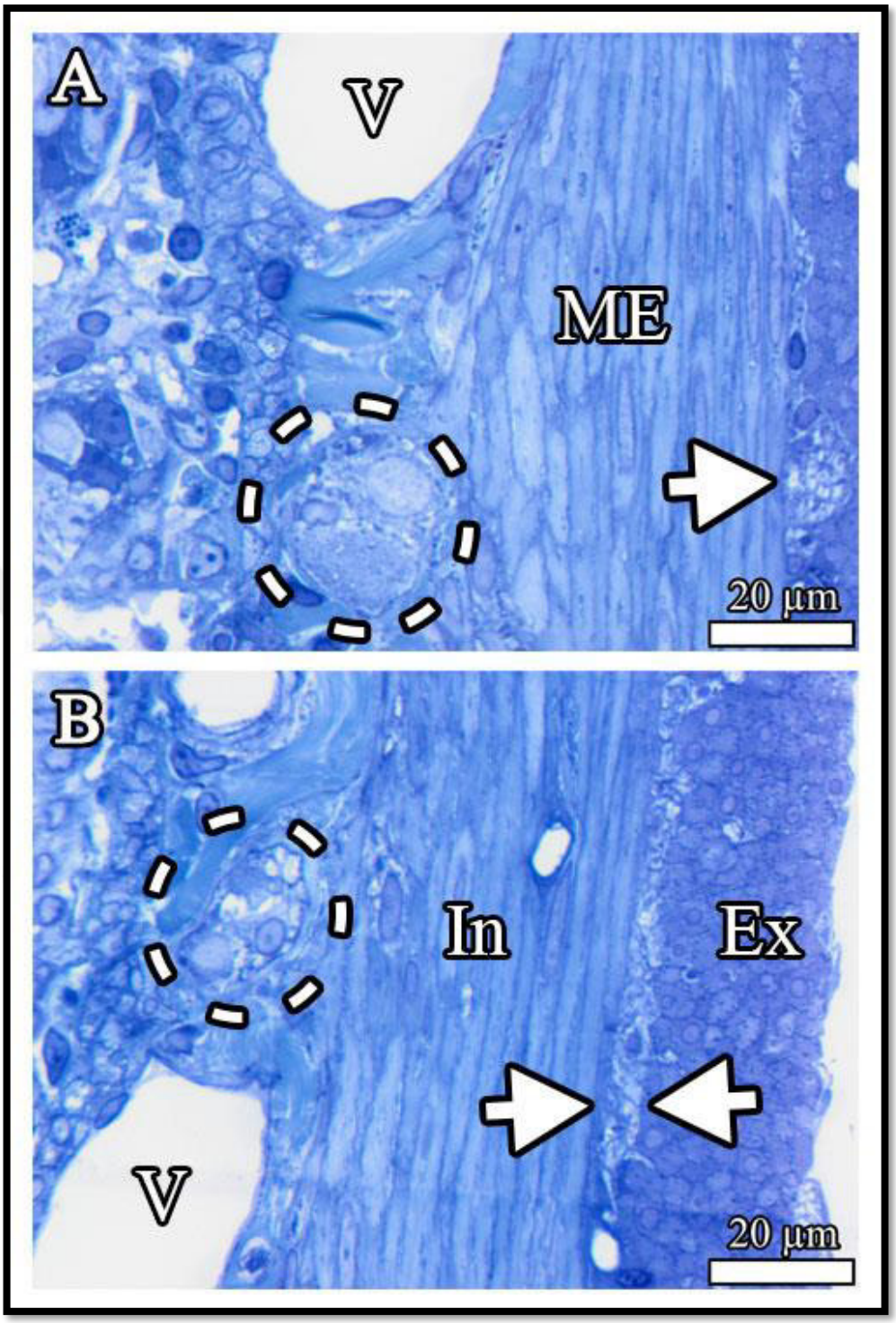

Figure 4. 113. (A, B) A high magnification of submucosa (SM) and muscularis externa that consists of two layers named interna (In) and externa (Ex) are seen. Between two layers of smooth muscles, a myenteric ganglion is observed (between arrows). The borders and structure of muscle cells can be seen. A large size of the vessel in the submucosa is found (V). Submucosal plexus (dashed line circle area) and large size vessel (V) are observed in the submucosa. Semithin section of resin embedded tissue (0.5 µm thickness) and stained with toluidine blue

4.1.2.3.3. Diclofenac Sodium + Gum Arabic Group

All layers of the large intestine in this group are seen intact. An expanded mucosa and big size Lieberkühn crypt (i.e. intestinal crypt) can be seen. The epithelium is of the simple columnar type, and the Lieberkühn crypt (i.e. intestinal crypt) has a healthy structure. The crypt contains several Goblet cells. The rest of the mucosal layers are covered by expanded muscularis mucosae. Lymphocytes are found infiltrating the gland's lumen. The submucosa of the large intestine wall contains vessels of various diameters. These vessels appear to be in good condition. In the submucosa, big size vessels, may be lymphatic vessel, can be seen. The muscularis mucosae appear to be in good health; no abnormal structures were found (Figures 4.114-4.123).

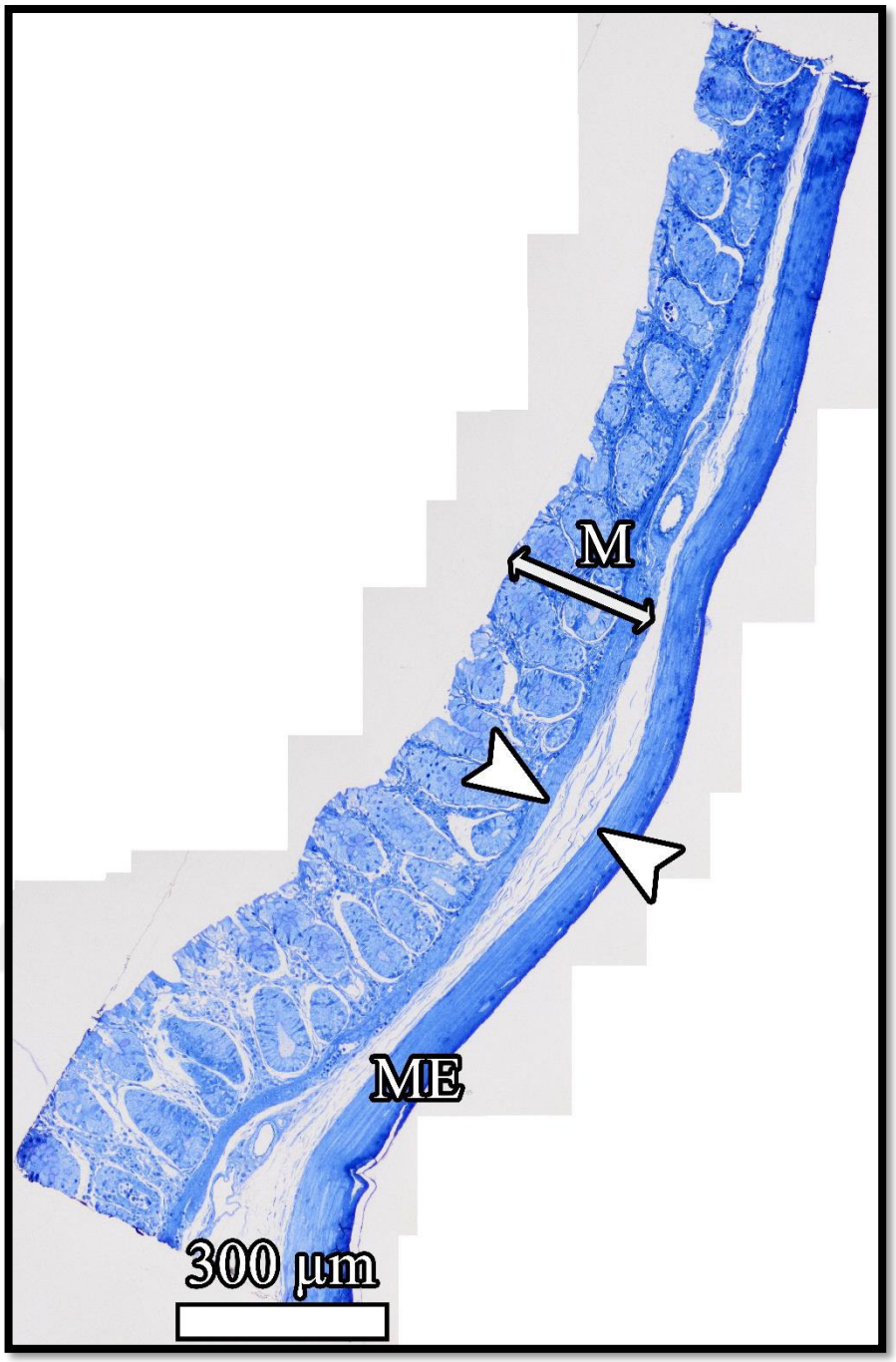

Figure 4. 114. A general view of the large intestine belongs to the diclofenac sodium + gum Arabic (DS + GA) group. All layers of the organ are seen in intact at this magnification. Partly an enlarged mucosa (M) and large size crypt of Lieberkühn (i.e. intestinal crypt) are observed. Arrowheads show the submucosa. (M), mucosa; (ME), muscularis externa. Semithin section of resin embedded tissue (0.5 µm thickness) and stained with toluidine blue

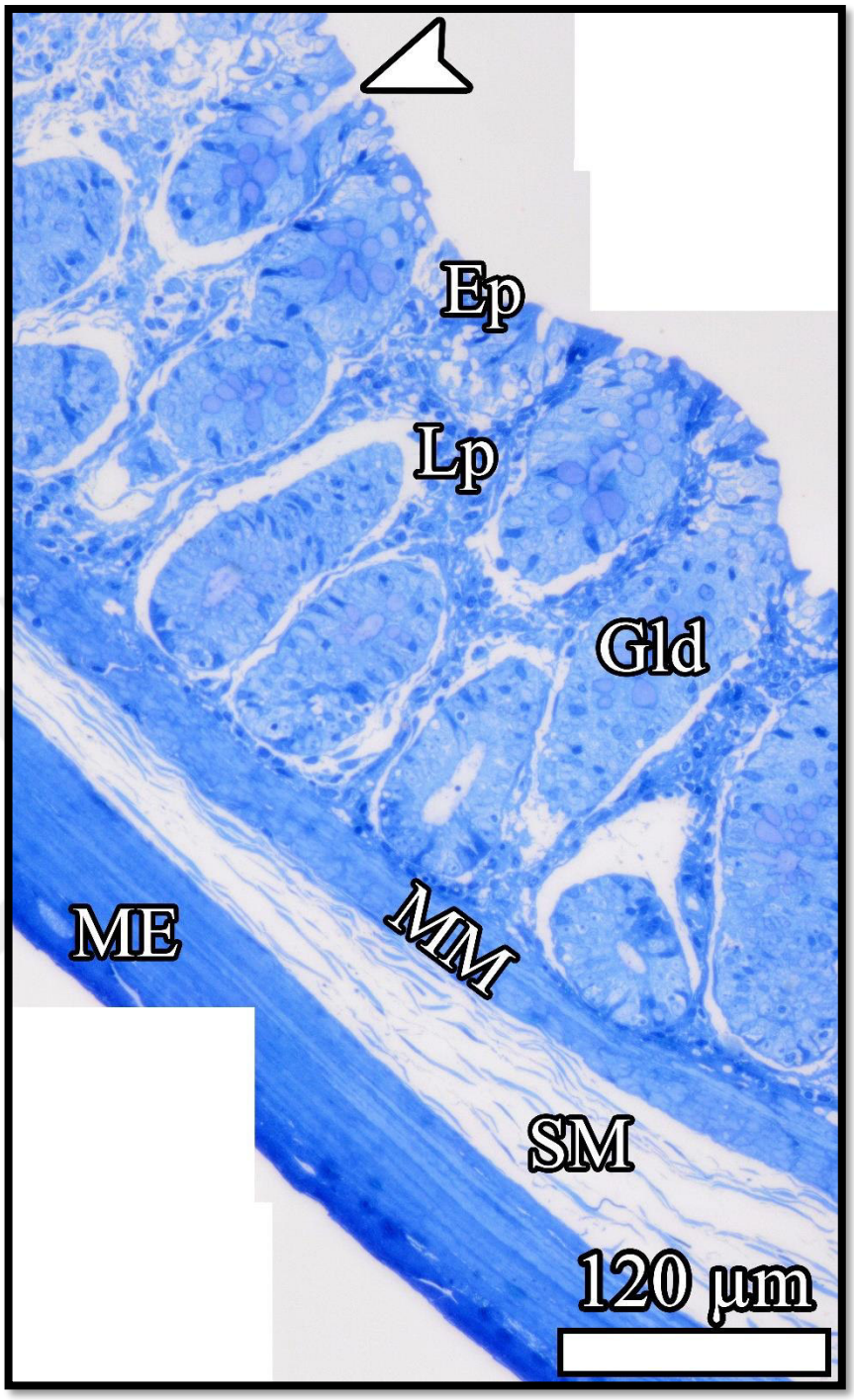

Figure 4. 115. A high magnification of the large intestine belongs to the diclofenac sodium + gum Arabic (DS + GA) group. All layers of the organ are seen in intact at this magnification. Partly an enlarged mucosa (M) and large size crypt of Lieberkühn (i.e. intestinal crypt) are found. Arrowheads show the submucosa (SM). (Ep), epithelium; (Gld), gland; (Lp), lamina propria; (M), mucosa; (ME), muscularis externa. Semithin section of resin embedded tissue (0.5 µm thickness) and stained with toluidine blue

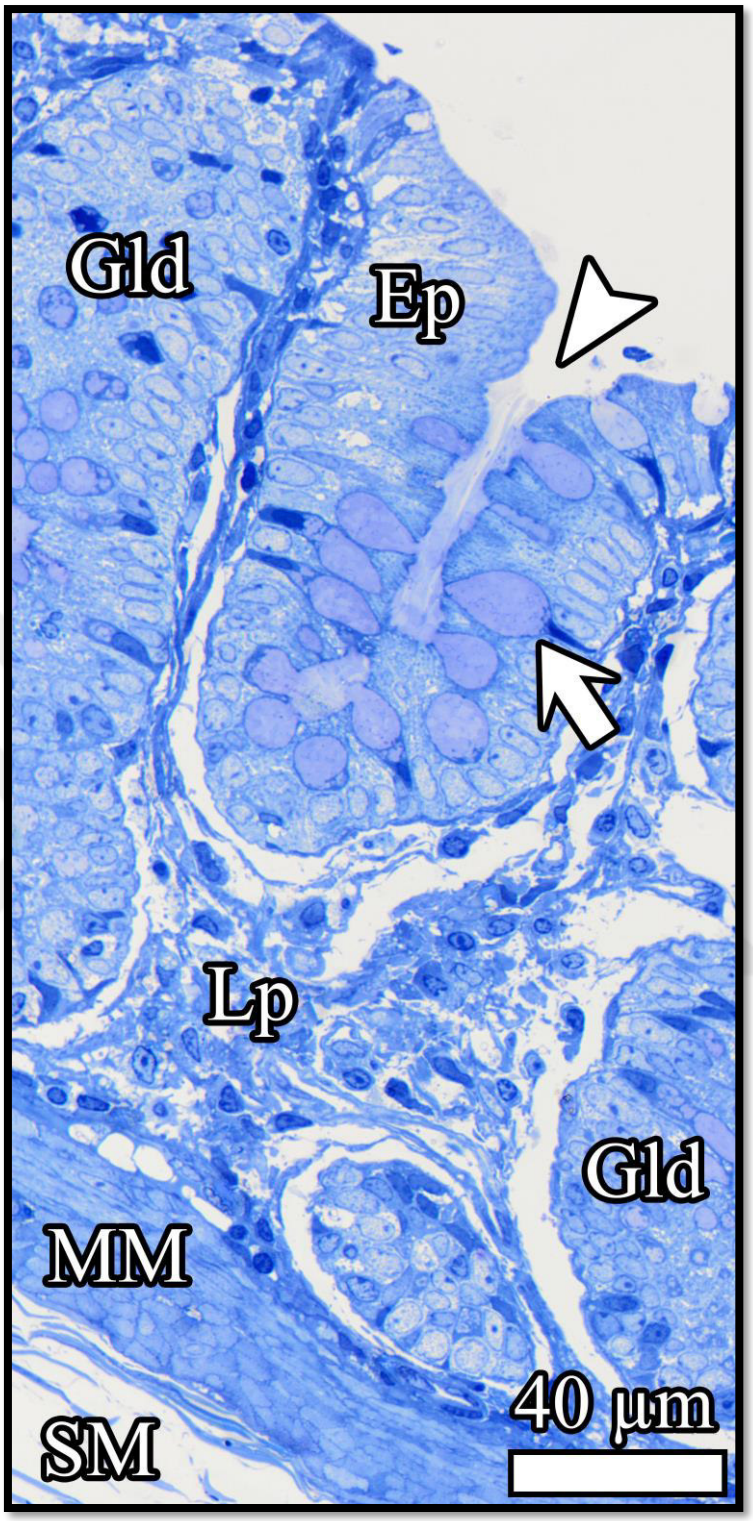

Figure 4. 116. A high magnification of the large intestine belongs to the diclofenac sodium + gum Arabic (DS + GA) group. All layers of the mucosa are observed intact. The epithelium has a simple columnar type (Ep) and the large size crypt of Lieberkühn (i.e. intestinal crypt) is seen as healthy structure (arrowhead). There are several Goblet cells (arrow) found in the crypt. An enlarged muscularis mucosae (MM) covers the rest of the mucosal layers. (SM), Submucosa; (Gld), gland; (Lp), lamina propria. Semithin section of resin embedded tissue (0.5 µm thickness) and stained with toluidine blue

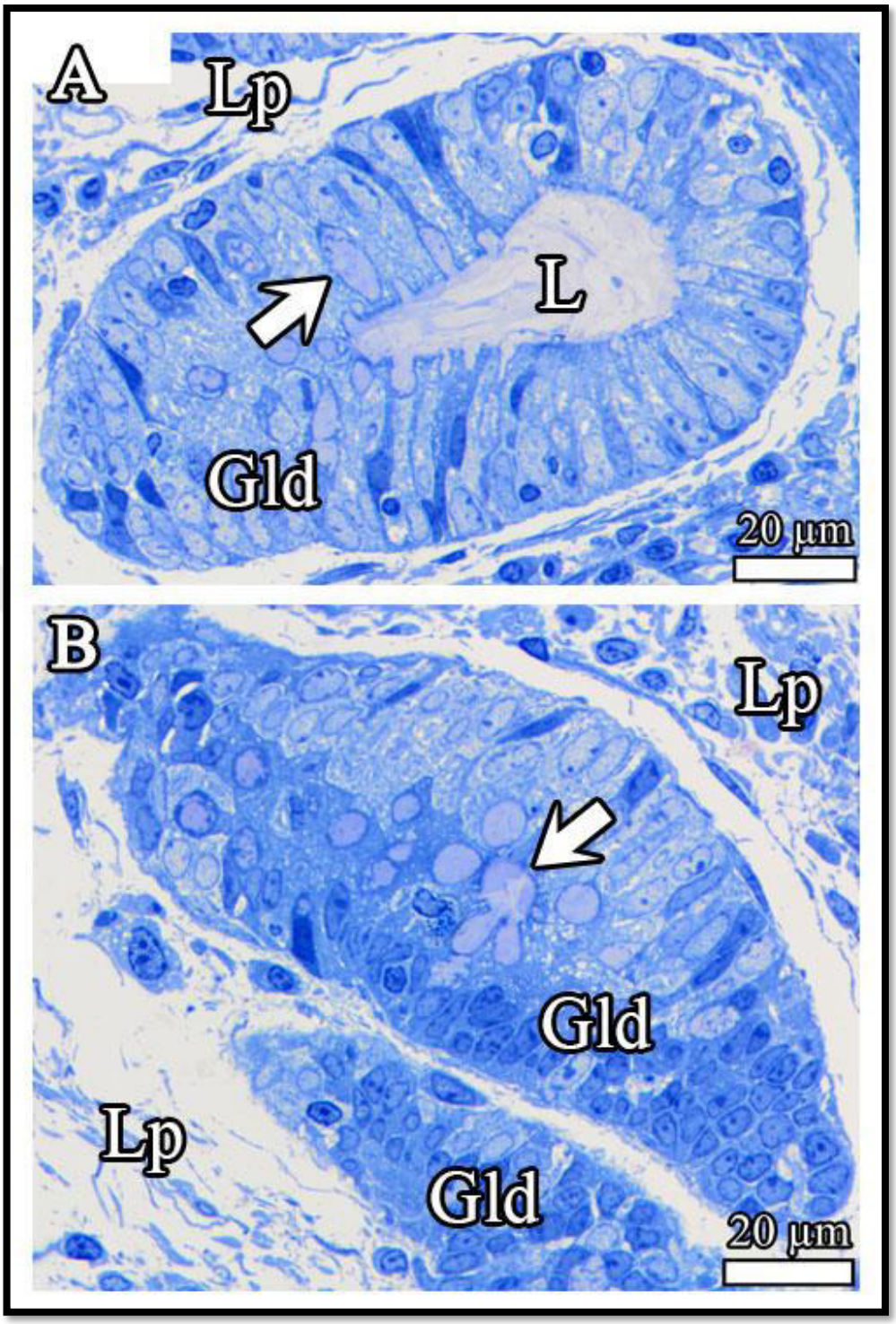

Figure 4. 117. (A, B) High magnification images of the large intestine belonging to the diclofenac sodium + gum Arabic (DS + GA) group are seen. Intestinal glands (Gld) structures are found healthy. **(A)** Gland epithelium has a simple columnar type and many Goblet cells. The lumen of the crypt of Lieberkühn (i.e. intestinal crypt) (L) is seen in normal. There are a number of Goblet cells (arrow) observed in the crypt. **(B)** A longitudinal section of intestinal glands and its Goblet cells are seen, the section was not passed from its lumen. (Lp), lamina propria. Semithin section of resin embedded tissue (0.5 µm thickness) and stained with toluidine blue

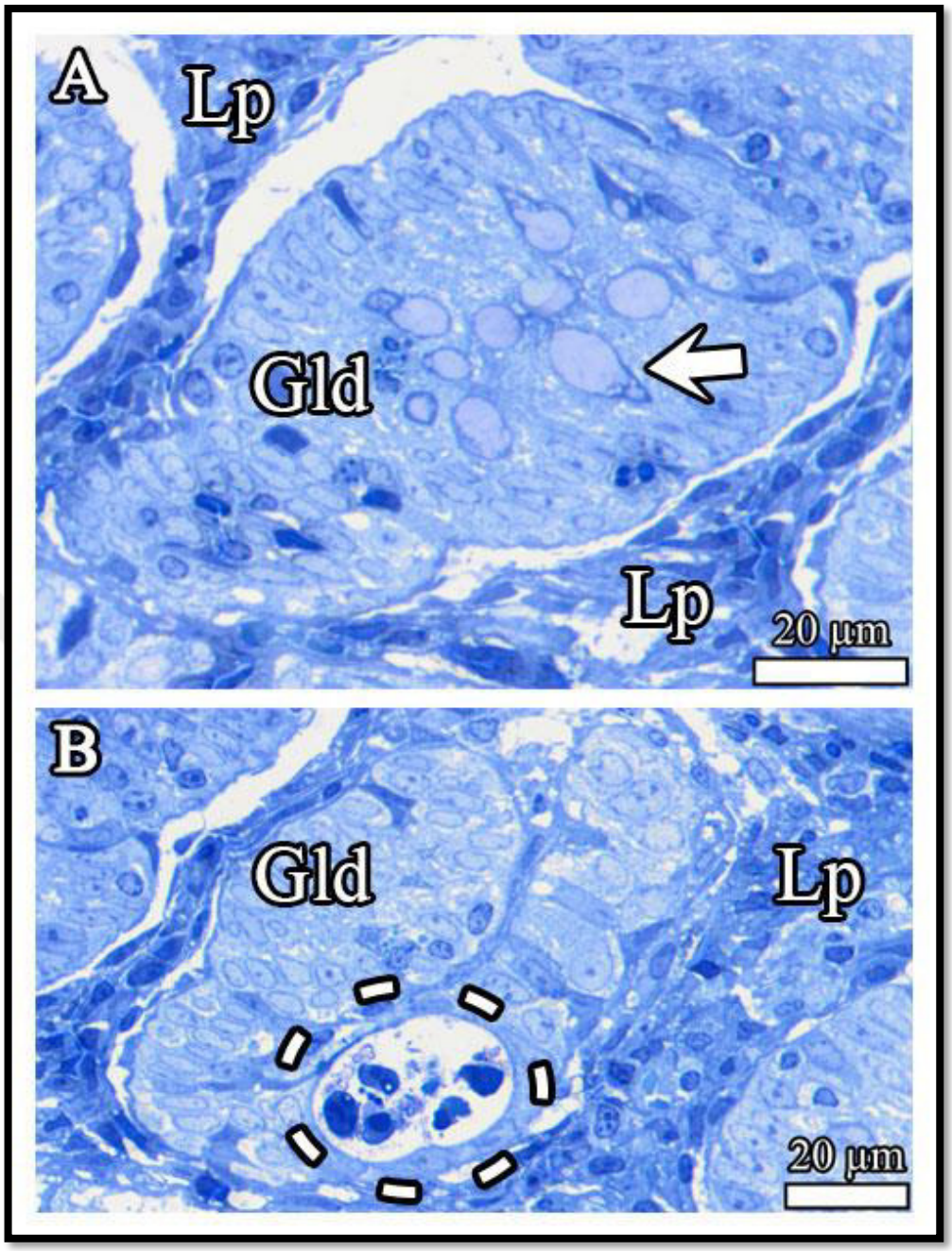

Figure 4. 118. (A, B) High magnification images of two large intestines belonging to the diclofenac sodium + gum Arabic (DS + GA) group are observed. **(A)** Although Goblet cells (arrow) in gland epithelium are seen clearly, but the borders of epithelium are not clearly observed. **(B)** Lymphocyte infiltration into gland epithelium (dashed circled area) is seen. Lamina propria (Lp) of mucosa was densely stained. Semithin section of resin embedded tissue (0.5 µm thickness) and stained with toluidine blue

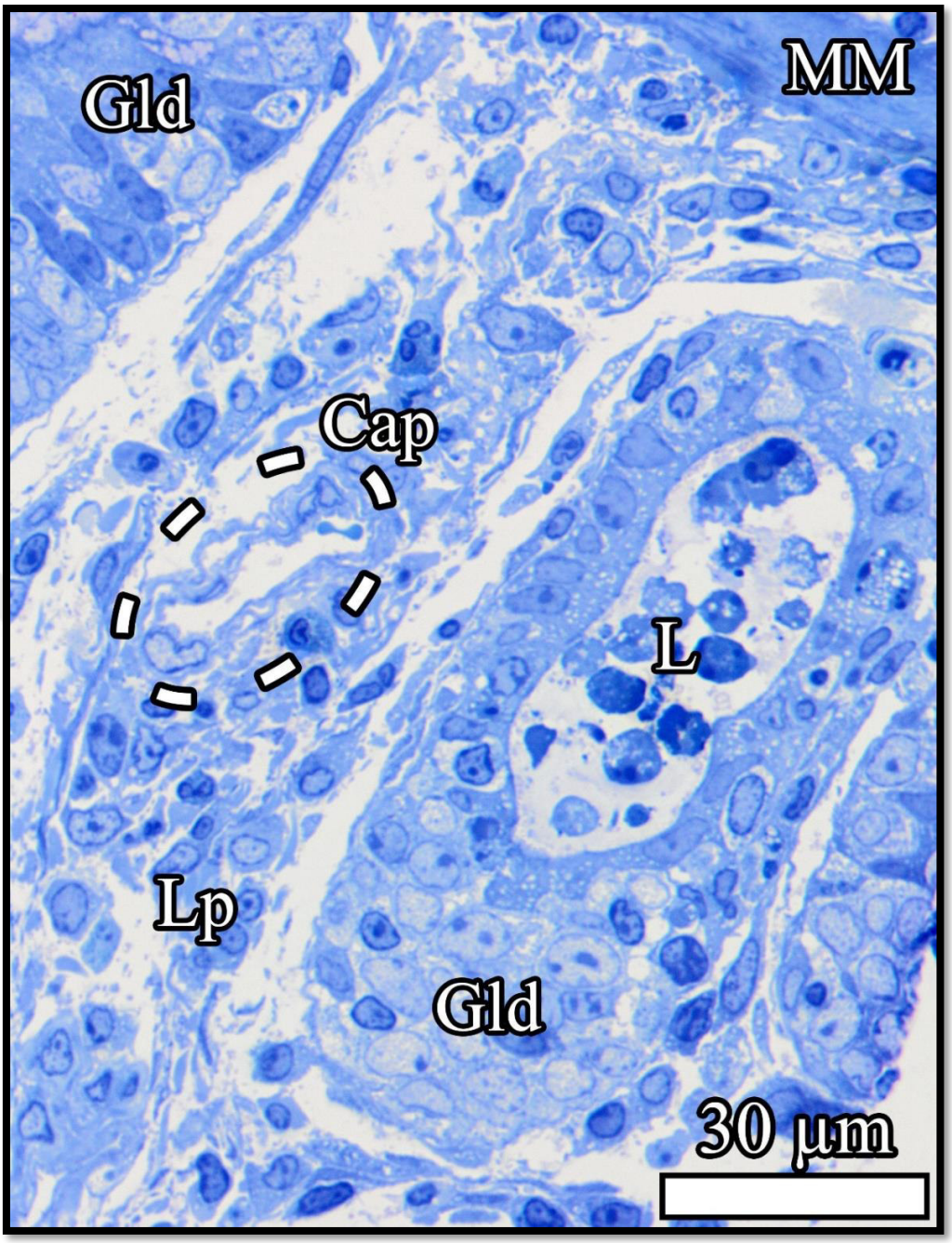

Figure 4. 119. A high magnification image of the large intestine belonging to the diclofenac sodium + gum Arabic (DS + GA) group is seen. Lymphocytes infiltration in the lumen (L) of the gland (Gld) is observed. The gland epithelium is so thin; it is hard to see Goblet cells in this layer. A loose connective tissue of lamina propria (LP) covers the glands. A large size capillary (Cap) is found in the lamina propria. (MM), muscularis mucosae. Semithin section of resin embedded tissue (0.5 µm thickness) and stained with toluidine blue

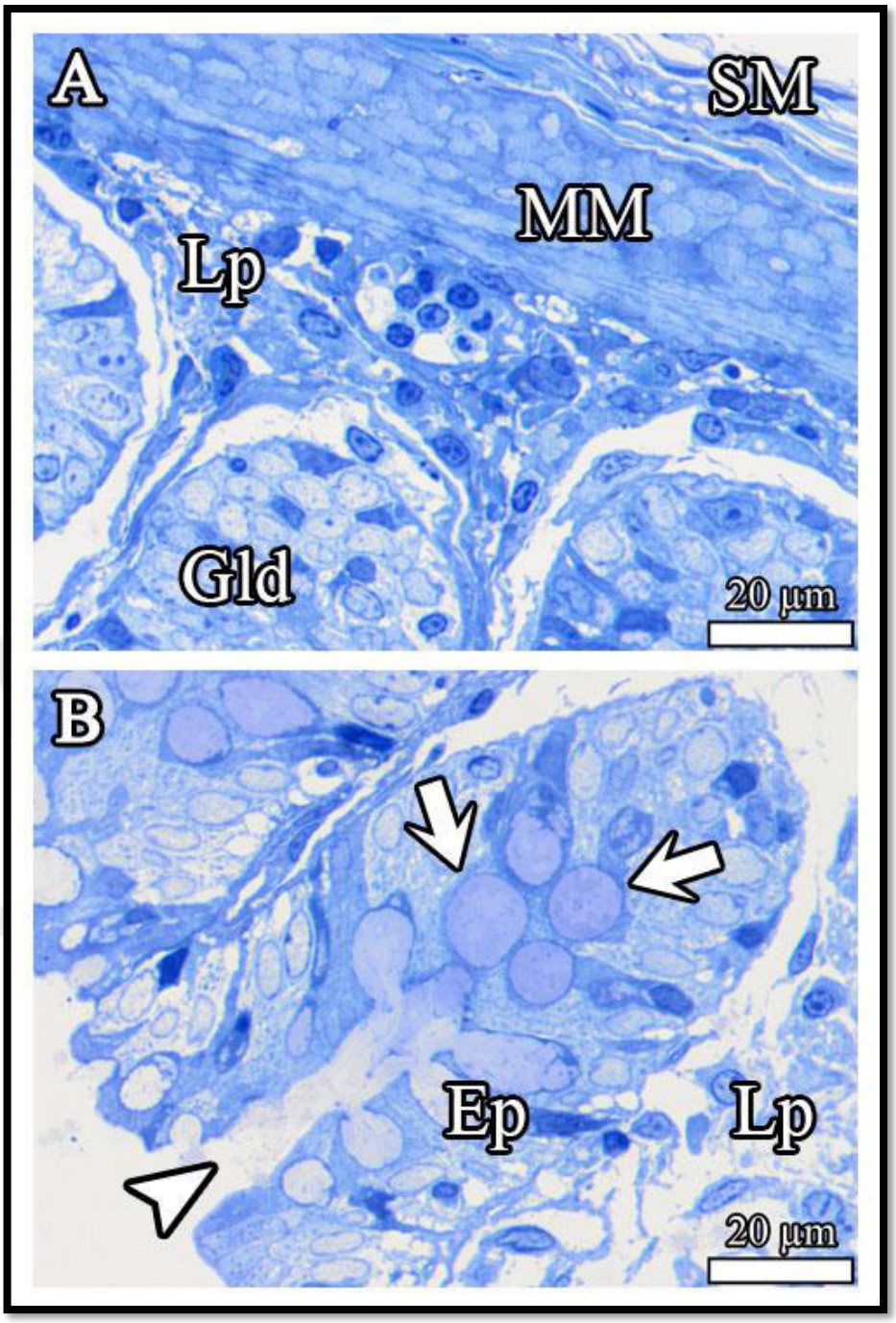

Figure 4. 120. (A, B) Images of the large intestine belonging to the diclofenac sodium + gum Arabic (DS + GA) group are seen. **(A)** A simple columnar surface epithelium (Ep), Lieberkühn crypts (arrowhead), and intestinal gland with many numbers of Goblet (arrow) cells are observed. **(B)** The base of glands (Gld), lamina propria (Lp), muscularis mucosae (MM), and submucosa of the large intestine are seen in healthy. These layers look healthy; there is no pathological structure. Semithin section of resin embedded tissue (0.5 µm thickness) and stained with toluidine blue

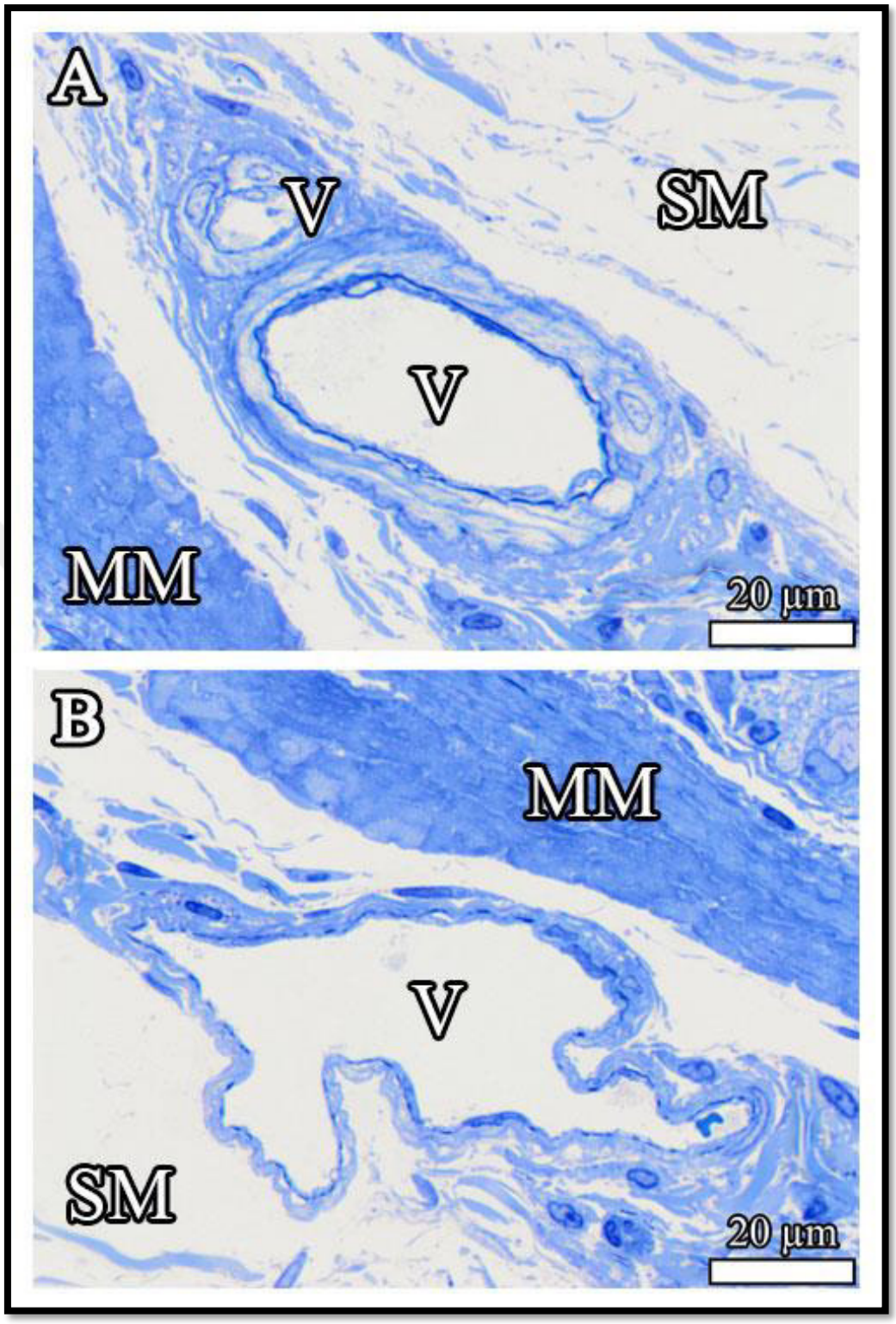

Figure 4. 121. (A, B) Images of large intestine belonging to the diclofenac sodium + gum Arabic (DS + GA) group is seen. **(A)** Different sizes of vessels (V) are found in the submucosa (SM) of the large intestine wall. These vessels look healthy. **(B)** The large size of the vessel (V), which might be a lymphatic, is seen in the submucosa (SM). Muscularis mucosae (MM) look healthy; there is no pathological structure. Semithin section of resin embedded tissue (0.5 µm thickness) and stained with toluidine blue

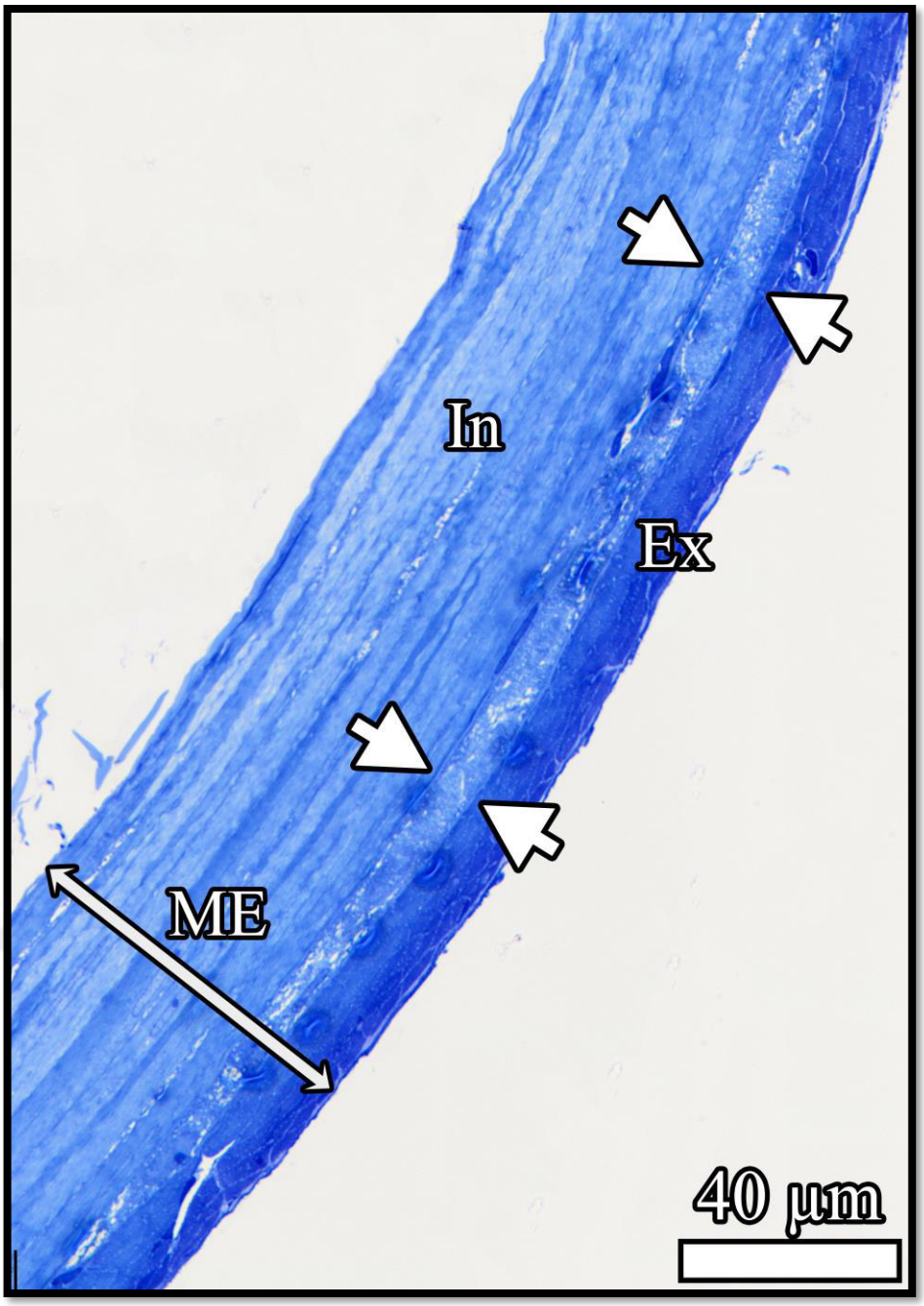

Figure 4. 122. An image of a large intestine belonging to the diclofenac sodium + gum Arabic (DS+ GA) group is seen. An intact muscularis externa (ME) has two layers, interna (In) and externa (Ex). Smooth muscles in both layers look healthy. Between them, myenteric plexus (arrows) is observed. Semithin section of resin embedded tissue (0.5 µm thickness) and stained with toluidine blue

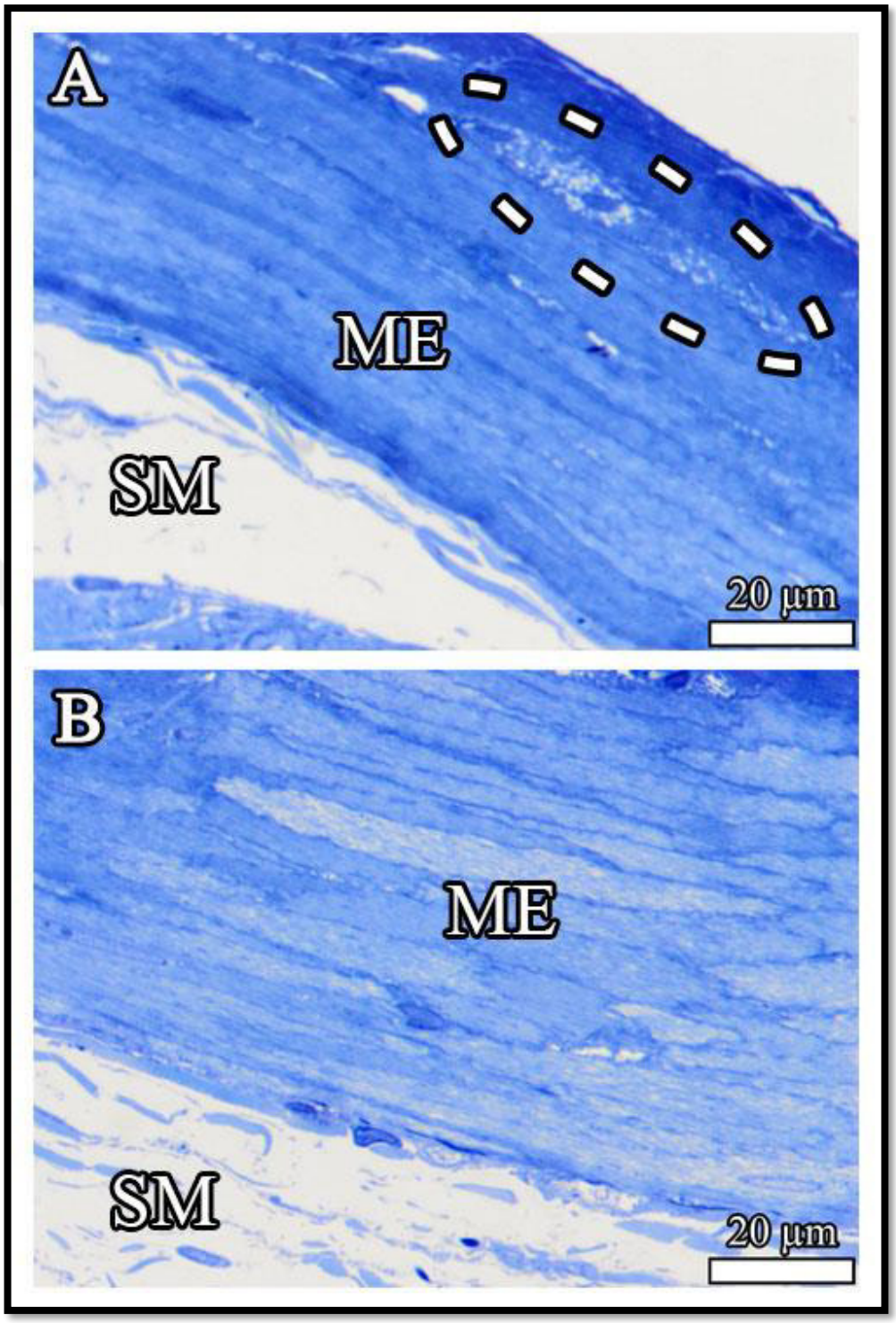

Figure 4. 123. **(A, B)** Images of the large intestine belonging to the diclofenac sodium + gum Arabic (DS+ GA) group are observed. Healthy muscularis externa (ME) that has two layers, interna and externa, between them (dashed circled area) a myenteric plexus is seen. (SM), submucosa. Semithin section of resin embedded tissue (0.5 µm thickness) and stained with toluidine blue

4.1.23.4. Gum Arabic Group

All the layers of the organ are seen partly healthy in this group. An expanded mucosa and big size of the Lieberkühn crypts (i.e. intestinal crypt) can be seen. Although the intestinal glands are normal, but their glandular cells are heavily stained, and many intermediate/Paneth cell-like cells are found at the base of these glands. Lieberkühn's crypt has few numbers of Goblet cells. Infiltrations of lymphocytes in the lamina propria were clearly visible. This organ has intact submucosal layer. The muscularis externa is made up of two healthy smooth muscle layers with healthy arteries between them (Figures 4.124-4.130).

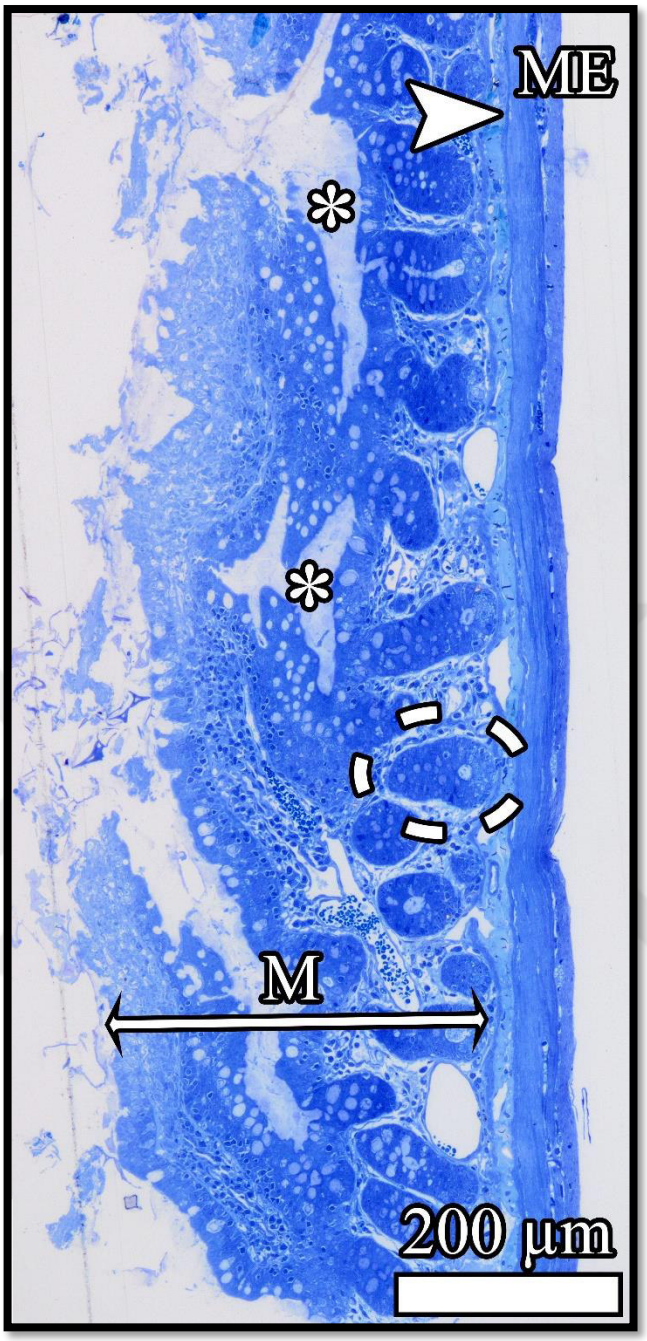

Figure 4. 124. A general view of the large intestine belongs to the gum Arabic (GA) group. All layers of the organ are seen intact except surface epithelium at this magnification. The simple columnar surface epithelium of mucosa in the large intestine was lost in most of area. This might be a result of poor fixation since other parts of the intestine look intact. Partly an enlarged mucosa (M) and large size crypt of Lieberkühn (i.e. intestinal crypt) (*) are observed. Intestinal glands are healthy structures (dashed circled area). Arrowhead shows the muscularis externa (ME). Semithin section of resin embedded tissue (0.5 µm thickness) and stained with toluidine blue

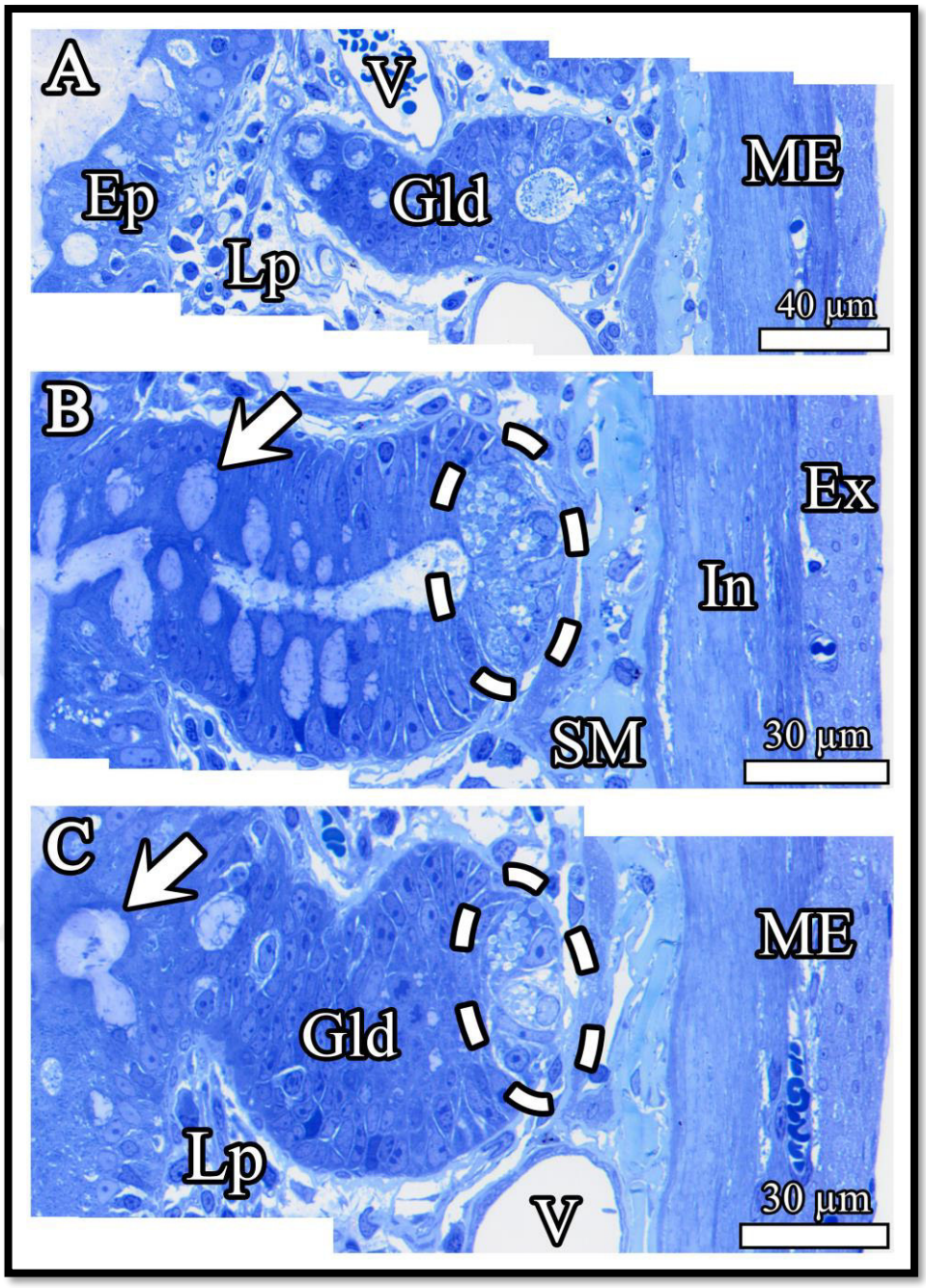

Figure 4. 125. (A, B, C) General views of the large intestine belong to the gum Arabic (GA) group. All layers of the organ are seen intact at this magnification. Partly an enlarged mucosa and large size crypt of Lieberkühn (i.e. intestinal crypt) are observed. Although intestinal glands are healthy structures, but their glandular cells were densely stained and there are many intermediate/Paneth cell-like cells at the base of glands (Gld) that were found (dashed circled area). There are a few numbers of Goblet cells (arrow) in the crypt of Lieberkühn. Lymphocytes infiltrations in the lamina propria (Lp) were clearly seen. Muscularis externa (ME) consists of two smooth muscle layers interna (In) and externa (Ex)). Semithin section of resin embedded tissue (0.5 µm thickness) and stained with toluidine blue

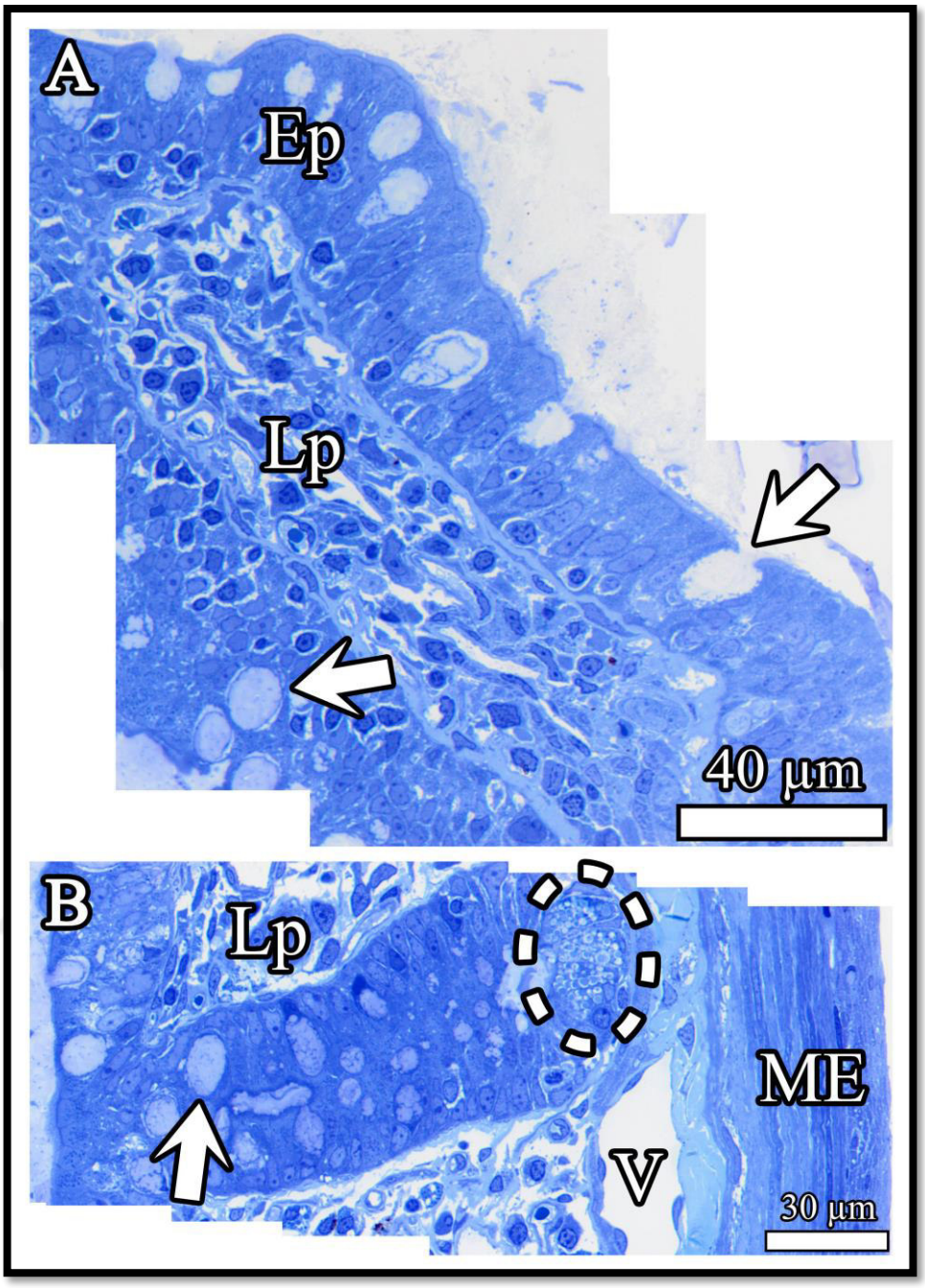

Figure 4. 126. (A, B) General views of the large intestine belong to the gum Arabic (GA) group. **(A)** Epithelium (Ep) and lamina propria (Lp) of mucosal layers in the organ is seen intact at this magnification. The epithelium (Ep) has few numbers of Goblet cells (arrows) and its basal membranes, as well as lamina propria (Lp) of the epithelium, look healthy. Lymphocytes infiltration into the epithelium is also observed. **(B)** An intestinal gland and an accumulation of intermediate cells (dashed lined area) at the base of it are seen. Few numbers of Goblet cells are observed (arrow). Muscularis externa (ME) consists of two smooth muscle layers. Semithin section of resin embedded tissue (0.5 µm thickness) and stained with toluidine blue

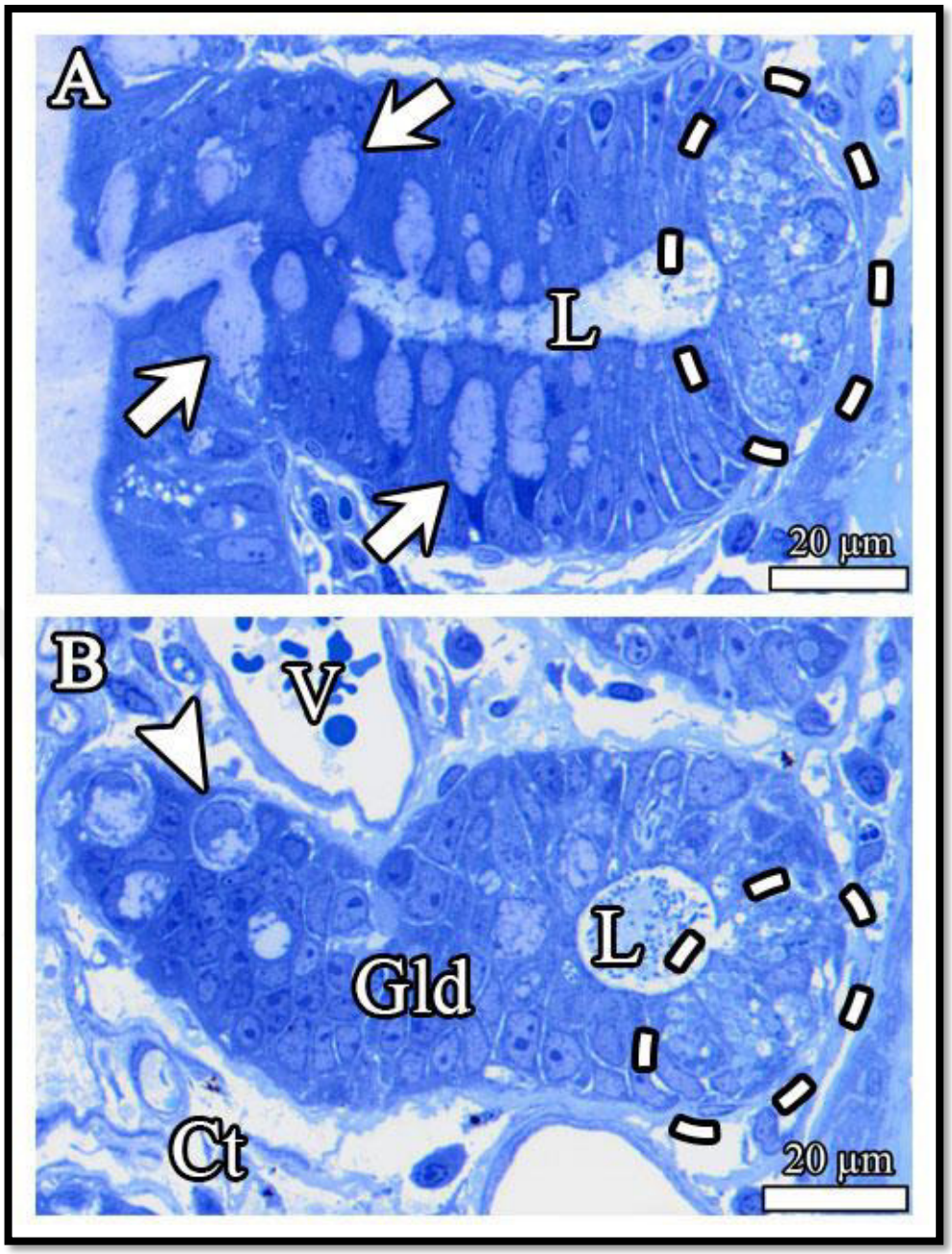

Figure 4. 127. (A, B) General views of the large intestine glands belong to the gum Arabic (GA) group. **(A)** An intestinal gland with many Goblet cells (arrows) and a large lumen (L) are seen. At the base of the gland, there are many intermediate/Paneth cell-like cells are observed (dashed circled area). **(B)** An intestinal gland (Gld) that covers by connective tissue (Ct) and a large lumen (L) are seen. Goblet cells (arrowhead) are found in the gland epithelium. At the base of the gland, there are many intermediate/Paneth cell-like cells are observed (dashed circled area). (V), vessel. Semithin section of resin embedded tissue (0.5 µm thickness) and stained with toluidine blue

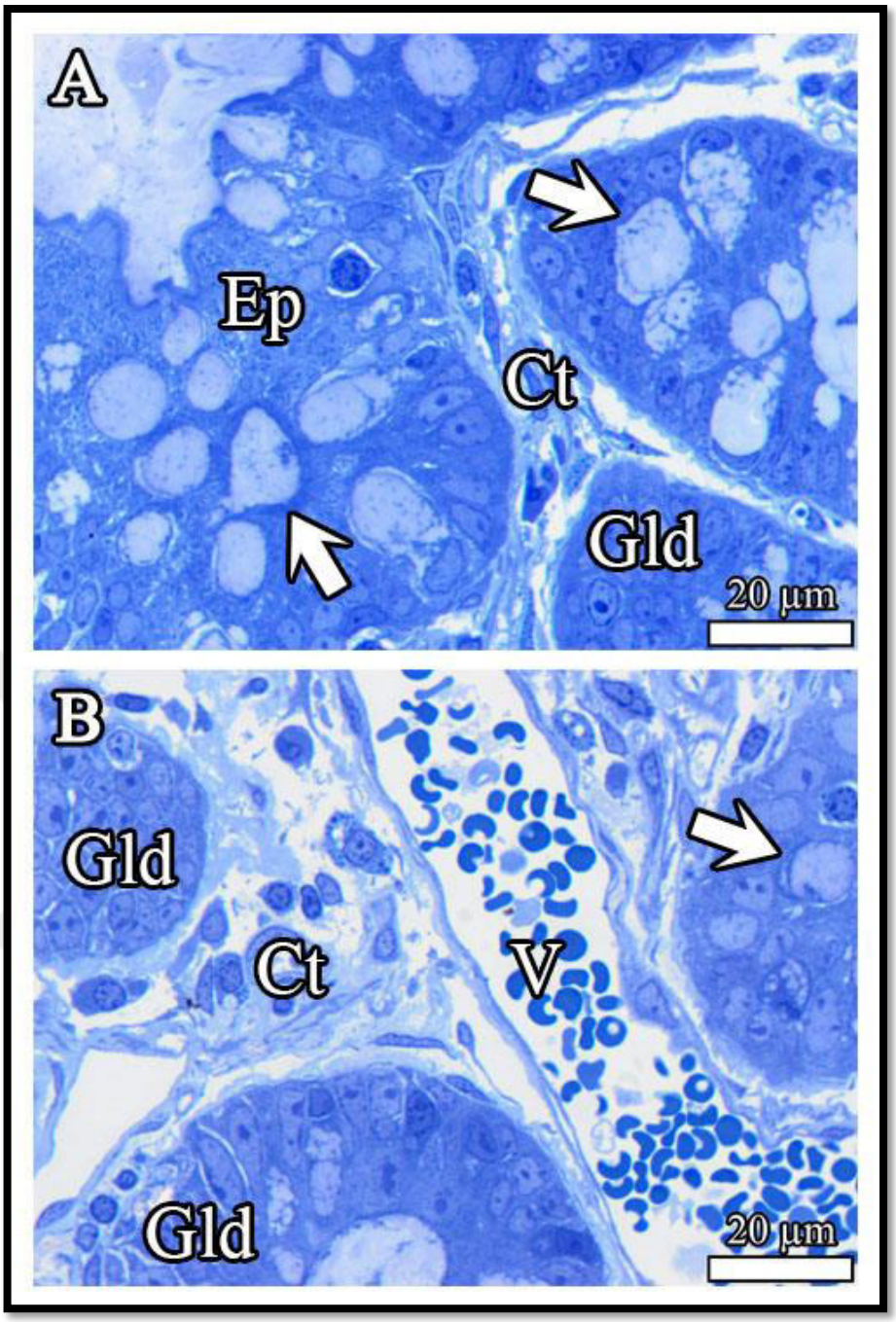

Figure 4. 128. (A, B) General views of the large intestine glands belong to the gum Arabic (GA) group. Three intestinal glands (Gld) with many Goblet cells (arrows) are partly seen. A lymphocyte infiltration is observed in the gland epithelium (Ep). Well-protected vessels (V) and connective tissue (Ct) are found in the sections. Semithin section of resin embedded tissue (0.5 µm thickness) and stained with toluidine blue

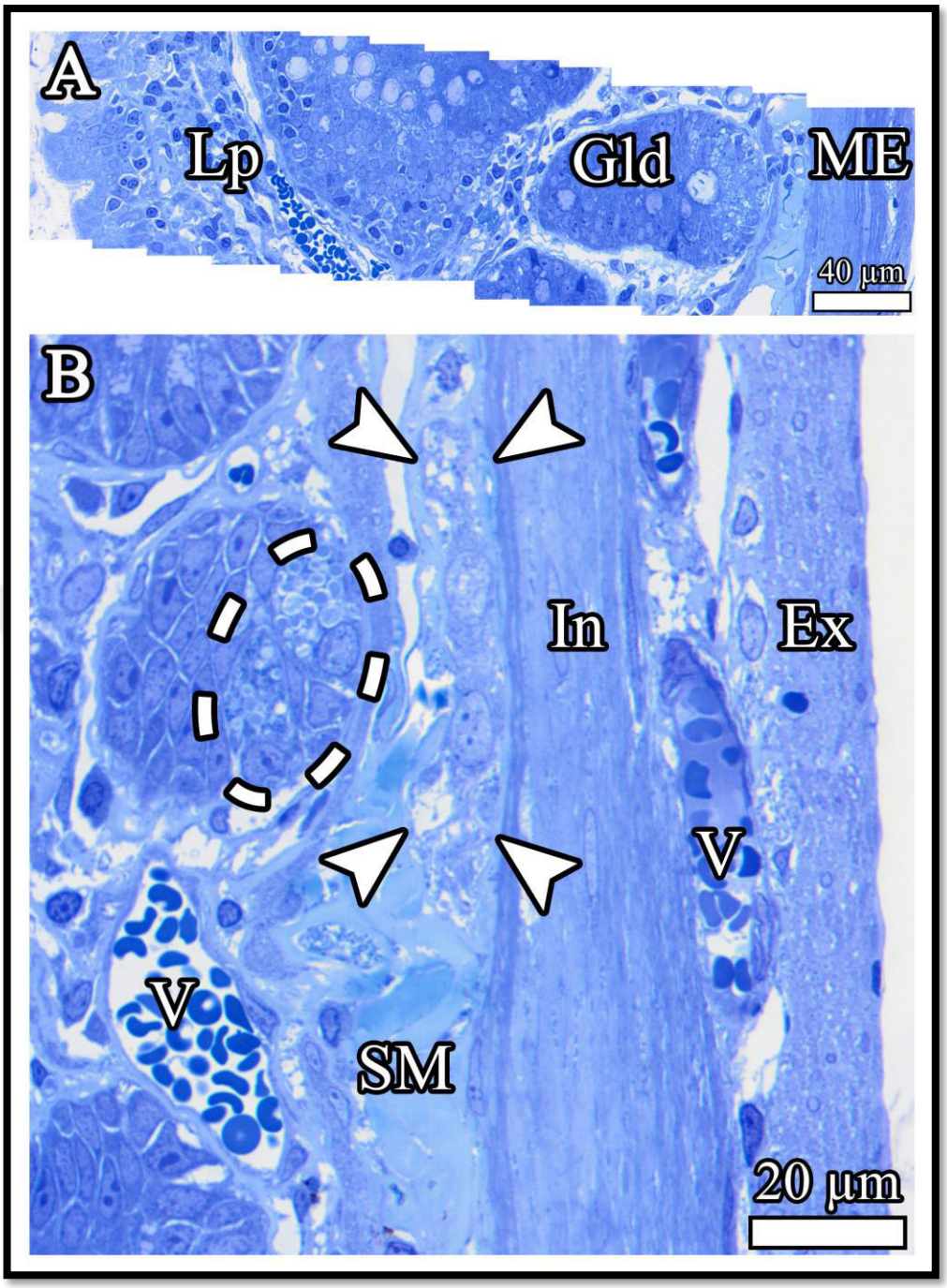

Figure 4. 129. (A, B) General views of the large intestine belong to the gum Arabic (GA) group. **(A)** Epithelium and lamina propria (Lp) of mucosal layers in the organ is seen intact at this magnification. The epithelium of the gland (Gld) has few numbers of Goblet cells. At the base of this gland, an accumulation of Paneth cells like cells/intermediate cells is observed. **(B)** An intestinal gland and an accumulation of Paneth cells like cells/intermediate cells (dashed lined area) at the base of it are seen. The intact submucosa layer (SM) of the large intestine is delineated by arrowheads. Muscularis externa (ME) consists of two smooth muscle layers (In and Ex) between them well healthy vessels are observed. Semithin section of resin embedded tissue (0.5 µm thickness) and stained with toluidine blue

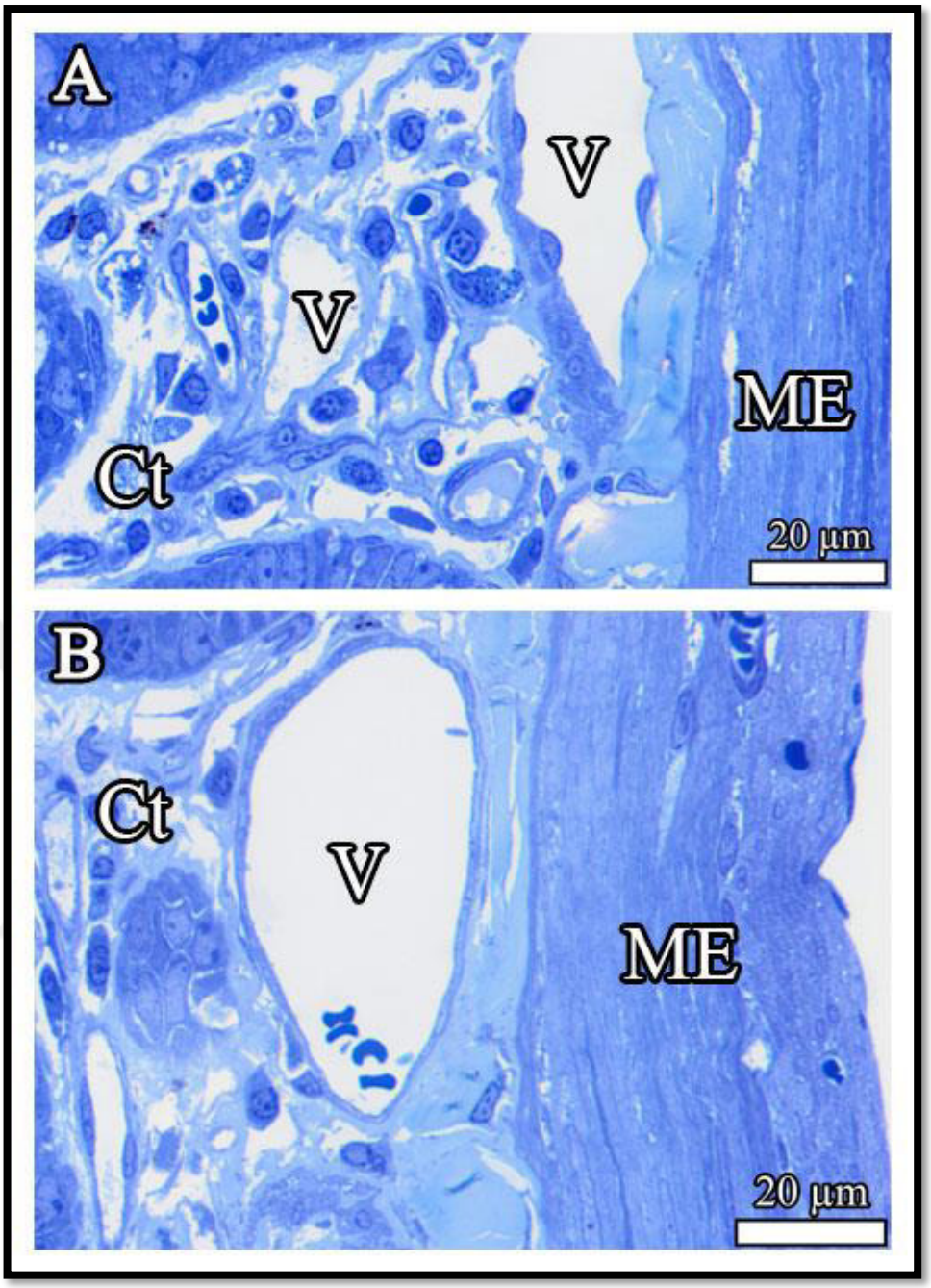

Figure 4. 130. (A, B) General views of the large intestine layers belong to the gum Arabic (GA) group. The submucosa that has many healthy vessels (V) and connective tissue (Ct) is seen. Muscularis externa of the intestine (ME) has healthy smooth muscles. Semithin section of resin embedded tissue (0.5 µm thickness) and stained with toluidine blue

4.2. Discussion

The purpose of this investigation was to explore if GA could protect the rat GIT mucosa from the mucosal effects of DS exposure. To assess the effects, stereological, light, and electron microscopic techniques were used. The functional state of the GIT mucosa is reflected in its morphological properties in terms of volume, volume fraction, numerical density, and the total number of cells. To acquire accurate and impartial results, it is critical to obtain quantitative data with statistical dependability. Stereology is at the core of the most effective tools in this regard. It is a methodological science that uses mathematical and statistical methods to drive three-dimensional information from two-dimensional images. Histological sections typically provide qualitative data that can determine whether or not the tissue is undergoing pathological changes. However, the only way to determine the significance of this shift in terms of statistically significant numbers is to use stereology. Where statistically significant changes can indicate the severity of pathological alterations or the effect of the experimental medicine under investigation.

Many people (67 million persons, or 25% of the adult population) are anticipated to have medically diagnosed arthritis, in accordance with the Centers for Disease Control and Prevention (CDC) by 2030, up from 46 million in 2003–2005 (Gupta and Eisen, 2009). Despite substantial improvements in the discovery of "disease-modifying" medications (like anti-cytokine treatments) and a very large frequency of serious negative consequences, NSAIDs remain the first-line therapy to treat osteoarthritis and rheumatoid arthritis. NSAIDs have a global market of more than $4 billion each year. After the cyclooxygenase (Cox)-2 inhibitors introduction the market surged. However, due to population aging in wealthier countries, it has been continuously rising (and the resulting rise in the prevalence of age-related disorders like arthritis). Aspirin, the first NSAID, has witnessed an upsurge in use due to its purported benefits in reducing the number of people who have heart attacks and strokes (Wallace, 2007).

With morbidity and burden in the lower in addition to the upper GI canals, the gastrointestinal (GI) system is the greatest common location of NSAID-related injury. The most prevalent adverse effect is dyspepsia, and it can have serious effects such as GI hemorrhage, erosions, membranous loops, stenosis, and colitis. When

employing the incidence density ratio, the research found an elevated entire death degree of 5.5 out of every 100.000 people-years after an upper GI incident (Abraham et al., 2008). The occurrence of NSAID-related adverse events rises in tandem with the usage of these drugs. However, because of the danger of gastrointestinal (GI) disorders, the prescription of NSAIDs is restricted. The consumption of NSAIDs has been linked to an increase in upper GI illnesses by three to five times (Henry and McGettigan, 2003). Despite the availability of gastroprotective medications, NSAID-induced GI injury still has a high mortality and morbidity rate. The expense of treating ulcer problems caused by NSAIDs is projected to be in the billions of dollars each year (Bidaut-Russell and Gabriel, 2001). The intake of selective cyclooxygenase (COX)-2 inhibitors have been linked to a decreased incidence of upper gastrointestinal disorders in clinical trials and observational research (Masso et al., 2010). However, they have also been connected to an elevated hazard of serious cardiovascular problems.

To discuss the effects of NSAIDs in general and diclofenac in particular on the GIT, the pathophysiology, and the methods used to treat or mitigate these effects, at the level of the stomach separate from the intestines because these procedures differ in the stomach and the intestine.

In this study, we found that after administration of DS for 15 days, either only or in conjunction with gum, the GIT mucosa was affected, in compare to the control group or gum arabic only given group. These findings resembled those previously published in the stomach, as Douthwaite and Lintott's endoscopic experiment in 1938 was the first to show that NSAIDs can make ulcers and bleeding in the upper gastrointestinal system (Douthwaite and Lintott, 1938). In that trial, the researchers established the aspirin's ability to injure the stomach. Stronger NSAIDs, such as indomethacin, phenylbutazone, and the fenamates, were introduced in the years that followed. In the 1960s and 1970s, case reports of melaena associated with aspirin and newer NSAIDs started to show up in the literature, and case-control studies on the GIT hazard of this class of medicine began to appear. In the following years, some academics have referred to the damage produced by NSAIDs to the upper gastrointestinal system as an "epidemic" (Gabriel and Bombardier, 1990; Singh et al., 1996). This is due in part to the widespread usage of these medications. After that, many studies confirmed that gastric inflammation, ulcers, and hemorrhages were

caused by the NSAID in both animals and humans (Naidu et al., 2009; Kinsey et al., 2011). Diclofenac sodium (100 mg/kg p.o.) injection to mice who are hungry produced stomach inflammation, causing soreness, spot erosions, and bleeding streaks six hours later (Russell, 2001) who report that endoscopic research has revealed that NSAIDs users had a 14–25 % prevalence percentage of stomach and duodenal ulcers. Understanding the mechanism of NSAID-induced GIT damage is critical because it may point to a method for preventing and treating NSAID-related organ damage.

The mucosa of the GIT is injured due to local flustering impacts and general effects mediated through prostaglandin synthesis reduction via inhibition of prostaglandin cyclooxygenase. Although all NSAIDs reduce the two types of COX found in the mucosa, the effects of individual NSAIDs on the two forms vary. The COX-1 is necessary for adequate protective stomach function, whereas COX-2 is elevated in inflammatory regions.

NSAIDs affect normal gastric defense mechanisms in several ways to cause gastropathy: first, they inhibit prostaglandin synthesis, which reduces mucus and bicarbonate secretion; second, through suppressing acid release and mucosal creation; third, by reducing local blood flow; and fourth, platelet aggregation and coagulation processes are disrupted by them (Bidaut-Russell and Gabriel, 2001).

The signs and symptoms that arise due to toxicity of NSAID on the lower GI distal to the duodenum are frequently vague, clinically silent, and difficult to diagnose. Side effects including the intestine's more distal parts are not only uncommon but also usually underestimated. NSAID-induced toxicity has now been proven to affect the entire GIT, including the small intestine, colon, and rectum (Thiéfin and Beaugerie, 2005). Also in this study, the damage of the NSAIDs was reported to be extended to the lower GIT, these findings matched those previously reported with different tools and methods like indirect markers to detect permeability and inflammation, as well as direct vision that is used Double-Balloon Enteroscopy (DBE) and CE, which are the most common approaches for evaluating small-bowel injuries. For example, in an early report, Bjarnason et al. used the ^{111} in-labeled leukocyte methodology to indicate that approximately two-thirds of NSAID users had indications of mild intestinal irritation (Bjarnason et al., 1987). In the neutrophils, there is a calcium binding protein called calprotectin, which has been

employed as an inflammatory bowel disease (IBD) recurrence marker in the GIT. The scope of this marker's use has been broadened to include the assessment of NSAID enteropathy. Maiden et al. discovered that 75% of healthy subjects had stool calprotectin concentrations that were greater than a baseline in a trial of healthy individuals managed with diclofenac or placebo (Maiden et al., 2005).

New endoscopic techniques made it easier to diagnose NSAID-induced enteropathy than ever before, revealing that it's just as prevalent and dangerous as upper GI problems (Shin et al., 2017). Many human studies DBE and CE were undertaken to assess the effects of NSAIDs on lower GIT. A study of people taking NSAIDs, DBE demonstrated mucosal breaches in 51% of the participants compared to a control group of 5% (Matsumoto et al., 2008). Graham et al. employed CE to analyze twenty-one arthritis-suffering patients who have already been utilizing diclofenac sodium for three months or extra and twenty control individuals to determine the prevalence of chronic NSAID use. According to the results, 71% of the NSAID group showed signs of small-bowel damage, matched to only 10% of the control group (Graham et al., 2005).

Goldstein and co-workers used CE to assess small intestine damage in volunteers who had no previous small intestine problems and were given diclofenac and PPI, a coxib, or a placebo for two weeks in a multicenter, randomized, controlled study. Patients who got a combination of NSAID and PPI possessed a higher proportion of lesions and more mucosal cracks on average than those who received coxib or placebo. In addition, they discovered the baseline frequency of small intestine mucosal damages is enough importance to be considered when evaluating the effects of NSAIDs (Goldstein et al., 2005). That suggests that taking a PPI to relieve upper GIT symptoms increases incidence of a lower GIT problem, demonstrating that NSAIDs cause enteropathy only when COX-1 and COX-2 inhibitors are administered simultaneously. These investigations confirm a significant rate of small-bowel injury (55–72%) linked to NSAIDs, with no evidence of mucosal damage in non-NSAID-using controls (7–10%) (Goldstein et al., 2005; Graham et al., 2005). Lower-GI damage is caused differently by NSAIDs than upper-GI injury. It relative depends on the molecule's pH and the degree of enhanced lower-intestine permeability caused by NSAIDs. Inflammation is constantly caused by increased permeability (Bjarnason et al., 2004). Long-term suppression of COX-1

and COX-2 together produces small intestine injury. Although COX-2-selective medicines had a lesser frequency of damage than non-selective NSAIDs, a capsule-endoscopy investigation indicated that COX-2-selective medications had a high prevalence of damage (Maiden et al., 2007). COX-2 is also needed for maintaining mucosal integrity and ulcer repair, hence stomach and intestine injuries only arise if together COX-1 and COX-2 are repressed (Halter et al., 2001). In addition, non-selective NSAIDs are mildly acidic and usually lipophilic, providing them the properties of a detergent. As a result, phospholipids are involved in their interaction, a key component of the brush boundary, producing injury to the surface epithelium (Bjarnason and Takeuchi, 2009). NSAIDs also lower intracellular adenosine triphosphate concentration by neutralizing mitochondrial oxidative phosphorylation. This alteration leads to a loss of integration between cells, such as intersections between cells, thus increasing the intestine permeability and consequent mucosal damage (Bjarnason and Takeuchi, 2009).

Bacteria have been concerned in the mechanism of pathophysiology by which NSAIDs induced enteropathy in many investigations. When germ-free rats and mice are administered an NSAID, they incur little or no intestinal damage, but when gram-negative bacteria colonize them, they become susceptible to NSAID-enteropathy (Wallace, 2013). In addition, bile and enterohepatic circulation play a part when it comes to the onset of intestinal injury (Wallace, 2013). It has been shown that intestinal epithelial cells cultured in the attendance of NSAIDs and bile are harmed. Bacteria can also trigger the production of toxic secondary bile acids (Syer et al., 2015). There is a clue that tying the bile duct in rats fed NSAIDs protects or decreases intestinal damage (Reuter et al., 1997). According to animal studies, NSAIDs do not cause serious intestine harm until they are circulated through the enterohepatic system. This could be due to the NSAID causing repeated epithelial injury as it circulates through the colon (Wallace, 2012).

Scientists have begun working on a cure for the effect of NSAIDs on the stomach rather than the intestines early because the harmful effects on the stomach prompt patients to seek treatment promptly. Proton pump inhibitors, for example, are antisecretory medications (PPIs), that can suppress acid output (Documents et al., 2010). They're widely used to prevent peptic ulcers and mucosal irritation caused by NSAIDs (Lanza et al., 2009). Despite the fact that PPIs have been shown to reduce

upper GI events, video-endoscopy examinations have indicated a significant risk of small-intestine injury in PPI-treated patients. Moreover, animal experiments have demonstrated that taking PPIs along with an NSAID increases the risk of NSAIDs enteropathy (Wallace, 2012). H2RAs are histamine 2-receptor antagonists that inhibit acid discharge, are also being researched to determine if they can help with NSAID-related adverse effects. H2RAs (e.g., famotidine and ranitidine) were preventative at large dosages, affording to a review of 14 trials, although they minimized the duodenal frequency but not stomach ulcers at commonly given doses (Rostom et al., 2009 a). Misoprostol (a prostaglandin analogue) preserves the mucosal layer of the GIT by increasing mucus/bicarbonate secretion and steadying barrier role (Dajani and Agrawal, 1989). When compared to NSAIDs alone, it reduces NSAID-related upper GI problems by about 40% (Bocanegra et al., 1998). It was discovered that using high-dose misoprostol with indomethacin reduced the effect of indomethacin on intestinal permeability to some extent (Davies et al., 2000). Due to diarrhea and stomach pain, misoprostol is rarely tolerated well, limiting its use; lesser dosages of misoprostol with fewer side effects possibly less efficient aiming to avoid GI disorders (Rostom et al., 2002). Antibiotics are able to guard against NSAID enteropathy in several investigations, particularly when they are effective at reducing gram-negative bacteria (Wallace, 2013). Fit volunteers have treated either diclofenac with omeprazole and rifaximin or diclofenac and omeprazole in a randomized controlled experiment. According to the data, rifaximin-treated volunteers developed fewer minor intestinal lesions than placebo-treated volunteers (Scarpignato et al., 2017). This adds to the growing body of data indicating enteric bacteria play a role in the genesis of NSAID enteropathy. While several researchers have investigated the effect of the DS on the GIT, we are unaware of any studies that have used stereology to examine the effects of the DS on the GIT mucosa.

Despite the fact that there are no major statistical differences in terms of stereological results among the groups on the stomach, small and large intestines, the diclofenac-treated groups appear to have pathological damage on the light microscopic findings. These findings could be explained by the short period of DS exposure in this experiment, the dose being too low to cause harm or the fact that diclofenac is safe at this dose for this duration.

Alternative and natural medications for treating various ailments have sparked increased interest in recent years, although scientific data is lacking. The usage of GA is often associated with the early dynastic period (3400 BC). It is a natural material composed of a compact fluid collected from the exudates of acacia trees. It is made up of a compound of polysaccharides and glycoproteins such as arabinose, rhamnose, galactose, and an organic acid, as well as minerals and amino acids. Because of its resistance to digestion, GA is employed as a natural prebiotic. Anaerobic microbiota converts GA to short-chain fatty acids (SCFs), which are critical for maintaining GIT homeostasis, structure, and function, as well as managing the overall luminal microbial ecology and suppressing pathogenic microorganisms. The cecum has the greatest bacteria in the GIT, and it is here that fermentation takes place. GA is a natural supplement that aids in the metabolism of the intestine and liver, among other things (Obaid, 2020; Al-Baadani et al., 2021). Indigenous Africans utilize it in food preparation, and for human and animal health. Various portions of acacia trees have been employed to pleasure a wide range of gastrointestinal ailments, such as diarrhea and typhoid fever, (Mahomoodally, 2013), and intestinal inflammation (Gamal el-din et al., 2003) for millennia.

The roles of the GA among different tissues were investigated and promising results were reported in the kidneys (Gado and Aldahmash, 2013; Khalid et al., 2021), the liver (Gamal el-din et al., 2003), the heart (Abd- Allah et al., 2002) and the gonads (Ahmed et al., 2016). However, some results were contradictory, whereas numerous investigations backed up GA's antioxidant efficiency (Kaddam et al., 2018). According to certain reports, its role is less important than previously thought (Cindoruk et al., 2007).

The gastric mucosa was protected and leucocyte penetration of the stomach wall was blocked in rats cured with GA, according to histology. GA, on the other hand, was able to undo the effect of DS, showing that gum's polysaccharides had anti-inflammatory and antioxidant properties in the gastric mucosa. This data is consistent with (Tanaka et al., 2010; Taha et al., 2020), who discovered that when rats were fed polysaccharides in gum prior to an intentionally induced stomach ulcer, it displayed clear gastroprotective properties. These findings are comparable to those of Helal et al., (2011), and Gohar and Zaki, (2014), who discovered that GA pre-treatment reduced stomach lesions caused by stress or indomethacin, respectively.

Furthermore, GA was identified by Al-Yahya and Asad, (2016) to reduced gastric damage generated by ethanol and indomethacin at both oral doses evaluated (500 mg, 1000 mg/kg) and confirm, the gastroprotective efficacy of GA alone or in conjunction with other anti-ulcer medicines. In indomethacin-induced gastric ulcer rats, GA has a respectable antiulcer result and potentiates or enhances the antiulcer effect of ranitidine. Furthermore, Khedr, (2017) demonstrated a dose-dependent antiulcer effect of GA in an adult rat with an ethanol-induced ulcer through a reduction in gastric juice, an increase in pH, and other cytoprotective effects; these effects were linked to polysaccharides, which demonstrated antiulcer properties by dragging to the mucosal lining and acting as a protective layer by increasing mucus formation or scavenging. This could be because GA contains antiulcer polysaccharides, such as arabinose, galactose, and AG, which affix to the mucosal surface and act as a defending covering. With 10% GA, the ulcer score was significantly reduced, and the stomach was protected from ulcers caused by ethanol, which was more efficient than the lesser doses.

Furthermore, GA treatment revealed stomach mucosa like normal with thin surface epithelium lining, collagen fibers in the lamina propria, and between the near-normal gastric glands. When polysaccharide was managed in rats created stomach ulcers in several tests, many researchers discovered gastroprotective characteristics (Galati et al., 2001; Tanaka et al., 2010). According to researchers, many theories proposed for polysaccharide antiulcer properties include their ability to suppress the secretion of acid and pepsin to protect the mucosa by boosting mucus production or scavenging radicals (Cipriani et al., 2009). According to others, plant polysaccharides have sparked a lot of interest because of their antiulcer potential (Ghildyal et al., 2010). The majority of these impacts are assumed to be caused by the complement system, as well as the macrophages, dendritic cells, and granulocytes production of ROS, NO, and cytokines.

In the current investigation, all samples of the intestinal tract were examined histopathologically and showed significant alterations in the mucosal layer of the intestine in diclofenac sodium-treated rats, as well as slight pathological alterations like superficial lesion and slight irritation in rats given both diclofenac sodium and gum therapy. Those who were given gum alone, on the other hand, had a completely different image from the control group. These figures were similar to those

previously published by Abd El-Mawla and Osman, (2011) who revealed the preventive impact of GA (1g/day) towards ulceration generated by meloxicam in the intestine of rats. GA does not degrade or break down significantly in the GIT, it also absorbs a lot of water, which makes it a mechanical laxative, according to previous research. GA also has the effect of increasing faucal nitrogen excretion, has no effect on starch digestion, and has no effect on the use of vitamin A, which is one of the most important components in ulcer healing (Abd El-Mawla and Osman, 2011). GA is an anti-oxidant with a lot of power, and it has been discovered that it protects against experimental liver, kidney, and heart toxicity by acting in the upper gut to regulate the phases of the free radical nitric oxide (NO), either by scavenging NO generated in the enterocytes and dispersing into the lumen, or by suppressing inducible NO synthase (Rehman et al., 2004). Sánchez et al. (2020) conducted a study to assess the melatonin effects as a protective substance of GI damage induced by DS. The findings reveal that melatonin (MLT) prevents intestinal tissue damage in an *ex vivo* design and at the stomach level in an *in vivo* investigation. Even though the samples treated with MLT and DS had high concentrations of COX-2 and iNOS, they had less GI damage. The antioxidant outcome of MLT, which enhances and promotes a healthy redox balance of enterocytes, is mostly responsible for this reduction (Sánchez et al., 2020).

Cations, particularly divalent cations, can be fixed by GA. Consequently, the calcium and magnesium levels in the caecum skyrocket, making calcium and magnesium absorption from the large intestine easier and GI ulcer healing faster. This is supported by the fact that gum is turned into a gelatinous condition at a higher concentration in the colon and is moved through the digestive tract more quickly (Wapnir et al., 1996).

It is also suggested that GA can pass through the gut and get absorbed to reach adequate concentrations in the circulation to apply its antioxidant effect into other organs rather than the intestine (Ali, 2004). However, we administered GA orally to mimic its use in folk medicine and traditions in the local community. Our study adds to the literature by confirming that GA has protective effects on the GIT that was exposed by DS. As far as we know, stereological investigation evaluating the GA's influence on the GIT histology has not been done before. This is the first study on the subject.

5. CONCLUSION AND RECOMMENDATION

5.1. Conclusion

1. Using a rat model, our findings contribute to the investigation of GA's potential as a preventive substance to GI injury when given together to DS during 15 days.
2. DS has harmful effects on the structure of adult GIT and function when administered by oral gavage for 15 days at a dose of 3.6 mg/kg.
3. To our knowledge, stereological analysis of the benefits of GA on the histology of the GIT was not done before. This is the first study in the subject; many reports praise the antioxidant role of GA in the kidneys, liver, gonads, and heart, with other contradicting reports suggesting that there is no role for GA as an antioxidant among oral administration.
4. It can be concluded that GA protects rats from diclofenac-induced mucosal lesions in the GI tract. The ability of polysaccharides to attach to the surface epithelium and act as a defensive covering, limiting pepsin and acid secretion, preserving mucosa via boosting mucus production, or scavenging radicals are just a few of the processes that could be responsible for these benefits.

5.2. Recommendation

Further investigations are required, considering the following points:

1. Administration of DS via the same, or other routes with a higher dose and for a longer duration.
2. Administration of GA through the same route and dose, but the starting date of administration should be before the DS exposure.
3. Using multiple antioxidants rather than one.
4. Biochemical analyses are to be done in both tissue samples and a blood sample.
5. Immunohistochemistry to be used for certain types of cells.
6. Physical or optical fractionator methods to be applied for stereological analysis.
7. Prospect study could pay attention to a comprehensive evaluation of GA as a substitute to traditional PPI-based therapy for the GI prevention harm produced by NSAIDs.

6. REFERENCES

Abd- Allah, A. R., Al- Majed, A. A., Mostafa, A. M., Al- Shabanah, O. A., Din, A. G. E., and Nagi, M. N. (2002). Protective effect of arabic gum against cardiotoxicity induced by doxorubicin in mice: Apossible mechanism of protection. *Journal of Biochemical and Molecular Toxicology, 16*(5), 254-259.

Abd El-Mawla, A. M., and Osman, H. E. H. (2011). Effects of Gum acacia aqueous extract on the histology of the intestine and enzymes of both the intestine and the pancreas of albino rats treated with Meloxicam. *Pharmacognosy Research, 3*(2), 114.

Abdalla, M., Badi, R., Ahmed, A., and Saeed, A. (2014). Human in vivo study: The effect of gum arabic on coagulation cascade. *International Research Journal of Pharmaceutical and Applied Sciences, 4*(6), 5-8.

Abraham, N., Castillo, D., and Hartman, C. (2008). National mortality following upper gastrointestinal or cardiovascular events in older veterans with recent nonsteroidal anti- inflammatory drug use. *Alimentary Pharmacology and Therapeutics, 28*(1), 97-106.

Abraham, N. S., Hlatky, M. A., Antman, E. M., Bhatt, D. L., Bjorkman, D. J., Clark, C. B., Laine, L. (2010). ACCF/ACG/AHA 2010 expert consensus document on the concomitant use of proton pump inhibitors and thienopyridines: A focused update of the ACCF/ACG/AHA 2008 expert consensus document on reducing the gastrointestinal risks of antiplatelet therapy and NSAID use. *Journal of the American College of Cardiology, 56*(24), 2051-2066.

Abuarra, A., Hashim, R., Bauk, S., Kandaiya, S., and Tousi, E. T. (2014). Fabrication and characterization of gum arabic bonded Rhizophora spp. particleboards. *Materials and Design, 60*, 108-115.

Adam, F. A., Abdellah, A. M., Abdel-Magid, H. M., and Osman, M. E. (2016). Effect of contamination by fungi and yeast on the physiochemical characteristics of gum arabic stored in semi-desert climate of khartoum city, Sudan. *Journal of Food Technology Research, 3*(1), 55-62.

Adjene, J. O., and Kendabie, K. (2007). Histological studies of the effects of red pepper on the stomach of adult wistar rats. *Electronic Journal of Biomedicine,* (3), 13-17.

Ahmed, A. A. (2018). Health benefits of gum arabic and medical use. In *Gum Arabic*, 183-210.

Ahmed, A. A., Fedail, J. S., Musa, H. H., Musa, T. H., and Sifaldin, A. Z. (2016). Gum arabic supplementation improved antioxidant status and alters expression of oxidative stress gene in ovary of mice fed high fat diet. *Middle East Fertility Society Journal, 21*(2), 101-108.

Al-Baadani, H. H., Al-Mufarrej, S. I., Al-Garadi, M. A., Alhidary, I. A., Al-Sagan, A. A., and Azzam, M. M. (2021). The use of gum arabic as a natural prebiotic in animals: A review. *Animal Feed Science and Technology*, 274, 114894.

Al-Yahya, A. A., and Asad, M. (2016). Antiulcer activity of gum arabic and its interaction with antiulcer effect of ranitidine in rats. *Biomedical Research (0970-938X), 27*(4).

Al Assaf, S., Phillips, G. O., and Williams, P. A. (2005). Studies on acacia exudate gums. Part I: the molecular weight of acacia senegal gum exudate. *Food Hydrocolloids, 19*(4), 647-660.

Alam, N. H., Meier, R., Schneider, H., Sarker, S. A., Bardhan, P. K., Mahalanabis, D., Gyr, N. (2000). Partially hydrolyzed guar gum–supplemented oral rehydration solution in the treatment of acute diarrhea in children. *Journal of Pediatric Gastroenterology and Nutrition, 31*(5), 503-507.

Ali, A. A., Ali, K. E., Fadlalla, A. E., and Khalid, K. E. (2008). The effects of gum arabic oral treatment on the metabolic profile of chronic renal failure patients under regular haemodialysis in Central Sudan. *Natural Product Research, 22*(1), 12-21.

Ali, B. H. (2004). Does gum arabic have an antioxidant action in rat kidney? *Renal Failure, 26*(1), 1-3.

Allison, M. C., Howatson, A. G., Torrance, C. J., Lee, F. D., and Russell, R. I. (1992). Gastrointestinal damage associated with the use of nonsteroidal antiinflammatory drugs. *New England Journal of Medicine, 327*(11), 749-754.

Altman, R., Bosch, B., Brune, K., Patrignani, P., and Young, C. (2015). Advances in NSAID development: Evolution of diclofenac products using pharmaceutical technology. *Drugs, 75*(8), 859-877.

Altunkaynak, B. Z., Onger, M. E., Altunkaynak, M. E., Ayranci, E., and Canan, S. (2012). A brief introduction to stereology and sampling strategies: Basic concepts of stereology. *NeuroQuantology, 10*(1), 31-43.

Amin, L., Jesmeen, T., Bishwajit Sutradhar, K., and Mannan, A. (2013). Development and in vitro evaluation of diclofenac sodium loaded mucoadhesive microsphere with natural gum for sustained delivery. *Current Drug Delivery, 10*(6), 765-770.

Andreasson, K. I., Savonenko, A., Vidensky, S., Goellner, J. J., Zhang, Y., Shaffer, A., Markowska, A. L. (2001). Age-dependent cognitive deficits and neuronal apoptosis in cyclooxygenase-2 transgenic mice. *Journal of Neuroscience, 21*(20), 8198-8209.

Antman, E. M., Bennett, J. S., Daugherty, A., Furberg, C., Roberts, H., and Taubert, K. A. (2007). Use of nonsteroidal antiinflammatory drugs: An update for clinicians: A scientific statement from the american heart association. *Circulation, 115*(12), 1634-1642.

Aoba, T. (2004). Solubility properties of human tooth mineral and pathogenesis of dental caries. *Oral Diseases, 10*(5), 249-257.

Avelino, A. L. N., Silva, N. V. R. e., Oliveira, G. B. D., Silva, A. A. D. S., Cavalcanti, B. C., Jamacaru, F. V. F., and Dornelas, C. A. (2021). Antioxidant and antigenotoxic actions of gum arabic on the intestinal mucosa, liver and bone marrow of swiss mice submitted to colorectal carcinogenesis. *Nutrition and Cancer*, 1-9.

Babiker, R., Merghani, T. H., Elmusharaf, K., Badi, R. M., Lang, F., and Saeed, A. M. (2012). Effects of gum arabic ingestion on body mass index and body fat percentage in healthy adult females: Two-arm randomized, placebo controlled, double-blind trial. *Nutrition Journal, 11*(1), 111.

Barker, N., Van Es, J. H., Kuipers, J., Kujala, P., Van Den Born, M., Cozijnsen, M., Peters, P. J. (2007). Identification of stem cells in small intestine and colon by marker gene Lgr5. *Nature, 449*(7165), 1003.

Bidaut-Russell, M., and Gabriel, S. E. (2001). Adverse gastrointestinal effects of NSAIDs: Consequences and costs. *Best Practice and Research Clinical Gastroenterology, 15*(5), 739-753.

Bjarnason, I., and Takeuchi, K. (2009). Intestinal permeability in the pathogenesis of NSAID-induced enteropathy. *Journal of Gastroenterology, 44*(19), 23-29.

Bjarnason, I., Takeuchi, K., Bjarnason, A., Adler, S., and Teahon, K. (2004). The grand unified theory of gut. *Scandinavian Journal of Gastroenterology, 39*(9), 807-815.

Bjarnason, I., Zanelli, G., Smith, T., Prouse, P., Williams, P., Smethurst, P., Levi, A. J. (1987). Nonsteroidal antiinflammatory drug-induced intestinal inflammation in humans. *Gastroenterology, 93*(3), 480-489.

Bliss, D. Z., Jung, H.-J., Savik, K., Lowry, A., LeMoine, M., Jensen, L., Schaffer, K. (2001). Supplementation with dietary fiber improves fecal incontinence. *Nursing Research, 50*(4), 203-213.

Blunt, H. S. (1926). Gum Arabic, with Special Reference to Its Production in the Sudan. *Nature,* 119, 11.

Bocanegra, T. S., Weaver, A. L., Tindall, E. A., Sikes, D. H., Ball, J. A., Wallemark, C. B., Fort, J. G. (1998). Diclofenac/misoprostol compared with diclofenac in the treatment of osteoarthritis of the knee or hip: A randomized, placebo controlled trial. Arthrotec Osteoarthritis Study Group. *The Journal of Rheumatology, 25*(8), 1602-1611.

Bombardier, C., Laine, L., Reicin, A., Shapiro, D., Burgos-Vargas, R., Davis, B., Hochberg, M. C. (2000). Comparison of upper gastrointestinal toxicity of rofecoxib and naproxen in patients with rheumatoid arthritis. *New England Journal of Medicine, 343*(21), 1520-1528.

Bresalier, R. S., Sandler, R. S., Quan, H., Bolognese, J. A., Oxenius, B., Horgan, K., Lanas, A. (2005). Cardiovascular events associated with rofecoxib in a colorectal adenoma chemoprevention trial. *New England Journal of Medicine, 352*(11), 1092-1102.

Brown, D. L. (2017). Bias in image analysis and its solution: Unbiased stereology. *Journal of Toxicologic Pathology, 30*(3), 183-191.

Brune, K., and Hinz, B. (2004). The discovery and development of antiinflammatory drugs. *Arthritis and Rheumatism: Official Journal of the American College of Rheumatology, 50*(8), 2391-2399.

Burgess, D. R. (1975). Morphogenesis of intestinal villi: II. Mechanism of formation of previllous ridges. *Development, 34*(3), 723-740.

Calame, W., Weseler, A. R., Viebke, C., Flynn, C., and Siemensma, A. D. (2008). Gum arabic establishes prebiotic functionality in healthy human volunteers in a dose-dependent manner. *British Journal of Nutrition, 100*(6), 1269-1275.

Calvert, R., and Pothier, P. (1990). Migration of fetal intestinal intervillous cells in neonatal mice. *The Anatomical Record, 227*(2), 199-206.

Chandana, G., Kishore, P., Raju, N., Sreenu, M., and Rao, G. S. (2013). Histological studies on the stomach of albino rat (Rattus norvegicus). *Indian Journal of Veterinary Anatomy, 25*(2), 107-108.

Cheng, K., Chalmers, I., and Sheldon, T. A. (2007). Adding fluoride to water supplies. *British Medical Journal, 335*(7622), 699-702.

Cindoruk, M., Kerem, M., Karakan, T., Salman, B., Akin, O., Alper, M., Ünal, S. (2007). Peroxisome proliferators-activated alpha agonist treatment ameliorates hepatic damage in rats with obstructive jaundice: An experimental study. *BMC Gastroenterology, 7*(1), 1-7.

Cipriani, T. R., Mellinger, C. G., Bertolini, M. L., Baggio, C. H., Freitas, C. S., Marques, M. C. A., Iacomini, M. (2009). Gastroprotective effect of a type I arabinogalactan from soybean meal. *Food Chemistry, 115*(2), 687-690.

Codipilly, C. N., Teichberg, S., and Wapnir, R. A. (2006). Enhancement of absorption by gum arabic in a model of gastrointestinal dysfunction. *Journal of the American College of Nutrition, 25*(4), 307-312.

Colony, P. C. (1983). Successive phases of human fetal intestinal development. *Nutritional adaption of the gastrointestinal tract in the newborn. Nestlé, Vevey, Raven Press, New York*, 3-28.

Crofford, L. J. (1997). COX-1 and COX-2 tissue expression: implications and predictions. *The Journal of Rheumatology. Supplement, 49*, 15-19.

Cullen, D., Bardhan, K., Eisner, M., Kogut, D., Peacock, R., Thomson, J., and Hawkey, C. (1998). Primary gastroduodenal prophylaxis with omeprazole for non-steroidal anti-inflammatory drug users. *Alimentary Pharmacologyand Therapeutics, 12*(2), 135-140.

Dajani, E., and Agrawal, N. (1989). Protective effects of prostaglandins against nonsteroidal anti-inflammatory drug-induced gastrointestinal mucosal injury. *International Journal of Clinical Pharmacology Research, 9*(6), 359-369.

Daoub, R. M., Elmubarak, A. H., Misran, M., Hassan, E. A., and Osman, M. E. (2018). Characterization and functional properties of some natural Acacia gums. *Journal of the Saudi Society of Agricultural Sciences, 17*(3), 241-249.

Davies, N. M., Saleh, J. Y., and Skjodt, N. M. (2000). Detection and prevention of NSAID-induced enteropathy. *Journal of Pharmacy and Pharmaceutical Sciences, 3*(1), 137-155.

De Groot, N., Spiegel, B., van Haalen, H., de Wit, N., Siersema, P., and van Oijen, M. (2013). Gastroprotective strategies in chronic NSAID users: A cost-effectiveness analysis comparing single-tablet formulations with individual components. *Value in Health, 16*(5), 769-777.

De Santa Barbara, P., Van Den Brink, G. R., and Roberts, D. J. (2003). Development and differentiation of the intestinal epithelium. *Cellular and Molecular Life Sciences, 60*(7), 1322-1332.

Dellmann, H.-D., and Eurell, J. A. (1998). Textbook of veterinary histology: 5(10), 298-301

Deniz, Ö. G., Kıvrak, E. G., Kaplan, A. A., and Altunkaynak, B. Z. (2017). Effects of folic acid on rat kidney exposed to 900 MHz electromagnetic radiation. *Journal of Microscopy and Ultrastructure, 5*(4), 198-205.

Desplanques, S., Renou, F., Grisel, M., and Malhiac, C. (2012). Impact of chemical composition of xanthan and acacia gums on the emulsification and stability of oil-in-water emulsions. *Food Hydrocolloids, 27*(2), 401-410.

Documents, A. C. o. C. F. T. F. o. E. C., Abraham, N. S., Hlatky, M. A., Antman, E. M., Bhatt, D. L., Bjorkman, D. J., Kahi, C. J. (2010). ACCF/ACG/AHA 2010 expert consensus document on the concomitant use of proton pump inhibitors and thienopyridines: A focused update of the ACCF/ACG/AHA 2008 expert consensus document on reducing the gastrointestinal risks of antiplatelet therapy and NSAID use. *Journal of the American College of Cardiology, 56*(24), 2051-2066.

Domenjoz, R. (1960). The pharmacology of phenylbutazone analogues. *Annals of the New York Academy of Sciences, 86*(1), 263-291.

Douthwaite, A., and Lintott, G. (1938). Gastroscopic observation of the effect of aspirin and certain other substances on the stomach. *The Lancet, 232*(6013), 1222-1225.

Dunn, J. S. (1967). The fine structure of the absorptive epithelial cells of the developing small intestine of the rat. *Journal of Anatomy, 101*(1), 57.

Ebell, M. H. (2004). NSAIDs vs. opiates for pain in acute renal colic. *American Family Physician, 70*(9), 1682-1682.

Egadu, S. P., Mucunguzi, P., and Obua, J. (2007). Uses of tree species producing gum arabic in karamoja, uganda. *African Journal of Ecology, 45*, 17-21.

El-Mawla, A. M. A., and Osman, H. E. H. (2011). Effects of gum acacia aqueous extract on the histology of the intestine and enzymes of both the intestine and the pancreas of albino rats treated with meloxicam. *Pharmacognosy Research, 3*(2), 114.

Fujimori, S., Gudis, K., Takahashi, Y., Seo, T., Yamada, Y., Ehara, A., Tanaka, S. (2010). Distribution of small intestinal mucosal injuries as a result of NSAID administration. *European Journal of Clinical Investigation, 40*(6), 504-510.

Funatsu, T., Chono, K., Hirata, T., Keto, Y., Kimoto, A., and Sasamata, M. (2007). Mucosal acid causes gastric mucosal microcirculatory disturbance in nonsteroidal anti-inflammatory drug-treated rats. *European Journal of Pharmacology, 554*(1), 53-59.

Gabriel, S., and Bombardier, C. (1990). NSAID induced ulcers. An emerging epidemic? *Journal of Rheumatology, 17*(1), 1-4.

Gado, A. M., and Aldahmash, B. A. (2013). Antioxidant effect of arabic gum against mercuric chloride-induced nephrotoxicity. *Drug Design, Development and Therapy, 7*, 1245.

Galati, E., Monforte, M., Tripodo, M., d'Aquino, A., and Mondello, M. (2001). Antiulcer activity of Opuntia ficus indica (L.) Mill.(Cactaceae): Ultrastructural study. *Journal of Ethnopharmacology, 76*(1), 1-9.

Gamal el-din, A. M., Mostafa, A. M., Al-Shabanah, O. A., Al-Bekairi, A. M., and Nagi, M. N. (2003). Protective effect of arabic gum against acetaminophen-induced hepatotoxicity in mice. *Pharmacological Research, 48*(6), 631-635.

Gans, S. (1961). Some new concepts in the embryology, anatomy, physiology and surgical correction of imperforate anus. *Western Journal of Surgery, Obstetrics, and Gynecology, 69*, 34-37.

Gazarian, M., and Graudins, L. V. (2006). Safe use of NSAIDs in infants and children. *Medicine Today*, 7(11), 71.

Ghildyal, P., Groslash, T. E., Skogsrud, M., Rolstad, B., Diallo, D., Michaelsen, T. E., Paulsen, B. S. (2010). Chemical composition and immunological activities of polysaccharides isolated from the Malian medicinal plant Syzygium guineense. *Journal of Pharmacognosy and Phytotherapy, 2*(6), 76-85.

Ghoshal, N., and Bal, H. (1989). Comparative morphology of the stomach of some laboratory mammals. *Laboratory Animals, 23*(1), 21-29.

Gohar, A. A., and Zaki, A. A. (2014). Assessment of some herbal drugs for prophylaxis of peptic ulcer. *Iranian Journal of Pharmaceutical Research, 13*(3), 1081.

Gokcimen, A., Rağbetli, M. Ç., Baş, O., Tunc, A. T., Aslan, H., Yazici, A. C., and Kaplan, S. (2007). Effect of prenatal exposure to an anti-inflammatory drug on neuron number in cornu ammonis and dentate gyrus of the rat hippocampus: A stereological study. *Brain Research, 1127*, 185-192.

Goldstein, J. L., Eisen, G. M., Lewis, B., Gralnek, I. M., Zlotnick, S., and Fort, J. G. (2005). Video capsule endoscopy to prospectively assess small bowel injury with celecoxib, naproxen plus omeprazole, and placebo. *Clinical Gastroenterology and Hepatology, 3*(2), 133-141.

Graham, D. Y., Opekun, A. R., Willingham, F. F., and Qureshi, W. A. (2005). Visible small-intestinal mucosal injury in chronic NSAID users. *Clinical Gastroenterology and Hepatology, 3*(1), 55-59.

Griffin, G. (2000). How safe and effective are nonsteroidal anti-inflammatory drugs (NSAIDs) in the treatment of acute or chronic nonspecific low back pain (LBP)? *Journal of Family Practice, 49*(9), 780-780.

Gupta, M., and Eisen, G. M. (2009). NSAIDs and the gastrointestinal tract. *Current Gastroenterology Reports, 11*(5), 345-353.

Halter, F., Tarnawski, A., Schmassmann, A., and Peskar, B. (2001). Cyclooxygenase 2—implications on maintenance of gastric mucosal integrity and ulcer healing: Controversial issues and perspectives. *Gut British Medical Journal, 49*(3), 443-453.

Helal, O. K., Yousef, M. M., and Elnaa, M. (2011). Possible protective effect of gum arabic on experimentally induced gastric ulcer in adult male albino rats: A histological and immunohistochemical study. *Egyptian Journal of Histology, 34*(3), 546-553.

Henry, D., and McGettigan, P. (2003). Epidemiology overview of gastrointestinal and renal toxicity of NSAIDs. *International Journal of Clinical Practice. Supplement*(135), 43.

Higuchi, K., Umegaki, E., Watanabe, T., Yoda, Y., Morita, E., Murano, M., Arakawa, T. (2009). Present status and strategy of NSAIDs-induced small bowel injury. *Journal of Gastroenterology, 44*(9), 879-888.

Hirose, K., Jyoyama, H., Kojima, Y., Eigyo, M., Hatakeyama, H., Asanuma, F., Yamaguchi, T. (1984). Pharmacological properties of 2-[4-(2-thiazolyloxy)-phenyl]-propionic acid (480156-S), a new non-steroidal antiinflammatory agent. *Arzneimittel-Forschung, 34*(3), 280-286.

Hooper, L., Brown, T. J., Elliott, R., Payne, K., Roberts, C., and Symmons, D. (2004). The effectiveness of five strategies for the prevention of gastrointestinal toxicity induced by non-steroidal anti-inflammatory drugs: Systematic review. *British Medical Journal, 329*(7472), 948.

Hu, B., Han, L., Gao, Z., Zhang, K., Al-Assaf, S., Nishinari, K., Fang, Y. (2018). Effects of temperature and solvent condition on phase separation induced molecular fractionation of gum arabic/hyaluronan aqueous mixtures. *International Journal of Biological Macromolecules, 116*, 683-690.

Huerta, C., Castellsague, J., Varas-Lorenzo, C., and Rodríguez, L. A. G. (2005). Nonsteroidal anti-inflammatory drugs and risk of ARF in the general population. *American Journal of Kidney Diseases, 45*(3), 531-539.

Ibrahim, M. A., Kohn, N., and Wapnir, R. A. (2004). Proabsorptive effect of gum arabic in isotonic solutions orally administered to rats: Effect on zinc and other solutes. *The Journal of Nutritional Biochemistry, 15*(3), 185-189.

Johnson, A. G. (1997). NSAIDs and increased blood pressure. *Drug Safety, 17*(5), 277-289.

Joshi, S., and Rapoport, A. M. (2017). Diclofenac potassium for oral solution (CAMBIA®) in the acute management of a migraine attack: clinical evidence and practical experience. *Therapeutic Advances in Neurological Disorders, 10*(4), 217-226.

Jüni, P., Reichenbach, S., and Egger, M. (2005). COX 2 inhibitors, traditional NSAIDs, and the heart. *British Medical Journal,* 330, 1342-1343.

Kaddam, L., Fdl-Elmula, I., and Saeed, A. (2018). Gum arabic beneficial effects, clinical applications, and future prospective. In *Gum Arabic*, 211-220.

Kaddam, L., FdleAlmula, I., Eisawi, O. A., Abdelrazig, H. A., Elnimeiri, M., Lang, F., and Saeed, A. M. (2015). Gum arabic as fetal hemoglobin inducing agent in sickle cell anemia; in vivo study. *BMC, Hematology, 15*(1), 19.

Kameda, N., Higuchi, K., Shiba, M., Machida, H., Okazaki, H., Yamagami, H., Tominaga, K. (2008). A prospective, single-blind trial comparing wireless capsule endoscopy and double-balloon enteroscopy in patients with obscure gastrointestinal bleeding. *Journal of Gastroenterology, 43*(6), 434-440.

Kammeraad, A. (1942). The development of the gastro- intestinal tract of the rat. I. Histogenesis of the epithelium of the stomach, small intestine and pancreas. *Journal of Morphology, 70*(2), 323-351.

Kaplan, S., Odaci, E., Canan, S., Onger, M. E., Aslan, H., and Unal, B. (2012). The disector counting technique. *NeuroQuantology, 10*(1).

Kashfi, K., and Rigas, B. (2005). Is COX-2 a 'collateral'target in cancer prevention? *Biochemical SocietyTransactions,* 33(4), 724-727

Katti, K. K., Kattumuri, V., Bhaskaran, S., Katti, K. V., and Kannan, R. (2009). Facile and general method for synthesis of sugar-coated gold nanoparticles. *International Journal of Green Nanotechnology: Biomedicine, 1*(1), 53-59.

Keskin, I., Kaplan, S., Kalkan, S., Sutcu, M., Ulkay, M. B., and Esener, O. B. (2015). Evaluation of neuroprotection by melatonin against adverse effects of prenatal exposure to a nonsteroidal anti-inflammatory drug during peripheral nerve development. *International Journal of Developmental Neuroscience, 41*, 1-7.

Khalid, S. A., Musa, A., Saeed, A., Ali, N. E. A., Abugroun, E. A., Mohamed, G., Phillips, G. O. (2021). Gum arabic in renal disease (GARDS Study): Clinical evidence of dietary supplementation impact on progression of renal dysfunction. *Journal of Functional Foods, 82*, 104515.

Khalid, S. A., Musa, A. M., Saeed, A. M., Abugroun, E. A., Ahmed, E. O. S., Ghalib, M. B., Abdelgader, A. (2014). Manipulating dietary fibre: Gum arabic making friends of the colon and the kidney. *Bioactive Carbohydrates and Dietary Fibre, 3*(2), 71-76.

Khedr, A. (2017). Antiulcer protective activity of gum arabic (Acacia Senegal) in adult rats. *Bulletin of the National Nutrition Institute of the Arab Republic of Egypt, 49*(1), 1-28.

Kinsey, S. G., Nomura, D. K., O'Neal, S. T., Long, J. Z., Mahadevan, A., Cravatt, B. F., Lichtman, A. H. (2011). Inhibition of monoacylglycerol lipase attenuates nonsteroidal anti-inflammatory drug-induced gastric hemorrhages in mice. *Journal of Pharmacology and Experimental Therapeutics, 338*(3), 795-802.

Kishimoto, A., Ushida, K., Phillips, G. O., Ogasawara, T., and Sasaki, Y. (2006). Identification of intestinal bacteria responsible for fermentation of gum arabic in pig model. *Current Microbiology, 53*(3), 173-177.

Kluth, D., Fiegel, H. C., and Metzger, R. (2011). Embryology of the hindgut. *Seminar in Pediatric Surgery,* 20*:*152-60.

Kluth, D., Jaeschke-Melli, S., and Fiegel, H. (2003). The embryology of gut rotation. *Seminar in Pediatric Surgery*, 12:175-79.

Kluth, D., Kaestner, M., Tibboel, D., and Lambrecht, W. (1995). Rotation of the gut: Fact or fantasy? *Journal of Pediatric Surgery, 30*(3), 448-453.

Kowalski, M., Makowska, J., Blanca, M., Bavbek, S., Bochenek, G., Bousquet, J., Gomes, E. (2011). Hypersensitivity to nonsteroidal anti- inflammatory drugs (NSAIDs)–classification, diagnosis and management: Review of the EAACI/ENDA and GA2LEN/HANNA. *Allergy, 66*(7), 818-829.

Kuramoto, T., Nakanishi, S., Ochiai, M., Nakagama, H., Voigt, B., and Serikawa, T. (2012). Origins of albino and hooded rats: Implications from molecular genetic analysis across modern laboratory rat strains. *PloS one, 7*(8), e43059.

Lanas, A., García-Rodríguez, L. A., Polo-Tomás, M., Ponce, M., Alonso-Abreu, I., Perez-Aisa, M. A., Muñoz, M. (2009). Time trends and impact of upper and lower gastrointestinal bleeding and perforation in clinical practice. *The American Journal of Gastroenterology, 104*(7), 1633.

Lanas, A., and Sopeña, F. (2009). Nonsteroidal anti-inflammatory drugs and lower gastrointestinal complications. *Gastroenterology Clinics, 38*(2), 333-352.

Langman, M. (2001). Ulcer complications associated with anti- inflammatory drug use. What is the extent of the disease burden? *Pharmacoepidemiology and Drug Safety, 10*(1), 13-19.

Lanza, F. L., Chan, F. K., Quigley, E. M., and Gastroenterology, P. P. C. o. t. A. C. o. (2009). Guidelines for prevention of NSAID-related ulcer complications. *Official Journal of the American College of Gastroenterology, 104*(3), 728-738.

Liebelt, A. G. (1998). Unique Features of Anatomy, Histology, and Ultrastructure Kidney, Mouse. In *Urinary System*, 37-57.

Liu, Y., Miyoshi, H., and Nakamura, M. (2007). Nanomedicine for drug delivery and imaging: A promising avenue for cancer therapy and diagnosis using targeted functional nanoparticles. *International Journal of Cancer, 120*(12), 2527-2537.

Macrae, R., Robinson, R. K., and Sadler, M. J. (1993). Encyclopaedia of food science, food technology and nutrition. *2nd edition. London, Academic Press*, 894-1017

Mahomoodally, M. F. (2013). Traditional medicines in Africa: An appraisal of ten potent African medicinal plants. *Evidence-Based Complementary and Alternative Medicine,* 1-14

Maiden, L. (2009). Capsule endoscopic diagnosis of nonsteroidal antiinflammatory drug-induced enteropathy. *Journal of Gastroenterology, 44*(19), 64-71.

Maiden, L., Thjodleifsson, B., Seigal, A., Bjarnason, I. I., Scott, D., Birgisson, S., and Bjarnason, I. (2007). Long-term effects of nonsteroidal anti-inflammatory drugs and cyclooxygenase-2 selective agents on the small bowel: A cross-sectional capsule enteroscopy study. *Clinical Gastroenterology and Hepatology, 5*(9), 1040-1045.

Maiden, L., Thjodleifsson, B., Theodors, A., Gonzalez, J., and Bjarnason, I. (2005). A quantitative analysis of NSAID-induced small bowel pathology by capsule enteroscopy. *Gastroenterology, 128*(5), 1172-1178.

Maksymowych, W. P. (2007). Update on the treatment of ankylosing spondylitis. *Therapeutics and Clinical Risk Management, 3*(6), 1125.

Masso Gonzalez, E. L., Patrignani, P., Tacconelli, S., and Rodríguez, L. A. G. (2010). Variability among nonsteroidal antiinflammatory drugs in risk of upper gastrointestinal bleeding. *Arthritis and Rheumatism, 62*(6), 1592-1601.

Matsui, H., Shimokawa, O., Kaneko, T., Nagano, Y., Rai, K., and Hyodo, I. (2011). The pathophysiology of non-steroidal anti-inflammatory drug (NSAID)-induced mucosal injuries in stomach and small intestine. *Journal of Clinical Biochemistry and Nutrition, 48*(2), 107-111.

Matsumoto, N., Riley, S., Fraser, D., Al-Assaf, S., Ishimura, E., Wolever, T., Phillips, A. O. (2006). Butyrate modulates TGF-β1 generation and function: Potential renal benefit for acacia (sen) SUPERGUM™(gum arabic)? *Kidney International, 69*(2), 257-265.

Matsumoto, T., Kudo, T., Esaki, M., Yano, T., Yamamoto, H., Sakamoto, C., Matsui, T. (2008). Prevalence of non-steroidal anti-inflammatory drug-induced enteropathy determined by double-balloon endoscopy: A Japanese multicenter study. *Scandinavian Journal of Gastroenterology, 43*(4), 490-496.

McCracken, K. W., and Wells, J. M. (2017). Mechanisms of embryonic stomach development. *Seminar in Cell and Developmental Biology*, 66, 36-42.

Meena, V. K., and Datta, S. (2015). Seedling morphology of some species of genus acacia and their taxonomic significance. *Journal of Tree Sciences, 34*(1), 56-63.

Miki, T., Satriotomo, I., Li, H.-P., Matsumoto, Y., Gu, H., Yokoyama, T., Takeuchi, Y. (2005). Application of the physical disector to the central nervous system: Estimation of the total number of neurons in subdivisions of the rat hippocampus. *Anatomical Science International, 80*(3), 153.

Min, Y. W., Park, S. U., Jang, Y. S., Kim, Y.-H., Rhee, P.-L., Ko, S. H., Chang, D. K. (2012). Effect of composite yogurt enriched with acacia fiber and Bifidobacterium lactis. *World Journal of Gastroenterology, 18*(33), 4563.

Moore, A., Bjarnason, I., Cryer, B., Garcia–Rodriguez, L., Goldkind, L., Lanas, A., and Simon, L. (2009). Evidence for endoscopic ulcers as meaningful surrogate endpoint for clinically significant upper gastrointestinal harm. *Clinical Gastroenterology and Hepatology, 7*(11), 1156-1163.

Musu, M., Finco, G., Antonucci, R., Polati, E., Sanna, D., Evangelista, M., Fanos, V. (2011). Acute nephrotoxicity of NSAID from the foetus to the adult. *European Review for Medical and Pharmacological Sciences, 15*(12), 1461-1472.

Naidu, P. S., Booker, L., Cravatt, B. F., and Lichtman, A. H. (2009). Synergy between enzyme inhibitors of fatty acid amide hydrolase and cyclooxygenase in visceral nociception. *Journal of Pharmacology and Experimental Therapeutics, 329*(1), 48-56.

Nasir, O., Artunc, F., Wang, K., Rexhepaj, R., Föller, M., Ebrahim, A., Walter, M. (2010). Downregulation of mouse intestinal Na+-coupled glucose transporter SGLT1 by gum Arabic (Acacia senegal). *Cellular Physiology and Biochemistry, 25*(2-3), 203-210.

Nasir, O., Babiker, S., and Salim, A. M. M. (2016). Protective effect of gum Arabic supplementation for type 2 diabetes mellitus and its complications. *International Journal of Multidisciplinary and Current Research*, *4*, 288-94.

Neighbour, H. (2014). Mechanisms of aspirin-intolerant asthma: Identifying inflammatory pathways in the pathogenesis of asthma. *International Archives of Allergy and Immunology, 163*(1), 1-2.

Nolte, T., Brander-Weber, P., Dangler, C., Deschl, U., Elwell, M. R., Greaves, P., Rogers, A. (2016). Nonproliferative and proliferative lesions ofthe gastrointestinal tract, pancreas and salivary glands of the rat and mouse. *Journal of Toxicologic Pathology, 29*(1), 1S-125S.

Obaid, S. S. (2020). The Medical uses of gum acacia-gum arabic (GA) in human. *Academic Journal of Research and Scientific Publishing, 1*(10).

Ojo, G. B., Caxton-Martins, E. A., and Odukoya, S. O. (2010). Morphometric effects of cola nitida extract on the stomach of adult male wistar rats. *Electronic Journal of Biomedicine* 2, 18-24.

Oliveira, D. S., Dzinic, S., Bonfil, A. I., Saliganan, A. D., Sheng, S., and Bonfil, R. D. (2016). The mouse prostate: A basic anatomical and histological guideline. *Bosnian Journal of Basic Medical Sciences, 16*(1), 8.

Onishi, T., Umemura, S., Yanagawa, M., Matsumura, M., Sasaki, Y., Ogasawara, T., and Ooshima, T. (2008). Remineralization effects of gum arabic on caries-like enamel lesions. *Archives of Oral Biology, 53*(3), 257-260.

Palaian, S., Ibrahim, M. I., and Mishra, P. (2010). Pattern of adverse drug reactions reported by the community pharmacists in nepal. *Pharmacy Practice, 8*(3), 201.

Pasquier, B., Armand, M., Castelain, C., Guillon, F., Borel, P., Lafont, H., and Lairon, D. (1996). Emulsification and lipolysis of triacylglycerols are altered by viscous soluble dietary fibres in acidic gastric medium in vitro. *Biochemical Journal, 314*(1), 269-275.

Patrignani, P., Tacconelli, S., Bruno, A., Sostres, C., and Lanas, A. (2011). Managing the adverse effects of nonsteroidal anti-inflammatory drugs. *Expert Review of Clinical Pharmacology, 4*(5), 605-621.

Phillips, G., and Williams, P. (2001). Tree exudate gums: Natural and versatile food additives and ingredients. *Food Ingredients and Analysis International*, 23:26, 28.

Phillips, G. O., and Williams, P. A. (2000). *Handbook of hydrocolloids*. 155-168

Poddubnyy, D., Song, I., and Sieper, J. (2009). A systematic comparison of rheumatoid-arthritis and ankylosing spondylitis: Non-steroidal anti-inflammatory drugs. *Clinical and Experimental Rheumatology, 27*(4), S148.

Rainsford, K. D. (1978). The effects of aspirin and other non-steroid anti-inflammatory/analgesic drugs on gastro-intestinal mucus glycoprotein biosynthesis in vivo: Relationship to ulcerogenic actions. *Biochemical Pharmacology, 27*(6), 877-885.

Rao, P., and Knaus, E. E. (2008). Evolution of nonsteroidal anti-inflammatory drugs (NSAIDs): Cyclooxygenase (COX) inhibition and beyond. *Journal of Pharmacy and Pharmaceutical Sciences, 11*(2), 81-110s.

Rao, P. P., Kabir, S. N., and Mohamed, T. (2010). Nonsteroidal anti-inflammatory drugs (NSAIDs): Progress in small molecule drug development. *Pharmaceuticals, 3*(5), 1530-1549.

Rehman, K. U., Codipilly, C. N., and Wapnir, R. A. (2004). Modulation of small intestinal nitric oxide synthase by gum arabic. *Experimental Biology and Medicine, 229*(9), 895-901.

Rehman, K. U., Wingertzahn, M. A., Teichberg, S., Harper, R. G., and Wapnir, R. A. (2003). Gum arabic (GA) modifies paracellular water and electrolyte transport in the small intestine. *Digestive Diseases and Sciences, 48*(4), 755-760.

Renard, D., Lavenant-Gourgeon, L., Ralet, M.-C., and Sanchez, C. (2006). Acacia s enegal gum: continuum of molecular species differing by their protein to sugar ratio, molecular weight, and charges. *Biomacromolecules, 7*(9), 2637-2649.

Reuter, B. K., Davies, N. M., and Wallace, J. L. (1997). Nonsteroidal anti-inflammatory drug enteropathy in rats: Role of permeability, bacteria, and enterohepatic circulation. *Gastroenterology, 112*(1), 109-117.

Rodge, A., Sonkamble, S., Salve, R., and Hashmi, S. (2012). Effect of hydrocolloid (guar gum) incorporation on the quality characteristics of bread. *Journal of Food Process Technology, 3*(2), 133-120.

Rostom, A., Dube, C., Wells, G., Tugwell, P., Welch, V., Jolicoeur, E., and McGowan, J. (2002). Prevention of NSAID-induced gastroduodenal ulcers (Cochrane Review). *The Cochrane Database Syst Rev,* 4:CD002296.

Rostom, A., Moayyedi, P., Hunt, R., and Group, C. A. o. G. C. (2009a). Canadian consensus guidelines on long- term nonsteroidal anti- inflammatory drug therapy and the need for gastroprotection: Benefits versus risks. *Alimentary Pharmacology and Therapeutics, 29*(5), 481-496.

Rostom, A., Muir, K., Dube, C., Lanas, A., Jolicoeur, E., and Tugwell, P. (2009b). Prevention of NSAID-related upper gastrointestinal toxicity: A meta-analysis of traditional NSAIDs with gastroprotection and COX-2 inhibitors. *Drug, Healthcare and Patient Safety, 1*, 47.

Russell, R. (2001). Non-steroidal anti-inflammatory drugs and gastrointestinal damage—problems and solutions. *Postgraduate Medical Journal, 77*(904), 82-88.

Sallmann, A. R. (1986). The history of diclofenac. *The American Journal of Medicine, 80*(4), 29-33.

Samter, M., and Beers, R. F. (1968). Intolerance to aspirin: Clinical studies and consideration of its pathogenesis. *Annals of Internal Medicine, 68*(5), 975-983.

Sánchez, A. B., Clares, B., Rodríguez-Lagunas, M. J., Fábrega, M. J., and Calpena, A. C. (2020). Study of melatonin as preventive agent of gastrointestinal damage induced by sodium diclofenac. *Cells, 9*(1), 180.

Sanchez, C., Renard, D., Robert, P., Schmitt, C., and Lefebvre, J. (2002). Structure and rheological properties of acacia gum dispersions. *Food Hydrocolloids, 16*(3), 257-267.

Scarpignato, C. (1995). Nonsteroidal anti-inflammatory drugs: How do they damage gastroduodenal mucosa? *Digestive Diseases, 13*(Suppl. 1), 9-39.

Scarpignato, C., Dolak, W., Lanas, A., Matzneller, P., Renzulli, C., Grimaldi, M., Bjarnason, I. (2017). Rifaximin reduces the number and severity of intestinal lesions associated with use of nonsteroidal anti-inflammatory drugs in humans. *Gastroenterology, 152*(5), 980-982. e983.

Scheiman, J. (2001). The impact of nonsteroidal anti-inflammatory drug-induced gastropathy. *The American Journal of Managed Care, 7*(1 Suppl), 10-14.

Scheiman, J. M. (1994). NSAID-lnduced Peptic Ulcer Disease: A critical review of pathogenesis and management. *Digestive Diseases, 12*(4), 210-222.

Schlansky, B., and Hwang, J. H. (2009). Prevention of nonsteroidal anti-inflammatory drug-induced gastropathy. *Journal of Gastroenterology, 44*(19), 44.

Schmidt, M., Sørensen, H. T., and Pedersen, L. (2018). Diclofenac use and cardiovascular risks: Series of nationwide cohort studies. *British Medical Journal, 362*, k3426.

Schmitz, C., Eastwood, B. S., Tappan, S. J., Glaser, J. R., Peterson, D. A., and Hof, P. R. (2014). Current automated 3D cell detection methods are not a suitable replacement for manual stereologic cell counting. *Frontiers in Neuroanatomy, 8*, 27.

Shin, S. J., Noh, C.-K., Lim, S. G., Lee, K. M., and Lee, K. J. (2017). Non-steroidal anti-inflammatory drug-induced enteropathy. *Intestinal Research, 15*(4), 446.

Silverstein, F. E., Graham, D. Y., Senior, J. R., Davies, H. W., Struthers, B. J., Bittman, R. M., and Geis, G. S. (1995). Misoprostol reduces serious gastrointestinal complications in patients with rheumatoid arthritis receiving nonsteroidal anti-inflammatory drugs: A randomized, double-blind, placebo-controlled trial. *Annals of Internal Medicine, 123*(4), 241-249.

Simon, L. S. (1997). Biologic effects of nonsteroidal anti-inflammatory drugs. *Current Opinion in Rheumatology, 9*(3), 178-182.

Singh, G., Ramey, D. R., Morfeld, D., Shi, H., Hatoum, H. T., and Fries, J. F. (1996). Gastrointestinal tract complications of nonsteroidal anti-inflammatory drug treatment in rheumatoid arthritis: A prospective observational cohort study. *Archives of Internal Medicine, 156*(14), 1530-1536.

Sinha, M., Gautam, L., Shukla, P. K., Kaur, P., Sharma, S., and Singh, T. P. (2013). Current perspectives in NSAID-induced gastropathy. *Mediators of Inflammation, 2013*.

Slavin, J. (2013). Fiber and prebiotics: Mechanisms and health benefits. *Nutrients, 5*(4), 1417-1435.

Sneader, W. (2000). The discovery of aspirin: A reappraisal. *British Medical Journal, 321*(7276), 1591-1594.

Snipes, R. L. (1981). Anatomy of the cecum of the laboratory mouse and rat. *Anatomy and Embryology, 162*(4), 455-474.

Solomon, S. D., McMurray, J. J., Pfeffer, M. A., Wittes, J., Fowler, R., Finn, P., Bertagnolli, M. (2005). Cardiovascular risk associated with celecoxib in a clinical trial for colorectal adenoma prevention. *New England Journal of Medicine, 352*(11), 1071-1080.

Steinmeyer, J. (2000). Pharmacological basis for the therapy of pain and inflammation with nonsteroidal anti-inflammatory drugs. *Arthritis Research and Therapy, 2*(5), 379.

Stephen, A. M., and Phillips, G. O. (2016). *Food polysaccharides and their applications*: CRC press.2nd edition 456-472

Stillman, M. T., and Schlesinger, P. A. (1990). Nonsteroidal anti-inflammatory drug nephrotoxicity: Should we be concerned? *Archives of Internal Medicine, 150*(2), 268-270.

Sun, W. H., Tsuji, S., Tsujii, M., Gunawan, E. S., Sawaoka, H., Kawai, N., Yasumaru, M. (2000). Cyclo- oxygenase- 2 inhibitors suppress epithelial cell kinetics and delay gastric wound healing in rats. *Journal of Gastroenterology and Hepatology, 15*(7), 752-761.

Sunada, K., and Yamamoto, H. (2009). Double-balloon endoscopy: Past, present, and future. *Journal of Gastroenterology, 44*(1), 1-12.

Syer, S. D., Blackler, R. W., Martin, R., de Palma, G., Rossi, L., Verdu, E., Langella, P. (2015). NSAID enteropathy and bacteria: A complicated relationship. *Journal of Gastroenterology, 50*(4), 387-393.

Szekely, C., and Zandi, P. (2010). Non-steroidal anti-inflammatory drugs and Alzheimer's disease: The epidemiological evidence. *CNS and Neurological Disorders-Drug Targets, 9*(2), 132-139.

Taha, M. S., El-Sherbiny, E. M., and Osman, H. F. (2020). Anti-ulcerogenic activity of gum arabic in gastric mucosal injury induced by ethanol in male albino rats. *Applied Physiology, Nutrition, and Metabolism, 45*(7), 731-736.

Tanaka, A., Hase, S., Miyazawa, T., Ohno, R., and Takeuchi, K. (2002). Role of cyclooxygenase (COX)-1 and COX-2 inhibition in nonsteroidal anti-inflammatory drug-induced intestinal damage in rats: relation to various pathogenic events. *Journal of Pharmacology and Experimental Therapeutics, 303*(3), 1248-1254.

Tanaka, L. Y. A., de Oliveira, A. J. B., Gonçalves, J. E., Cipriani, T. R., de Souza, L. M., Marques, M. C. A., Sassaki, G. L. (2010). An arabinogalactan with anti-ulcer protective effects isolated from Cereus peruvianus. *Carbohydrate Polymers, 82*(3), 714-721.

Thiéfin, G., and Beaugerie, L. (2005). Toxic effects of nonsteroidal antiinflammatory drugs on the small bowel, colon, and rectum. *Joint Bone Spine, 72*(4), 286-294.

Tonon, R. V., Grosso, C. R., and Hubinger, M. D. (2011). Influence of emulsion composition and inlet air temperature on the microencapsulation of flaxseed oil by spray drying. *Food Research International, 44*(1), 282-289.

Trelle, S., Reichenbach, S., Wandel, S., Hildebrand, P., Tschannen, B., Villiger, P. M., Jüni, P. (2011). Cardiovascular safety of non-steroidal anti-inflammatory drugs: Network meta-analysis. *British Medical Journal, 342*, c7086.

Treuting, P. M., Dintzis, S. M., Liggitt, D., and Frevert, C. W. (2011). Comparative anatomy and histology: *A Mouse and Human Atlas,* 1(3), 20-25.

Treuting, P. M., Valasek, M. A., and Dintzis, S. M. (2012). Upper gastrointestinal tract. In *Comparative Anatomy and Histology*, 155-175.

Turvill, J., Wapnir, R., Wingertzahn, M., Teichberg, S., and Farthing, M. (2000). Cholera toxin-induced secretion in rats is reduced by a soluble fiber, gum arabic. *Digestive Diseases and Sciences, 45*(5), 946-951.

Ulrich, C. M., Bigler, J., and Potter, J. D. (2006). Non-steroidal anti-inflammatory drugs for cancer prevention: Promise, perils and pharmacogenetics. *Nature Reviews Cancer, 6*(2), 130.

Vane, J. R., and Botting, R. M. (1998). Mechanism of action of anti-inflammatory drugs: An overview. In Selective COX-2 Inhibitors. *Pharmacology, Clinical Effects and Therapeutic Potentials,* 1-17.

Venerito, M., Wex, T., and Malfertheiner, P. (2010). Nonsteroidal anti-inflammatory drug-induced gastroduodenal bleeding: Risk factors and prevention strategies. *Pharmaceuticals, 3*(7), 2225-2237.

Verbeken, D., Dierckx, S., and Dewettinck, K. (2003). Exudate gums: Occurrence, production, and applications. *Applied Microbiology and Biotechnology, 63*(1), 10-21.

Verma, S., and Singh, S. (2008). Current and future status of herbal medicines. *Veterinary World, 1*(11), 347.

Wallace, J. (2007). Building a better aspirin: Gaseous solutions to a century- old problem. *British Journal of Pharmacology, 152*(4), 421-428.

Wallace, J. L. (2012). NSAID gastropathy and enteropathy: Distinct pathogenesis likely necessitates distinct prevention strategies. *British Journal of Pharmacology, 165*(1), 67-74.

Wallace, J. L. (2013). Mechanisms, prevention and clinical implications of nonsteroidal anti-inflammatory drug-enteropathy. *World Journal of Gastroenterology, 19*(12), 1861.

Wallace, J. L., and Chin, B. C. (1997). Inflammatory mediators in gastrointestinal defense and injury. *Proceedings of the Society for Experimental Biology and Medicine, 214*(3), 192-203.

Walton, K. D., Kolterud, Å., Czerwinski, M. J., Bell, M. J., Prakash, A., Kushwaha, J., Gumucio, D. L. (2012). Hedgehog-responsive mesenchymal clusters direct patterning and emergence of intestinal villi. *Proceedings of the National Academy of Sciences, 109*(39), 15817-15822.

Walton, K. D., Mishkind, D., Riddle, M. R., Tabin, C. J., and Gumucio, D. L. (2018). Blueprint for an intestinal villus: Species- specific assembly required. *Wiley Interdisciplinary Reviews: Developmental Biology, 7*(4), 317.

Wapnir, R. A., Teichberg, S., Go, J. T., Wingertzahn, M. A., and Harper, R. G. (1996). Oral rehydration solutions: Enhanced sodium absorption with gum arabic. *Journal of the American College of Nutrition, 15*(4), 377-382.

Wapnir, R. A., Wingertzahn, M. A., Moyse, J., and Teichberg, S. (1997). Gum arabic promotes rat jejunal sodium and water absorption from oral rehydration solutions in two models of diarrhea. *Gastroenterology, 112*(6), 1979-1985.

Warner, T. D., Giuliano, F., Vojnovic, I., Bukasa, A., Mitchell, J. A., and Vane, J. R. (1999). Nonsteroid drug selectivities for cyclo-oxygenase-1 rather than cyclo-oxygenase-2 are associated with human gastrointestinal toxicity: A full in vitro analysis. *Proceedings of the National Academy of Sciences, 96*(13), 7563-7568.

Watanabe, T., Sugimori, S., Kameda, N., Machida, H., Okazaki, H., Tanigawa, T., Oshitani, N. (2008). Small bowel injury by low-dose enteric-coated aspirin and treatment with misoprostol: a pilot study. *Clinical Gastroenterology and Hepatology, 6*(11), 1279-1282.

Watson, A. J., and Pritchard, D. M. (2000). VII. Apoptosis in intestinal epithelium: lessons from transgenic and knockout mice. *American Journal of Physiology-Gastrointestinal and Liver Physiology, 278*(1), 1-5.

Weeks, A. (2015). The prevention and treatment of postpartum haemorrhage: What do we know, and where do we go to next?. *An International Journal of Obstetrics and Gynaecology, 122*(2), 202-210.

Whelton, A. (1999). Nephrotoxicity of nonsteroidal anti-inflammatory drugs: Physiologic foundations and clinical implications. *The American Journal of Medicine, 106*(5), 13S-24S.

Williams, J. M., Duckworth, C. A., Vowell, K., Burkitt, M. D., and Pritchard, D. M. (2016). Intestinal preparation techniques for histological analysis in the mouse. *Current Protocols in Mouse Biology, 6*(2), 148-168.

Younes, H., Egret, N., Hadj-Abdelkader, M., Rémésy, C., Demigné, C., Gueret, C., Alphonse, J.-C. (2006). Fermentable carbohydrate supplementation alters nitrogen excretion in chronic renal failure. *Journal of Renal Nutrition, 16*(1), 67-74.

Younes, H., Garleb, K., Behr, S., Rémésy, C., and Demigné, C. (1995). Fermentable fibers or oligosaccharides reduce urinary nitrogen excretion by increasing urea disposal in the rat cecum. *The Journal of Nutrition, 125*(4), 1010-1016.

CURRICULUM VITAE

Mohamed Kheir Eltigani Awad Elkarim Ahmed was graduated from Omdurman Islamic University – Faculty of Basic Medical Sciences (1996) in Khartoum, Sudan, then went on to complete the M.Sc. of Human Anatomy at University of Khartoum, Faculty of Medicine (2002) in Khartoum, Sudan, and finally the M.B.B.S. at Kassala University, Faculty of Medicine. Eventually, he received his PhD from Ondokuz Mayis University, Faculty of Medicine, Department of Histology and Embryology, 2022 Samsun- Turkey. He was the father of two sons and two daughters.

ORCID number: 0000-0002-7476-3073

Publications

Mohamed Kheir E.A. ElKarim. Mohamed A/Salam Nurein, Mohamed A. Hassan (2014). Thyroid gland morphology with special considerations of the recurrent laryngeal nerves variations. *Khartoum Medical Journal*, 7(3), 1040-1042.

Rashid Awad Abdalla Salih, Mohammed AhmedAbdallah, MohamedkheirE.Awad, Mohammed H.Ali, AbuobiedaBalaAbusharib, and Mohammed A. Hammad (2015). Primary lymphoma of the thyroid gland: A case report. *International Journal of Recent Scientific Research*, 6(10), 6699-6701.